

REV LTR

THE **BOEING** COMPANY

AIRPLANE DIVISION
P.O. BOX 707
RENTON, WASHINGTON 98055

CODE IDENT. NO. 81205

NUMBER D6-15000

NASA CR-62036

TITLE: Large Transport Landing Characteristics as
Simulated in Flight and on the Ground

FOR LIMITATIONS IMPOSED ON THE USE OF THE INFORMATION
CONTAINED IN THIS DOCUMENT AND ON THE DISTRIBUTION
OF THIS DOCUMENT, SEE LIMITATIONS SHEET.

MODEL 367-80 CONTRACT NAS2-3224

ISSUE NO. 26 ISSUED TO: Nasa Ames

PREPARED BY	<u>J. W. Kerrigan</u>	<u>2/4/66</u>
	J. W. Kerrigan	
PREPARED BY	<u>R. G. Root</u>	<u>2/4/66</u>
	R. G. Root	
SUPERVISED BY	<u>L. G. Kimbrel</u>	
APPROVED BY	<u>H. C. Higgins</u>	
APPROVED BY	_____	(DATE)

ACTIVE SHEET RECORD

SHEET NUMBER	REV LTR	ADDED SHEETS				SHEET NUMBER	REV LTR	ADDED SHEETS			
		SHEET NUMBER	REV LTR	SHEET NUMBER	REV LTR			SHEET NUMBER	REV LTR	SHEET NUMBER	REV LTR
Title Page						VI-43					
1						VI-44					
ii						VI-45					
iii						VI-46					
iv						VI-47					
2						VI-48					
3						VI-49					
I-4						VI-50					
II-5						VI-51					
III-6						VI-52					
III-7						VI-53					
III-8						VI-54					
III-9						VI-55					
IV-10						VI-56					
IV-11						VI-57					
IV-12						VII-58					
IV-13						VII-59					
IV-14						VII-60					
V-15						VII-61					
V-16						VII-62					
VI-17						VII-63					
VI-18						VII-64					
VI-19						VII-65					
VI-20						VII-66					
VI-21						VII-67					
VI-22						VII-68					
VI-23						VII-69					
VI-24						VII-70					
VI-25						VII-71					
VI-26						VII-72					
VI-27						VII-73					
VI-28						VII-74					
VI-29						VII-75					
VI-30						VII-76					
VI-31						VII-77					
VI-32						VII-78					
VI-33						VII-79					
VI-34						VII-80					
VI-35						VII-81					
VI-36						VII-82					
VI-37						VII-83					
VI-38						VII-84					
VI-39						VII-85					
VI-40						VII-86					
VI-41						VII-87					
VI-42						VII-88					

ACTIVE SHEET RECORD											
SHEET NUMBER	REV LTR	ADDED SHEETS				SHEET NUMBER	REV LTR	ADDED SHEETS			
		SHEET NUMBER	REV LTR	SHEET NUMBER	REV LTR			SHEET NUMBER	REV LTR	SHEET NUMBER	REV LTR
VII-89											
VII-90						IX-135					
VII-91						X-136					
VII-92						X-137					
VII-93						X-138					
VII-94						X-139					
VII-95						X-140					
VII-96						X-141					
VII-97						X-142					
VII-98						X-143					
VII-99						X-144					
VII-100						X-145					
VII-101						X-146					
VIII-102						X-147					
VIII-103						A1-1					
VIII-104						A1-2					
VIII-105						A1-3					
VIII-106						A1-4					
VIII-107						A1-5					
VIII-108						A1-6					
VIII-109						A1-7					
VIII-110						A1-8					
VIII-111						A1-9					
VIII-112		VIII-112A				A1-10					
VIII-113						A1-11					
VIII-114						A1-12					
VIII-115						A1-13					
VIII-116						A1-14					
VIII-117						A1-15					
VIII-118						A1-16					
VIII-119						A1-17					
VIII-120						A1-18					
VIII-121						A1-19					
VIII-122						A1-20					
IX-123						A1-21					
IX-124						A1-22					
IX-125						A1-23					
IX-126						A2-1					
IX-127						A2-2					
IX-128						A2-3					
IX-129						A2-4					
IX-130						A2-5					
IX-131						A2-6					
IX-132						A2-7					
IX-133						A2-8					
IX-134						A2-9					
						A2-10					

ACTIVE SHEET RECORD

SHEET NUMBER	REV LTR	ADDED SHEETS				SHEET NUMBER	REV LTR	ADDED SHEETS			
		SHEET NUMBER	REV LTR	SHEET NUMBER	REV LTR			SHEET NUMBER	REV LTR	SHEET NUMBER	REV LTR
A3-1											
A3-2											
A4-1											
A4-2											
A4-3											
A4-4											
A4-5											
A4-6											
A4-7											
A4-8											
A4-9											
A4-10											
A4-11											
A4-12											
A5-1											
A5-2											
A5-3											
A5-4											
A5-5											
A5-6											
A5-5											
A5-6											
A6-1											
A6-2											
A6-3											

REVISIONS

REV SYM	DESCRIPTION	DATE	APPROVAL

F

REV SYM
TD 4572A

BOEING NO. D6-15000
PAGE 1v

6-7000

Table of Contents

	<u>Page</u>
I. Summary	
II. References	
III. List of Illustrations	
IV. List of Symbols	
V. Introduction	
VI. Documentation of Basic Configuration	
A. Airborne Simulation	
B. Ground Based Simulation	
VII. Longitudinal Configuration Characteristics	
A. Airborne Simulation	
B. Ground Based Simulation	
VIII. Lateral Configuration Characteristics	
A. Airborne Simulation	
B. Ground Based Simulation	
IX. Documentation of the 367-80 with Boundary Layer Control	
X. Inflight - Ground-Based Simulator Comparison	

APPENDIX

1. Description of the Ames Large Transport Configurations
 - A. Airborne Simulator
 - B. Ground Based Simulation
2. Basic 367-80 Description
3. Control Force Characteristics

Table of Contents (cont'd)

4. Derivation of Theory
5. Ground Based Analog Simulation Description
6. Description of Documentation Maneuvers

I. SUMMARY

32624

The stability and control characteristics during low speed landing approaches of various Ames large transport configurations were evaluated using the Boeing 367-80 airplane and the Ames moving base analog simulator. This report documents comparisons of the 367-80 and the moving base simulators to the theoretically calculated characteristic responses of the large transport configurations. For all maneuvers performed the simulation accuracy was satisfactory.

AUT NOR

II References

1. D6-19860. 367-80 Airplane Variable Stability Simulation System
(NASA Ames Large Transport Simulation Program). (NASA CR-62037)
2. Etkin, Bernard; Dynamics of Flight. John Wiley & Sons, Inc., 1962.

III. LIST OF ILLUSTRATIONS

Fig. No.	Description	Page
1	367-80 Schematic	V-16
2-10	Documentation of the basic longitudinal inflight configuration	VI-18 to 27
11-22	Documentation of the basic lateral inflight configuration	VI-29 to 41
23-36	Documentation of the typical ground based configurations	VI-43 to 57
37	Summary of normalized pitch rate reversals for inflight configurations	VII-62
38-39	Column steps for inflight configurations	VII-63 to 64
40-55	Wind up turns for inflight configurations	VII-65 to 80
56-63	Speed stability tests for inflight configurations	VII-81 to 88
64	Pitch attitude change for an inflight configuration	VII-89
65-67	Elevator pulses for inflight configurations	VII-90 to 92
68-69	Column steps for ground based configurations	VII-97 to 98
70-72	Elevator pulses for ground based configurations	VII-99 to 101
73	Summary plot of steady roll rates for inflight configurations	VIII-104
74-77	Roll rate reversals for inflight configurations	VIII-106 to 109
78	A 20° heading change for an inflight configuration	VIII-110
79-81	Roll response to wheel steps for varying ground based augmentation systems	VIII-115 to 117

Fig. No.	Description	Page
32	Effect of τ_R on roll response to a wheel step for ground based configurations	VIII-118
33	Effect of τ_R on roll response to an aileron step for ground based configurations	VIII-119
34-36	Wheel step for ground based configurations	VIII-120 to 122
37-96	Documentation of the 367-80 with boundary layer control	IX-124 to 135
97	Wheel step comparing inflight and ground based configurations	X-138
98	Wheel pulse comparing inflight and ground based configurations	X-139
99	Rudder pulse comparing inflight and ground based configurations	X-140
100	Elevator pulse comparing inflight and ground based configurations	X-141
101	Column step comparing inflight and ground based configurations	X-142
102	Flight Data Comparison for Column Step	X-143
103	Ground Data Comparison for Column Step	X-144
104	Ground-Flight Comparison for Column Step	X-145
105	Ground-Flight Comparison for Column Step	X-146
106	Ground-Flight Comparison for Column Step	X-147
A2-1 to A2-4	Characteristics of 367-80 speed brakes	A2-6
A2-5	Pitching moment characteristics of the 367-80 thrust reversers	to A2-9 A2-10
A3-1	Control system force characteristics for the airborne and ground based simulators	A3-2

Table No.	Description	Page
1	Airborne simulation longitudinal run log	VII-59
2	Phugoid characteristics for inflight configurations	VII-61
3	Ground based simulation longitudinal run log	VII-94 to 96
4	Airborne simulation lateral run log	VIII-103
5	Wheel step results for inflight configurations	VIII-105
6	Ground based simulation lateral run log	VIII-112 to 114
Al-1	Aerodynamic characteristics for the basic inflight configurations	Al-2 to 5
Al-2	Variations of aerodynamic characteristics for simulated configurations	Al-6
Al-3	367-80 BLC aerodynamic characteristics	Al-8 to 12
Al-4	Ground based configuration description	Al-4
Al-5	Ground based simulation longitudinal run log	Al-15 to 17

Table No.	Description	Page
A1-6	Ground based simulation lateral run log	A1-18 to 21
A1-7	Lateral directional stability augmentation system	A1-22
A1-8	Equivalent lateral-directional aerodynamic coefficients	A1-23
A2-1	367-80 longitudinal characteristics (unaugmented)	A2-2 to 5
A5-1	Ground based simulation equations of motion	A5-2 to 4
A5-2	Ground based simulation system capabilities	A5-6

12

IV. SYMBOLS

Coefficients and Derivatives

C_D	Drag Coefficient, Drag/ qS_w
C_L	Lift Coefficient, Lift/ qS_w
C_l	Rolling Moment Coefficient, Rolling Moment/ $qS_w b$
C_m	Pitching Moment Coefficient, Pitching Moment/ $qS_w \bar{c}$
C_n	Yawing Moment Coefficient, Yawing Moment/ $qS_w b$
C_y	Side Force Coefficient, Side Force/ qS_w
$C_{D\alpha=0}$	Drag Coefficient at $\alpha = 0$
$C_{D\alpha}$	Drag-Curve Slope, $\partial C_D / \partial \alpha$
$C_{L\alpha=0}$	Lift Coefficient at $\alpha = 0$
$C_{L\alpha}$	Lift-Curve Slope, $\partial C_L / \partial \alpha$
$C_{L\dot{\alpha}}$	Lift Coefficient Due to Angle-of-Attack Rate $\partial C_L / \partial \dot{\alpha}$
$C_{L\delta}$	Lift Coefficient Due to Surface Deflection $\partial C_L / \partial \delta$
$C_{L i_H}$	Lift Coefficient Due to Horizontal Stabilizer Incidence $\partial C_L / \partial i_H$
$C_{L q}, C_{L \dot{\theta}}$	Lift Coefficient Due to Pitch Rate, $\partial C_L / \partial q$
$C_{l\beta}$	Effective Dihedral Derivative, $\partial C_l / \partial \beta$
$C_{l\delta}$	Roll Control Derivative, $\partial C_l / \partial \delta$
$C_{l p}, C_{l \dot{\phi}}$	Rolling Moment Due to Roll Rate, $\partial C_l / \partial p$
$C_{l r}, C_{l \dot{\psi}}$	Rolling Moment Due to Yaw Rate, $\partial C_l / \partial r$
$C_{m\alpha=0}$	Pitching moment Coefficient at $\alpha = 0$
$C_{m\alpha}$	Static Longitudinal Stability Derivative, $\partial C_m / \partial \alpha$
$C_{m\dot{\alpha}}$	Pitching Moment Coefficient Due to Angle-of-Attack Rate, $\partial C_m / \partial \dot{\alpha}$

$C_{m\delta}$	Pitch Control Power Derivative, $\partial C_m / \partial \delta$
$C_{m\dot{1}_H}$	Pitching Moment Due to Horizontal Stabilizer Incidence, $\partial C_m / \partial \dot{1}_H$
$C_{mq}, C_{m\dot{\theta}}$	Pitching Moment Coefficient Due to Pitch Rate, $\partial C_m / \partial q$
$C_{n\beta}$	Static Directional Stability Derivative, $\partial C_n / \partial \beta$
$C_{n\delta}$	Yawing Moment Coefficient Due to Surface Deflection, $\partial C_n / \partial \delta$
$C_{np}, C_{n\dot{\phi}}$	Yawing Moment Coefficient Due to Roll Rate, $\partial C_n / \partial p$
$C_{nr}, C_{n\dot{\psi}}$	Yawing Moment Coefficient Due to Yaw Rate, $\partial C_n / \partial r$
$C_{Y\beta}$	Side-Force Derivative, $\partial C_Y / \partial \beta$
$C_{Y\delta}$	Side-Force Coefficient Due to Surface Deflection, $\partial C_Y / \partial \delta$
$C_{Yp}, C_{Y\dot{\phi}}$	Side-Force Coefficient Due to Roll Rate, $\partial C_Y / \partial p$
$C_{Yr}, C_{Y\dot{\psi}}$	Side-Force Coefficient Due to Yaw Rate, $\partial C_Y / \partial r$
C_A	BLC Blowing Coefficient
$(\dot{\quad})$	Time derivative $d(\quad) / dt$
General	
a.c.	Aerodynamic Center
a_y	Side Acceleration Normal to the Flight Path
a_z	Vertical Acceleration Normal to the Flight Path (positive downward)
b	Wing Span
c	Chord
\bar{c}	Mean Aerodynamic Chord

F	Control Force
g	Gravitational Constant, 32.2 feet/second ²
GW	Gross Weight
h	Altitude
I	Moment of Inertia Slug-feet ²
IRIG	Clock Time
i _H	Horizontal Stabilizer Incidence Relative to the Wing Chord Plane
L	$\left\{ \begin{array}{l} \text{Rolling Acceleration, } C_{l_s} \delta \text{ MAX } qSb/I_{xx} \\ \text{Lift Acceleration, } a_z/V, \frac{C_{L\alpha} \alpha qS}{mv}, \frac{C_{L_s} \delta qS}{mv} \end{array} \right.$
m	Mass
M	$\text{Pitching acceleration } \frac{C_{m_s} \delta \text{ max } qS\bar{c}}{I_{yy}}$
MAC or m.a.c.	Mean Aerodynamic Chord
M _{CG}	Pitching Moment about CG
n, n _z	Load Factor, g's (body axis)
P	Damped Period
p	Rolling Velocity
q	Dynamic Pressure, Pitching Velocity
r	Yawing Velocity
S	Area
T, TH	Thrust
T _{1/2} , t _{1/2}	Time to Half Amplitude
t _{sa max}	Time to maximum aileron
U	Change in Velocity
V _e	Equivalent Airspeed
V _i	Indicated air speed

V_S	Velocity at Stall
V_T	True Airspeed
W	Weight
α	Angle of Attack of Horizontal Reference Line
α_w	Angle of Attack of the wing mean chord
β	Sideslip Angle
β_{NB}	Sideslip Angle measured at nose boom
δ	Surface Deflection
γ	Flight Path Angle
ζ	Damping Ratio
θ	Angle between the Horizontal Reference Line and the Horizon
τ	Time Constant
ϕ	Roll Angle
ψ	Yaw Angle
$ \phi/\beta $	Roll Angle to Sideslip Ratio
ω_d	Dutch Roll Undamped Natural Frequency
ω_n	Undamped Natural Frequency
ω_D	Damped Natural Frequency

Subscripts

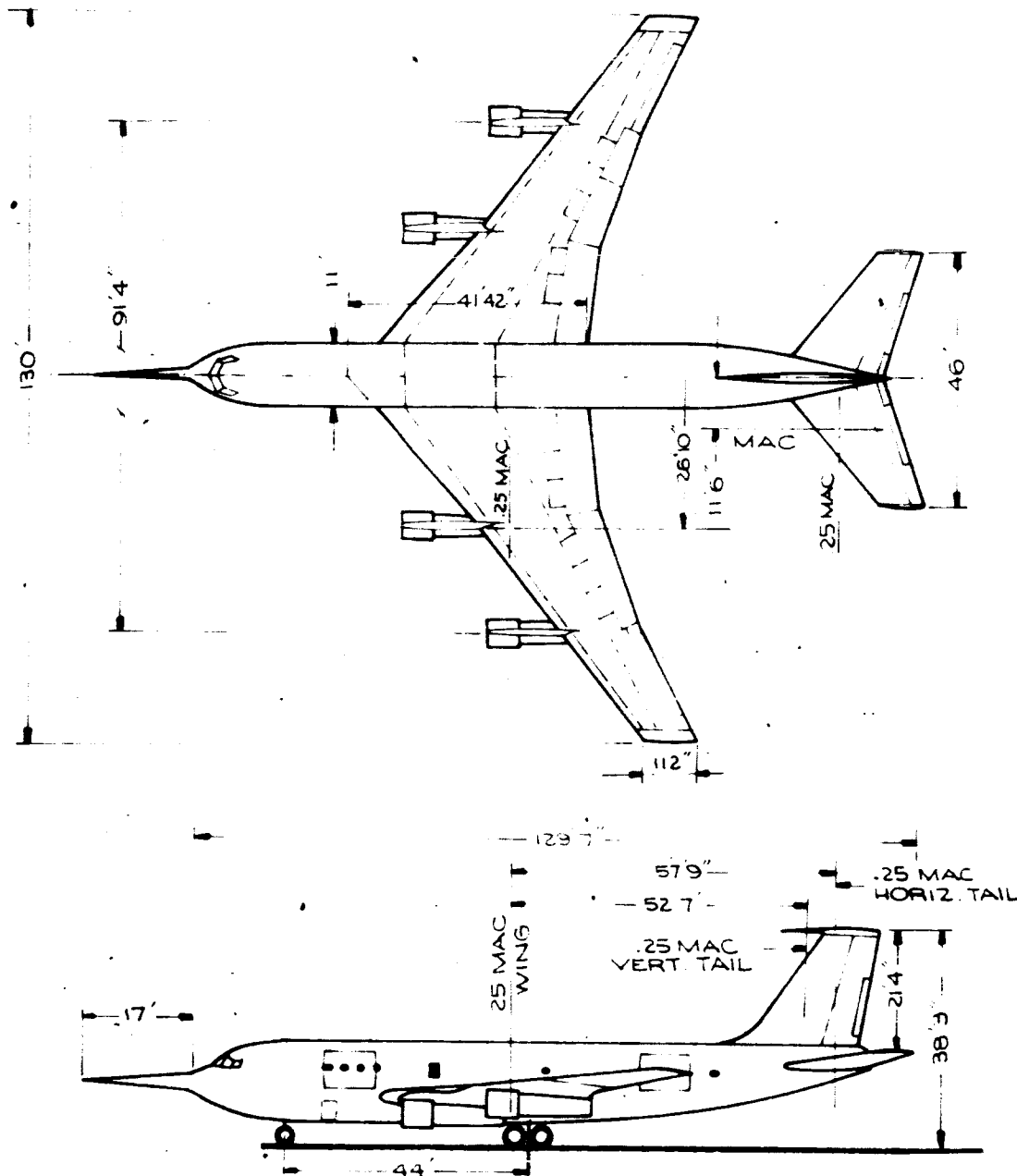
a, A	Aileron
a.c.	Aerodynamic Center
C	Thrust modulator clamshell door
CG	Center of Gravity
Col	Column
d	Dutch Roll
e, E	Elevator
H	Horizontal Stabilizer
MAX	Maximum
N	Net
O	Reference, Free Stream
P	Pedal
r, R	Rudder, Roll mode
s	Spoiler
SB	Speed Brake
S.P.	Short Period
ss	Steady State
trim	Trim Condition
W, WH	Wheel
XX,)	Moment of Inertia Designation
YY,)	
ZZ,)	
XZ,)	

BOEING**V. INTRODUCTION**

Large transport airplanes of the type capable of making shortfield landings at 500,000 lb gross weight were evaluated using the Boeing 367-80 in-flight dynamic simulator in conjunction with the Ames Moving Base Transport Simulator, during late 1965 (7 September to 14 December). Stability and control characteristics in the landing approach were evaluated by NASA/Ames pilots. The ground based simulation was used to investigate a large number of configurations while the in-flight simulation was used to substantiate the results.

The purpose of this report is to describe and document the configurations evaluated on the 367-80 and the ground-based simulators. The accuracy and validity of the simulations are shown in Section VI where response characteristics are presented in detail for basic or typical configurations. Response characteristics of other important configurations are shown in Sections VII, VIII and IX along with a tabulation of dynamic characteristics for all of the configurations evaluated. Section IX presents the response characteristics of the Boeing 367-80 with boundary layer control, one of the configurations evaluated. Section X compares the inflight and ground based simulations of several configurations. The documentation maneuvers performed to measure these characteristics are described in Appendix 6.

The Boeing 367-80 airplane (707 prototype) is shown in Fig. 1. Its description as a five-degree-of-freedom variable stability airplane for in-flight dynamic simulation of a large transport airplane is detailed in Reference 1. A description of the Ames moving base transport simulation system is given in Appendix 5.



WING :		HORIZONTAL TAIL :		VERTICAL TAIL :	
AREA	2821.36FT ²	AREA	625FT ²	AREA	312 FT ²
ASPECT RATIO	6.0	ASPECT RATIO	3.37	ASPECT RATIO	1.46
SWEEP @ .25c	35.0°	SWEEP @ .25c	35.0°	SWEEP @ .25c	31.0°
INCIDENCE	2.0°	TAPER RATIO	.421	TAPER RATIO	.45
DIHEDRAL	7.0°	DIHEDRAL	7.0°	VV	.0447
MAC	20.05FT.	V _H	.638		

CALC			REVISED	DATE	367-80 CHARACTERISTICS	06-158
CHECK						FIG. 1
APR.						PAGE
APR.						V 16
					THE BOEING COMPANY	
					RENTON, WASHINGTON	

VI. Documentation of the Basic Configuration

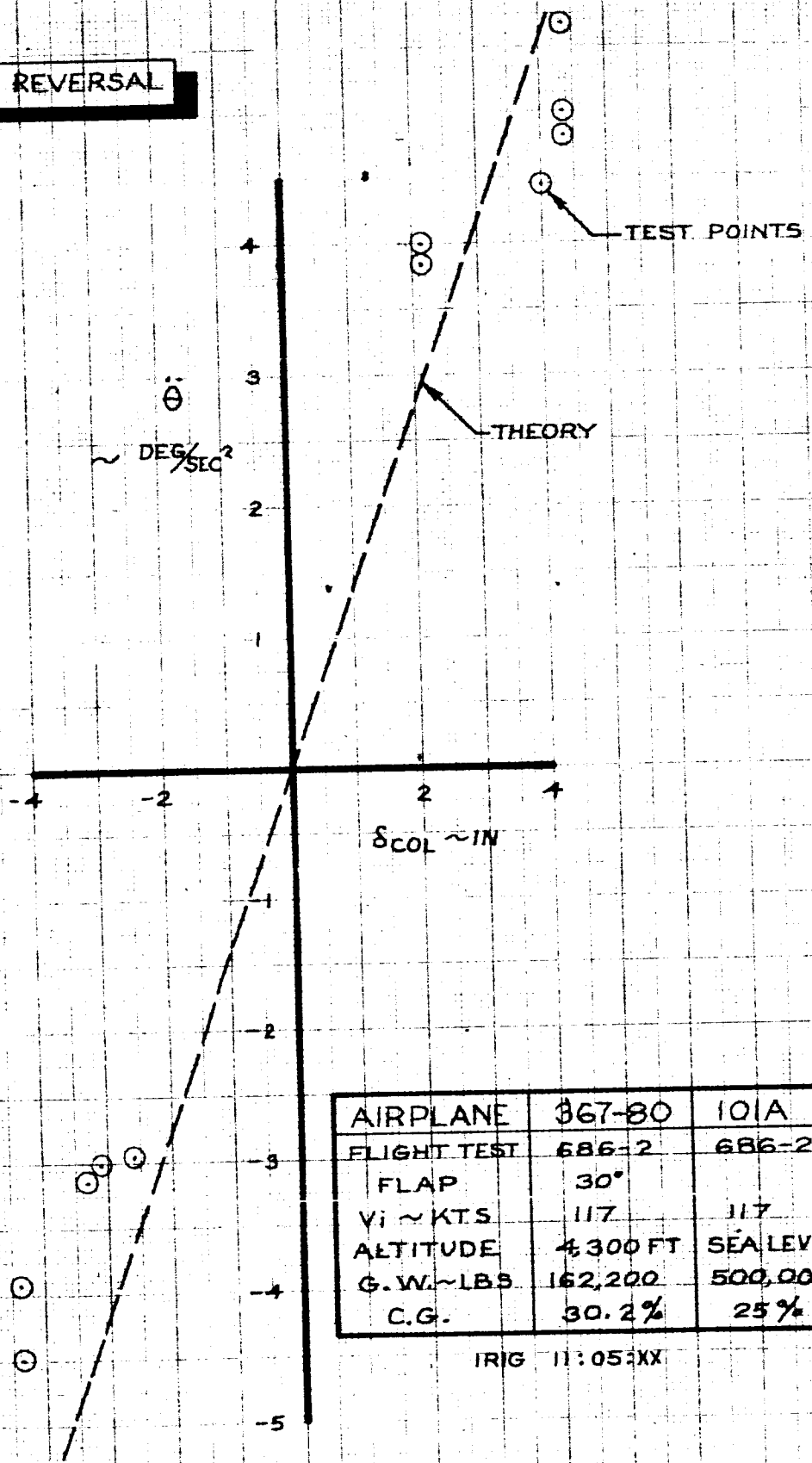
A. Airborne Simulation

The characteristics of the basic longitudinal configuration (designated 101A) and the basic lateral configuration (designated 1209) for a large transport aircraft are presented in Figs. 2 to 21. The maneuvers performed to determine the aerodynamic characteristics are listed below along with brief comments on the agreement between flight test data and theory. The theoretical characteristics shown are derived in Appendix 4.

Longitudinal:

Maneuver	Comments
Pitch Rate Reversal	Fig. 2. The 367-80 accurately simulated the basic 101A configuration for a pitch rate reversal. An example of how the data was obtained is shown in Fig. 3.
Column Step	Fig. 4. A time lag is evident in the flight test time history when compared to a theoretically calculated column step. This is probably caused by aerodynamic and control surface lags which are not included in the theory. The column step was usually reversed prematurely before the peak load factor was reached.
Wind Up Turn	Figs. 5 & 6. The wind up turn flight test data agrees quite well with theory when the data are shifted to allow for mis-trim during the flight test.
Speed Stability	Fig. 7. The flight test data shows a slight mis-trim but otherwise agrees quite well with theory for configuration 101A.

PITCH RATE REVERSAL

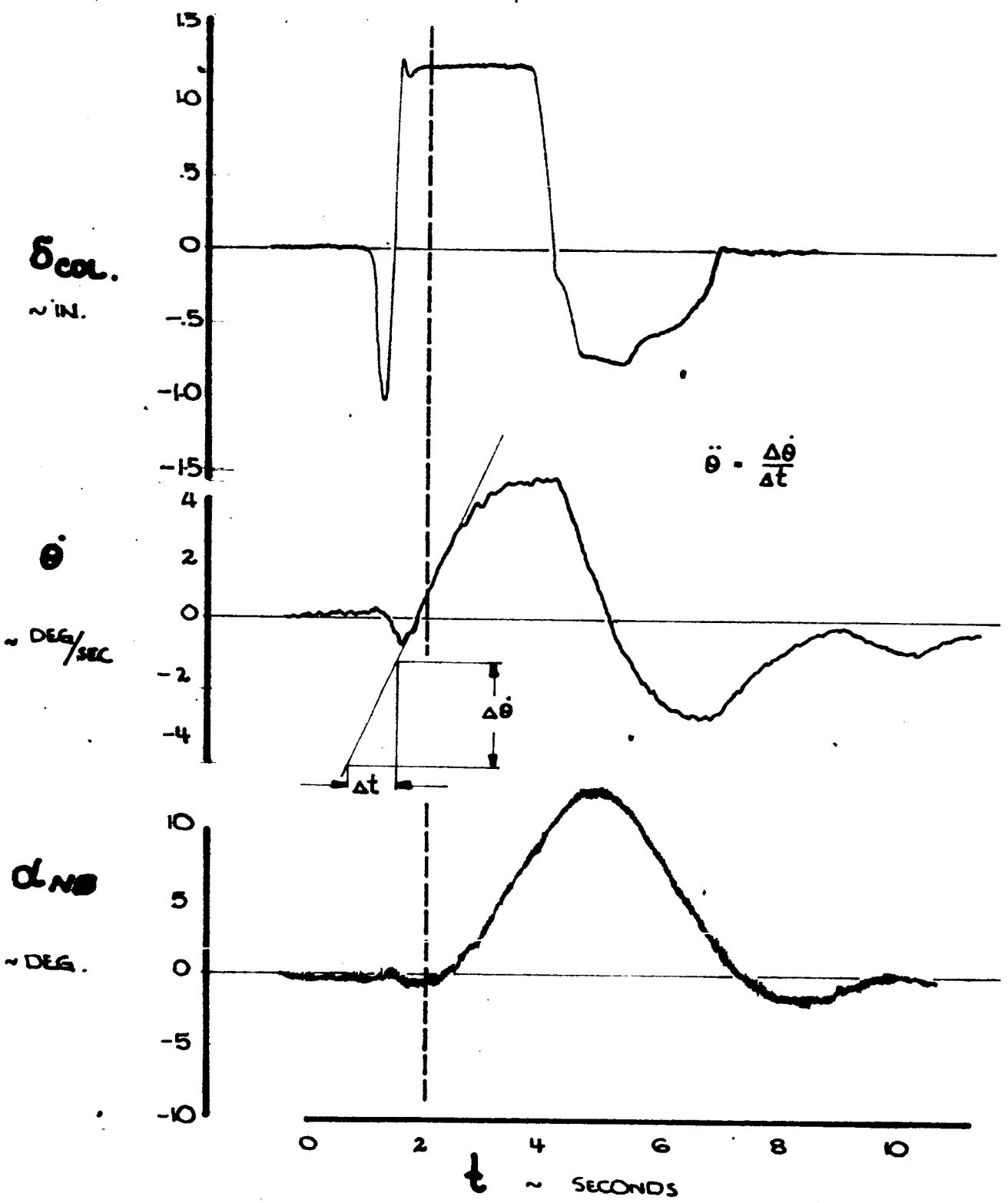


AIRPLANE	367-80	101A
FLIGHT TEST	686-2	686-2
FLAP	30°	
V _i ~ KTS	117	117
ALTITUDE	4,300 FT	SEA LEVEL
G.W. ~ LBS	162,200	500,000
C.G.	30.2%	25%

IRIG 11:05:XX

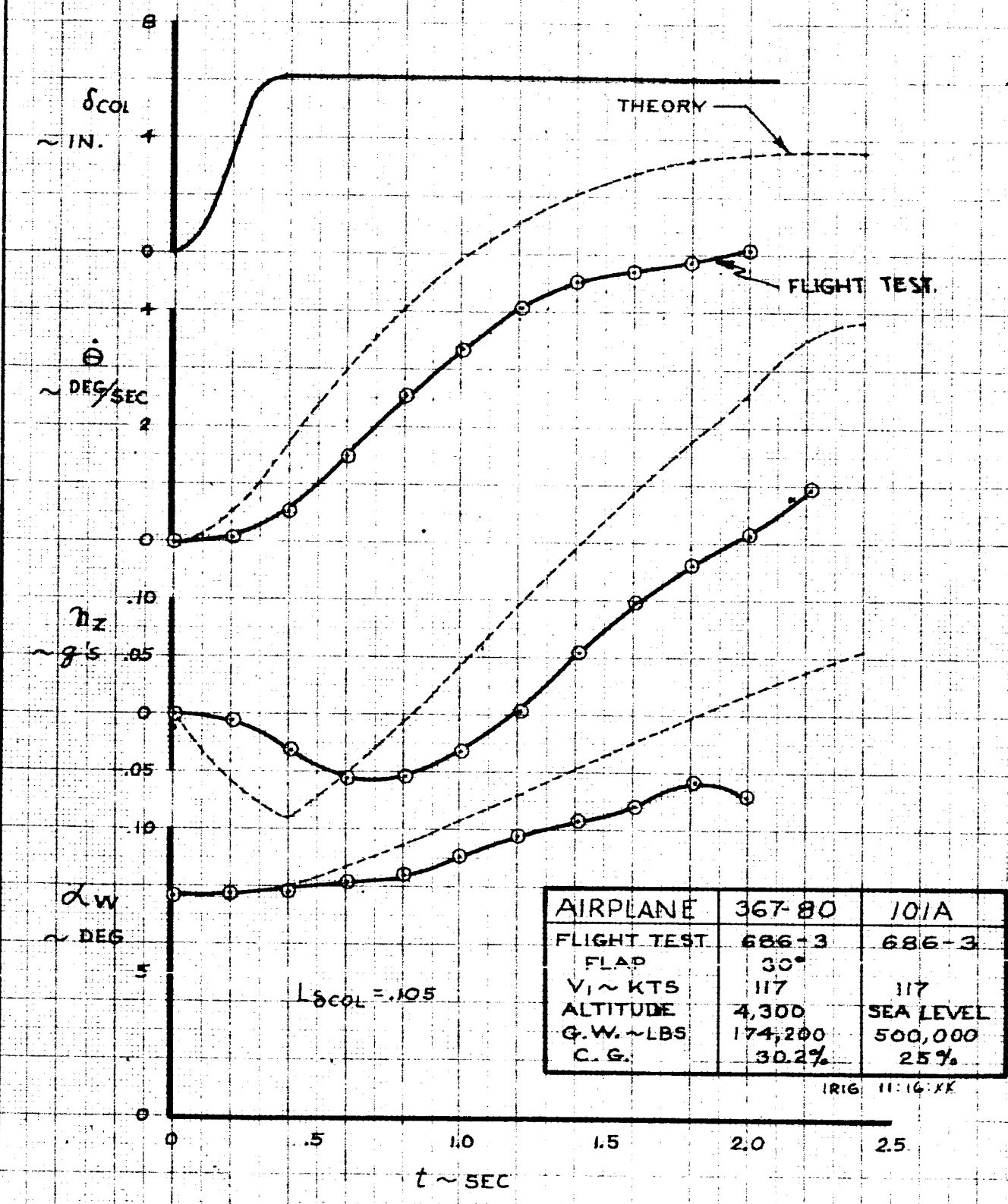
CALC			REVISED	DATE	PITCH RATE REVERSAL FLIGHT TEST 686-2 CONFIGURATION 101A THE BOEING COMPANY	367-80
CHECK						FIG. 2
APR						PAGE
APR						VI-18
						06-15000

PITCH RATE REVERSALS



ENGR.			REVISED	DATE	SAMPLE OF FLIGHT TEST DATA FOR PITCH RATE REVERSALS	D6-15000
CHECK						FIG. 3
APR					THE BOEING COMPANY RENTON, WASHINGTON	VI-19
APR						

**COLUMN STEP
CONFIG. 101A**

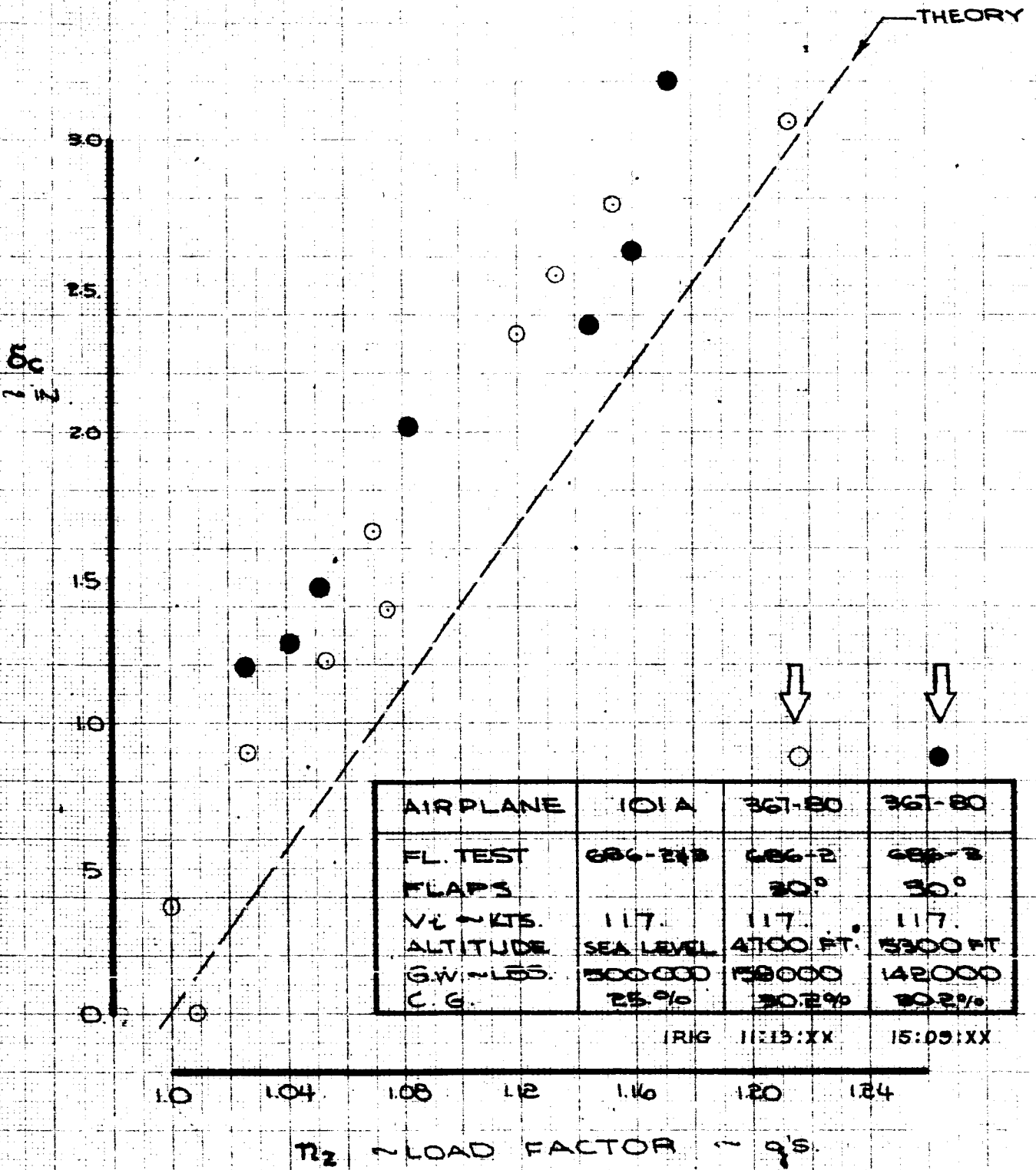


AIRPLANE	367-80	101A
FLIGHT TEST	686-3	686-3
FLAP	30°	
V ₁ ~ KTS	117	117
ALTITUDE	4,300	SEA LEVEL
G.W. ~ LBS	174,200	500,000
C.G.	30.2%	25%

IRIG 11:16:XX

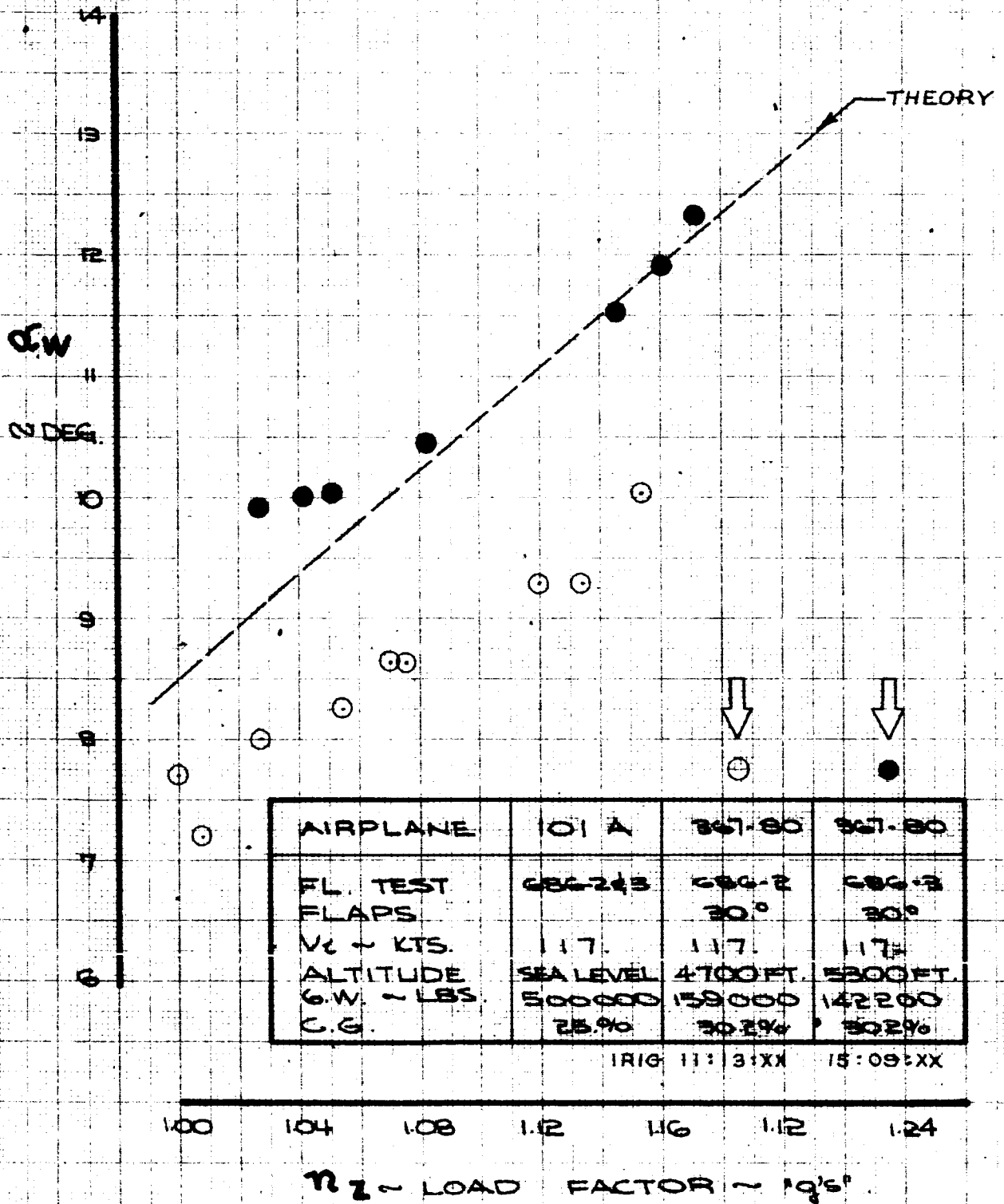
CALC		REVISED	DATE	COLUMN STEP FLIGHT TEST 686-3 CONFIGURATION 101A THE BOEING COMPANY D6-15000	367-80
CHECK					FIG. 4
APR					PAGE
APR					VI-20

WINDUP TURN



CALC			REVISED	DATE	WINDUP TURN FL. TEST: 686-2 & -3 CONFIG.: 101A	367-80	
CHECK						FIG. 5	
APR						THE BOEING COMPANY 06-15000	PAGE VI-21
APR							

WINDUP TURN



AIRPLANE	101 A	367-80	367-80
FL. TEST	686-2 & 3	686-2	686-3
FLAPS		30°	30°
V _c - KTS.	117.	117.	117.
ALTITUDE	SEA LEVEL	4700 FT.	5300 FT.
G.W. - LBS.	500000	159000	142200
C.G.	25%	30.2%	30.2%

IRIG 11:31XX 15:09XX

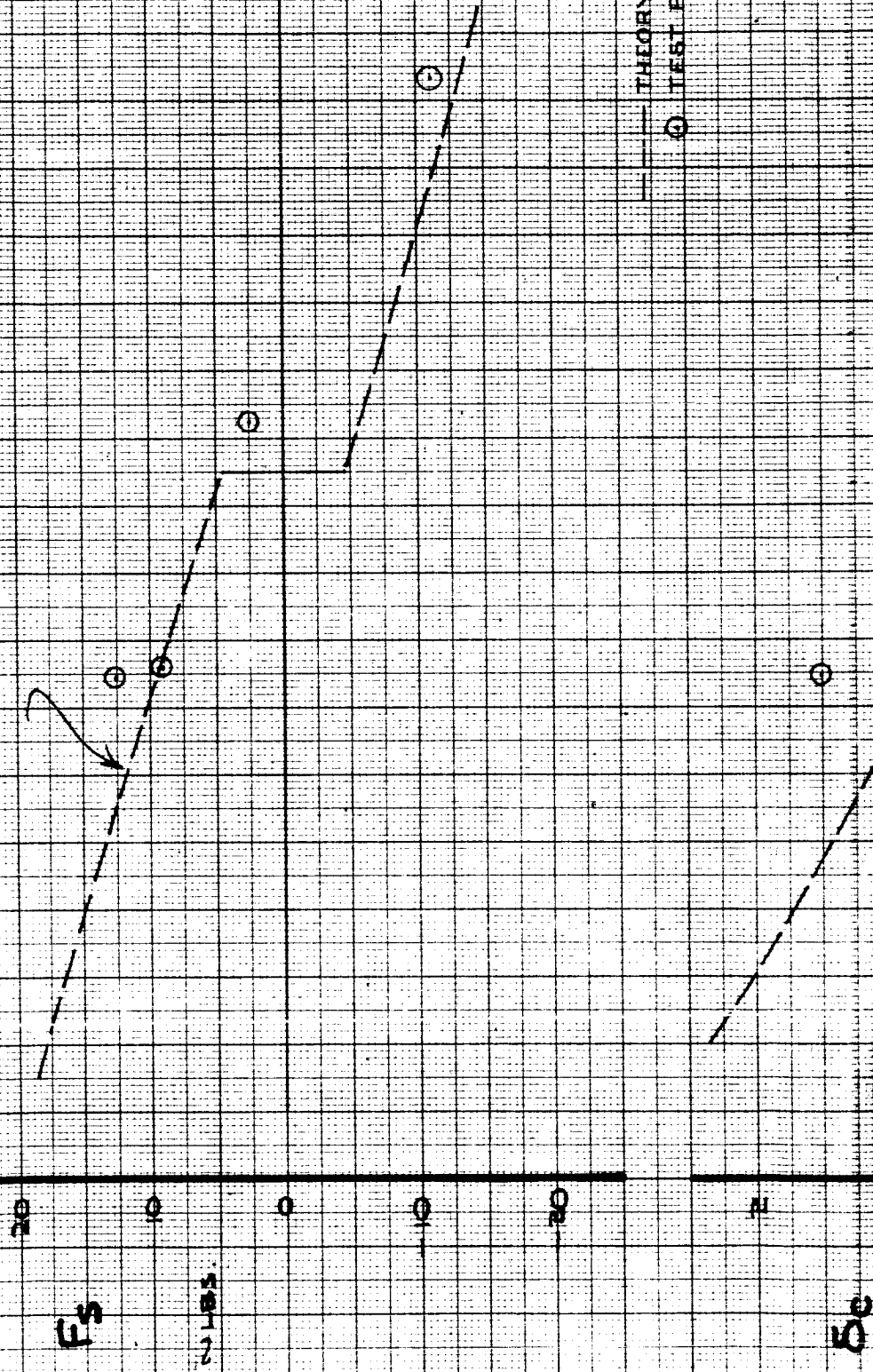
CALC			REVISED	DATE	WINDUP TURN FL. TEST 686-2 & 3 CONFIG. : 101A THE BOEING COMPANY DG-15000	367-80
CHECK						FIG. 6
APR						PAGE
APR						VI-22

SPEED STABILITY

AIRPLANE	367-80	101-A
FL TEST	686-2	686-2
FLAPS	30°	
VE - KTS.	117	117
ALTITUDE	4760 FT.	SEA LEVEL
G.W. - LBS.	159000	100000
C.G.	28.8%	25.0%

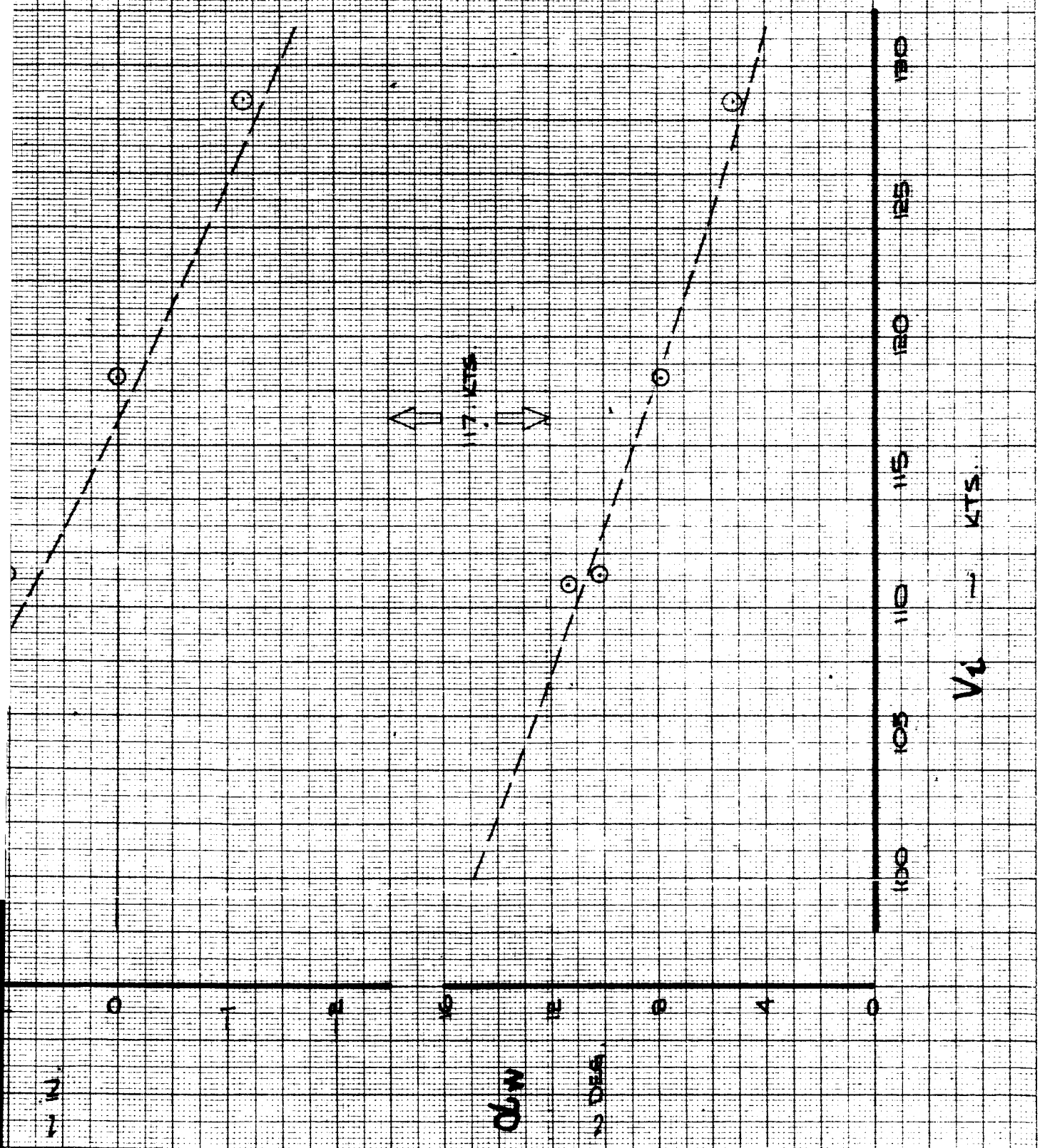
IRIG 11151XX

*Theoretical Force
variation for
Aves large
Transport?*



CALC		REVISED	DATE	SPEED STABILITY FL. TEST: 686-2 CONFIG. 101A THE BOEING COMPANY 06-15000	367-80
CHECK					FIG. 7
APPD.					PAGE VI-23
APPD.					7

VI-23-2



Phugoid

Fig. 8. The measured period of the phugoid agrees very well with the theoretical while the measured damping ratio is approximately 40% of the theoretical value. The damping ratio, however, is very difficult to measure accurately since only one cycle of the phugoid was recorded.

Pitch Attitude

Fig. 9. Approximately 3 seconds are required for a change in pitch attitude of 8 degrees.

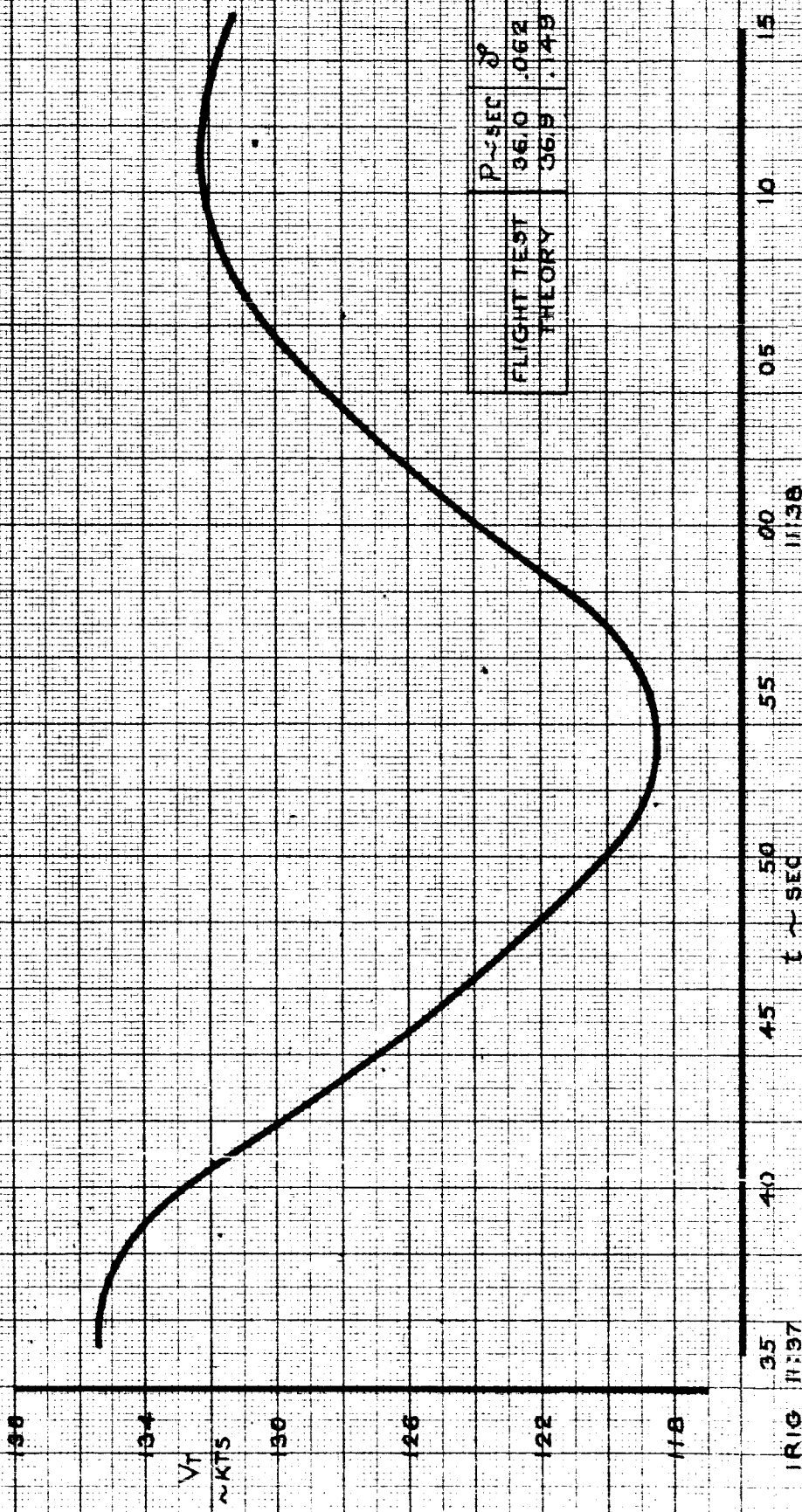
Elevator Pulse

Fig. 10. The 367-80 simulated the elevator pulse of the basic configuration accurately.

PHUGOID CHARACTERISTICS

AIRPLANE	367-80	101A
FLIGHT TEST	686-2	686-2
FLAP	30°	
V _L , KTS	117	117
ALTITUDE	4,900FT	SEA LEVEL
G.W., LBS	151,500	500,000
C.G.	30.2%	25%

IRIG 11:27:XX



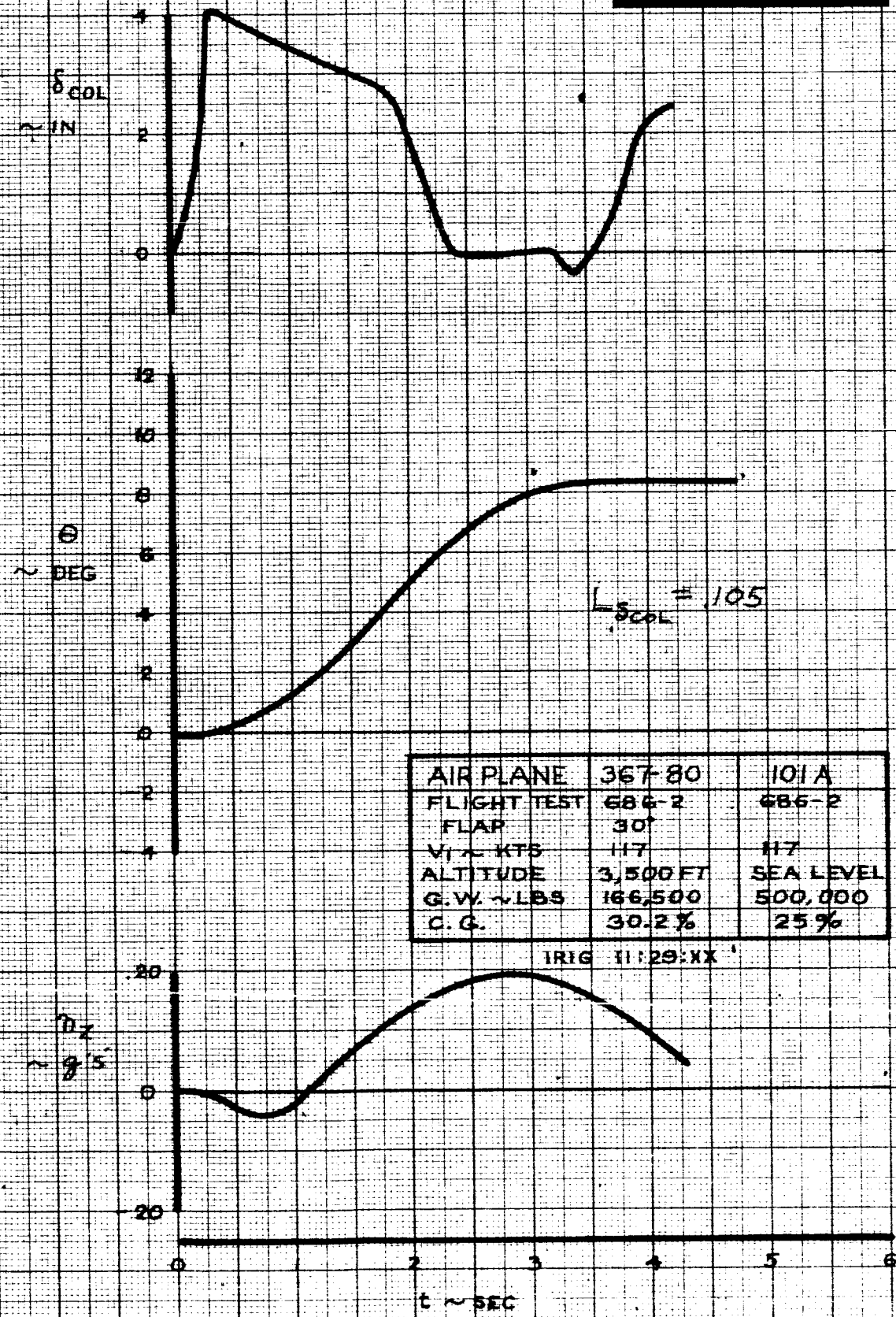
CALC		REVISED	DATE
CHECK			
APR			
APR			

PHUGOID CHARACTERISTICS
 FLIGHT TEST 686-2
 COFIGURATION 101A

367-80
 FIG. 8
 PAGE VI-25

THE BOEING COMPANY
 DC-15000

PITCH ATTITUDE



AIR PLANE	367-80	101A
FLIGHT TEST	686-2	686-2
FLAP	30°	
V _I ~ KTS	117	117
ALTITUDE	3,500 FT	SEA LEVEL
G.W. ~ LBS	166,500	500,000
C.G.	30.2%	25%

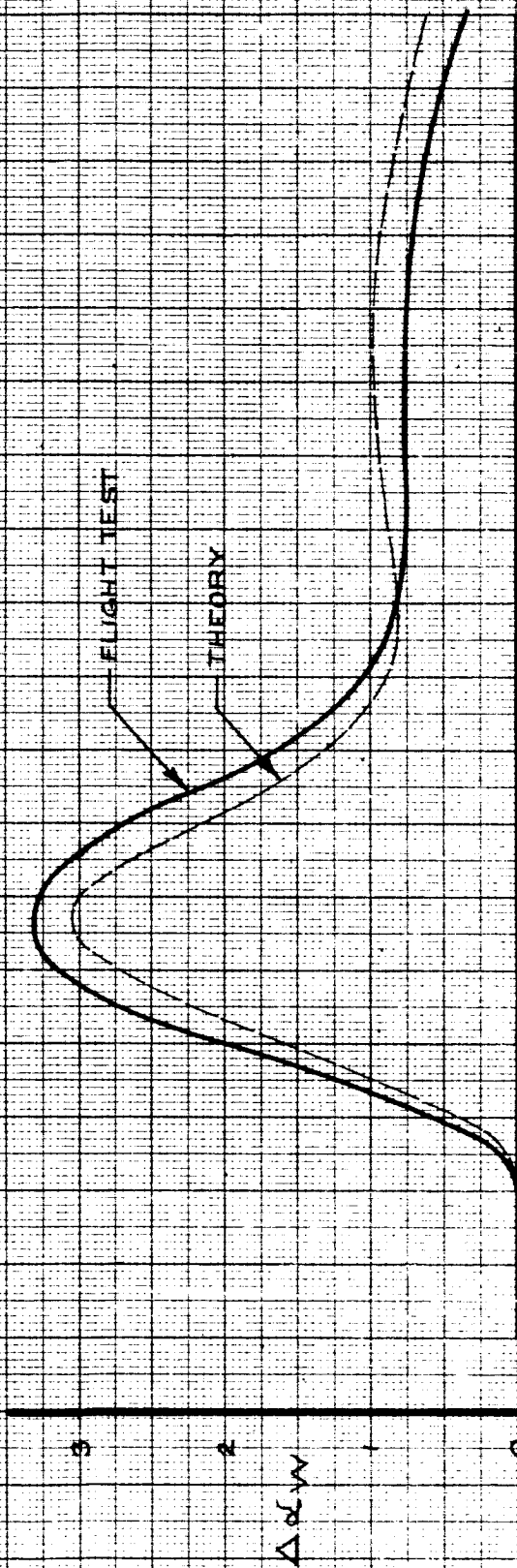
CALC		REVISED	DATE
CHECK			
APR			
APR			

PITCH ATTITUDE
 FLIGHT TEST 686-2
 CONFIGURATION 101A

THE BOEING COMPANY
 D6-15000

367-80
 FIG. 9
 PAGE VI-26

ELEVATOR PULSE

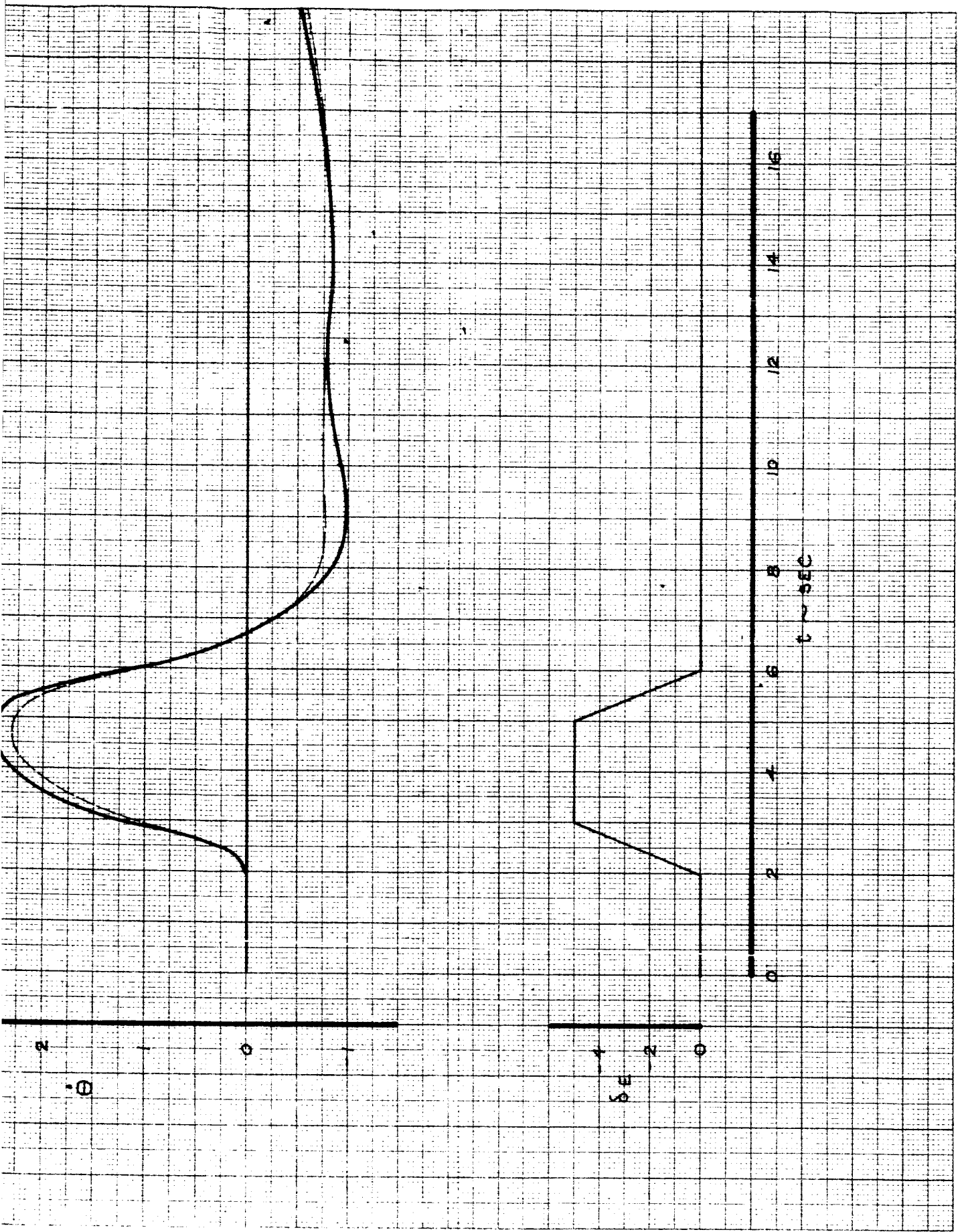


$M_{ref} = .506$

$M_{\delta} = .587$

AIRPLANE	367-80	101A
FLIGHT TEST	686-2	686-2
FLAPS	30°	
V _I ~ KTS	117	117
ALTITUDE	4,500 FT	SEA LEVEL
G.W. ~ LBS	162,600	500,000
C.G.	30.2%	25%

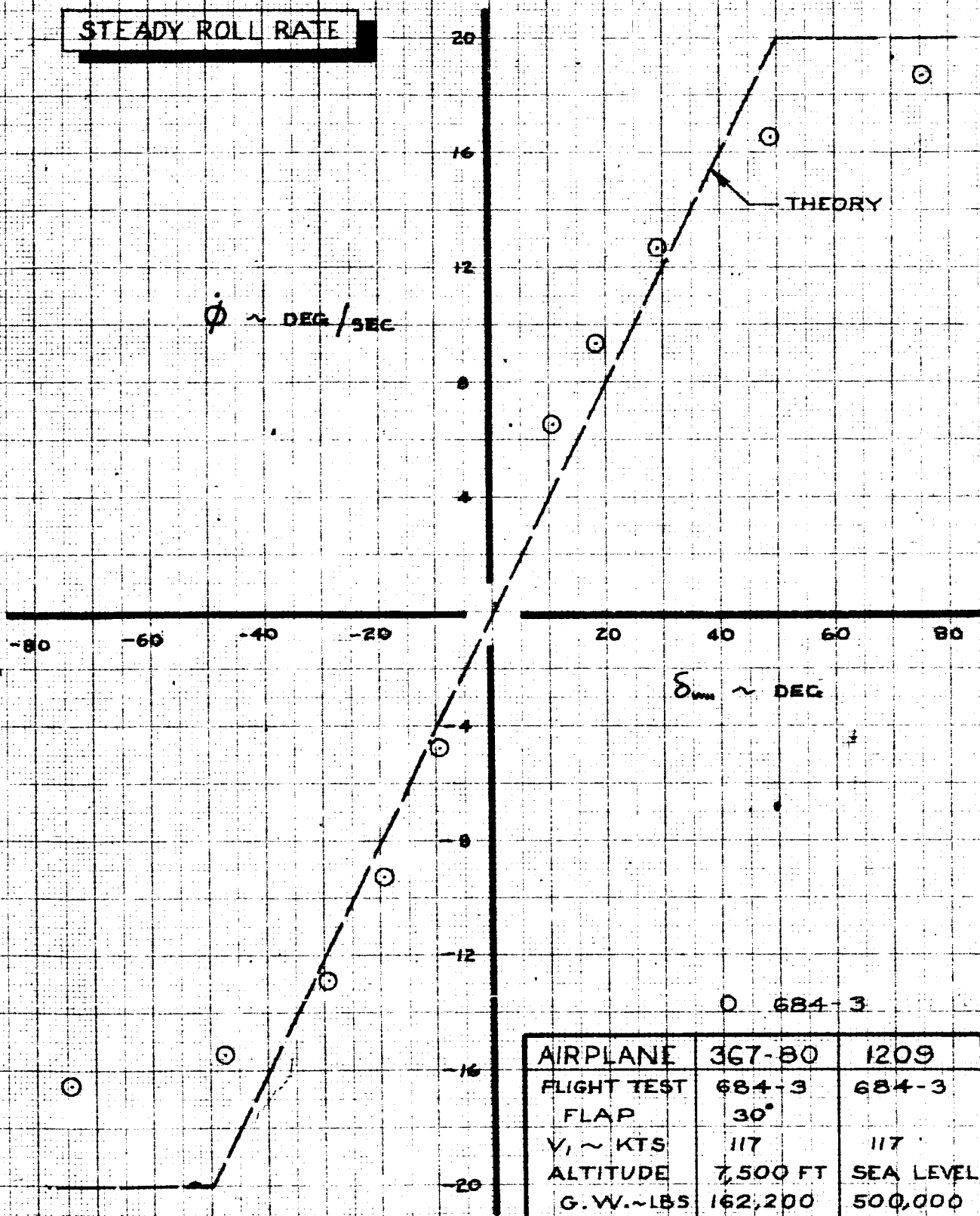
CALC			REVISED	DATE	ELEVATOR PULSE FLIGHT TEST 686-2 CONFIGURATION 101A	367-80
CHECK						FIG. 10
APPD.						THE BOEING COMPANY
APPD.						DG-15000
						PAGE VI-21-1



VI-27.2

Lateral: Maneuver	Comments
Steady Roll Rate	Fig. 11. The Steady State roll rate characteristics of the 367-80 were nonlinear whereas the theory is linear. The maximum roll rate achieved in flight was somewhat less than theory predicts. A sample of how the flight test data was reduced is shown in Fig. 12.
Roll Rate Reversal	Fig. 13. The 367-80 accurately simulated the basic 1209 configuration roll acceleration. Fig. 14 shows how the flight data were reduced.
Yaw Rate Reversal	Fig. 15. The yaw acceleration was slightly larger than predicted by the theory. Fig. 16 shows how flight data were reduced.
Steady Sideslip	Fig. 17. The 367-80 exhibited a low lateral control deflection to balance the sideslip angles generated,
Spiral Stability	Fig. 18. Theory gives the time to half amplitude as 18.3 seconds. Flight Test data indicated a time to half amplitude on the order of 100 seconds.
20° Heading Change	Fig. 19. A 20° heading change was accomplished in approximately 10.5 seconds. Opposite wheel is required to stop the roll at the desired bank angle.

STEADY ROLL RATE

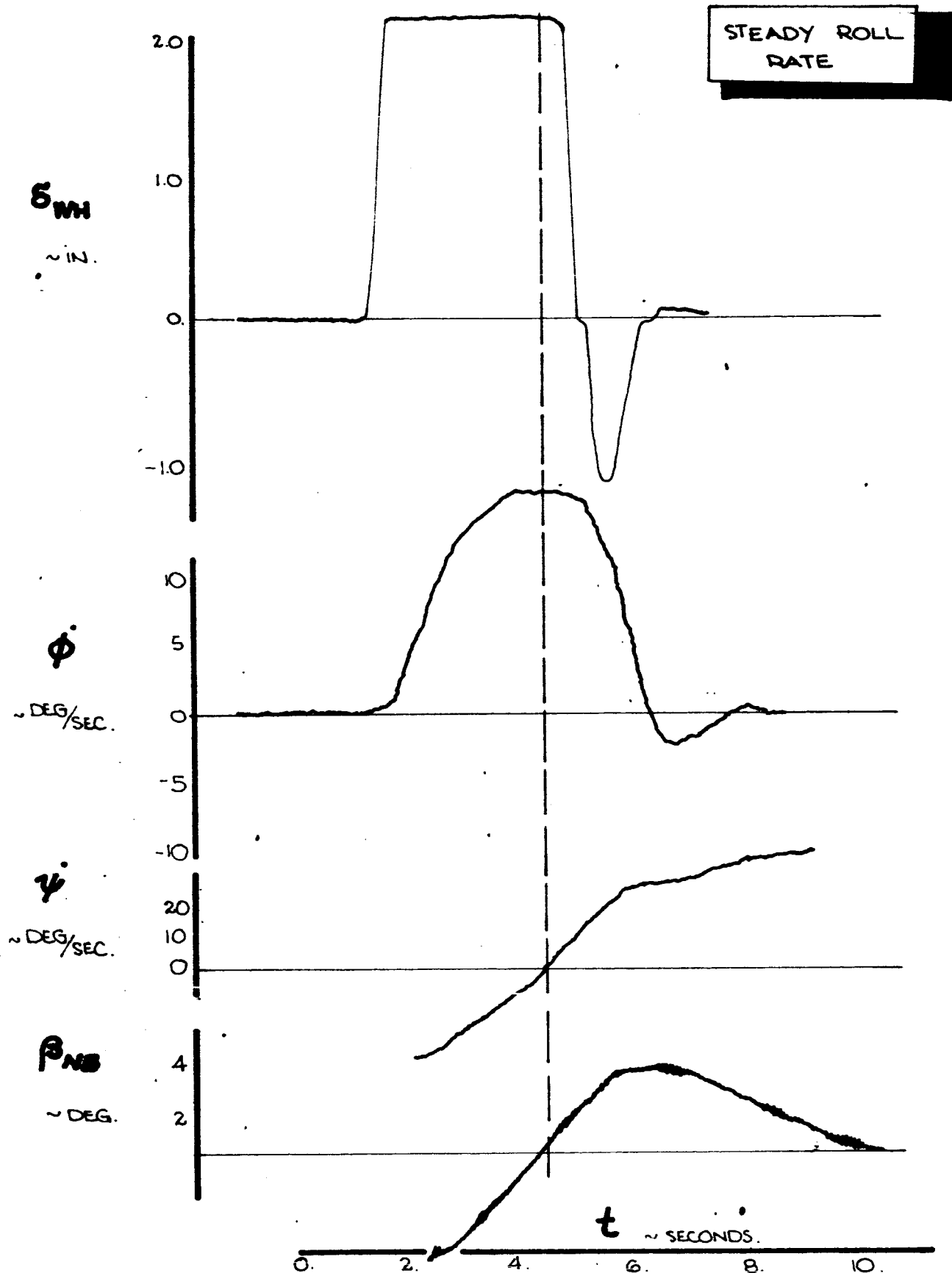


CALC			REVISED	DATE
CHECK				
APR				
APR				

STEADY ROLL RATE
 FLIGHT TEST 684-3
 CONFIGURATION 1209

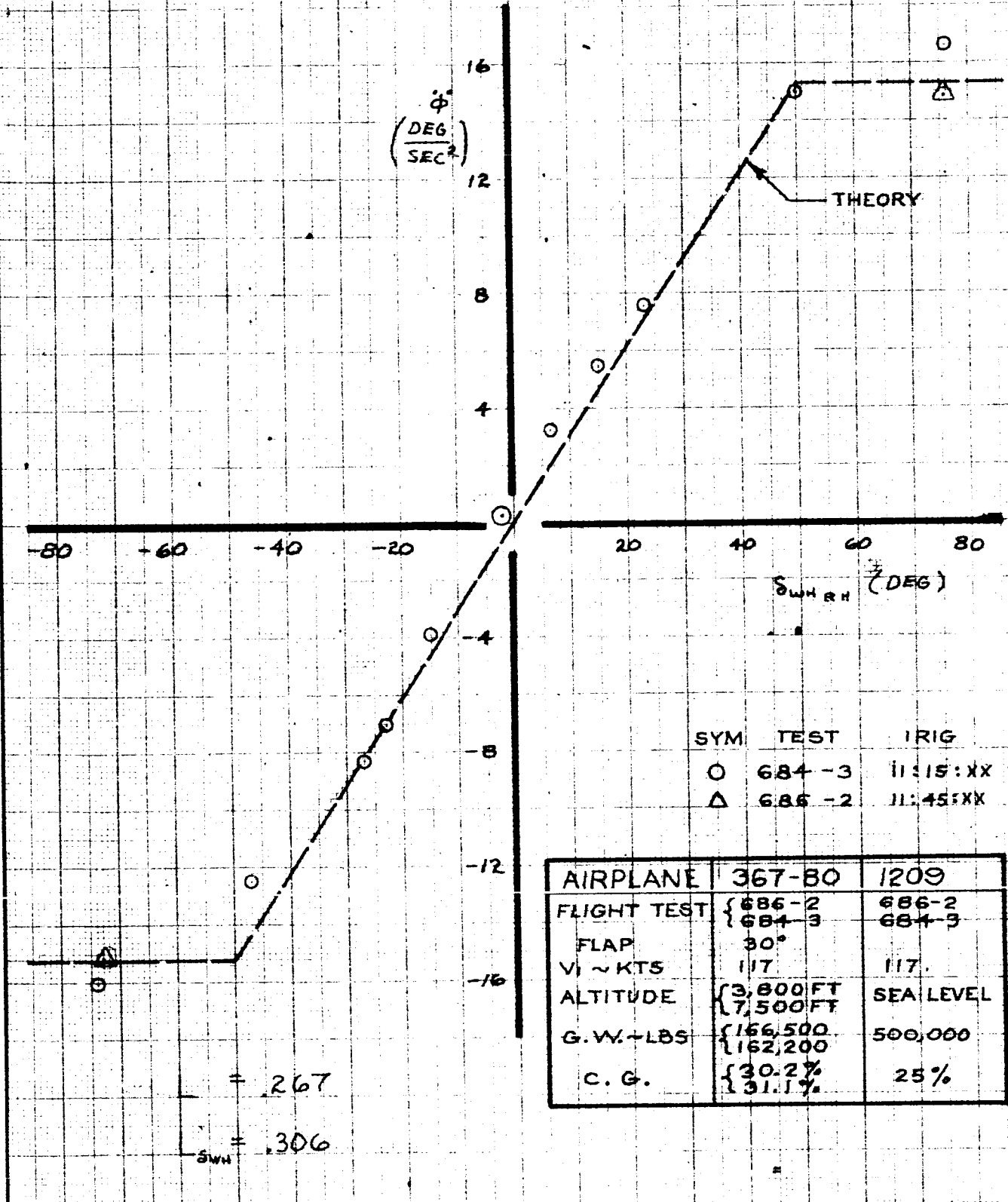
367-80
 FIG. 11
 PAGE VI-29

THE BOEING COMPANY
 DG-15000



ENGR.			REVISED	DATE	SAMPLE OF FLIGHT TEST DATA FOR STEADY ROLL RATE.	D6-15000
CHECK						FIG. 12
APR					THE BOEING COMPANY RENTON, WASHINGTON	VI-30
APR						

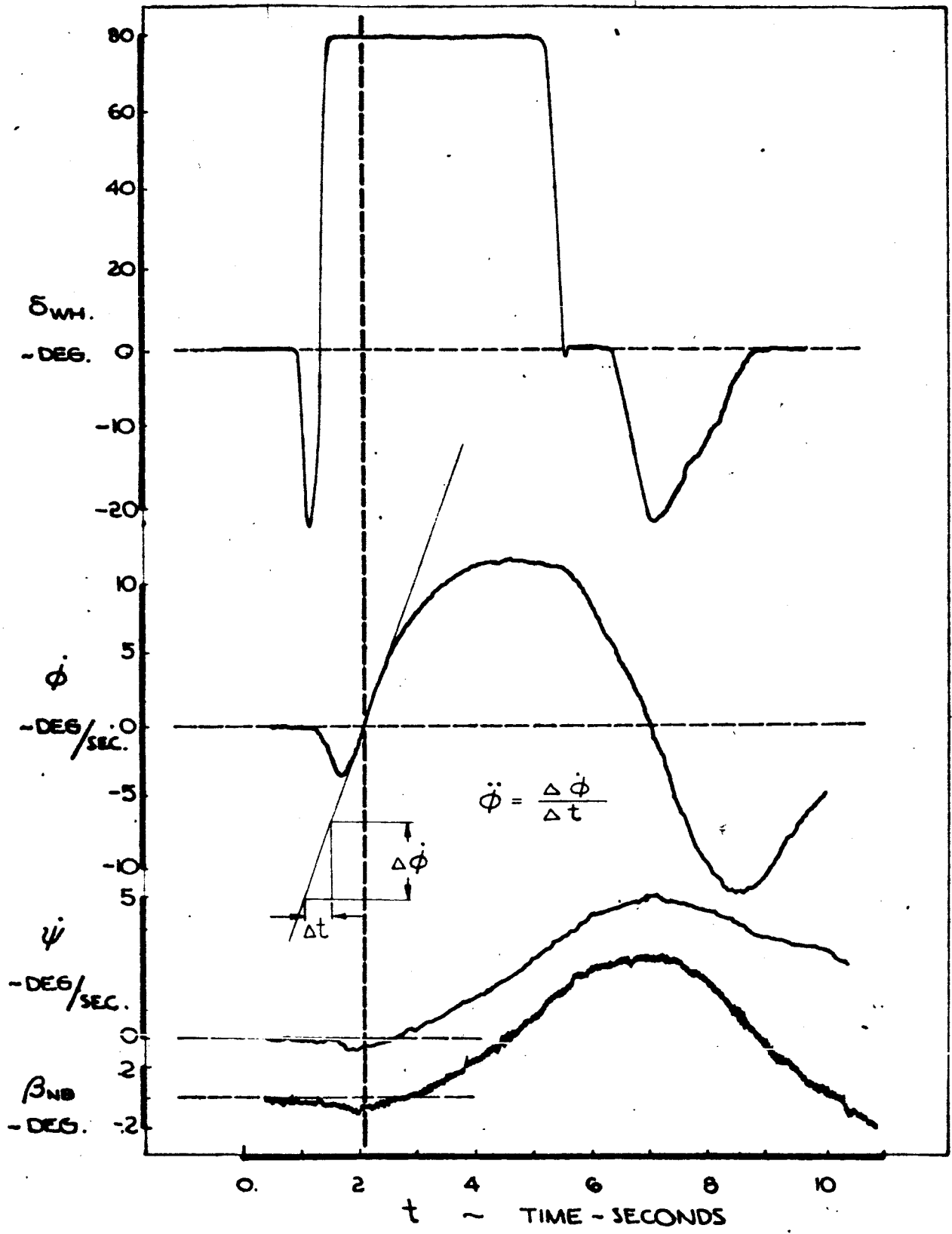
ROLL RATE REVERSAL



SYM TEST TRIG
 O 684-3 11:15:XX
 Δ 686-2 11:45:XX

AIRPLANE	367-80	1209
FLIGHT TEST	{ 686-2 684-3	686-2 684-3
FLAP	30°	
V ₁ ~ KTS	117	117
ALTITUDE	{ 3,800 FT 7,500 FT	SEA LEVEL
G. W. + LBS	{ 166,500 162,200	500,000
C. G.	{ 30.2% 31.1%	25%

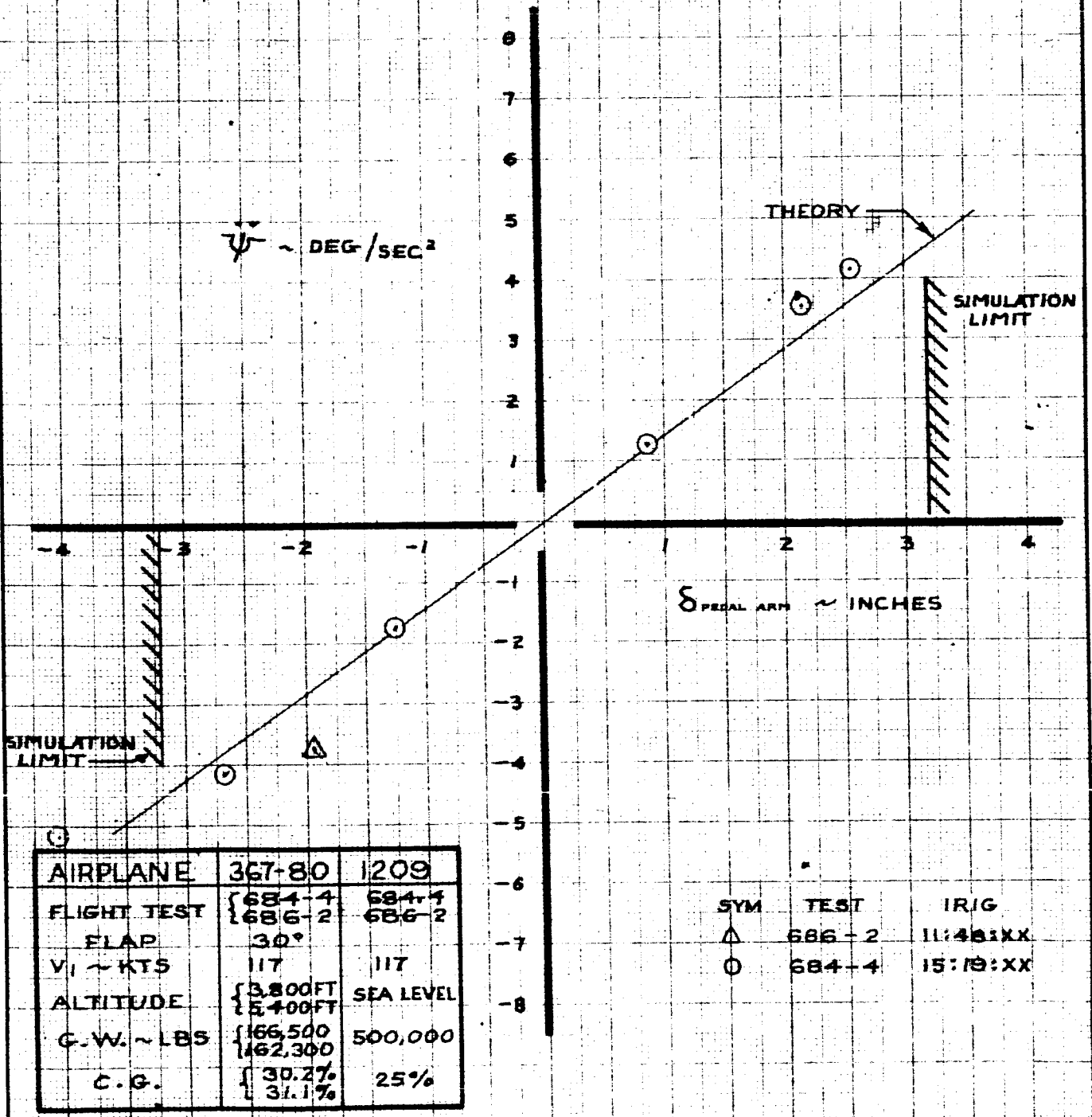
CALC	REVIS	REVISED	DATE	ROLL RATE REVERSAL FLIGHT TEST 686-2 & 684-3 CONFIGURATION 1209 THE BOEING COMPANY D6-15000	367-80
CHECK					FIG. 13
APR					PAGE
APR					VI-31



ENGR.			REVISED	DATE	SAMPLE OF FLIGHT TEST DATA FOR ROLL RATE REVERSAL.	367-80
CHECK						FIG. 14
APR						VI-32
APR						THE BOEING COMPANY RENTON, WASHINGTON DG-15000

25

YAW RATE REVERSAL



AIRPLANE	367-80	1209	
FLIGHT TEST	{ 684-4	{ 684-4	
FLAP	{ 686-2	{ 686-2	
VI ~ KTS	117	117	
ALTITUDE	{ 3,800FT	SEA LEVEL	
	{ 5,400FT		
G.W. ~ LBS	{ 166,500	500,000	
	{ 162,300		
C.G.	{ 30.2%	25%	
	{ 31.1%		

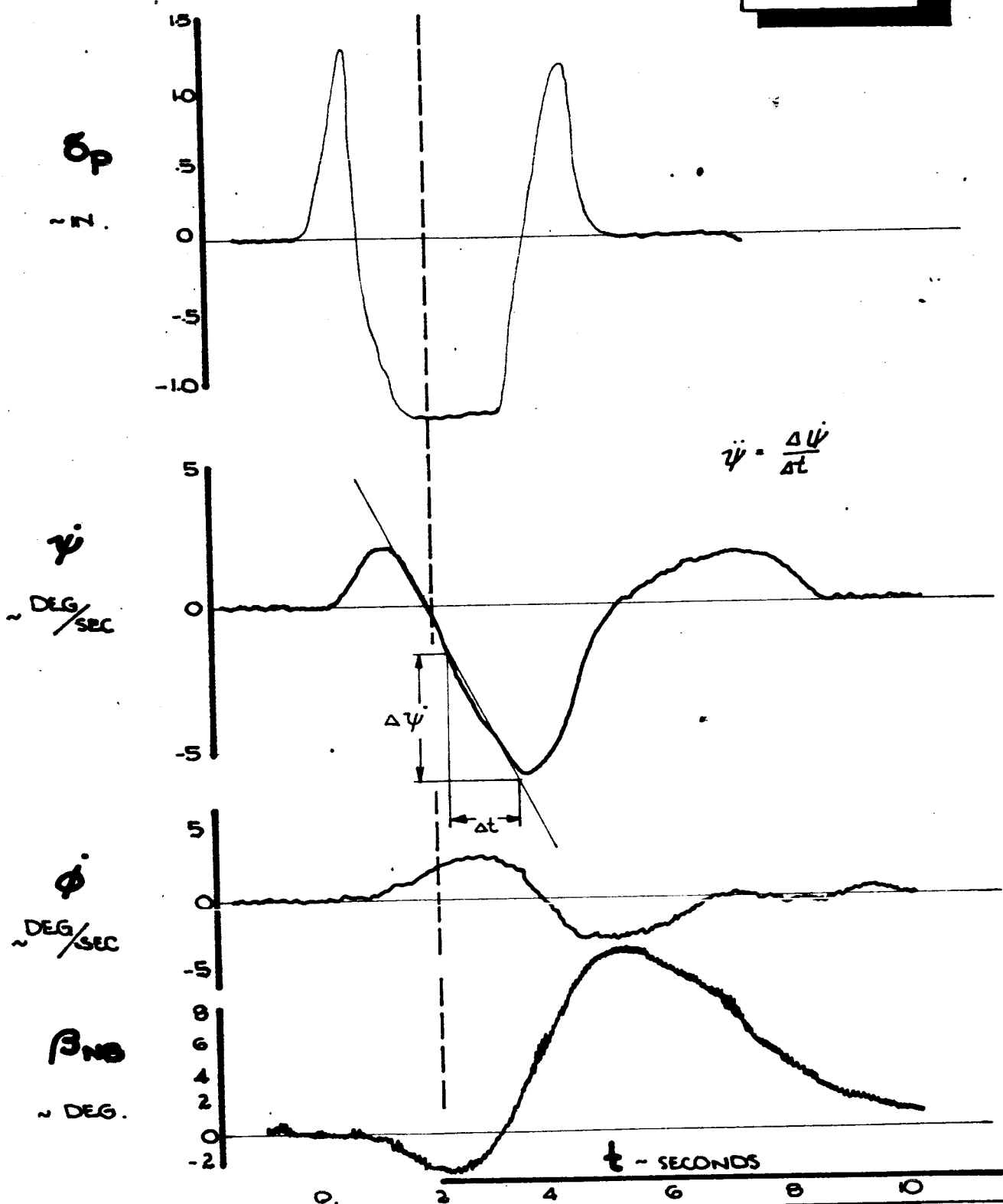
CALC		REVISED	DATE
CHECK			
APR			
APR			

YAW RATE REVERSAL
FLIGHT TEST 684-4 & 686-2
CONFIGURATION 1209

THE BOEING COMPANY
D6-15000

367-80
FIG.15
PAGE
VI-33

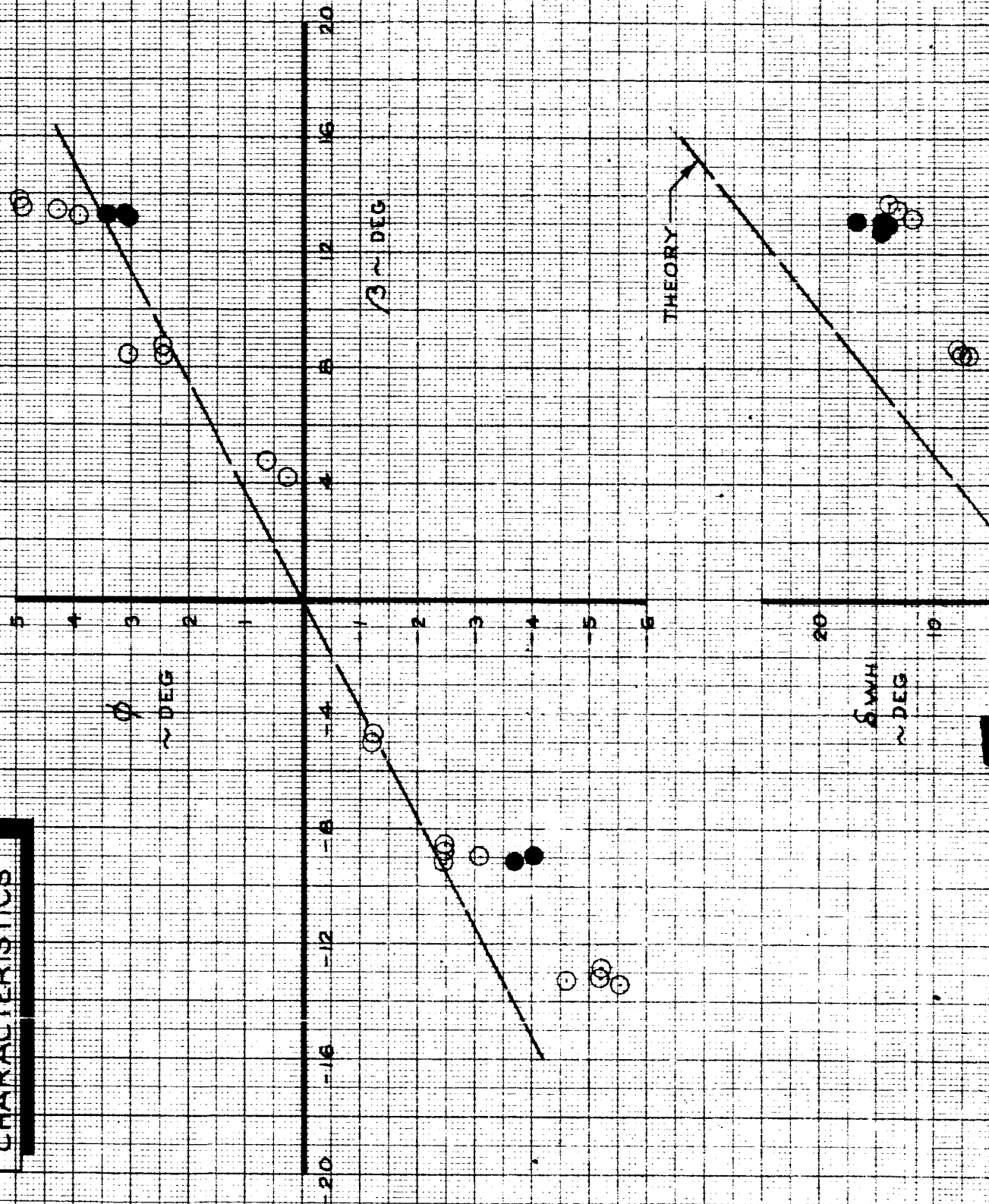
YAW RATE REVERSAL



ENGR.			REVISED	DATE	SAMPLE OF FLIGHT TEST DATA FOR YAW RATE REVERSALS.	D6-15000
CHECK						FIG. 16
APR						
APR						
					THE BOEING COMPANY RENTON, WASHINGTON	VI-34

57

STEADY SIDESLIP CHARACTERISTICS

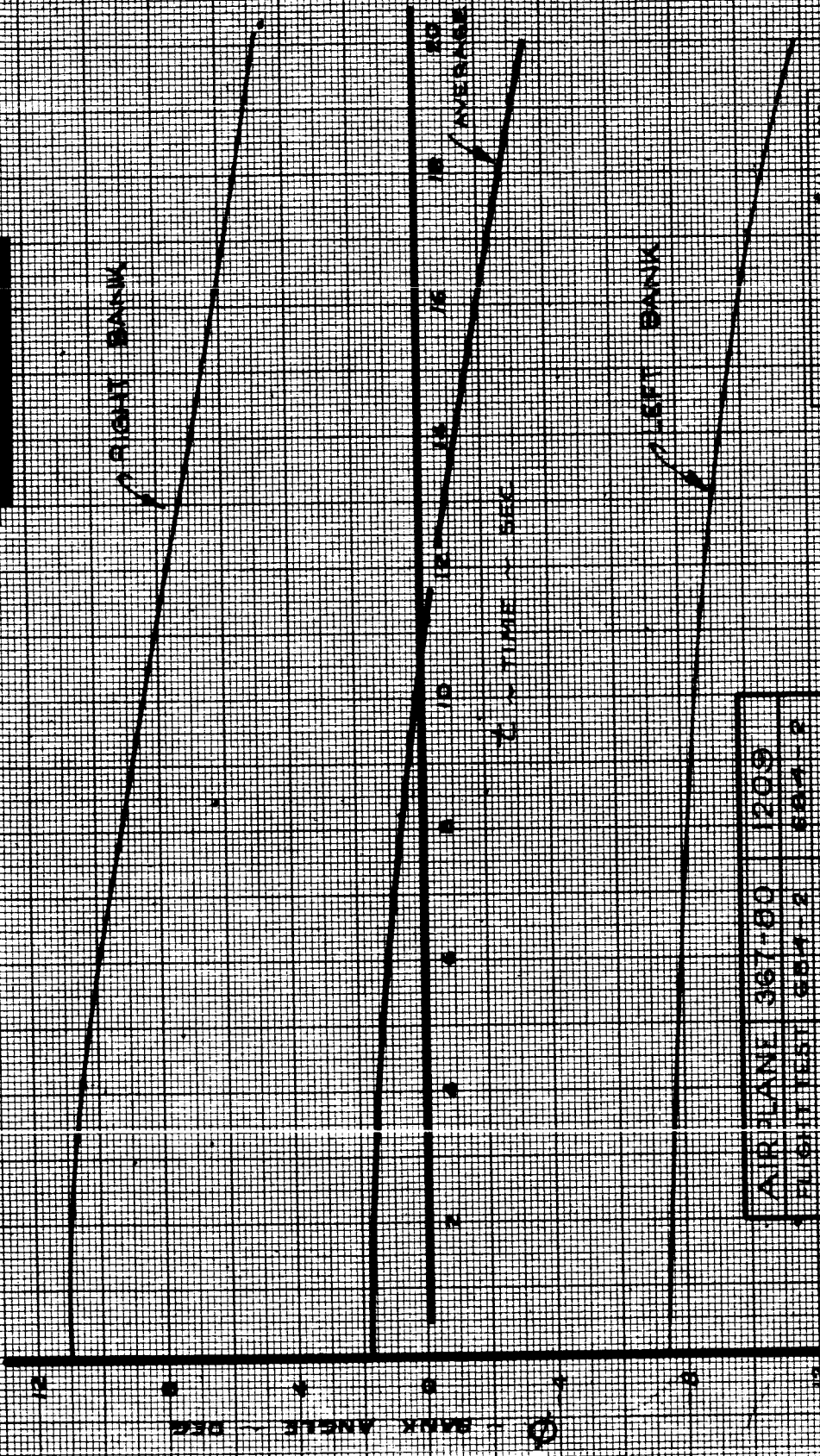


CALC			REVISED	DATE	STEADY SIDESLIP CHARACTERISTICS FLIGHT TEST 684-2, 686-2 CONFIGURATION 1209	367-80
CHECK						FIG. 17
APPD.						
APPD.						
					THE BOEING COMPANY D6-15000	PAGE VI-52

SPIRAL MODE

RIGHT BANK

LEFT BANK



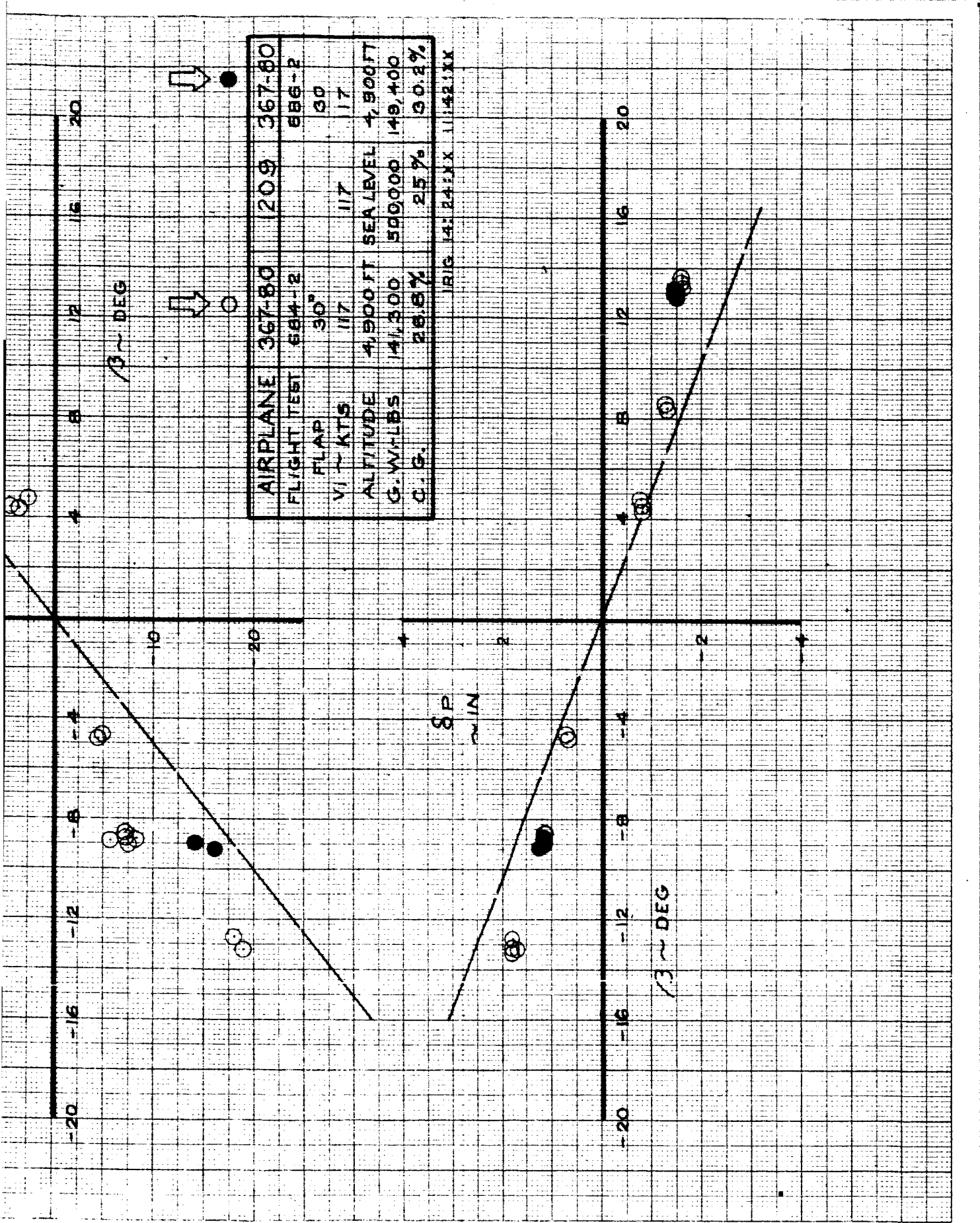
FLIGHT TEST LONG THEORY 100'S

AIRPLANE	367-80	1209
FLIGHT TEST	684-2	684-2
CLAMP	20°	
WING KTS	117	117
ALTITUDE	5,000 FT	SEA LEVEL
G.W. - LBS	141,300	500,000
C.G.	25.8%	25%

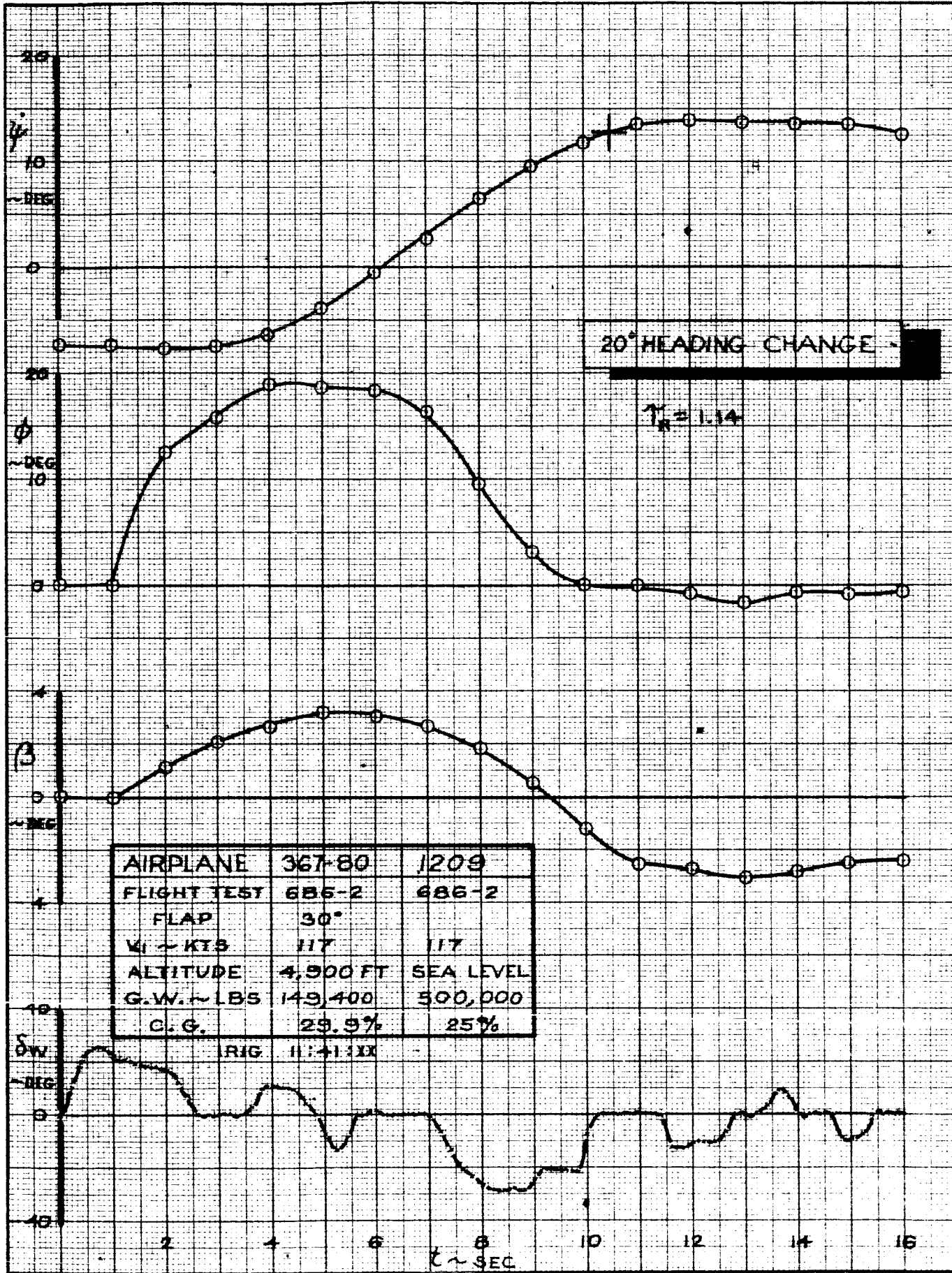
FIG. 18

CALC		REVISED	DATE	SPIRAL STABILITY FLIGHT TEST 684-2 CONFIGURATION 1209 THE BOEING COMPANY D6-15000	367-80
CHECK					FIG. 18
APR					PAGE
APR					VI-36

39



VI-35-2



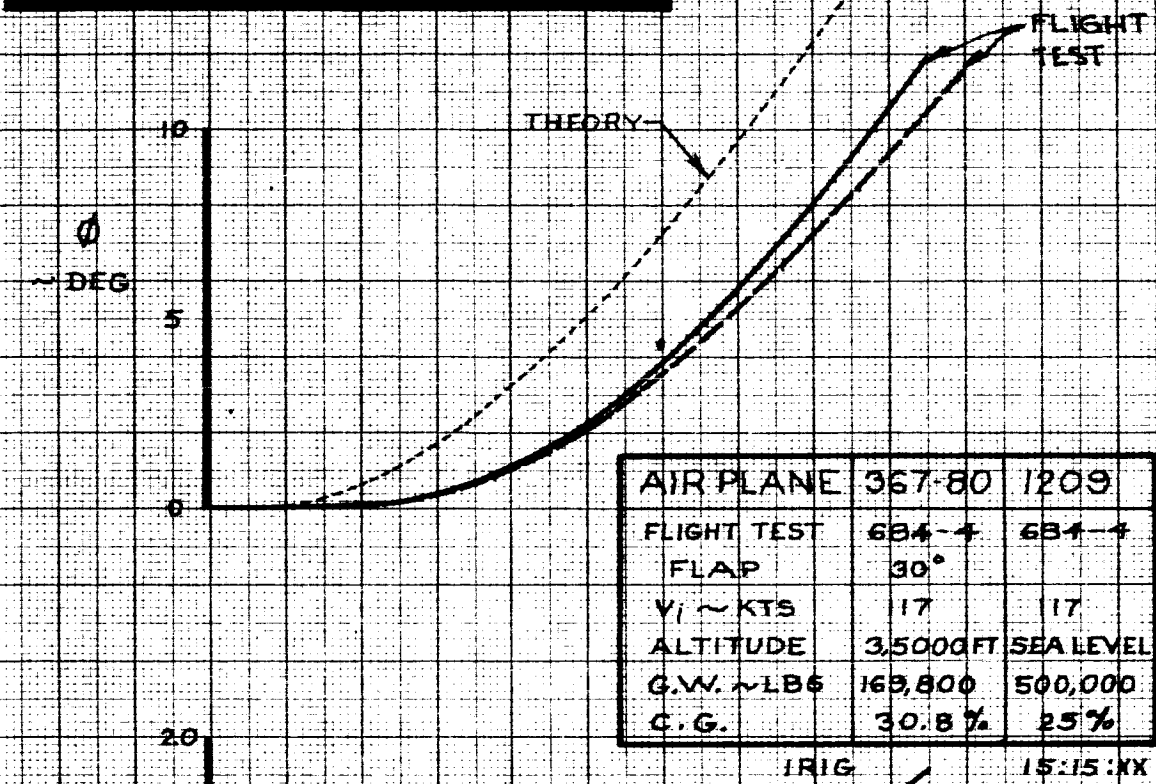
AIRPLANE	367-80	1209
FLIGHT TEST	686-2	686-2
FLAP	30°	
V _I ~ KTS	117	117
ALTITUDE	4,900 FT	SEA LEVEL
G.W. ~ LBS	149,400	500,000
C.G.	29.9%	25%

RIG. 11:41:XX

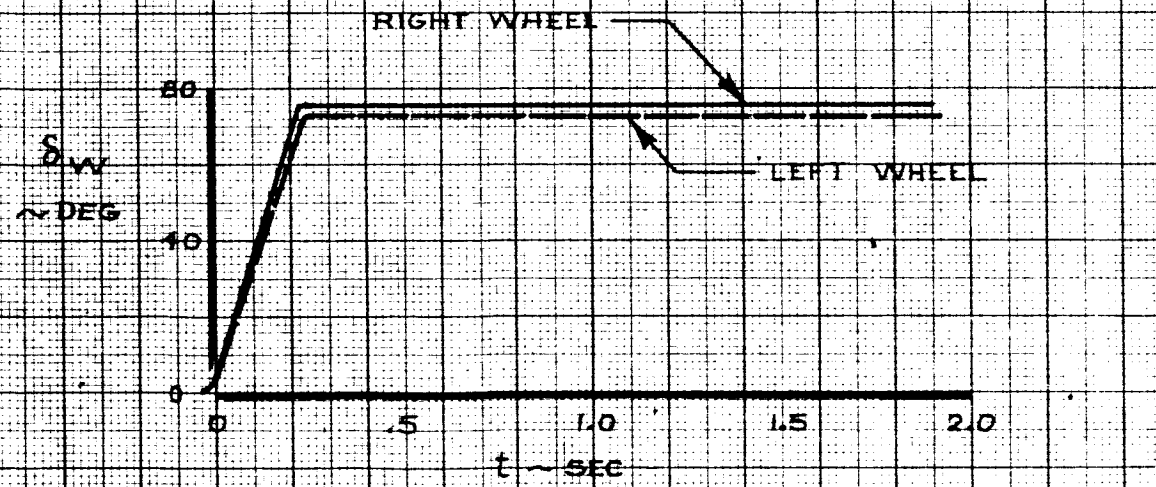
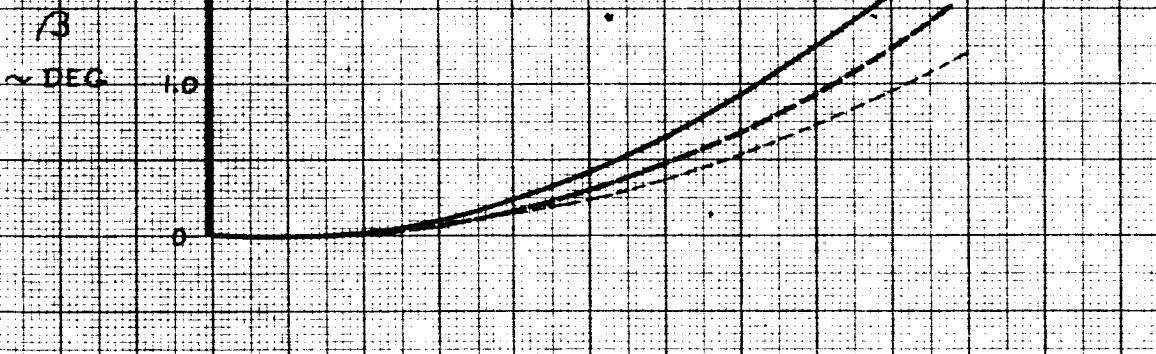
CALC		REVISED	DATE	20° HEADING CHANGE FLIGHT TEST 686-2 CONFIGURATION 1209	367-80	
CHECK					FIG. 19	
APR					THE BOEING COMPANY	PAGE VI-37
APR					D6-15000	

07

WHEEL STEP CHARACTERISTICS



AIR PLANE	367-80	1209
FLIGHT TEST	684-4	684-4
FLAP	30°	
V _i ~ KTS	17	17
ALTITUDE	3,500 FT SEA LEVEL	
G.W. ~ LBS	163,800	500,000
C.G.	30.8%	25%



CALC		REVISED	DATE	WHEEL STEP CHARACTERISTICS FLIGHT TEST 684-4 CONFIGURATION 1209	367-80
CHECK					FIG. 20
APR					THE BOEING COMPANY
APR					D6-15000
					PAGE VI-38

17

Wheel Step

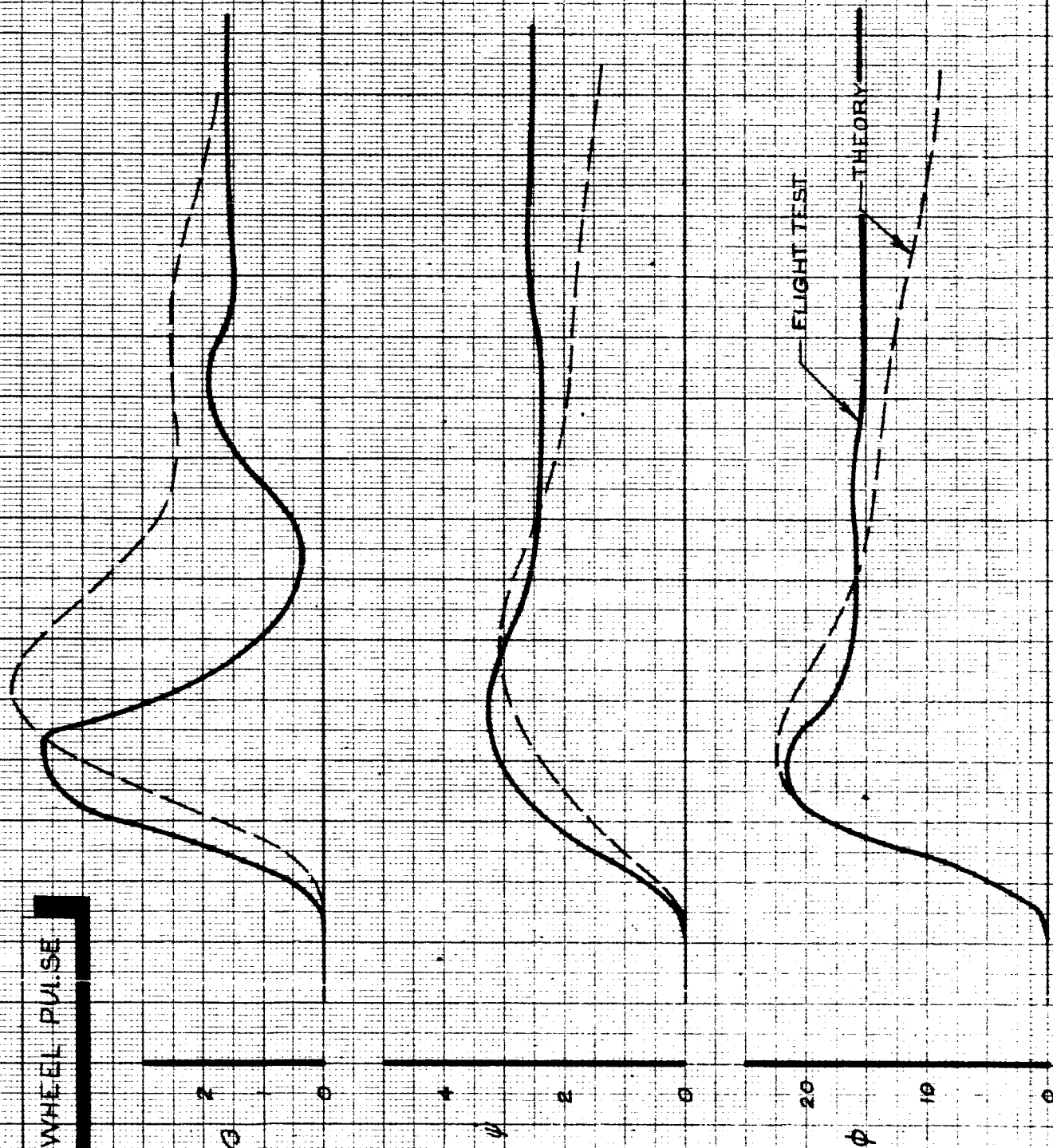
Fig. 20. Flight test roll angle data lags behind the six degree of freedom digital computer values for the wheel step shown. This is probably due to the aerodynamic and control surface lags which are not incorporated into the digital computer program.

Wheel Pulse

Fig. 21. Flight test data shows a good correlation with the theory for the basic 1209 configuration with the exception of sideslip angle.

Rudder Pulse

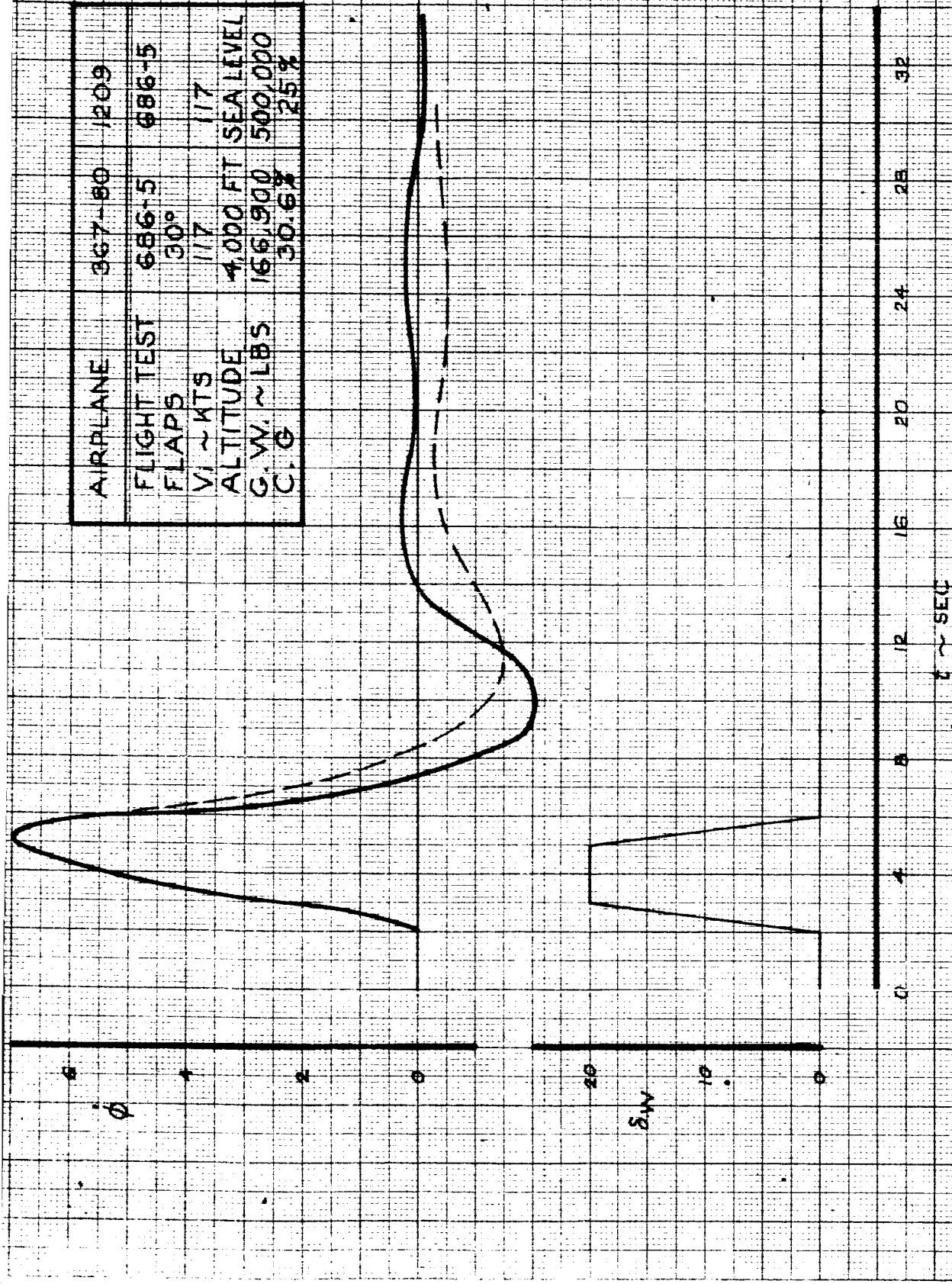
Fig. 22. Good correlation is evident with the exception of sideslip angle at the first reversal.



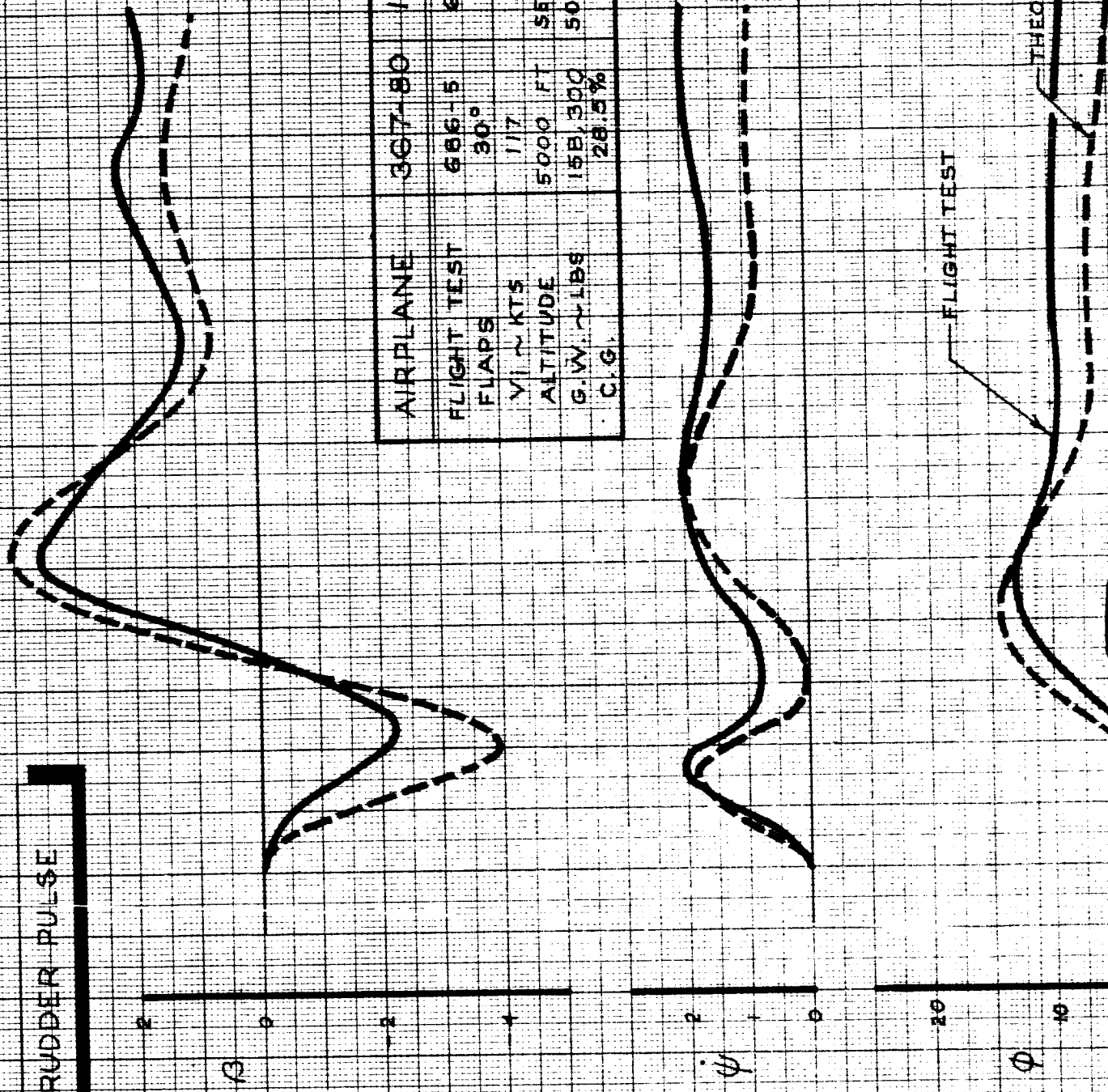
CALC			REVISED	DATE	WHEEL PULSE FLIGHT TEST 686-5 CONFIGURATION: 1209 THE BOEING COMPANY 06-15000	367-80
CHECK						FIG. 21
APPD.						PAGE
APPD.						VI-40-

VI-10-2

AIRPLANE	867-80	1209
FLIGHT TEST	686-5	686-5
FLAPS	30°	
V _i ~ KTS	117	117
ALTITUDE	4,000 FT	SEA LEVEL
G. W. ~ LBS	166,900	500,000
C. G.	30.6%	25%



RUDDER PULSE



AIRPLANE	367-80	1209
FLIGHT TEST	686-5	686-5
FLAPS	30°	
VI ~ KTS	117	117
ALTITUDE	5000 FT	SEA LEVEL
G.W. ~ LBS	158,300	500,000
C.G.	28.5%	25%

CALC			REVISED	DATE
CHECK				
APPD.				
APPD.				

RUDDER PULSE
 FLIGHT TEST 686-5
 CONFIGURATION: 1209

THE BOEING COMPANY

D6-15000

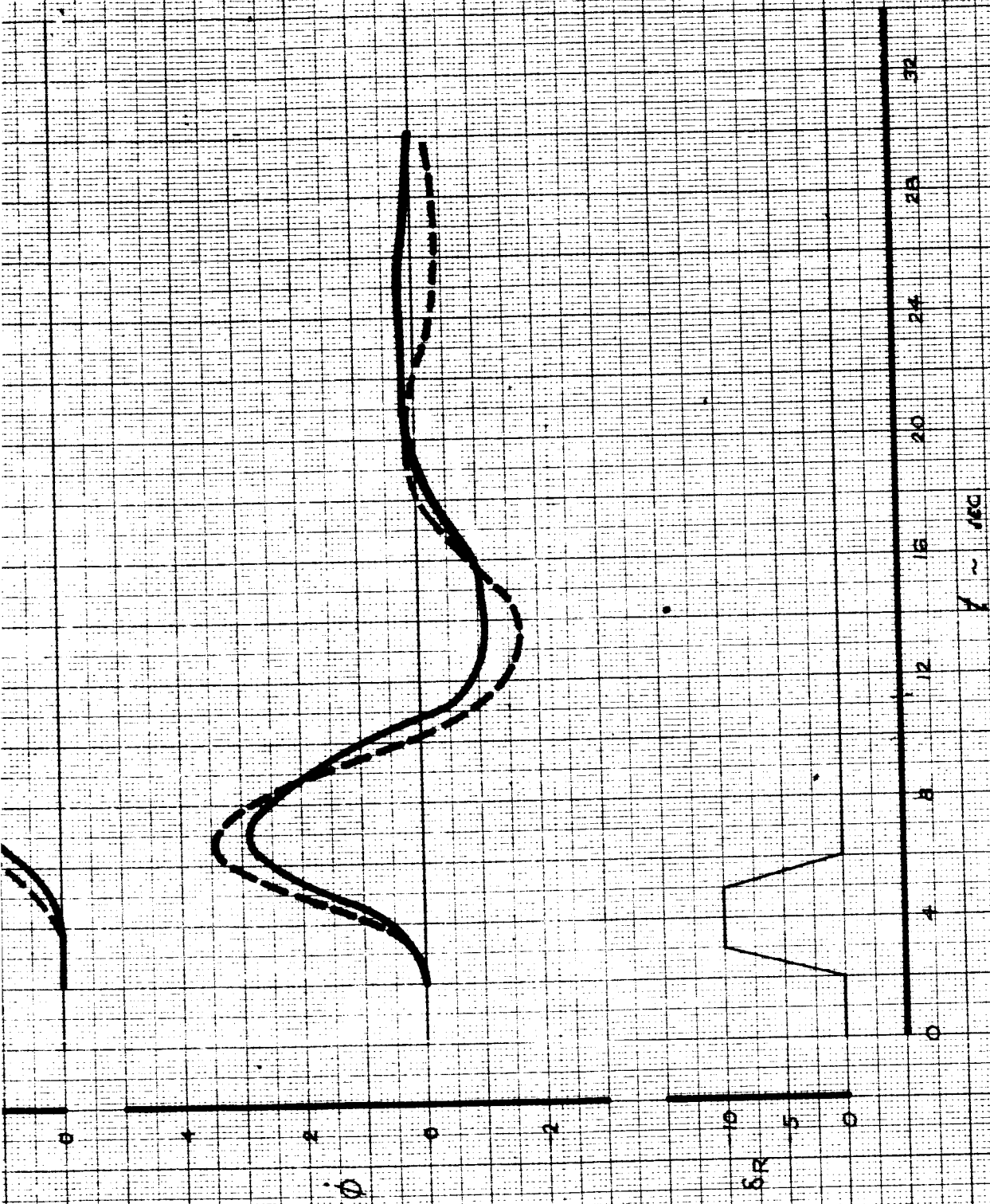
FIG. 22

PAGE VI-41

hm

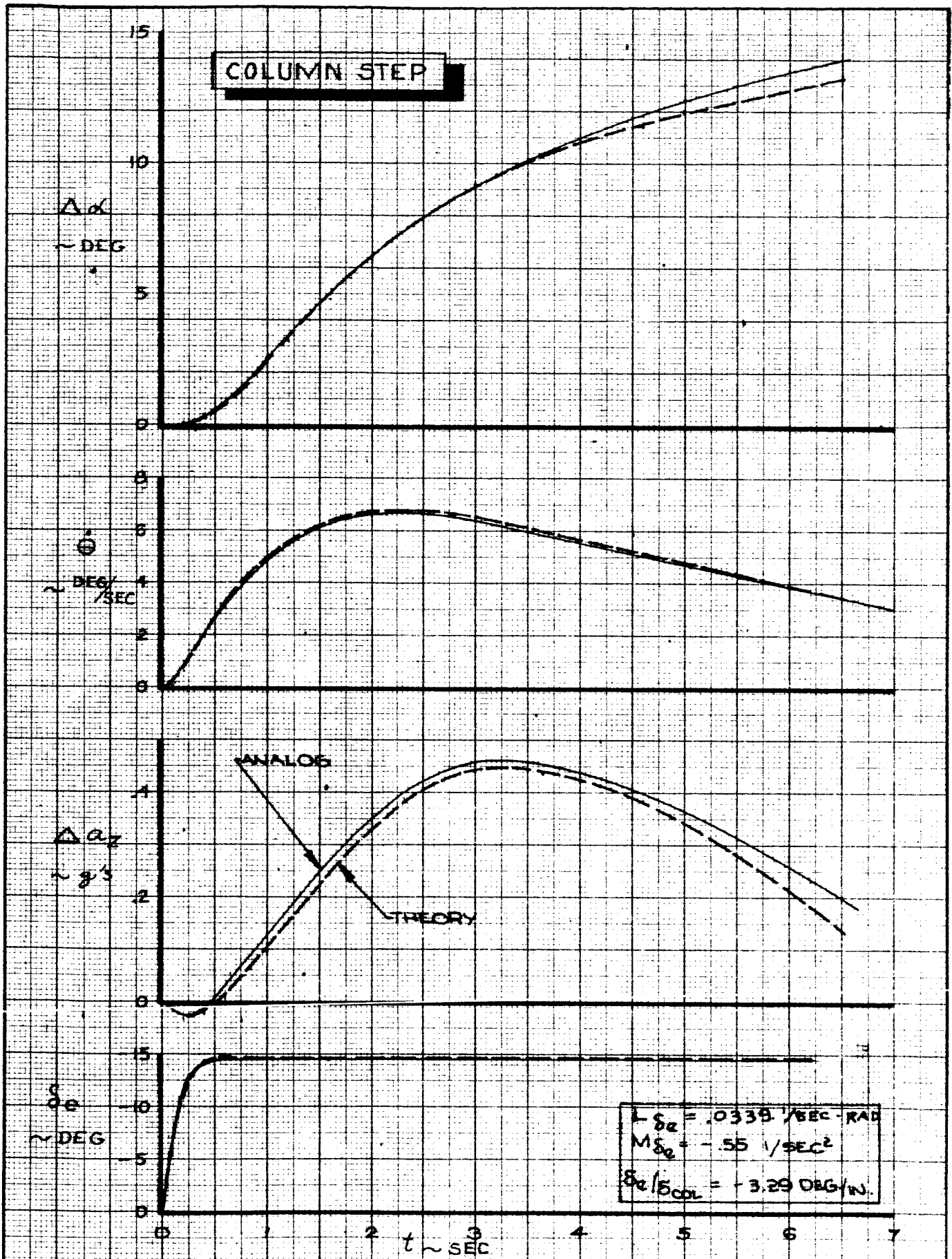
-1

VI-41
- 2



B. Ground Based Simulation

The characteristics of a typical longitudinal configuration (G 100) and lateral directional configuration (G1202A), are presented in Figs. 23 thru 36. The theoretical characteristics shown are derived using the methods of Appendix 4. The parameters presented in these figures were used to validate the accuracy of the ground based simulation. Figs. 23 thru 36 indicate that the simulation was an accurate representation of the desired configurations.



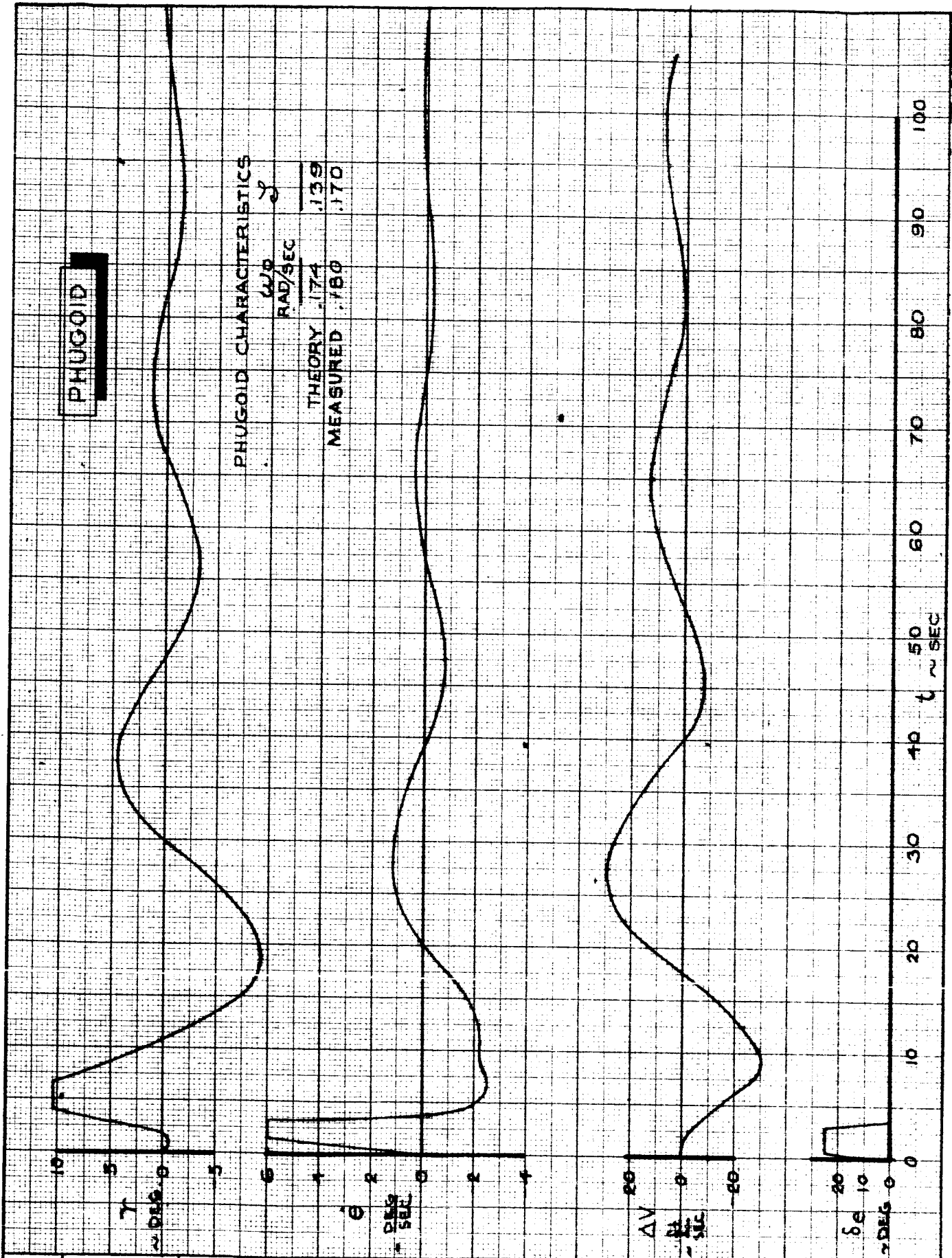
CALC	R. Root	2-2-66	REVISED	DATE	COLUMN STEP GROUND BASED SIMULATOR CONFIGURATION G101A	D6-15000 FIG. 23
CHECK						
APR					THE BOEING COMPANY	PAGE VI-43
APR				5		

PHUGOID

PHUGOID CHARACTERISTICS

ω_D
RAD/SEC

THEORY	.174	.139
MEASURED	.180	.170



CALC	R. Root	2-1-66	REVISED	DATE
CHECK				
APR				
APR				

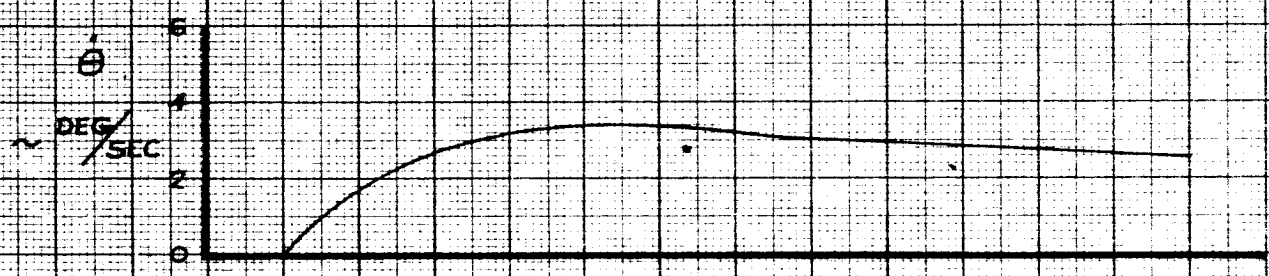
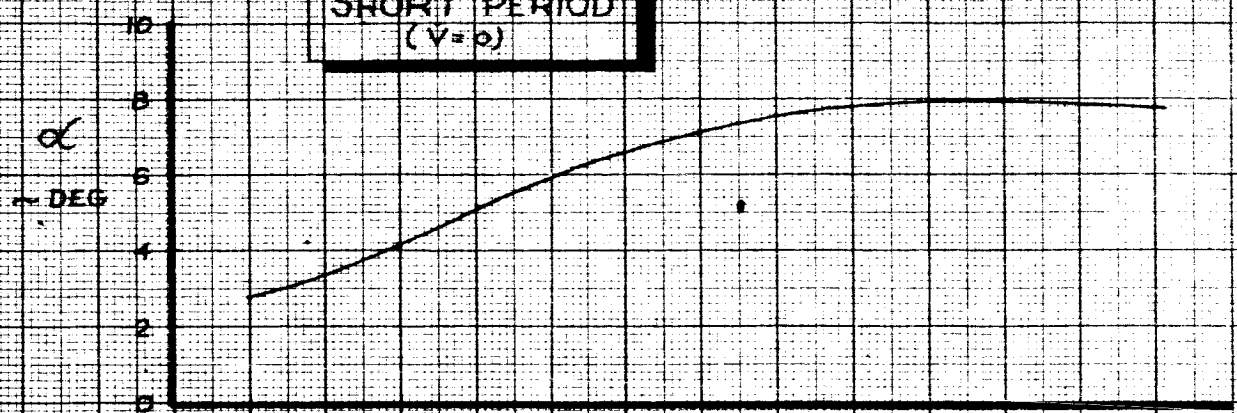
PHUGOID CHARACTERISTICS
GROUND BASED SIMULATOR
CONFIGURATION G100

THE BOEING COMPANY

D6-15000
FIG. 24
PAGE VI-44

47

**SHORT PERIOD
($\gamma=0$)**

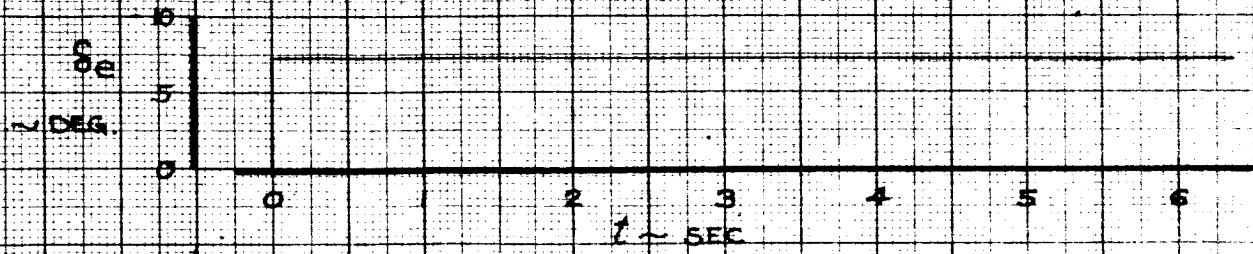


SHORT PERIOD CHARACTERISTICS

	ω_D RAD/SEC	ζ
THEORY	.544	.728
MEASURED	.63	.7-B



$\frac{d\alpha}{dt} = -329 \text{ DEG/N}$
 $M_{\alpha} = -.55 / \text{SEC}^2$



CALC	R. Root	2-1-66	REVISED	DATE
CHECK				
APR				
APR				

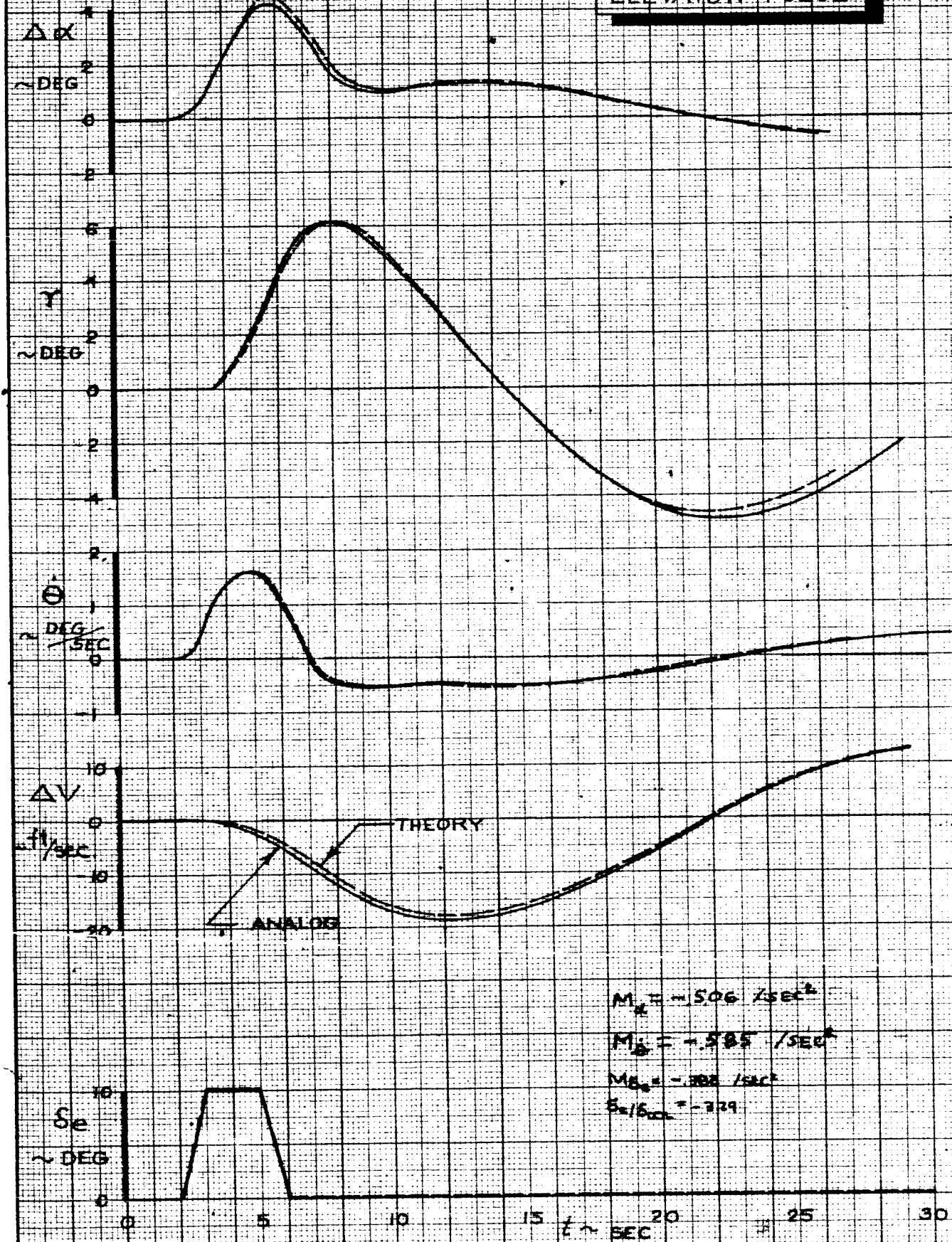
**SHORT PERIOD CHARACTERISTICS
GROUND BASED SIMULATOR
CONFIGURATION GIOIA**

THE BOEING COMPANY

D6-15000
 FIG. 25
 PAGE VI-45

48

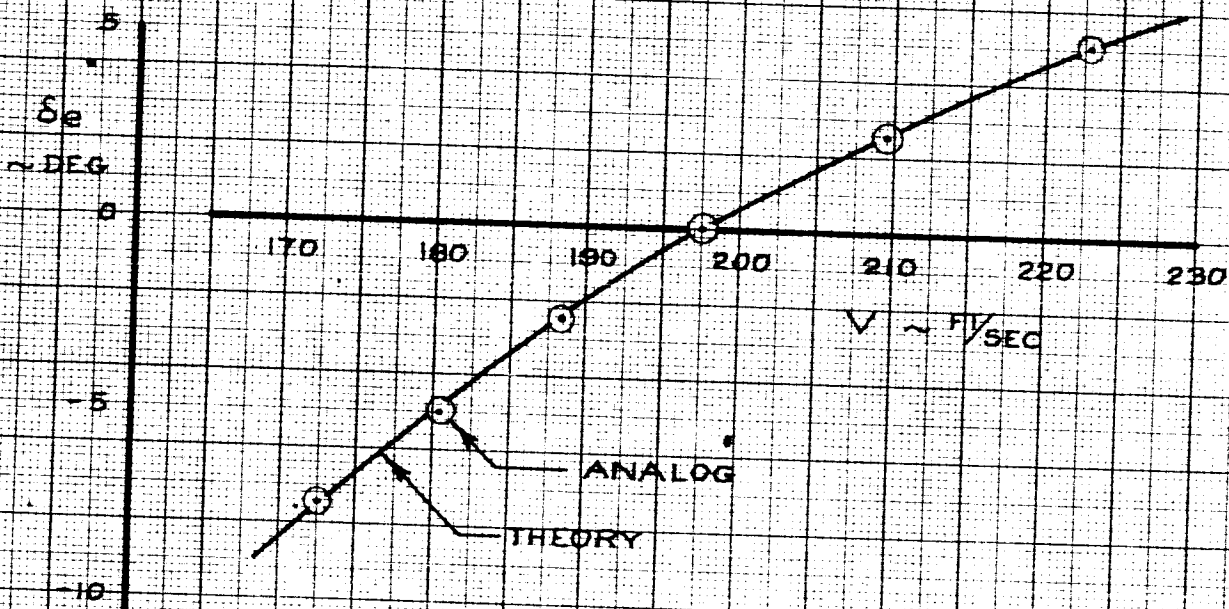
ELEVATOR PULSE



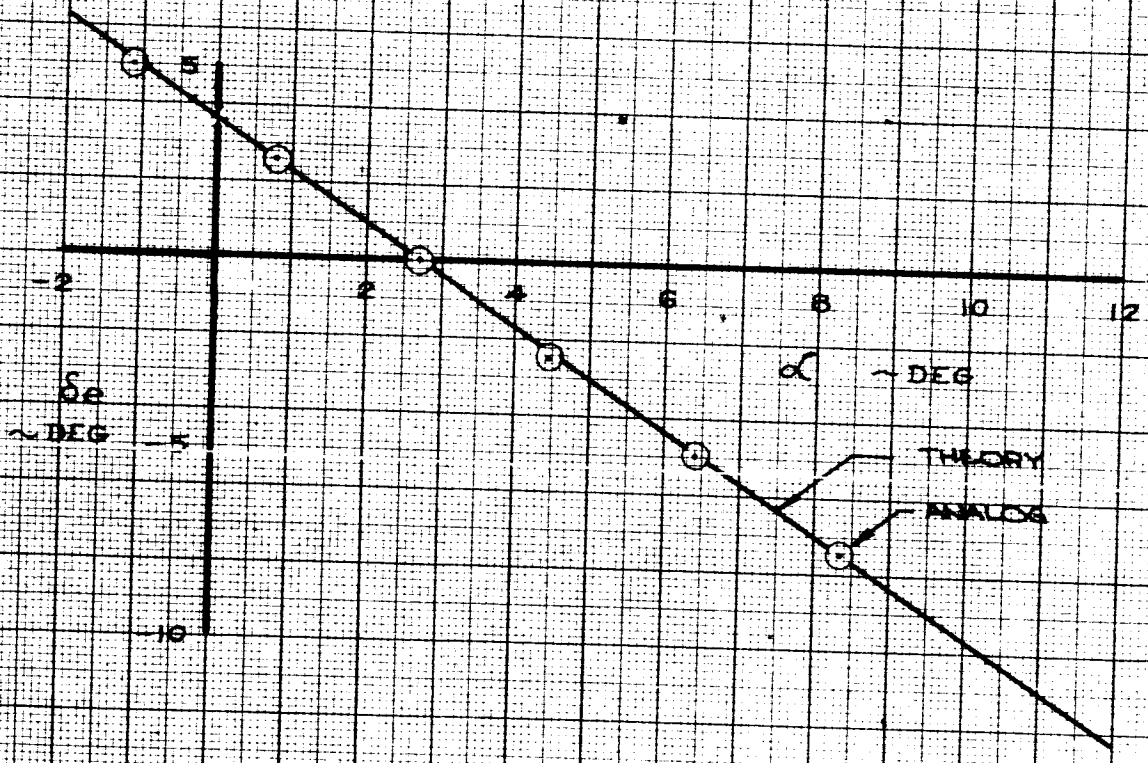
CALC	R. Root	2-2-66	REVISED	DATE	ELEVATOR PULSE GROUND BASED SIMULATOR CONFIGURATION G100 THE BOEING COMPANY	D6-15000
CHECK						FIG. 26
APR						PAGE
APR						VI-46

49

SPEED STABILITY



$M_{\dot{\delta}_e} = -3.62 / \text{SEC}^2$
 $\dot{\delta}_e / \text{FOOT} = -3.29 \text{ DEG/IN.}$



CALC	R. Root	2-2-66	REVISED	DATE
CHECK				
APR				
APR				

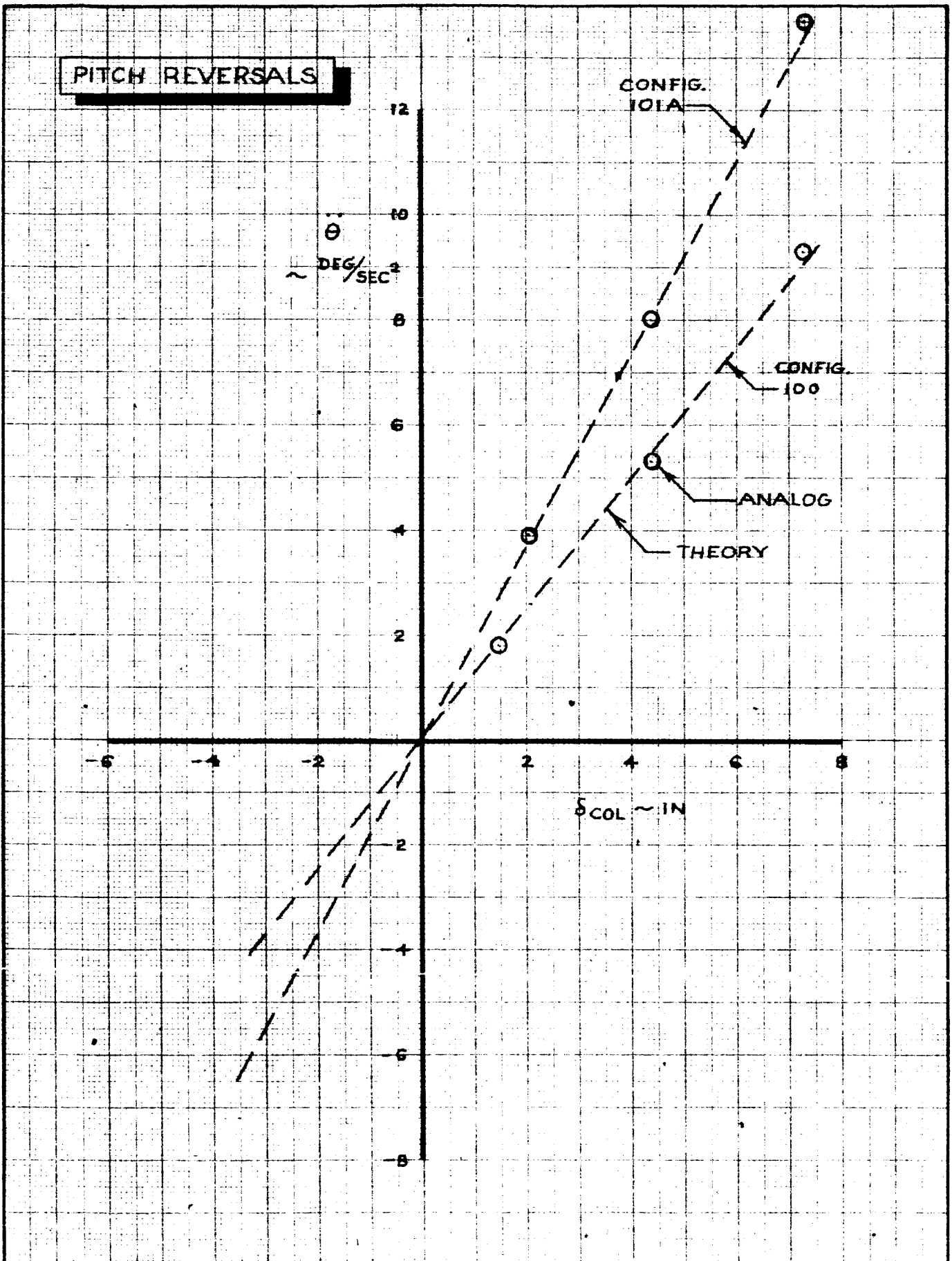
SPEED STABILITY
GROUND BASED SIMULATOR
CONFIGURATION G100

THE BOEING COMPANY

D6-15000
 FIG. 27
 PAGE
 VI-47

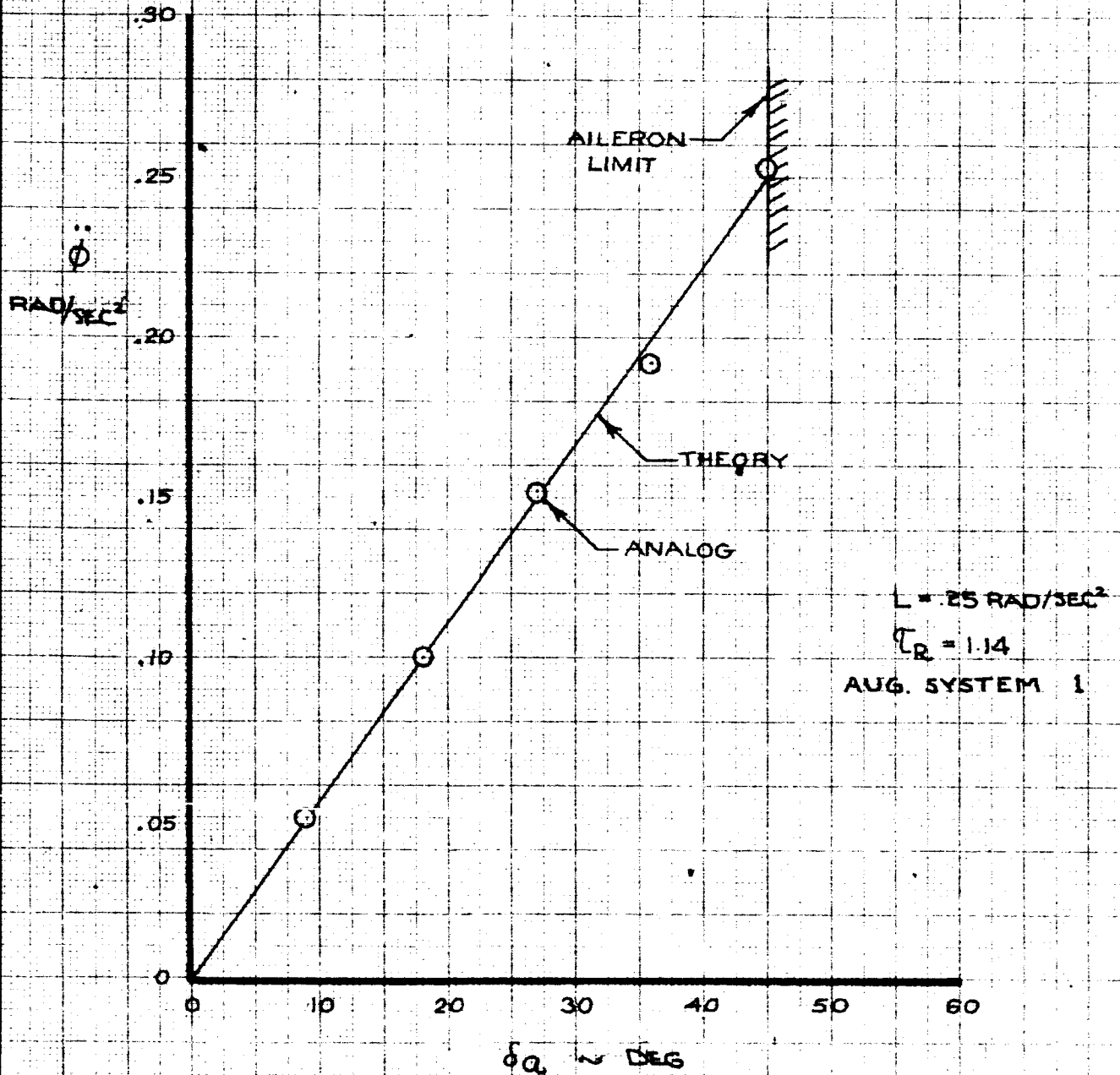
50

PITCH REVERSALS



CALC	R. Root	2-2-66	REVISED	DATE	PITCH REVERSALS GROUND BASED SIMULATOR CONFIGURATION G100 & G101A THE BOEING COMPANY	D6-15000
CHECK						
APR						PAGE
APR						VI-48

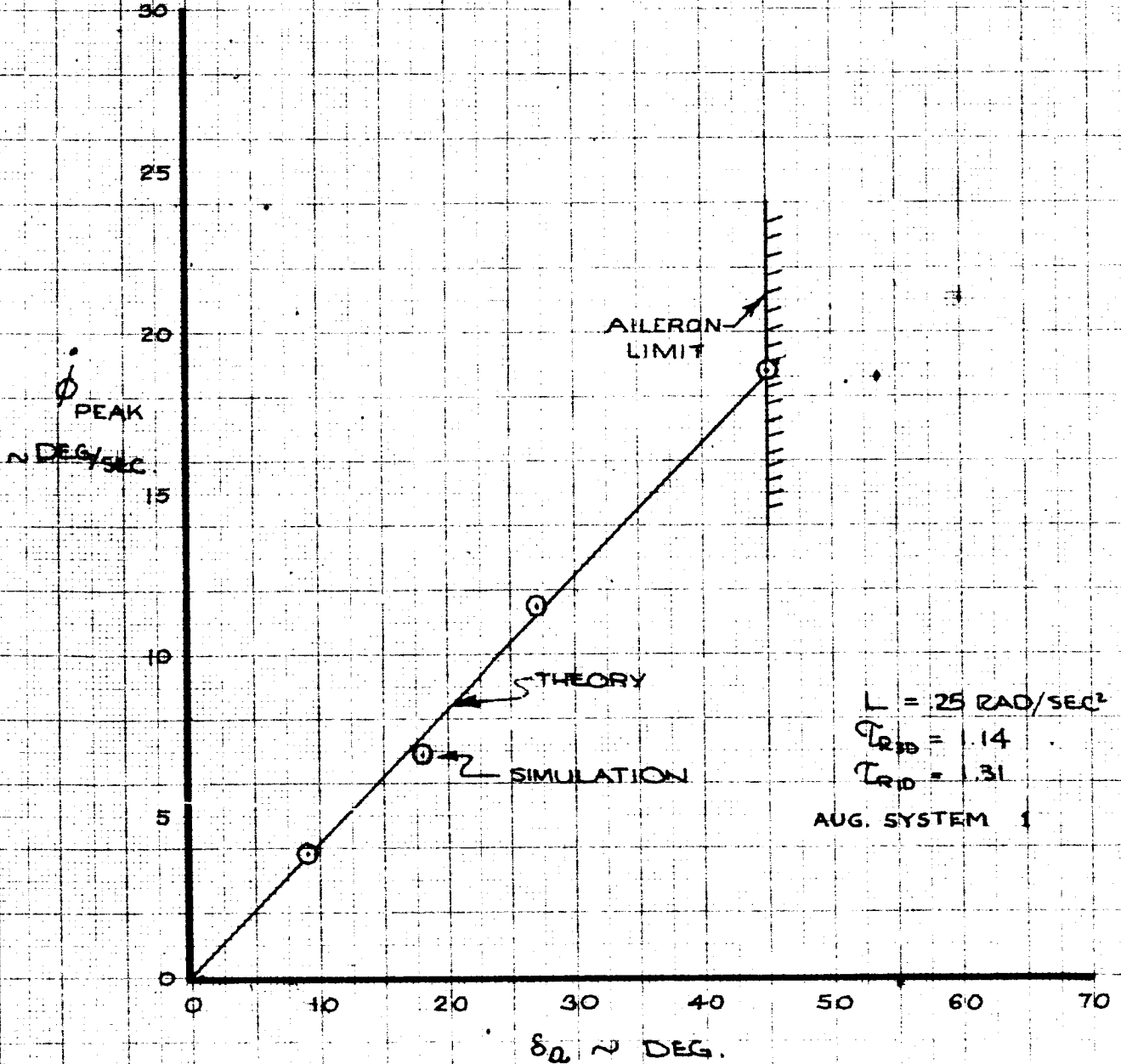
WHEEL REVERSAL



CALC	R. Root	2-2-66	REVISED	DATE	WHEEL REVERSAL GROUND BASED SIMULATOR CONFIGURATION G1202A	D6-15000 FIG.29
CHECK					THE BOEING COMPANY	PAGE VI-49
APR						
APR						

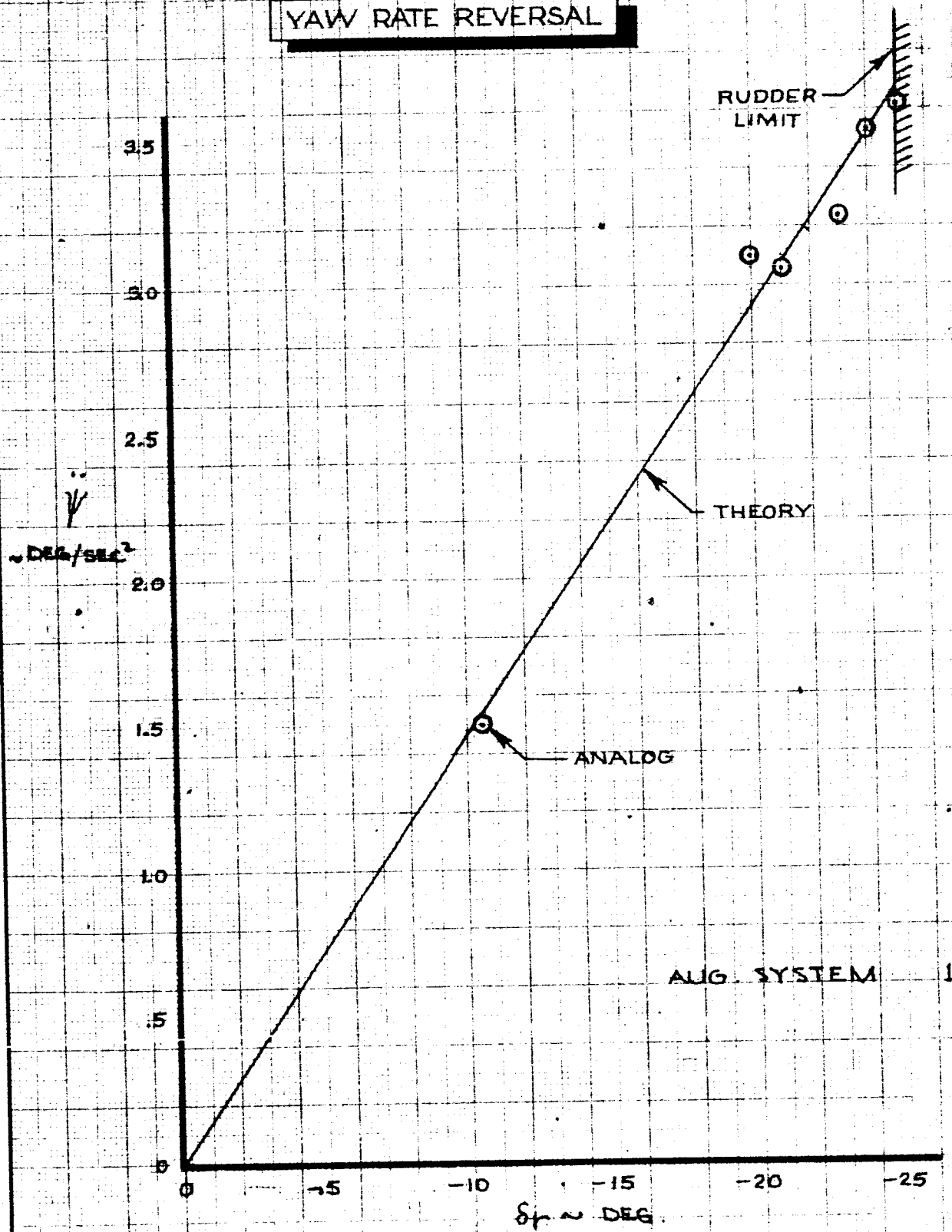
ROLL RATE

ONE DEGREE OF FREEDOM



CALC	R. Root	2-2-66	REVISED	DATE	ROLL RATE GROUND BASED SIMULATOR CONFIGURATION G1202A THE BOEING COMPANY	D6-15000
CHECK						FIG. 30
APR						PAGE
APR						VI-50

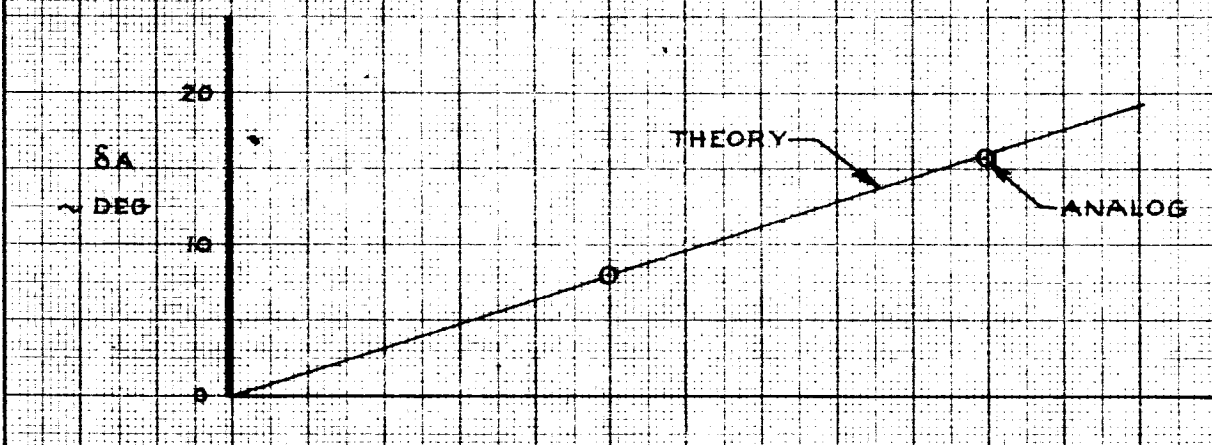
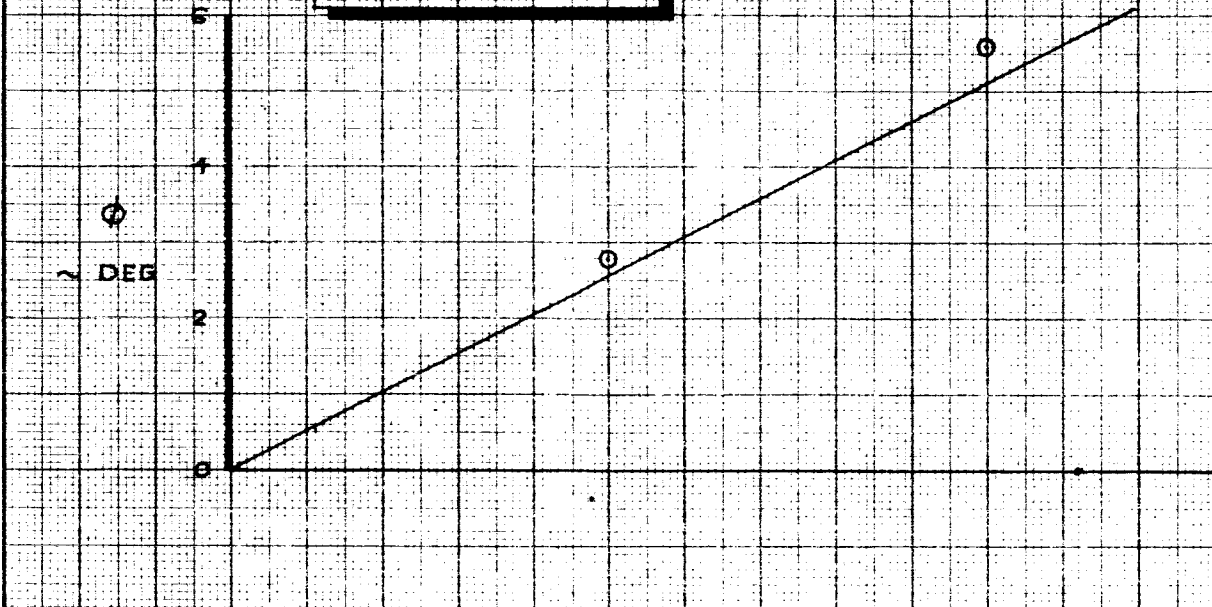
YAW RATE REVERSAL



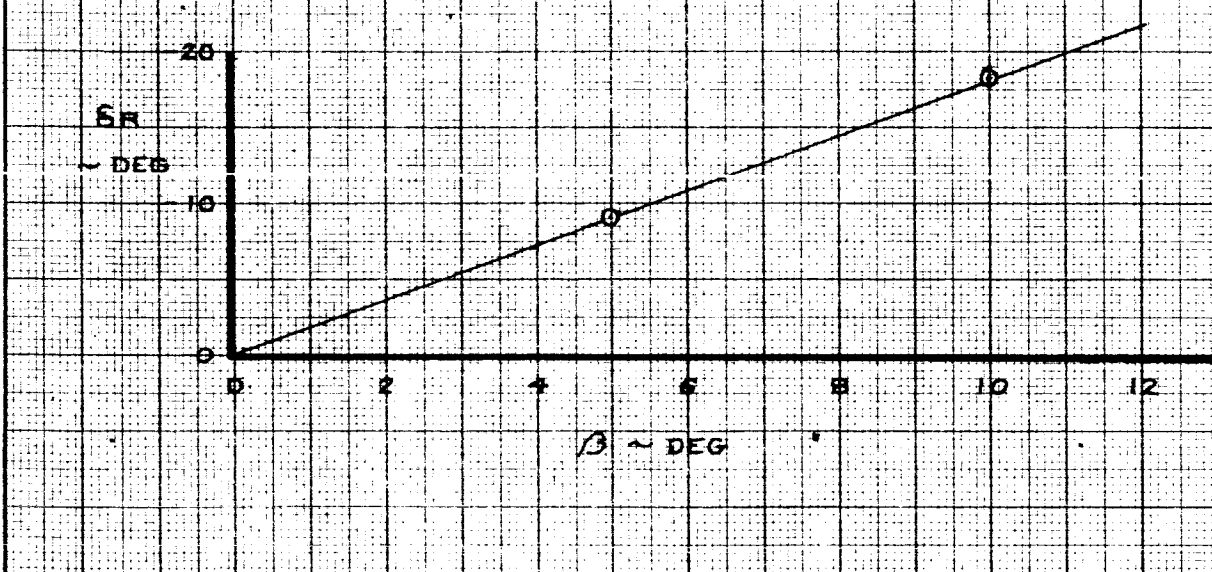
CALC	R. Root	2-2-66	REVISED	DATE	YAW RATE REVERSAL GROUND BASED SIMULATOR CONFIGURATION G1202A THE BOEING COMPANY	DD-15000
CHECK				FIG. 31		
APR				PAGE		
APR				VI-51		

54

STEADY SIDESLIP

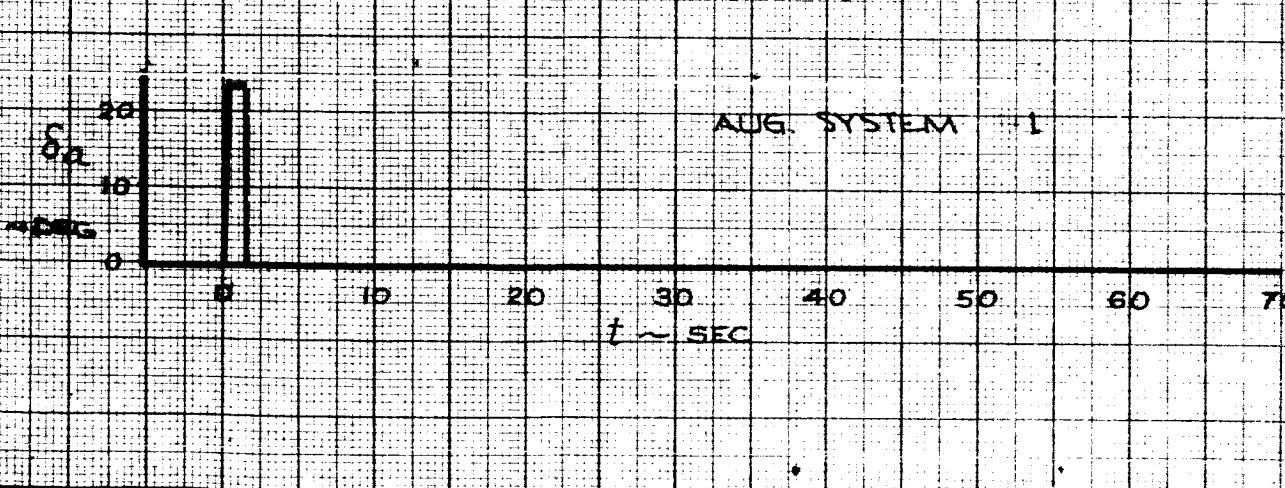
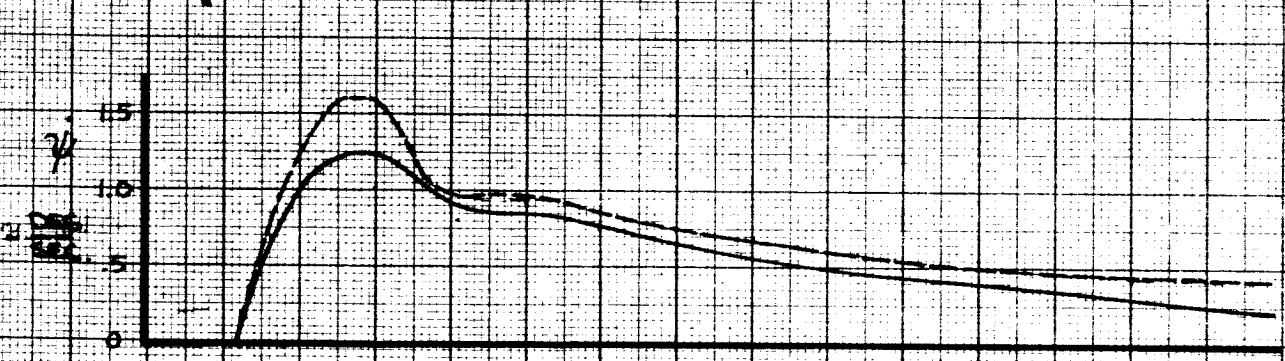
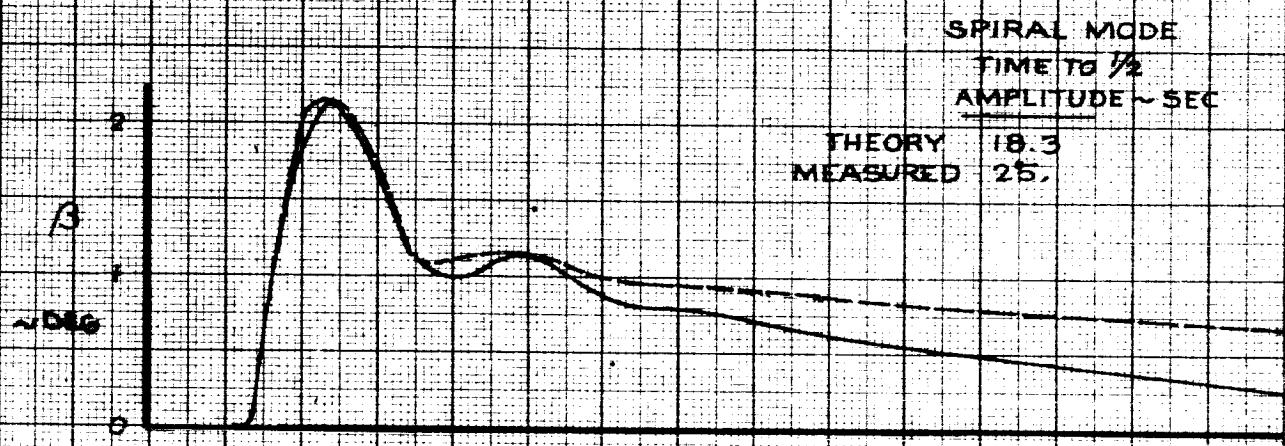
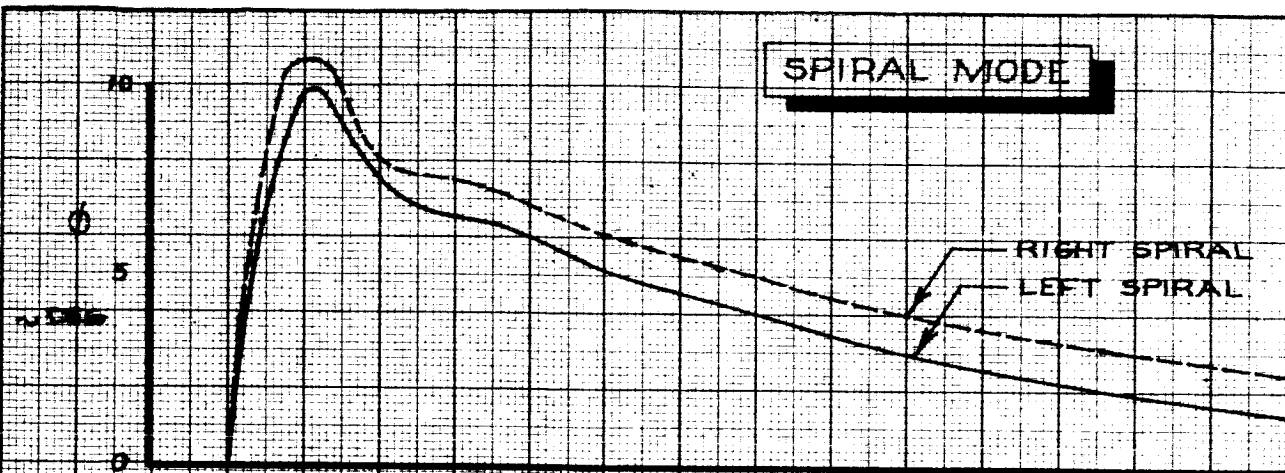


AUG. SYSTEM I
 $L = .30$
 $T_R = .14$



CALC	R. Root	2-2-66	REVISED	DATE	STEADY SIDESLIP CHARACTERISTICS GROUND BASED SIMULATOR CONFIGURATION G1202	D6-15000
CHECK						FIG. 31A
APR						PAGE
APR						VI-52
					THE BOEING COMPANY	

55



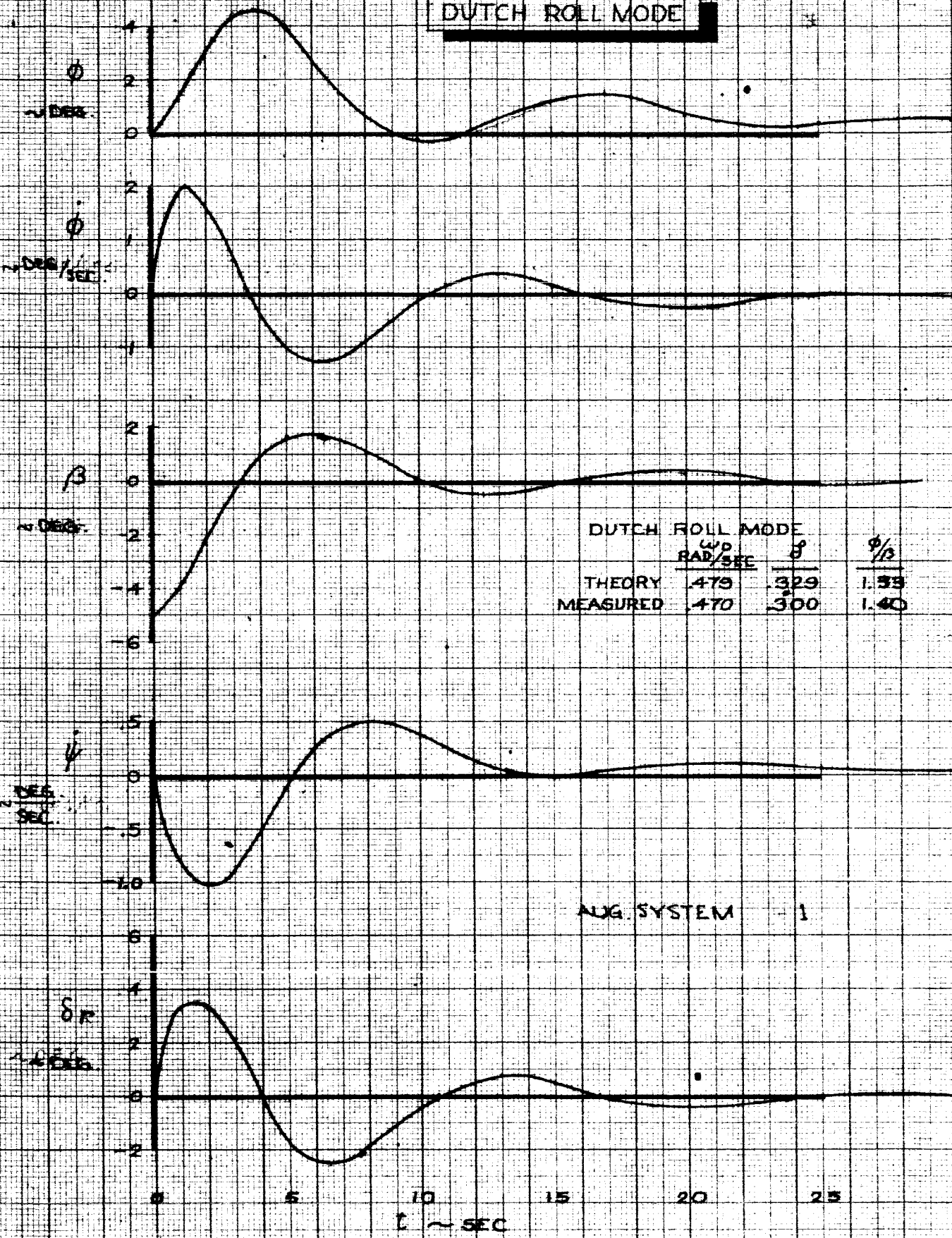
CALC	R. Root	2-2-66	REVISED	DATE
CHECK				
APR				
APR				

SPIRAL MODE
 GROUND BASED SIMULATOR
 CONFIGURATION G1202 A
 THE BOEING COMPANY

D6-15000
 FIG.32
 PAGE
 VI-53

56

DUTCH ROLL MODE



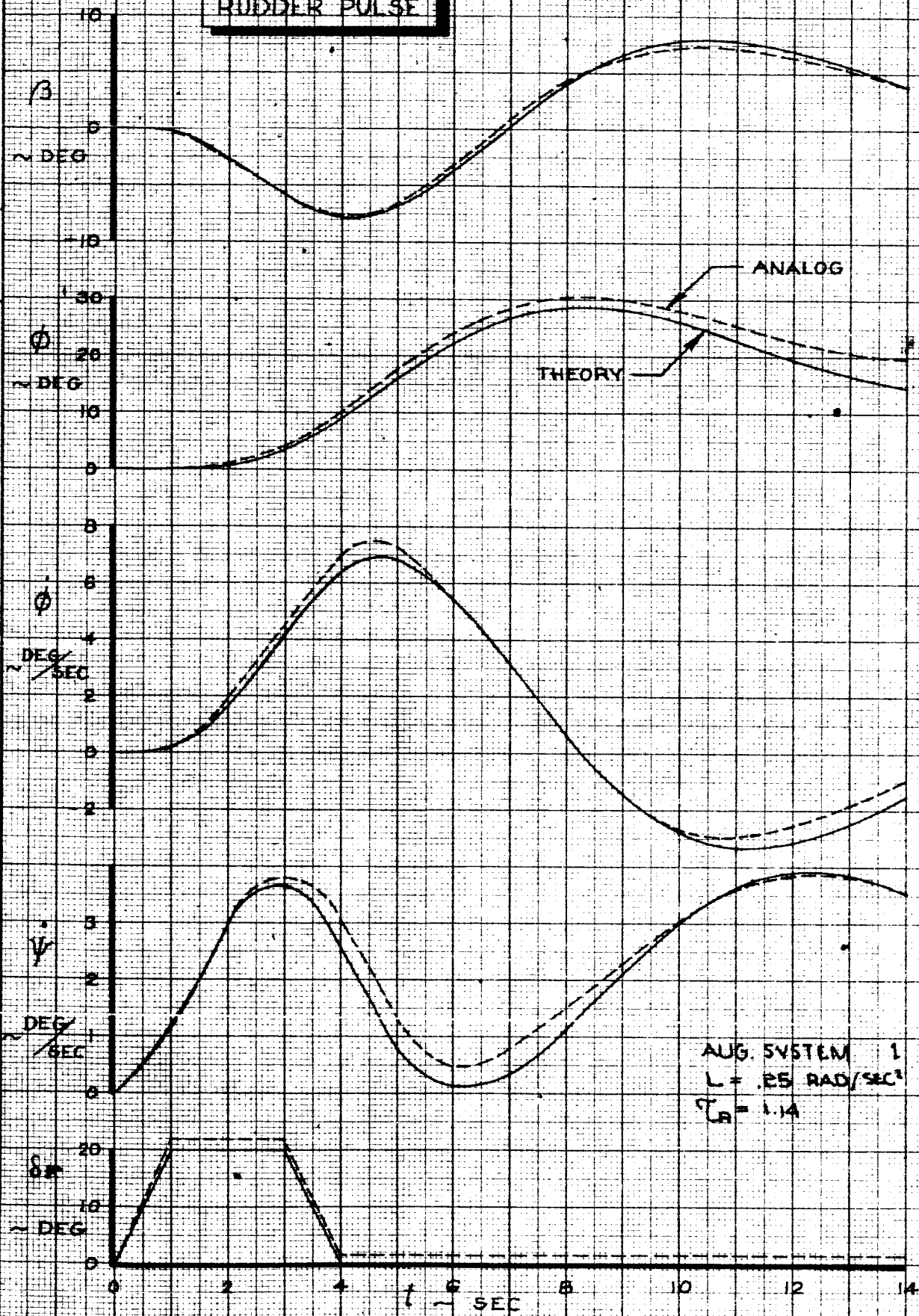
DUTCH ROLL MODE			
	ω_D	δ	ϕ/β
	RAD/SEC		
THEORY	479	329	1.33
MEASURED	470	300	1.40

AUG. SYSTEM - 1

CALC	R. Root	2-2-66	REVISED	DATE	DUTCH ROLL MODE GROUND BASED SIMULATOR CONFIGURATION G1202A THE BOEING COMPANY	D6-15000
CHECK						FIG. 33
APR						PAGE VI-54
APR						

57

RUDDER PULSE

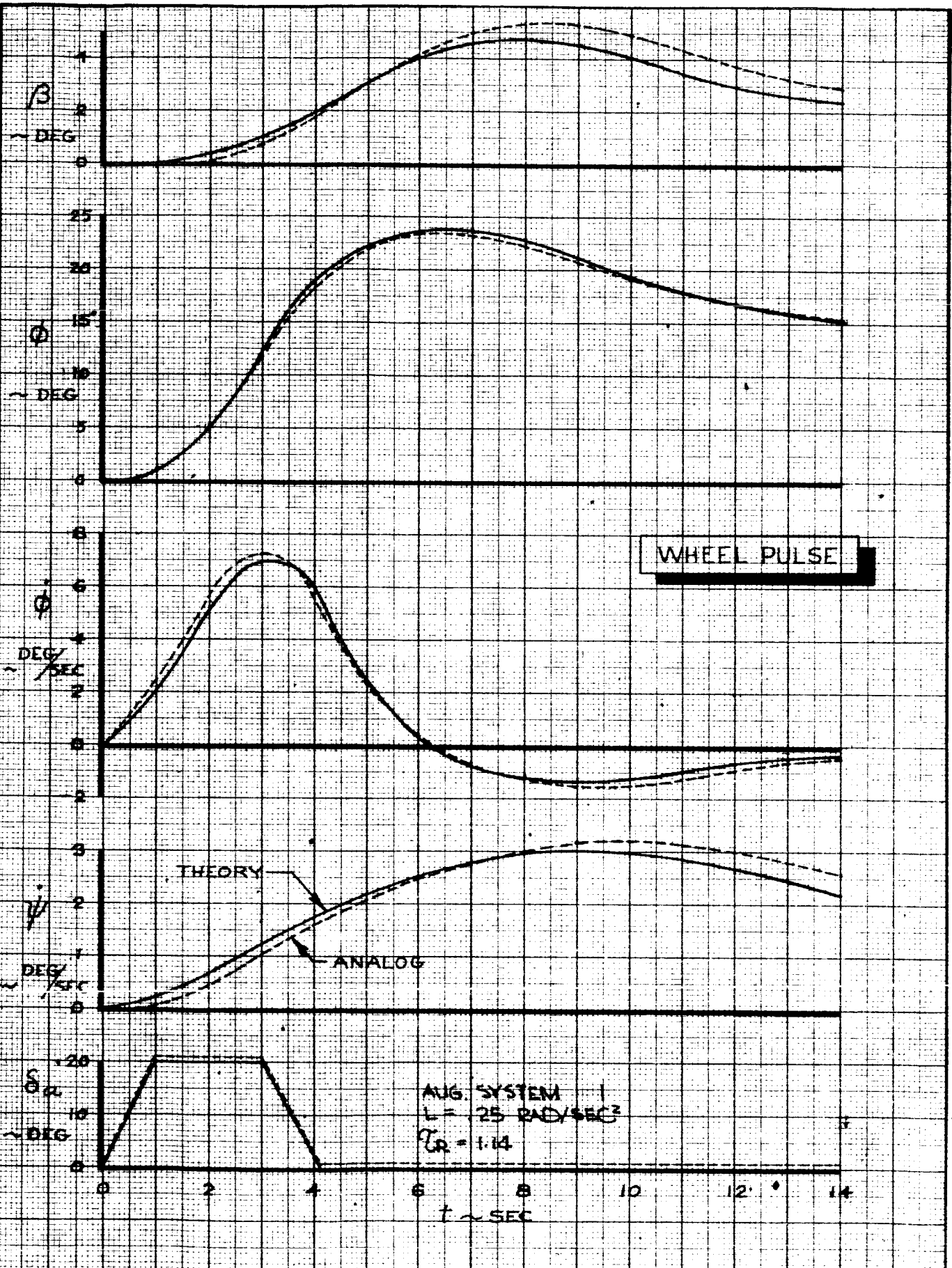


CALC	R. Root	2-2-66	REVISED	DATE
CHECK				
APR				
APR				

RUDDER PULSE
 GROUND BASED SIMULATOR
 CONFIGURATION G1202A
 THE BOEING COMPANY

D6-15000
 FIG. 34
 PAGE VI-55

58



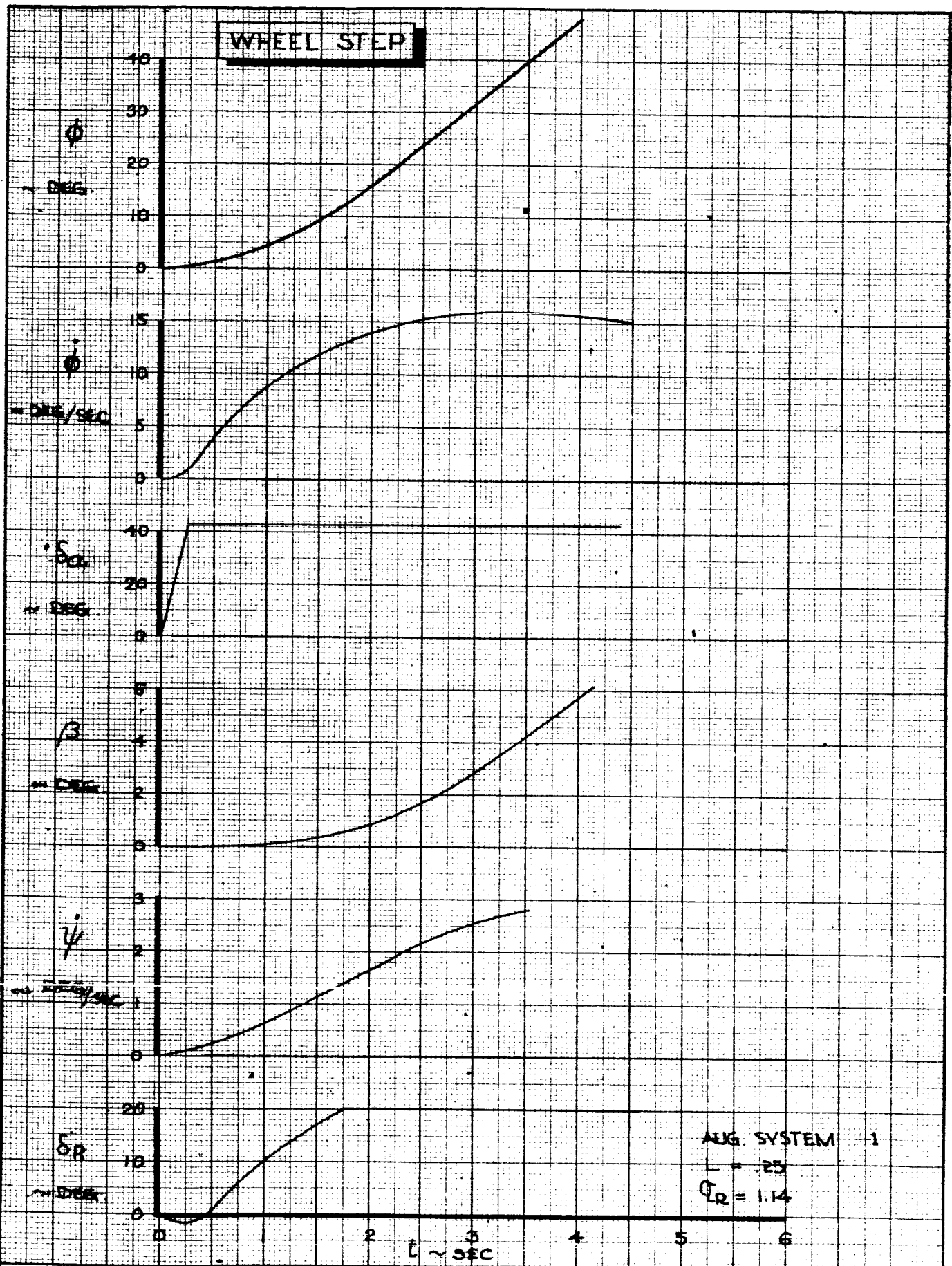
CALC	R. Root	2-2-66	REVISED	DATE
CHECK				
APR				
APR				

WHEEL PULSE
 GROUND BASED SIMULATOR
 CONFIGURATION G1202A
 THE BOEING COMPANY

D6-15000
 FIG. 35
 PAGE VI-56

59

WHEEL STEP



AUG. SYSTEM 1
 $L = .25$
 $C_R = 1.14$

CALC	R. Root	2-2-66	REVISED	DATE
CHECK				
APR				
APR				

WHEEL STEP
 GROUND BASED SIMULATOR
 CONFIGURATION G1202A

THE BOEING COMPANY

D6-15000
 FIG. 36
 PAGE
 VI-57

VII. LONGITUDINAL CONFIGURATION

A. Airborne Simulation

Eight variations of the basic longitudinal configuration are discussed in this section. The documentation maneuvers performed with each configuration are summarized in a single Figure or Table whenever possible. They are eliminated entirely when the response does not change significantly from that of the basic configuration. For the purposes of evaluating and documenting the longitudinal mode the lateral configuration was always the basic 1209.

Table 1 contains a summary of the longitudinal configurations evaluated on the Airborne Simulation. The numbers shown are theoretical values equivalent to the theoretical lines shown on the Figures. The longitudinal aerodynamic coefficients used to obtain these characteristics are listed in Appendix 1.

CONFIG.	L α /SEC-RAD	M α /SEC ²	L δ col. /SEC-IN/RAD	M δ col. /SEC ²	L $\dot{\epsilon}$ /RAD	SHORT PERIOD		PHUGOID		COMMENTS INCREASED (+) DECREASED (-)
						W h RAD/SEC	ζ	W h RAD/SEC	ζ	
101A	.521	-.506	.00313	.0252	.0516	.907	.7033	.1720	.1490	BASIC
100			.00262	.0167						- SENSITIVITY
105A			.00625	.0504						+ SENSITIVITY - LIFT WITH δ COL.
105*			.00792							+ SENSITIVITY -- LIFT WITH δ COL.
151B			.00010	.0252						++ LIFT WITH δ COL.
151C			.00164							+ LIFT WITH δ COL.
151D			.00020	.0504						+ SENSITIVITY ++ LIFT WITH δ COL.
158A	.552	-1.012	.00635		.0984	1.330	.7205	.1693	.1845	+ SENS. - LIFT WITH δ COL. + DAMPING + STATIC STABILITY
159A	.521	-.506	.00316	.0252	.0984	1.071	.8647	.1446	.2352	+ DAMPING
159B	.521	-.506	.00635	.0504	.0984	1.071	.8647	.1446	.2352	+ SENS. - LIFT WITH δ COL. + DAMPING
161B	.497	-.128	.00635		.0516	.650	.9423	.1200	.3320	+ SENS - LIFT WITH δ COL. - STATIC STAB.
-80 BLC	.459	-.469	.00278	.0641	0	1.347	.5245	.1352	.1244	+ DAMPING + STATIC STABILITY

ENGR		REVISED	DATE	AIRBORNE SIMULATION LONGITUDINAL RUN LOG	TABLE 1
CHECK					D6-15000
APR				THE BOEING COMPANY RENTON, WASHINGTON	VII-59
APR					

A summary of pitch rate reversals for all configurations is shown in Fig. 37 normalized to the pitch control sensitivity of the basic 101A configuration. This curve shows some scatter in the data but generally good agreement with the theoretical for all configurations.

Column steps are shown in Figs. 38 & 39 for two configurations, 151B and 151C, which point out changes in lift due to column deflection when compared to the basic 101A configuration (Fig. 4). A lag is apparent in the flight test data that does not show up in the theoretical results. This could be due to an aerodynamic lag or a lag in the lift control (spoilers) which does not appear in the theory.

The wind up turn data is shown for all configurations in Figs. 40 through 55 and matches the theoretical calculations accurately.

Speed stability tests were performed and correlation with the theoretical static characteristics was good. Results are shown in Figs. 56 through 63.

A summary of phugoid characteristics for all configurations is shown in Table 2. The damping ratios were difficult to measure accurately since only one cycle of the phugoid was recorded and they do not compare accurately with the theoretical. The period, on the other hand, was easily determined and agrees closely with theory.

TABLE 2

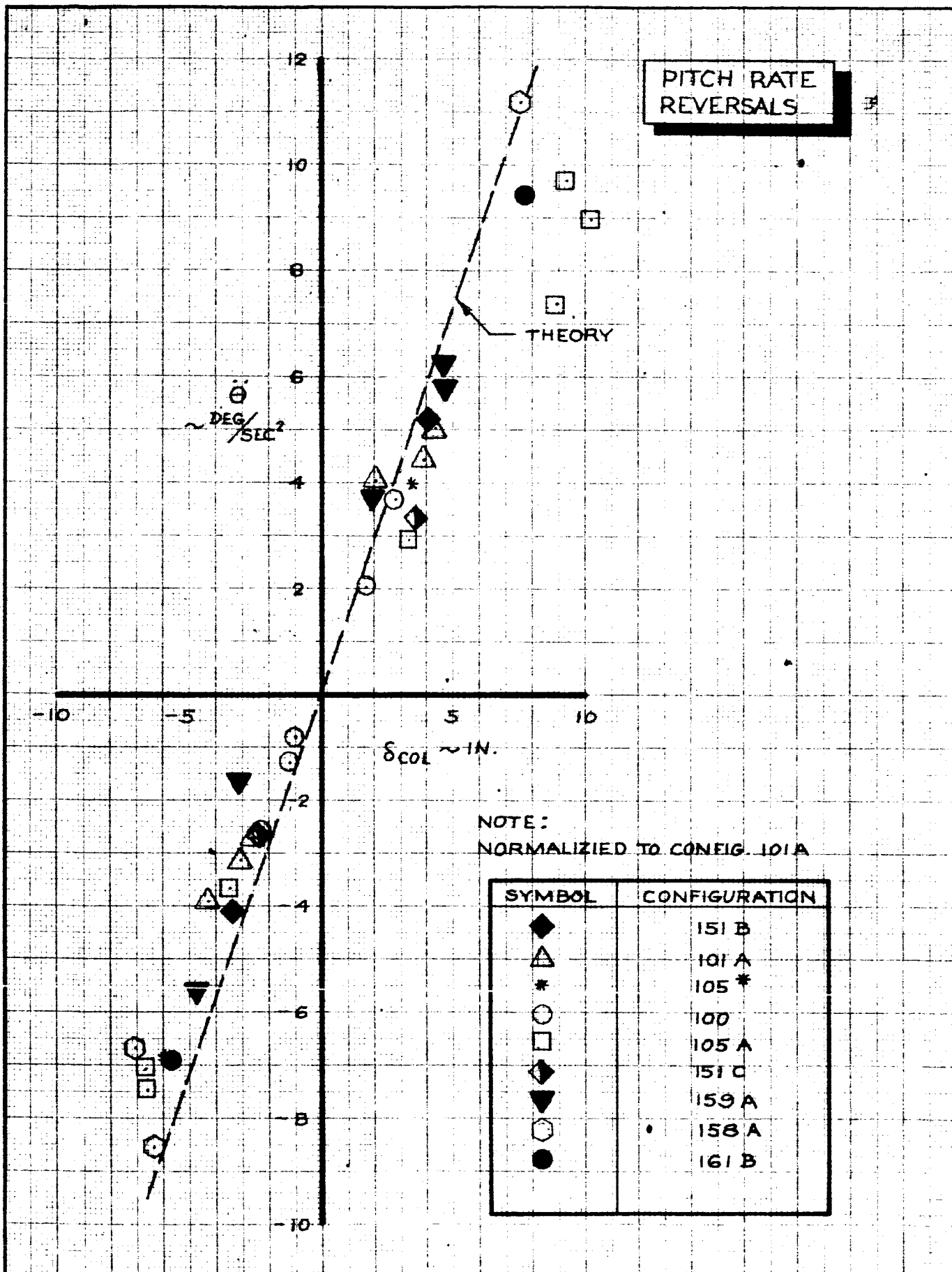
PHUGOID CHARACTERISTICS

CONFIGURATION	PERIOD (SEC)		DAMPING RATIO	
	Flight Test	Theory	Flight Test	Theory
-80B	40.9	46.5	.140	.1244
100	36.6	36.9	.078	.1490
101A	36.0	36.9	.062	.1490
105*	29.6	36.9	.058	.1490
105A	30.0	36.9	.063	.1490
151B	26.2	36.9	.093	.1490
151C	31.2	36.9	.070	.1490
158A	35.8	37.8	.102	.1845
159A	40.8	44.5	.128	.2352
161B	31.3	55.5	.090	.3320

A pitch attitude change is shown for configuration 158A in Fig. 64.

Comparison with the basic 101A configuration (Fig. 9) shows the effect of changing lift with column deflection.

Elevator pulses are shown in Figs. 65 thru 67 for three configurations, 158A, 159A and 161B. Comparison of these pulses with the 101A configuration (Fig. 10) and with one another shows the effect static stability and pitch damping.



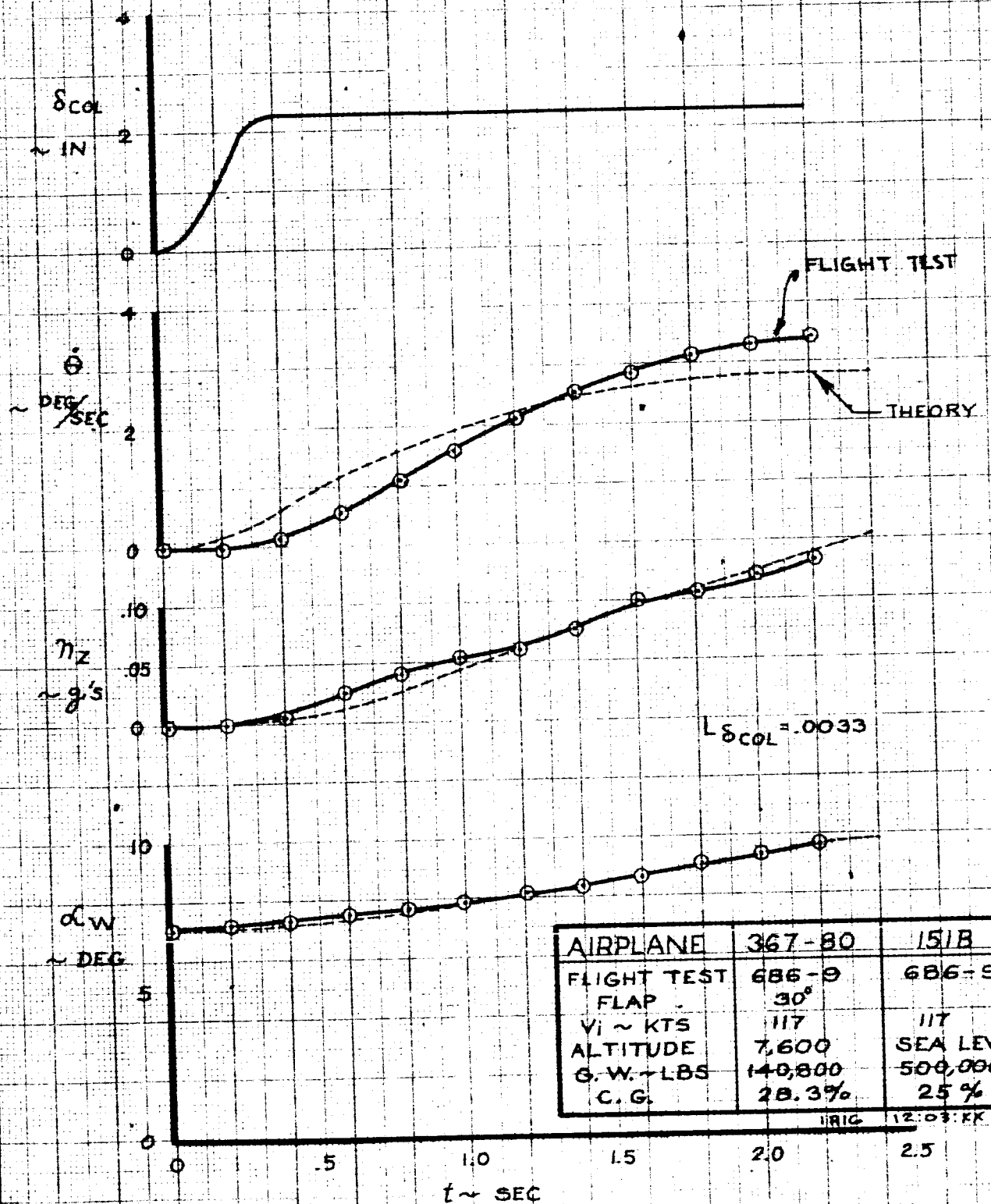
CALC		REVISED	DATE
CHECK			
APR			
APR			

NORMALIZED PITCH RATE REVERSALS - SUMMARY

367-80
FIG. 37
PAGE VII-62

THE BOEING COMPANY
D6-15000

**COLUMN STEP
CONFIGURATION 151B**



AIRPLANE	367-80	151B
FLIGHT TEST	686-9	686-9
FLAP	30°	
V _I ~ KTS	117	117
ALTITUDE	7,600	SEA LEVEL
G. W. ~ LBS	140,800	500,000
C. G.	28.3%	25%

IRIG 12:03:KK

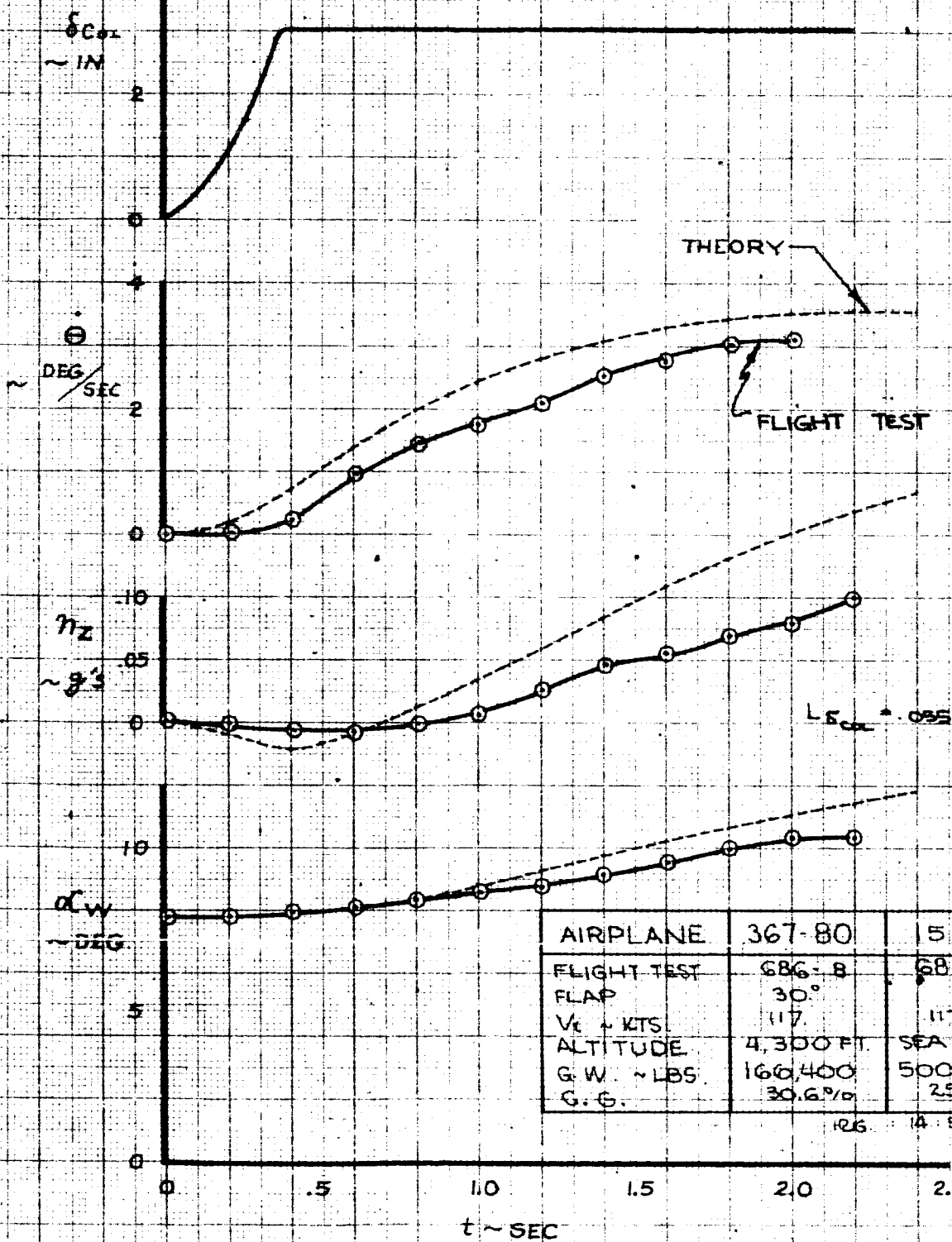
CALC		REVISED	DATE
CHECK			
APR			
APR			

COLUMN STEP
FLIGHT TEST 686-9
CONFIGURATION 151 B

THE BOEING COMPANY
D6-15000

367-80
FIG. 38
PAGE VII-63

**COLUMN STEP
CONFIG. 151C**

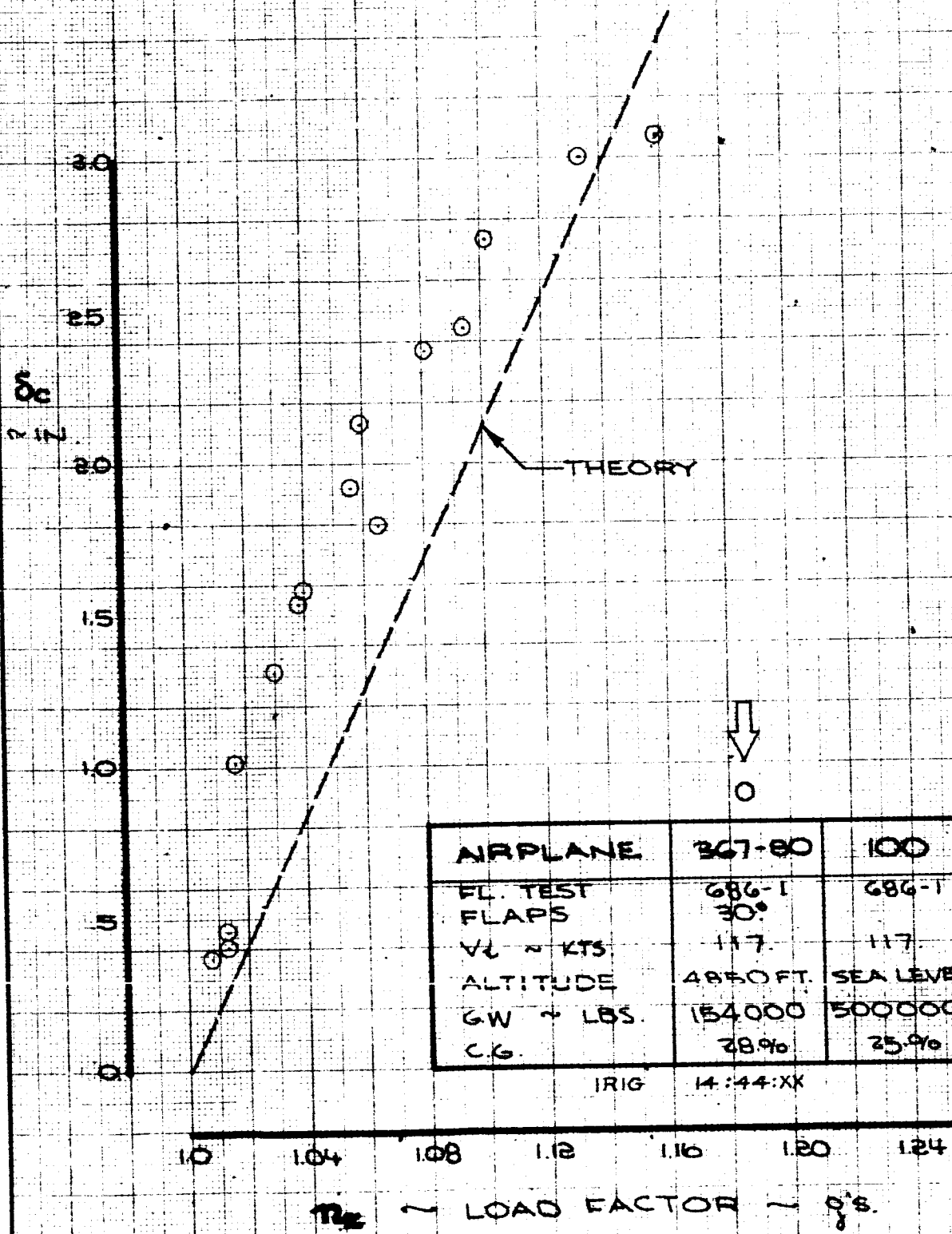


AIRPLANE	367-80	151C
FLIGHT TEST	686-B	686-B
FLAP	30°	
V_e ~ KTS.	117.	117.
ALTITUDE	4,300 FT.	SEA LEVEL
G.W. ~ LBS.	166,400	500,000
G.G.	30.6%	25.0%

1916 14:34:xx

CALC		REVISED	DATE	COLUMN STEP FLIGHT TEST 686-B CONFIGURATION 151C THE BOEING COMPANY DG-15000	367-80
CHECK					FIG. 39
APR					PAGE
APR					VII-64

WINDUP TURN

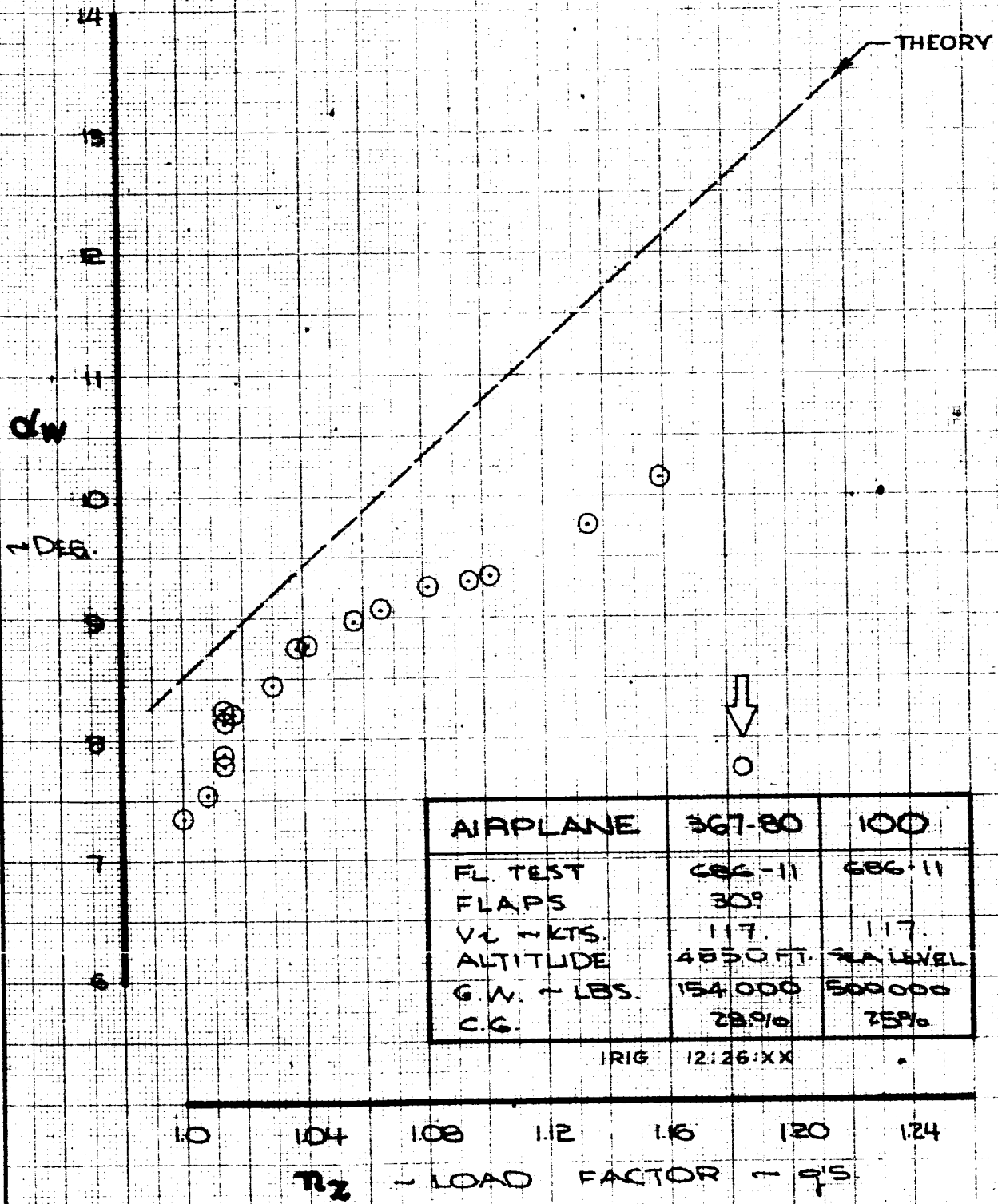


AIRPLANE	367-80	100
FL. TEST	686-1	686-1
FLAPS	30°	
V _L ~ KTS	117	117
ALTITUDE	4850 FT.	SEA LEVEL
GW ~ LBS.	154000	500000
C.G.	28.9%	25.9%

IRIG 14:44:XX

CALC		REVISED	DATE	WINDUP TURN FL. TEST : 686-1 CONFIG. : 100 THE BOEING COMPANY DG-15000	367-80
CHECK					FIG. 40
APR					PAGE
APR					VII-65

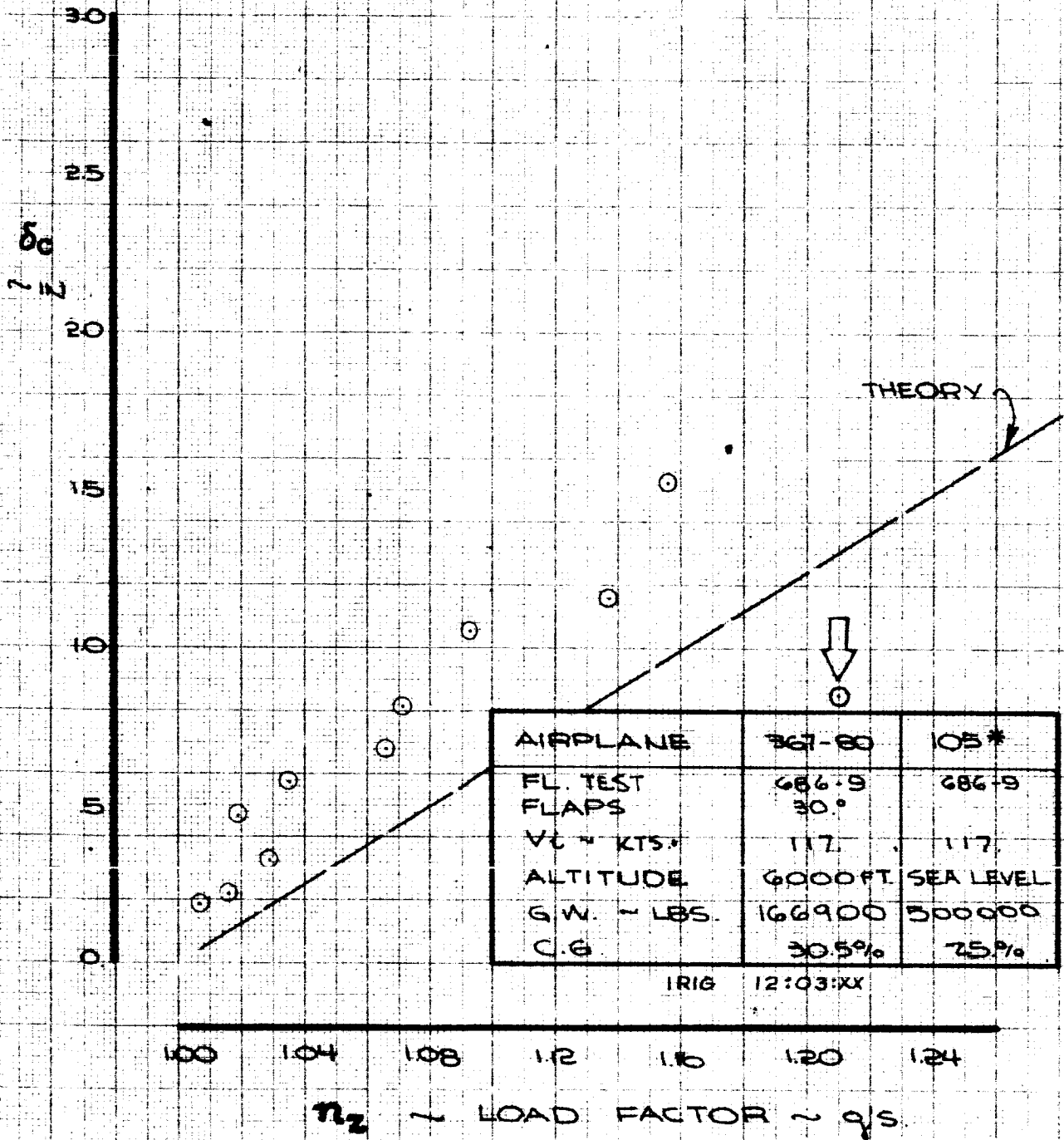
WINDUP TURN



CALC			REVISED	DATE	WINDUP TURN FL. TEST : 686-11 CONFIG. : 100	367-80
CHECK						FIG.41
APR						PAGE
APR						VII-66
					THE BOEING COMPANY DG-15000	

109

WINDUP TURN



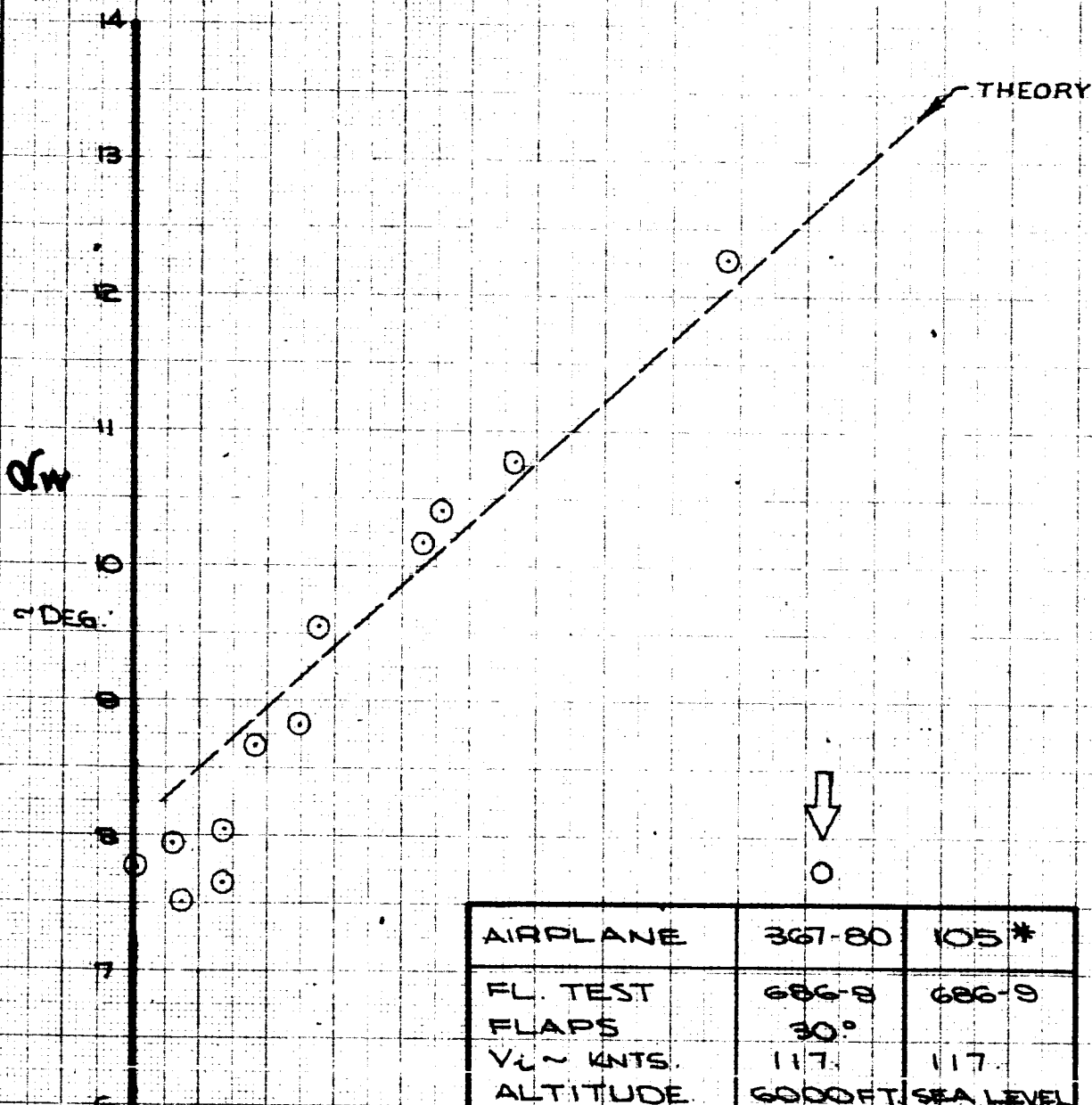
AIRPLANE	367-80	105*
FL. TEST	686.9	686.9
FLAPS	30°	
V _C ~ KTS.	117	117
ALTITUDE	6000 FT. SEA LEVEL	
G.W. ~ LBS.	166900	300000
C.G.	30.5%	25%

IRIG 12:03:XX

CALC		REVISED	DATE	WINDUP TURN FL. TEST : 686.9 . CONFIG. 105 *	367-80
CHECK					FIG. 42
APR					
APR					THE BOEING COMPANY D6-15000

70

WINDUP TURN



AIRPLANE	367-80	105*
FL. TEST	686-8	686-9
FLAPS	30°	
V _L ~ KNTS.	117.	117.
ALTITUDE	6000 FT.	SEA LEVEL
G.W. ~ LBS.	166000	500000
C.G.	30.5%	25%

RIG 12:03:XX

1.0 1.04 1.08 1.12 1.16 1.20 1.24

n_z ~ LOAD FACTOR ~ 9/5

CALC		REVISED	DATE	WINDUP TURN FL. TEST: 686-9 CONFIG. : 105*	367-80
CHECK					FIG.43
APR					THE BOEING COMPANY
APR					D6-15000
					PAGE VII-68

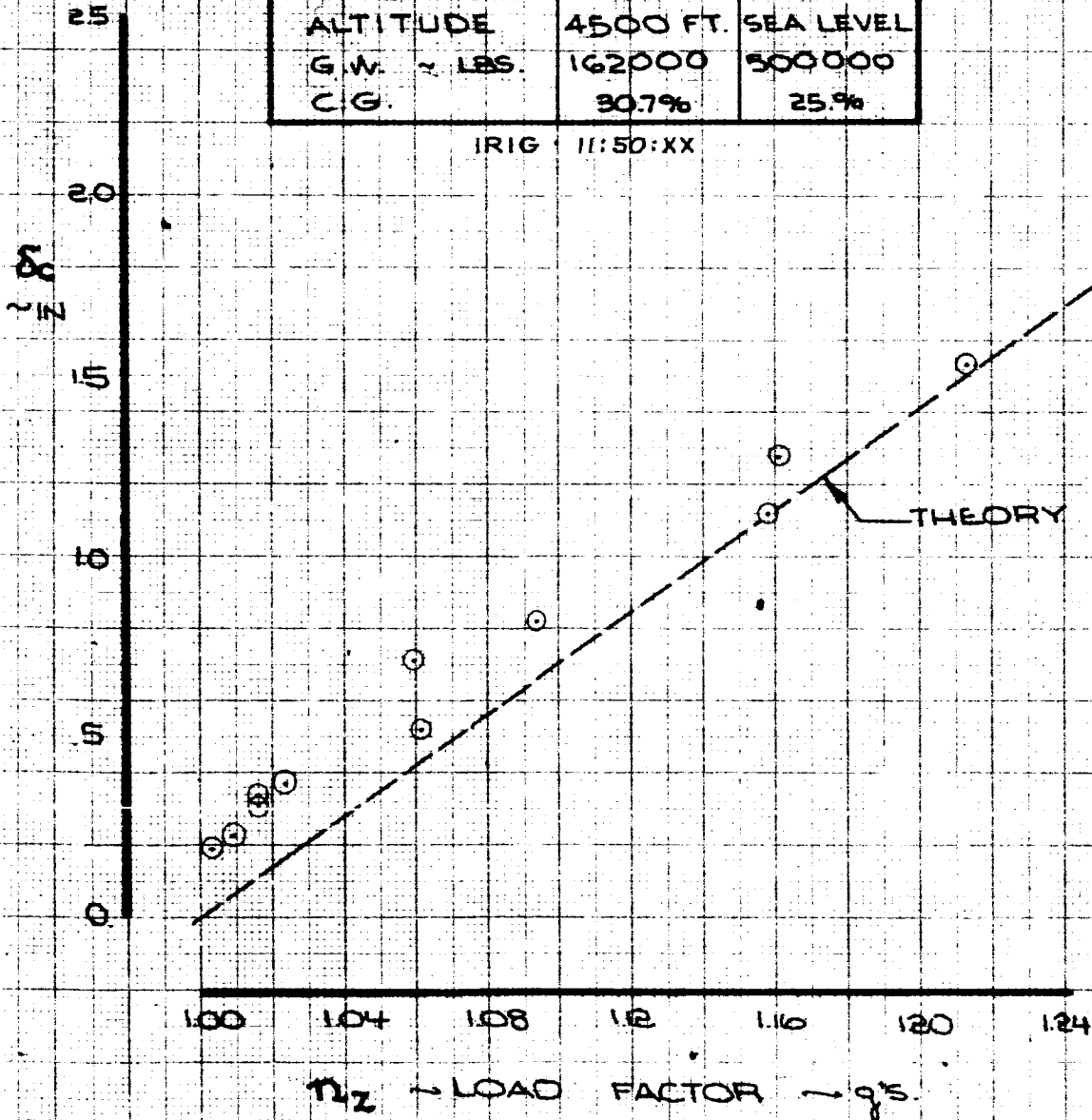
WINDUP TURN



○

AIRPLANE	367-80	105A
FL. TEST	686-7	686-7
FLAPS	30°	
VE (KTS)	117	117
ALTITUDE	4500 FT.	SEA LEVEL
G.W. (LBS)	162000	500000
C.G.	30.7%	25%

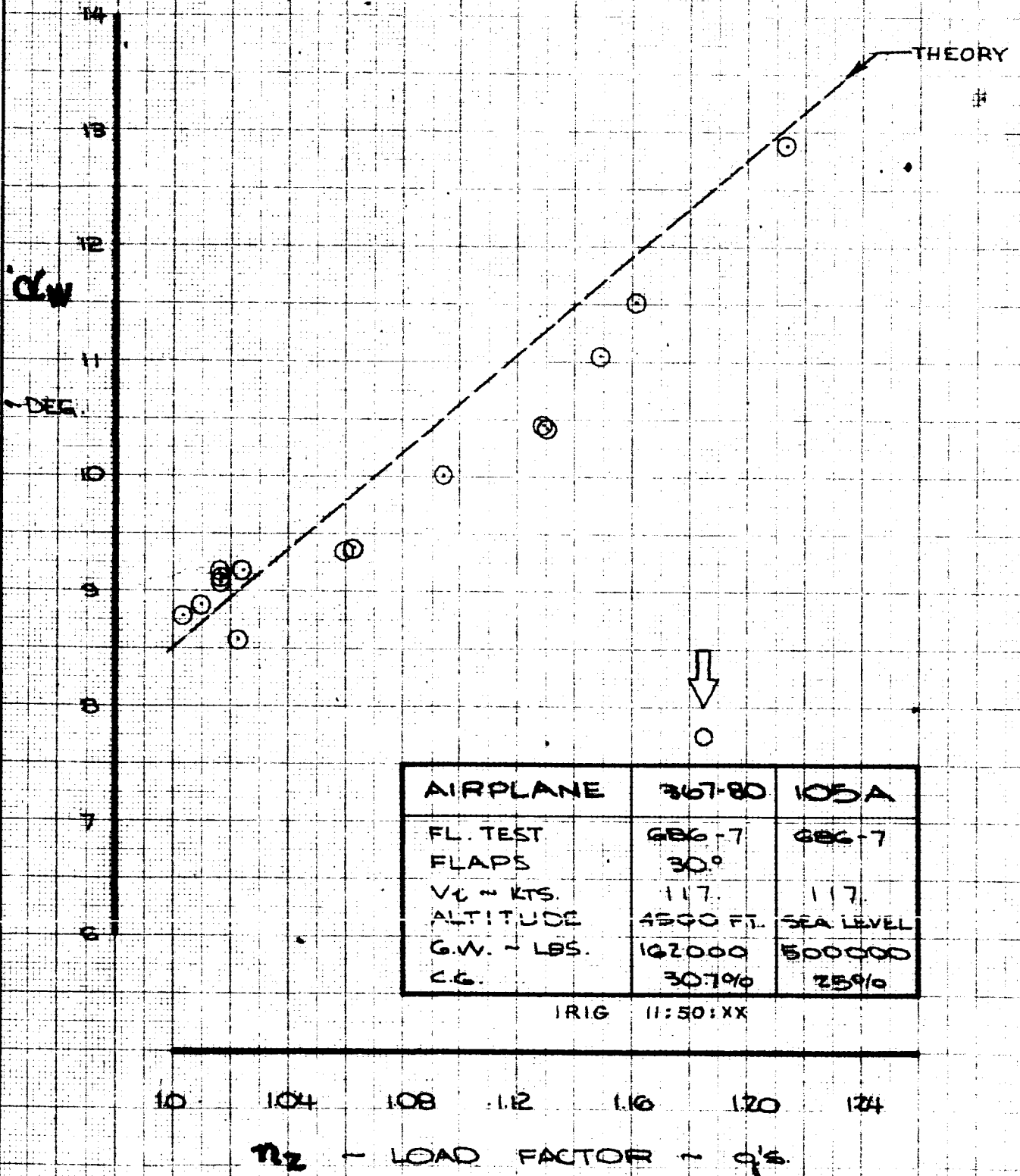
IRIG 11:50:XX



CALC			REVISED	DATE	WINDUP TURN	367-80
CHECK					FL. TEST : 686-7	
APR					CONFIG. : 105A	FIG. 44
APR					THE BOEING COMPANY	PAGE VII-69
					D6-15000	

72

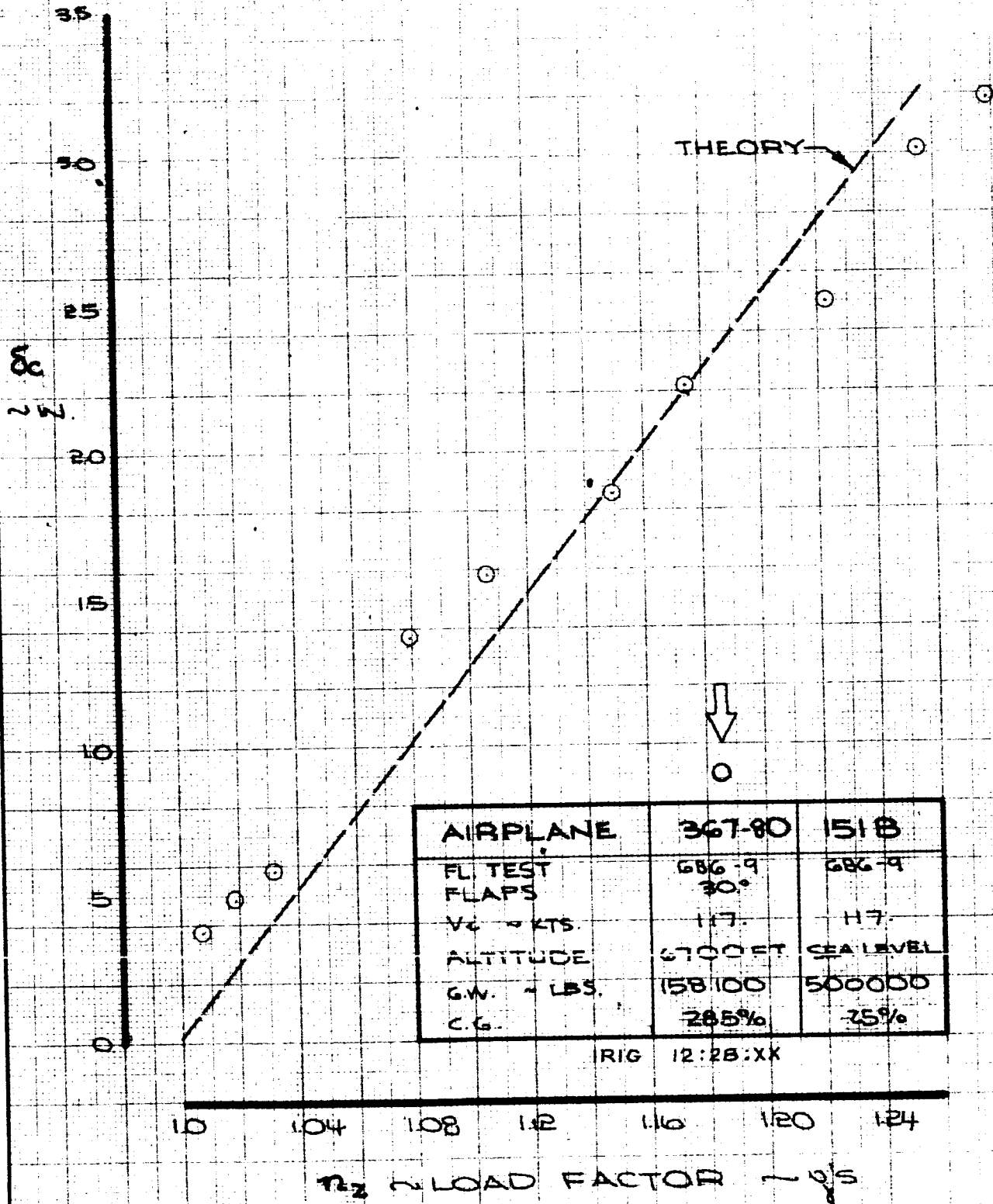
WINDUP TURN



CALC		REVISED	DATE	WINDUP TURN FL. TEST : 686-7 CONFIG. : 105A THE BOEING COMPANY D6-15000	105A
CHECK					FIG. 45
APR					PAGE
APR					VII-70

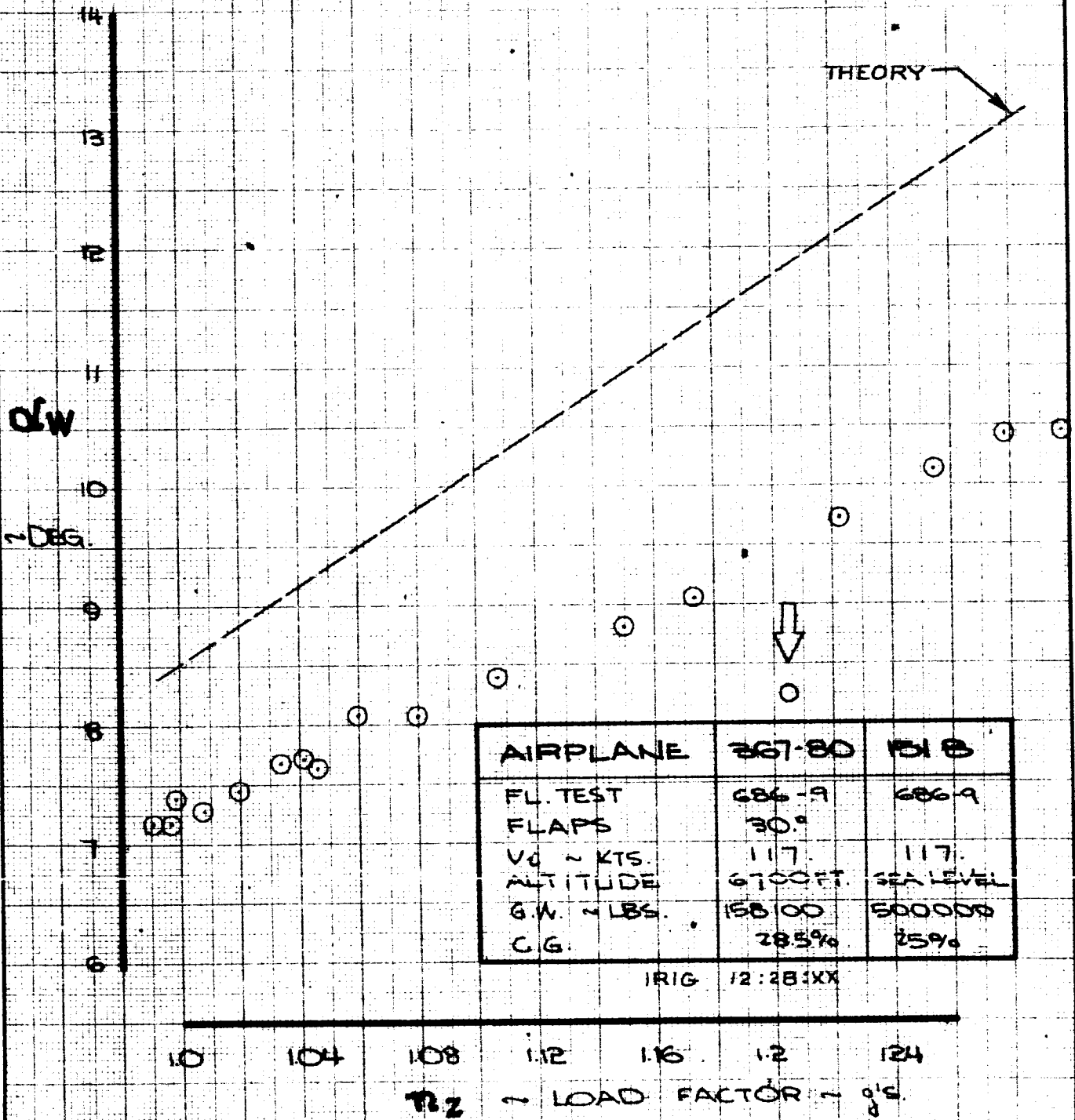
73

WINDUP TURN



CALC		REVISED	DATE	WINDUP TURN FL. TEST: 686-9 CONFIG. 151B THE BOEING COMPANY D6-15000	367-80
CHECK					FIG. 46
APR					PAGE
APR					VII-71

WINDUP TURN



AIRPLANE	267-80	151B
FL. TEST	686-9	686-9
FLAPS	30°	
V_0 ~ KTS.	117	117
ALTITUDE	6700 FT.	SEA LEVEL
G.W. ~ LBS.	15800	50000
C.G.	28.5%	25%

IRIG 12:28:XX

CALC		REVISED	DATE
CHECK			
APR			
APR			

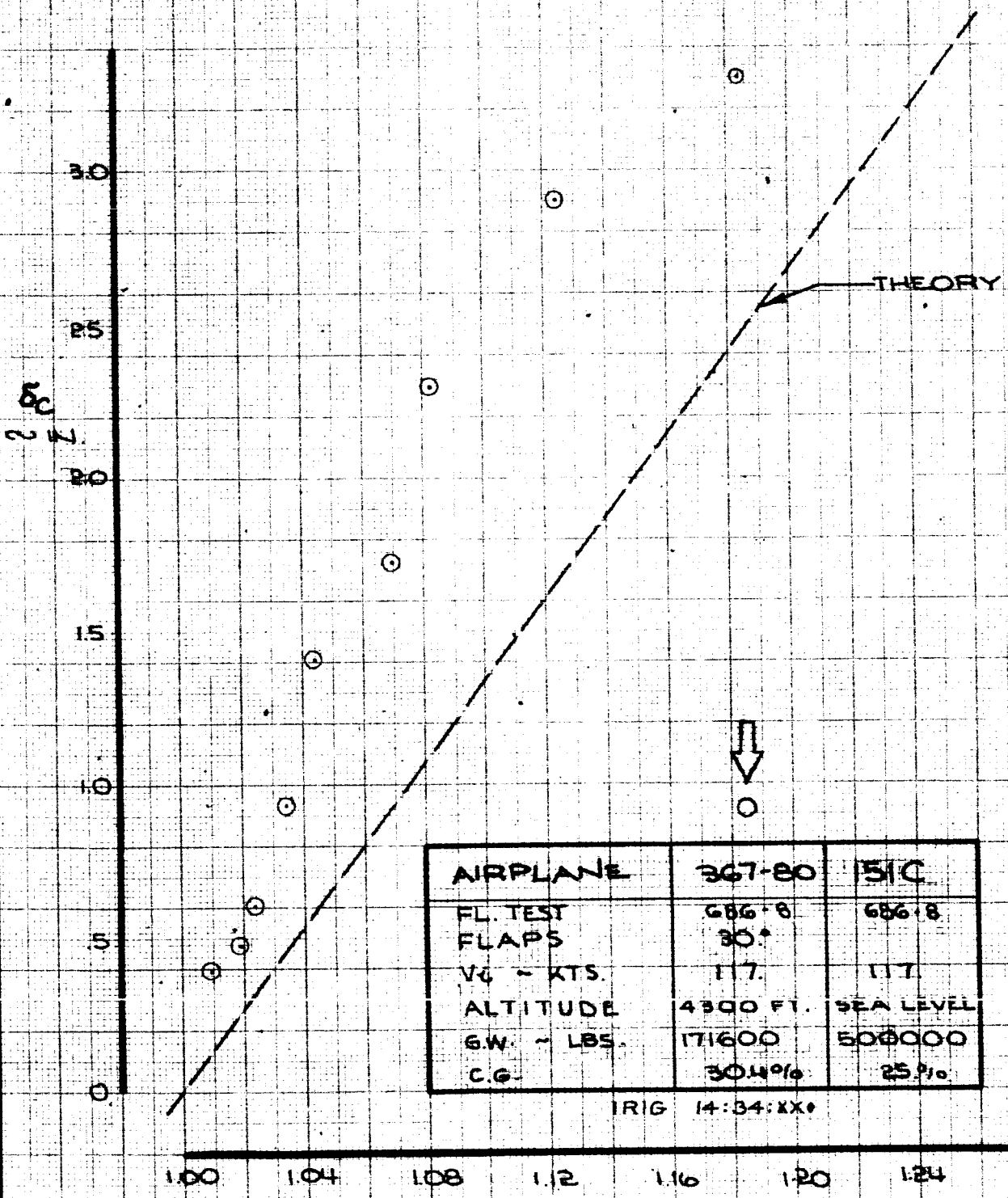
WINDUP TURN
 FL. TEST : 686-9
 CONFIG. : 151B

THE BOEING COMPANY
 DG-15000

151-B
 FIG. 47
 PAGE VII-72

75

WINDUP TURN



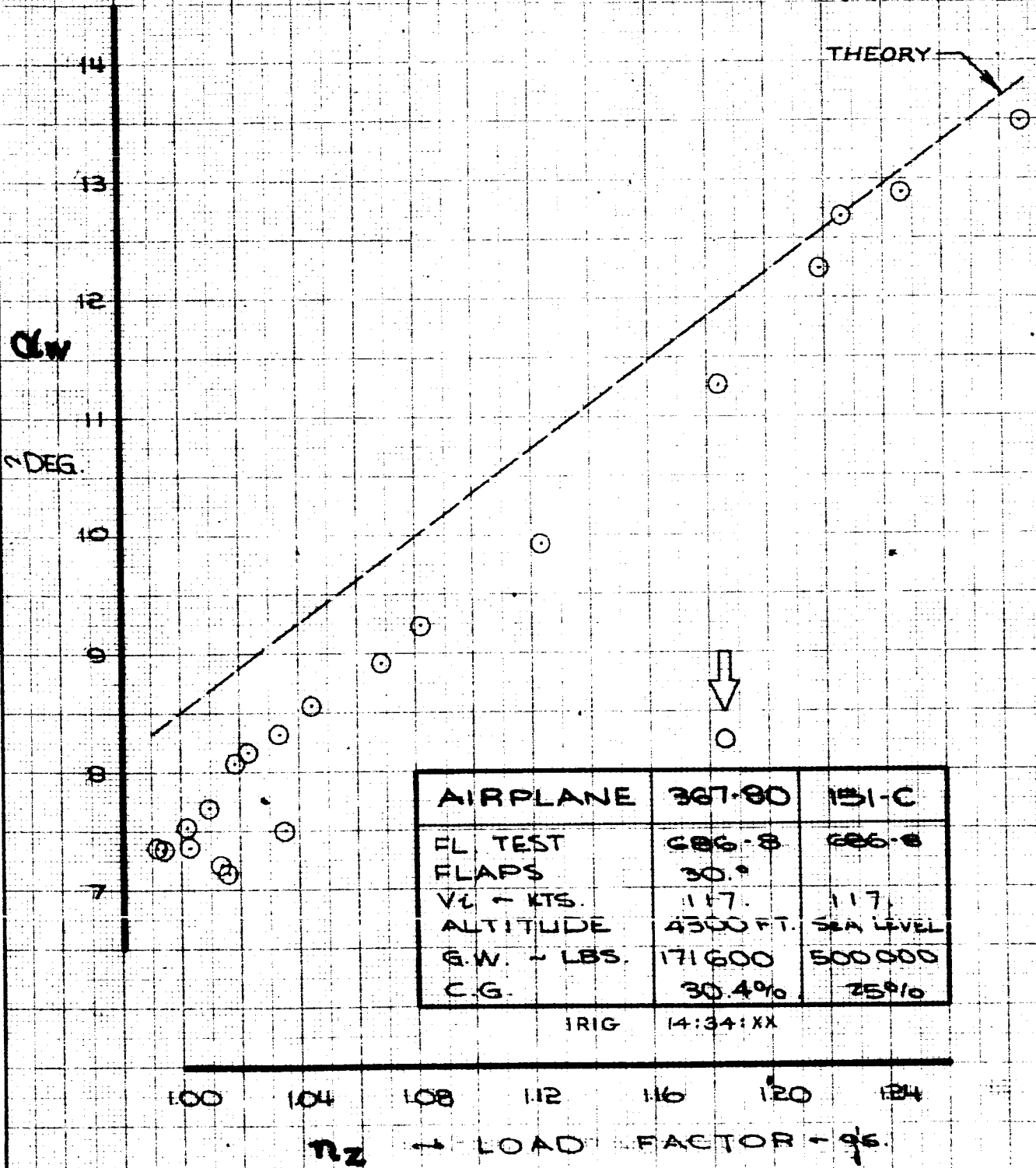
AIRPLANE	367-80	151C
FL. TEST	686-8	686-8
FLAPS	30°	
V ₀ - KTS.	117	117
ALTITUDE	4300 FT.	SEA LEVEL
G.W. - LBS.	171600	500000
C.G.	30.4%	25%

IRIG 14:34:XX*

$n_z \sim$ LOAD FACTOR \sim g's.

CALC			REVISED	DATE	WINDUP TURN FL. TEST. : 686-8 CONFIG. 151C	367-80
CHECK						FIG. 48
APR						PAGE
APR					THE BOEING COMPANY	VII-73
					D6-15000	

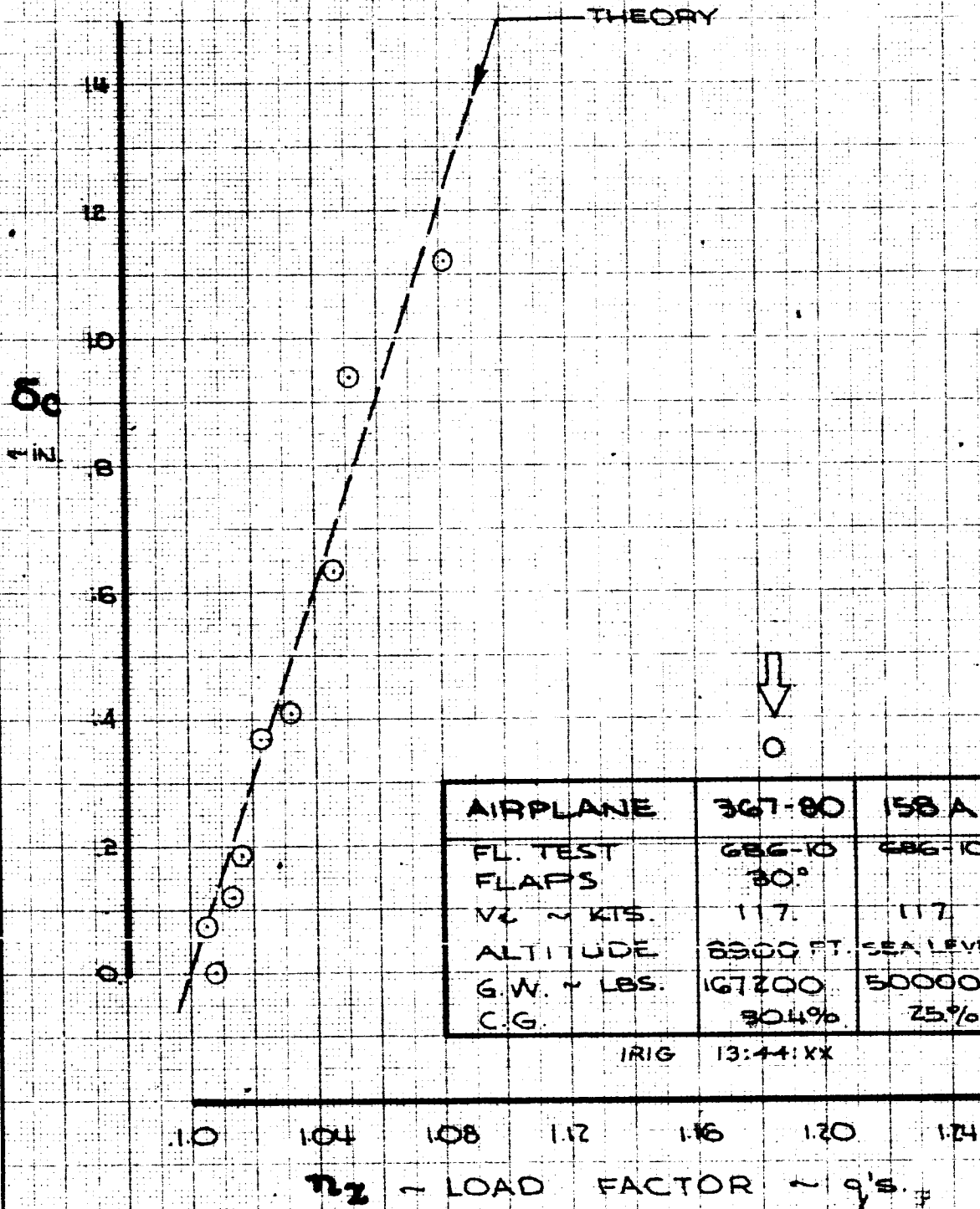
WINDUP TURN



CALC		REVISED	DATE	WINDUP TURN FL. TEST : 686-B CONFIG. : 151-C	151-C	
CHECK					FIG. 49	
APR					THE BOEING COMPANY	PAGE VII-74
APR					D6-15000	

77

WINDUP TURN



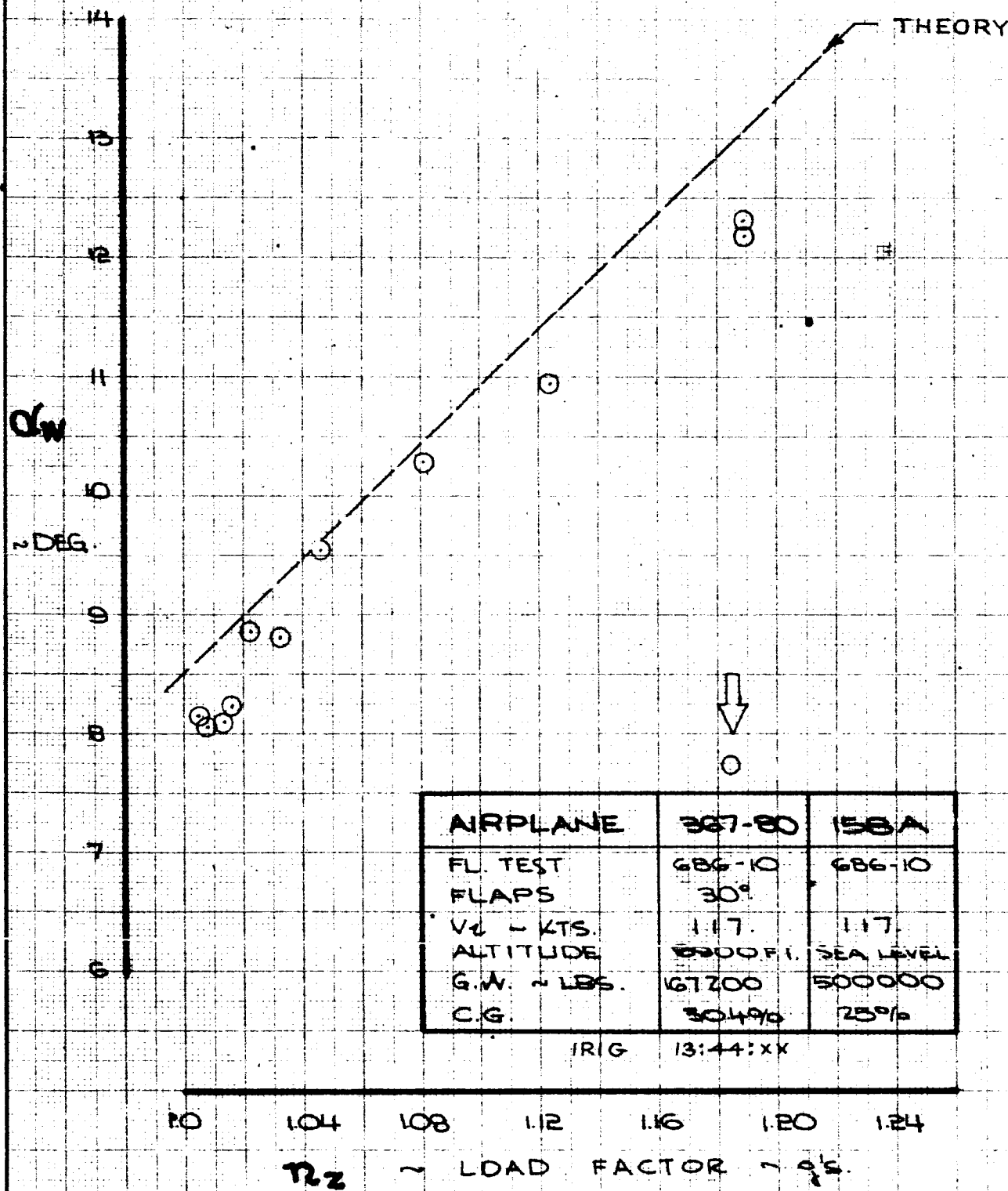
AIRPLANE	367-80	158A
FL. TEST	686-10	686-10
FLAPS	30°	
V _L ~ KTS.	117	117
ALTITUDE	6500 FT.	SEA LEVEL
G.W. ~ LBS.	167200	500000
C.G.	304%	75%

IRIG 13:44:XX

IRIG 13-44-18

CALC			REVISED	DATE	WINDUP TURN FL. TEST: 686-10 CONFIG.: 158A THE BOEING COMPANY DG-15000	367-80
CHECK						FIG. 50
APR						PAGE
APR						VII-75

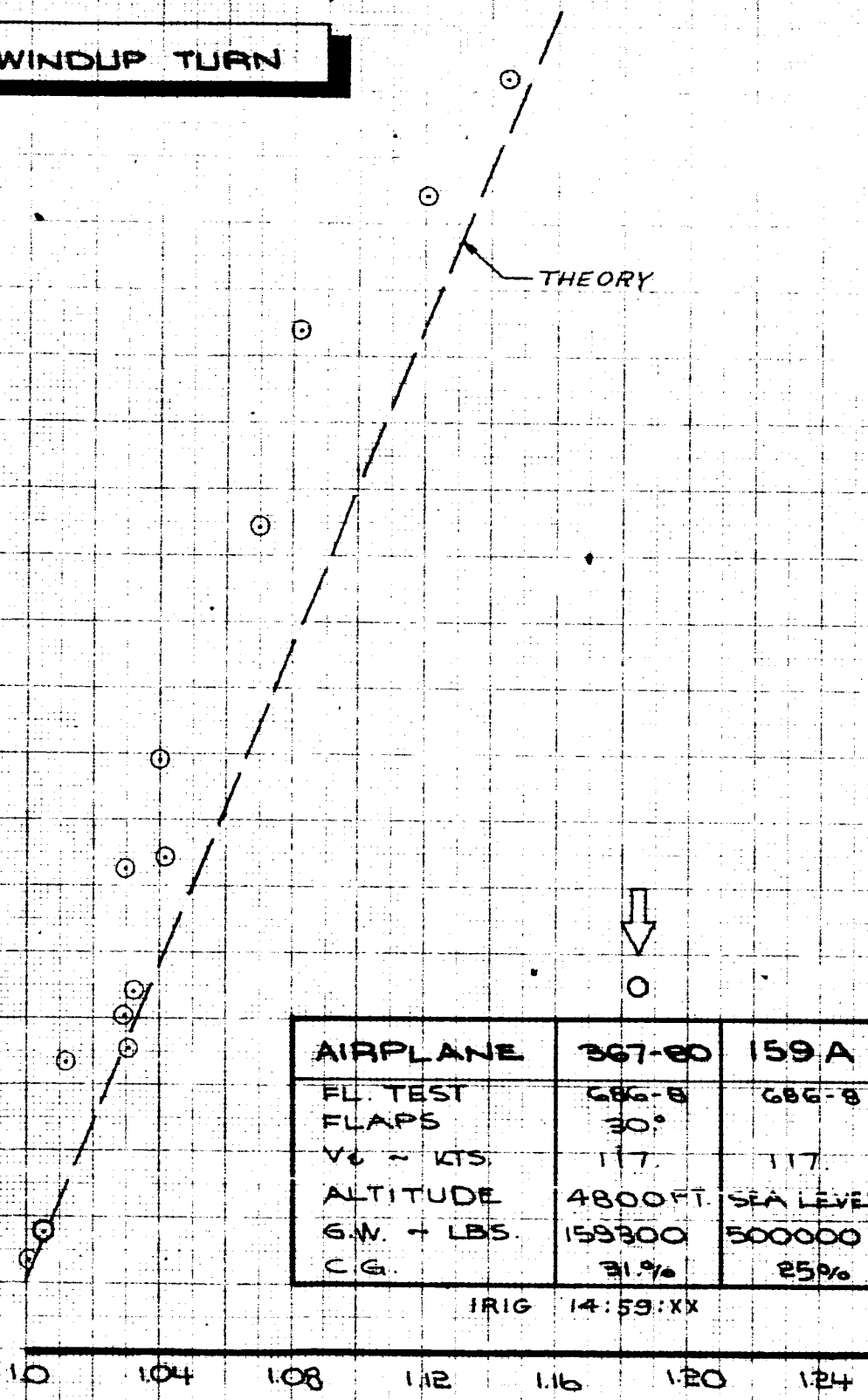
WINDUP TURN



CALC			REVISED	DATE	WINDUP TURN FL. TEST. 686-10 CONFIG. : 158A THE BOEING COMPANY DG-15000	158A
CHECK						FIG. 51
APR						PAGE
APR						VII-76

WINDUP TURN

n_z
 30
 25
 20
 15
 10
 5
 0



AIRPLANE	367-80	159A
FL. TEST	686-B	686-B
FLAPS	30°	
V ₀ - KTS.	117	117
ALTITUDE	4800 FT.	SEA LEVEL
G.W. - LBS.	159300	500000
C.G.	31%	25%

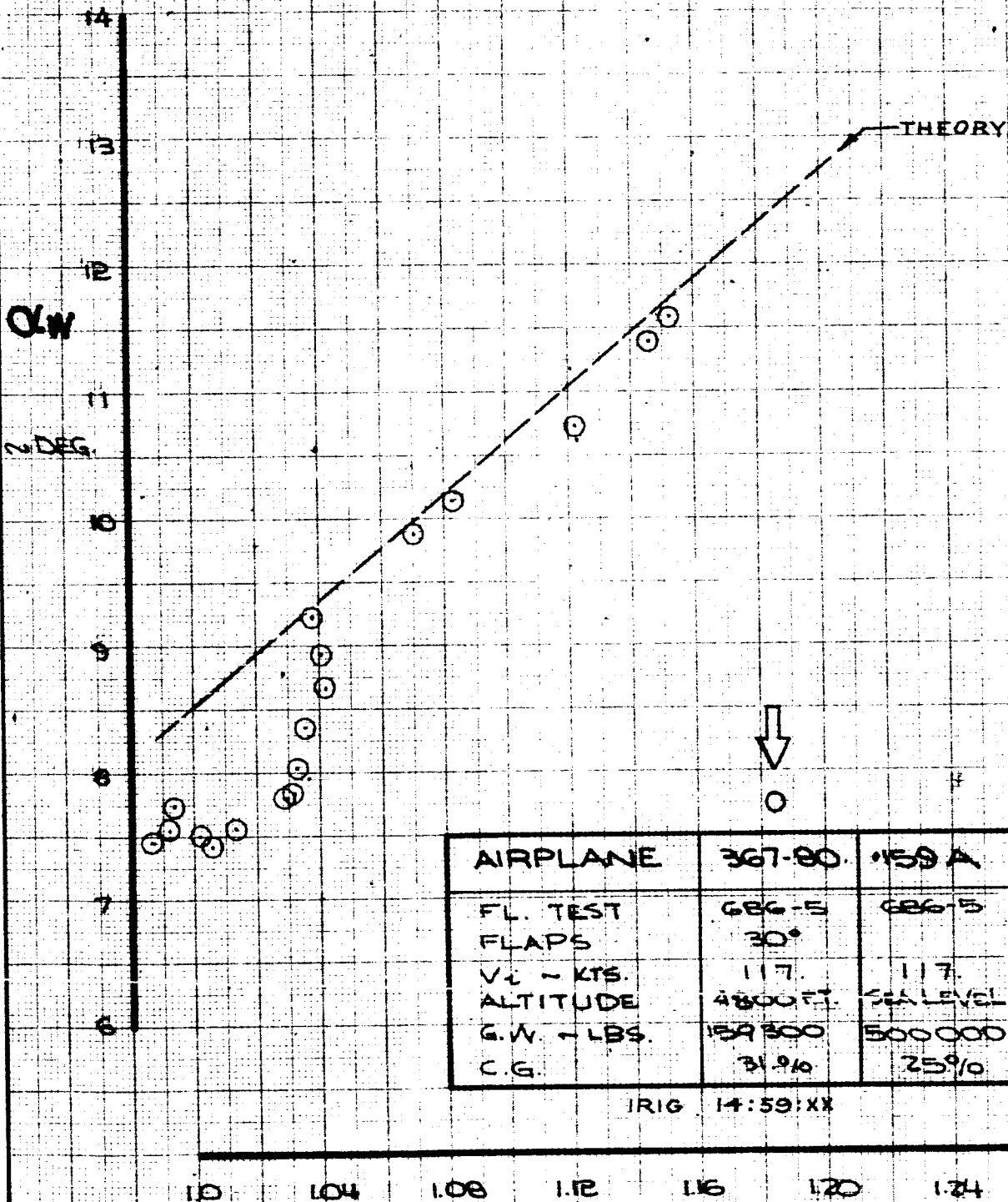
IRIG 14:59:XX

1.0 1.04 1.08 1.12 1.16 1.20 1.24

n_z ~ LOAD FACTOR - g's.

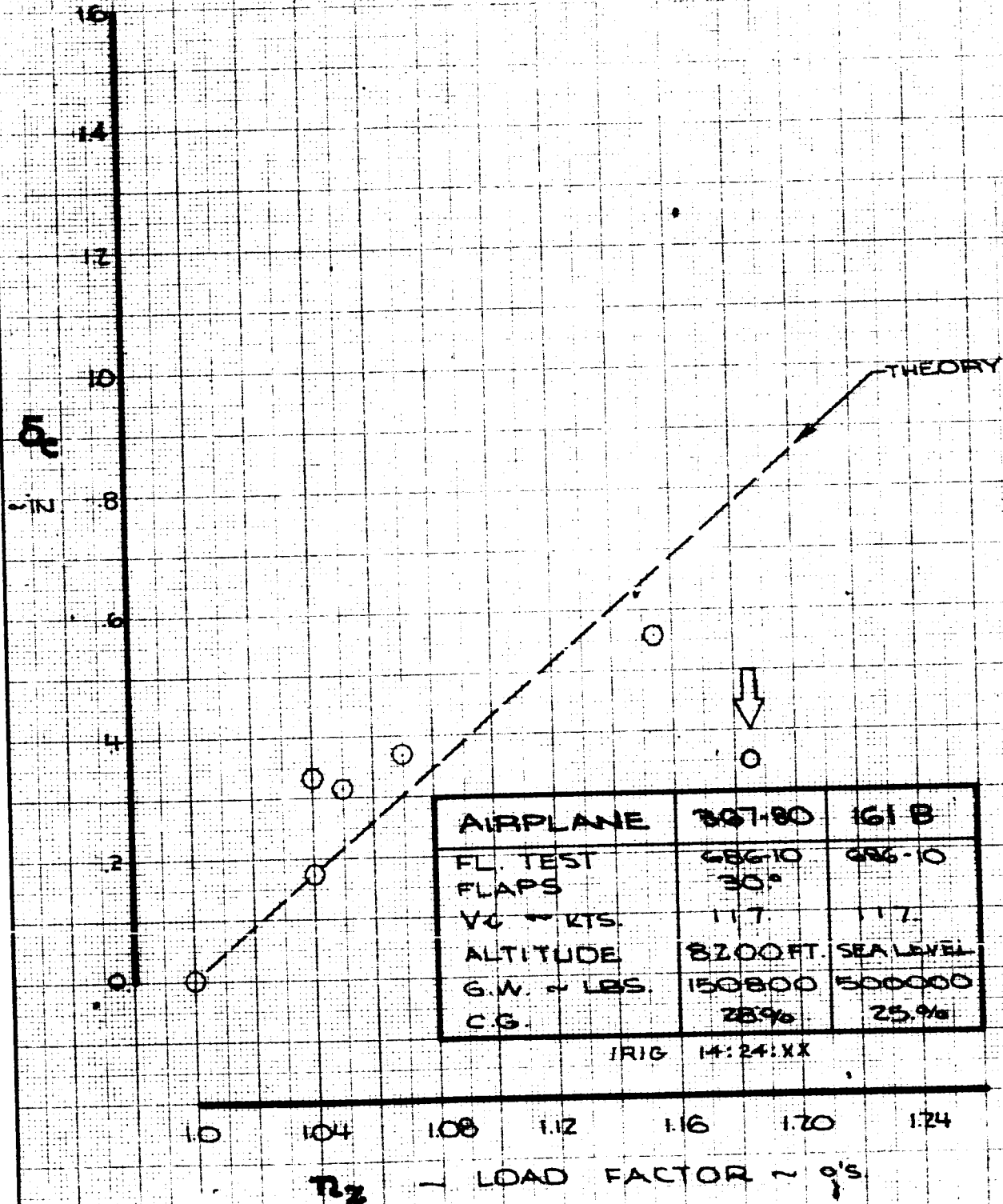
CALC			REVISED	DATE	WINDUP TURN FL. TEST : 686-B CONFIG. 159A THE BOEING COMPANY DG-15000	367-80
CHECK						FIG. 52
APR						
APR						PAGE VII-77

WINDUP TURN



CALC		REVISED	DATE	WINDUP TURN FL. TEST : 686-5 CONFIG. : 159A	159A	
CHECK					FIG. 53	
APR					THE BOEING COMPANY DG-15000	PAGE
APR						VII-78

WINDUP TURN



AIRPLANE	367-80	161 B
FL. TEST	686-10	686-10
FLAPS	30°	
V _C ~ KTS.	117	117
ALTITUDE	8200 FT.	SEA LEVEL
G.W. ~ LBS.	150800	500000
C.G.	28%	25%

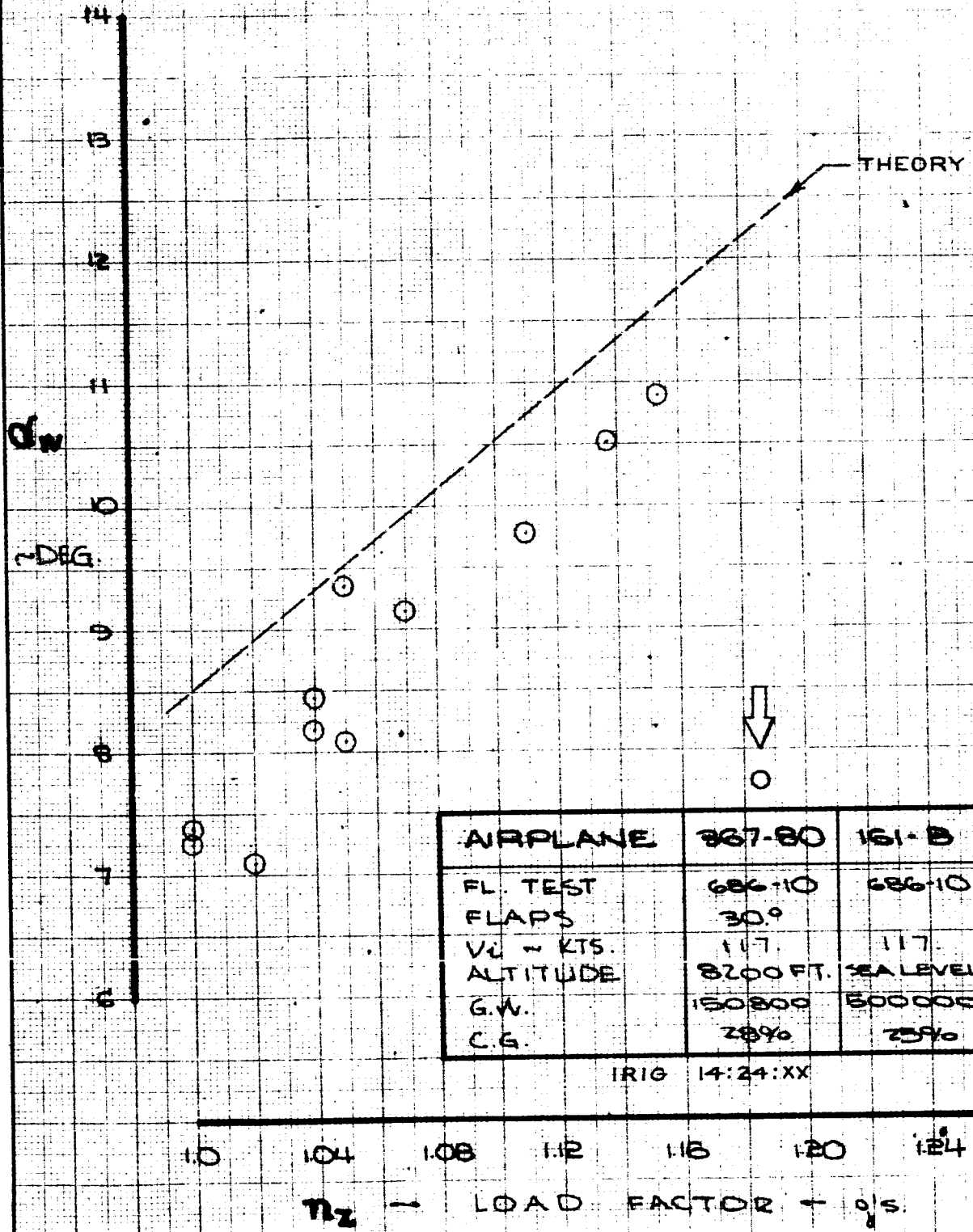
IRIG 14:24:XX

1.0 1.04 1.08 1.12 1.16 1.20 1.24

n_z — LOAD FACTOR ~ 9's

CALC			REVISED	DATE	WINDUP TURN FL. TEST : 686-10 CONFIG. : 161 B THE BOEING COMPANY 26-15000	367-80
CHECK						FIG. 54
APR						PAGE
APR						VII-79

WINDUP TURN



AIRPLANE	767-80	161-B
FL. TEST	686-10	686-10
FLAPS	30°	
V _L - KTS.	117	117
ALTITUDE	8200 FT.	SEA LEVEL
G.W.	150800	500000
C.G.	28%	25%

IRIG 14:24:XX

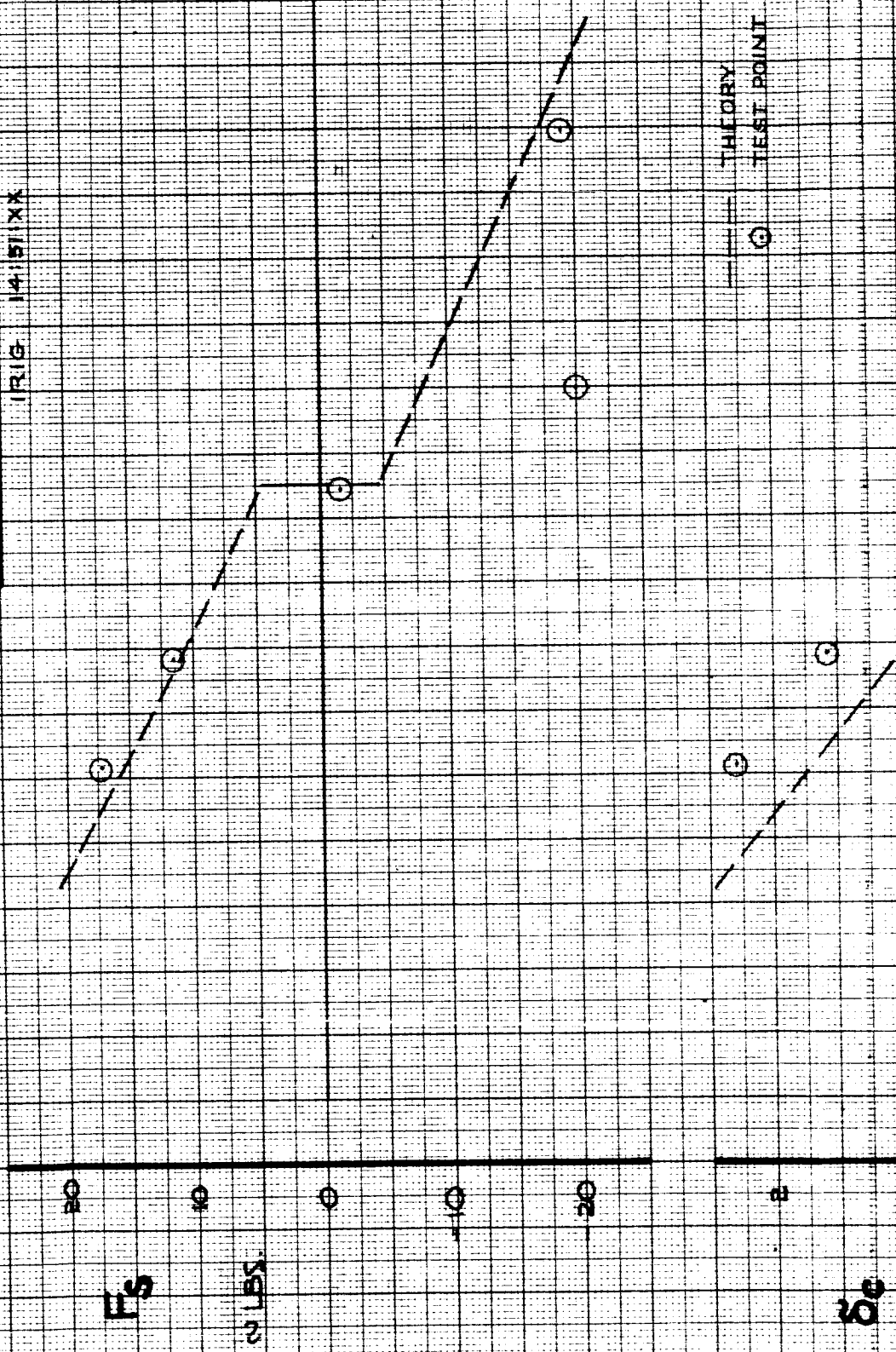
CALC			REVISED	DATE	WINDUP TURN FL. TEST : 686-10 CONFIG. : 161B THE BOEING COMPANY DG-15000	161 B
CHECK						FIG.55
APR						PAGE
APR						VII-80

23

SPEED STABILITY

AIRPLANE :	367-80	100
FL. TEST	686-1	686-1
FLAPS	30°	
V _R - KTS	117	117
ALTITUDE	4800 FT. SEA LEVEL	
G.W. - LBS.	154000	150000
C.G.	25% _{MAC}	25% _{MAC}

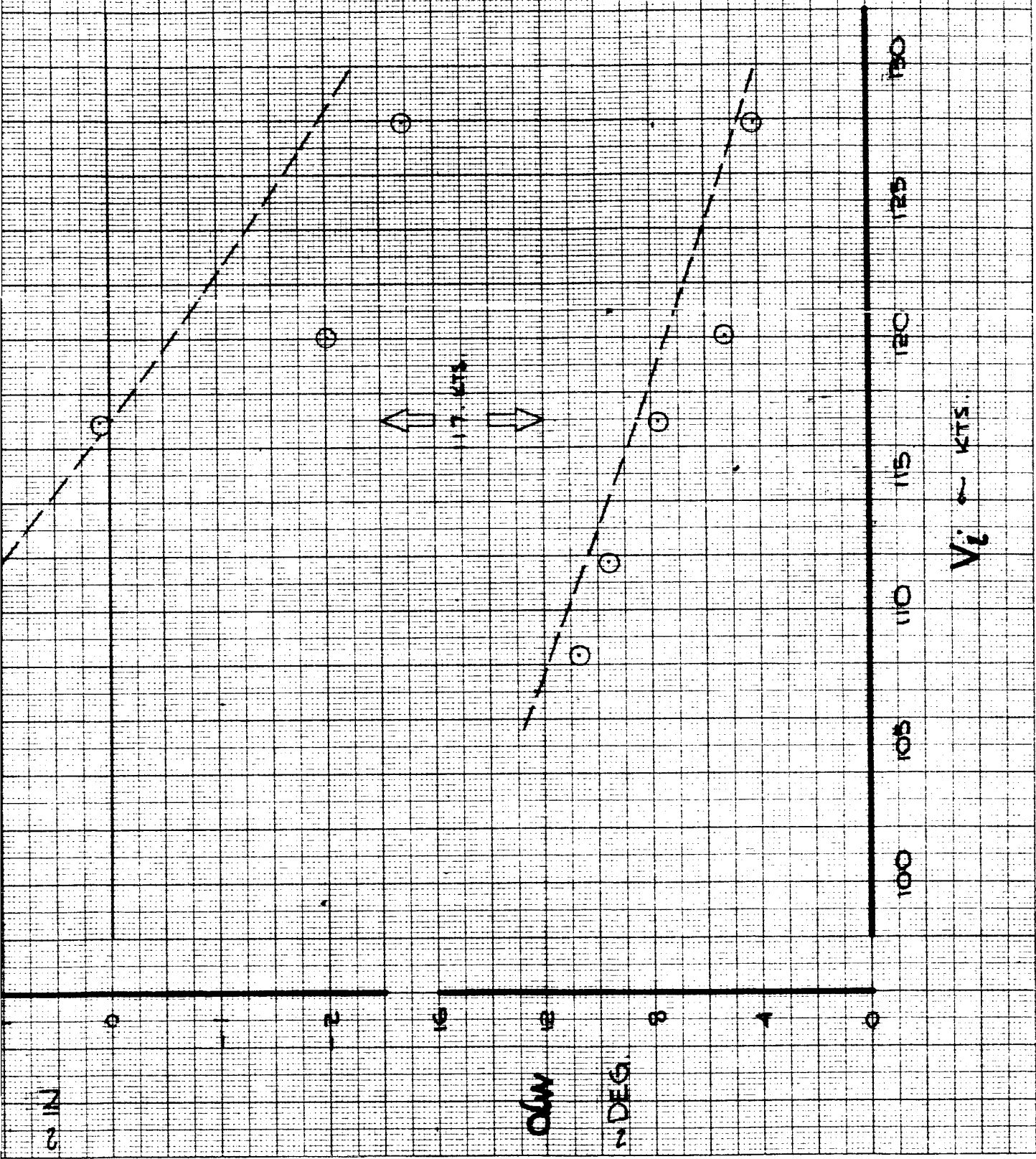
IRIG 14-151XX



THEORY
TEST POINT

CALC		REVISED	DATE	SPEED STABILITY FL. TEST : 686-1 CONFIG. : 100 THE BOEING COMPANY DG-15000	367-80
CHECK					FIG. 56
APPD.					PAGE
APPD.					VII-31

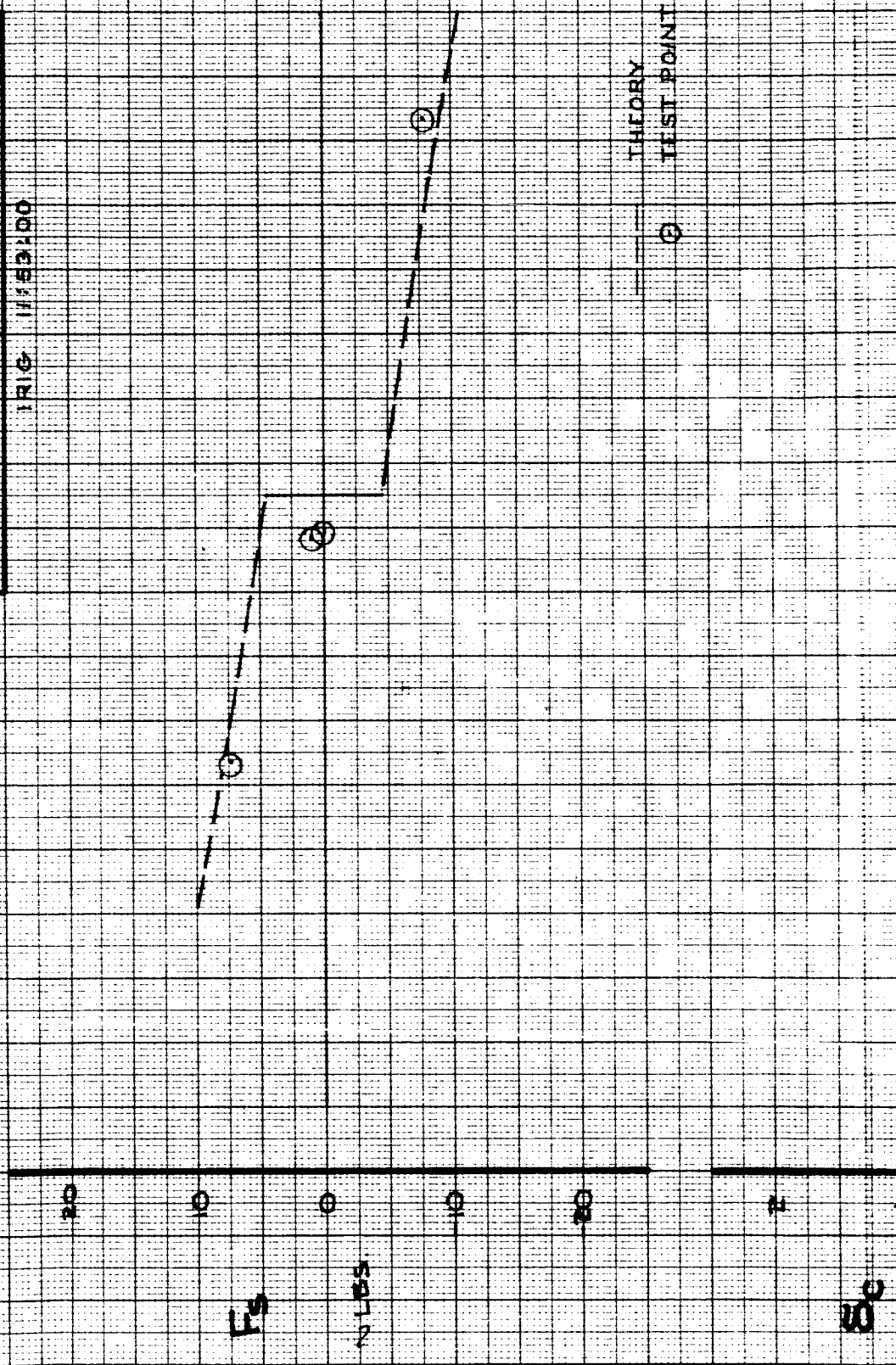
VII-81
1/2



SPEED STABILITY

AIRPLANE	367-80	105-A
FL TEST	686-7	686-7
FLAPS	30°	
VL + KTS	117	117
ALTITUDE	4000 FT.	SEA LEVEL
G.W. + LBS.	151600	500000
S.G.	25.9%	25%

TRIG 11:53:00



CALC		REVISED	DATE
CHECK			
APPD.			
APPD.			

SPEED STABILITY
 FL. TEST : 686-7
 CONFIG. 105-A

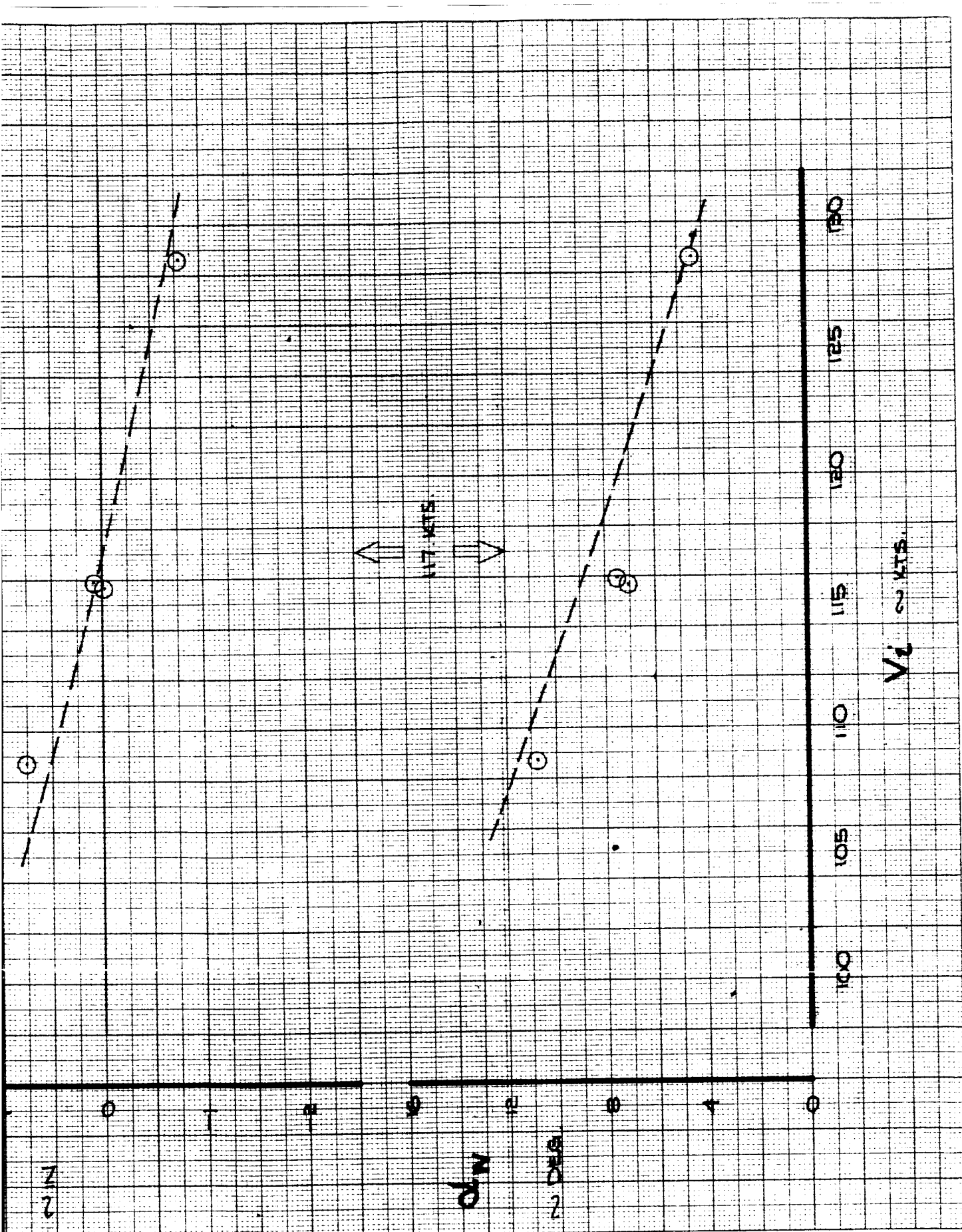
367-80
 FIG. 57

THE BOEING COMPANY
 D6-15000

PAGE
 VII-32

52

—



VII-82
29

98

SPEED STABILITY

AIRPLANE :	367-80	105*
FL TEST	686-9	686-9
FLAPS	30°	
V ₂ KTS	117	117
ALTITUDE	5000 FT. SEA LEVEL	
GW - LBS.	170000	800000
C.G.	30.5%	25%

IRIG 12:05:1X

20
10
0
-10
-20
-30

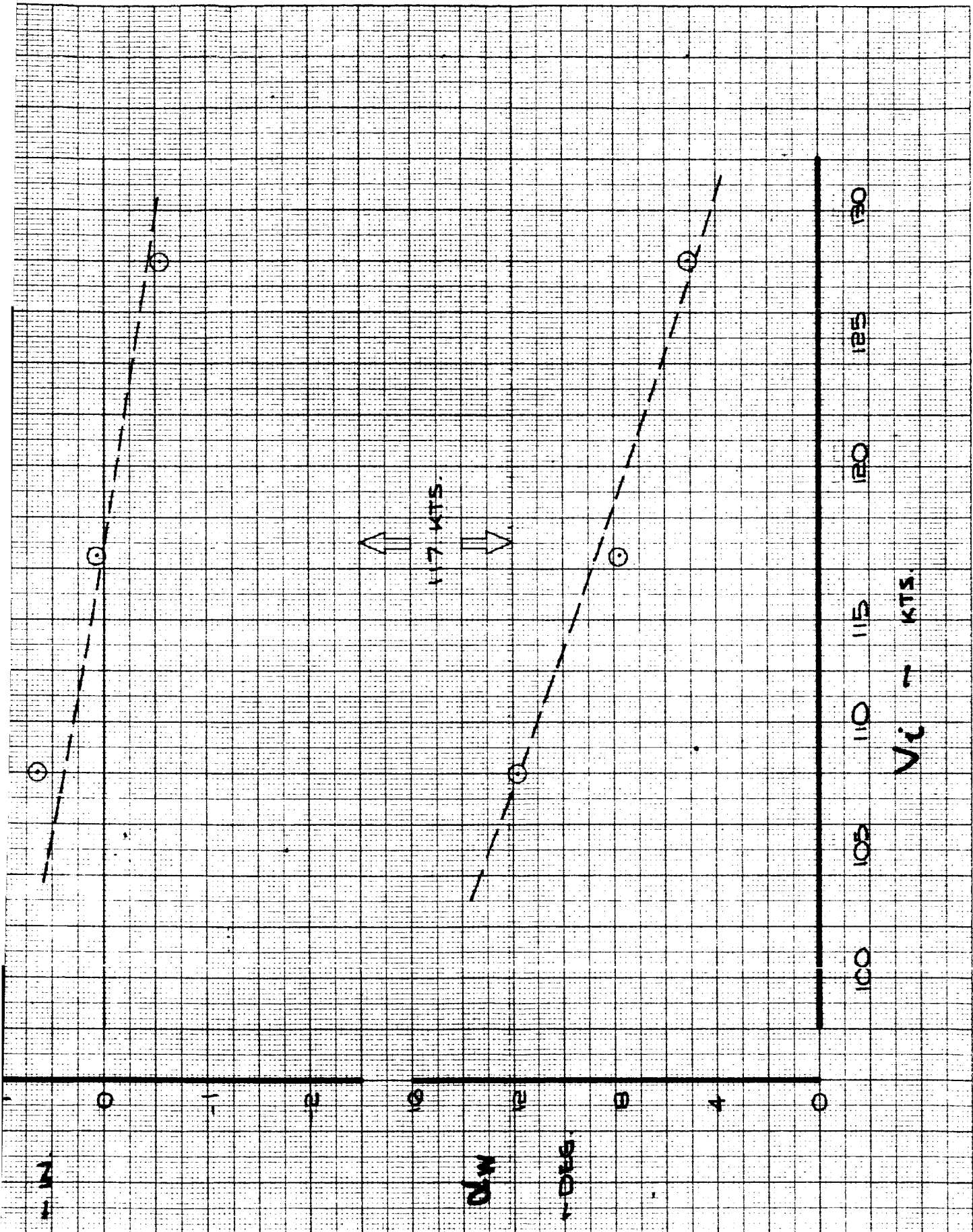
F_s

~LBS.

30

--- THEORY
○ TEST POINT

CALC		REVISED	DATE	SPEED STABILITY FL. TEST : 686-9 CONFIG. : 105*	367-80
CHECK					FIG. 58
APPD.				THE BOEING COMPANY	PAGE VII-33
APPD.				D6-15000	

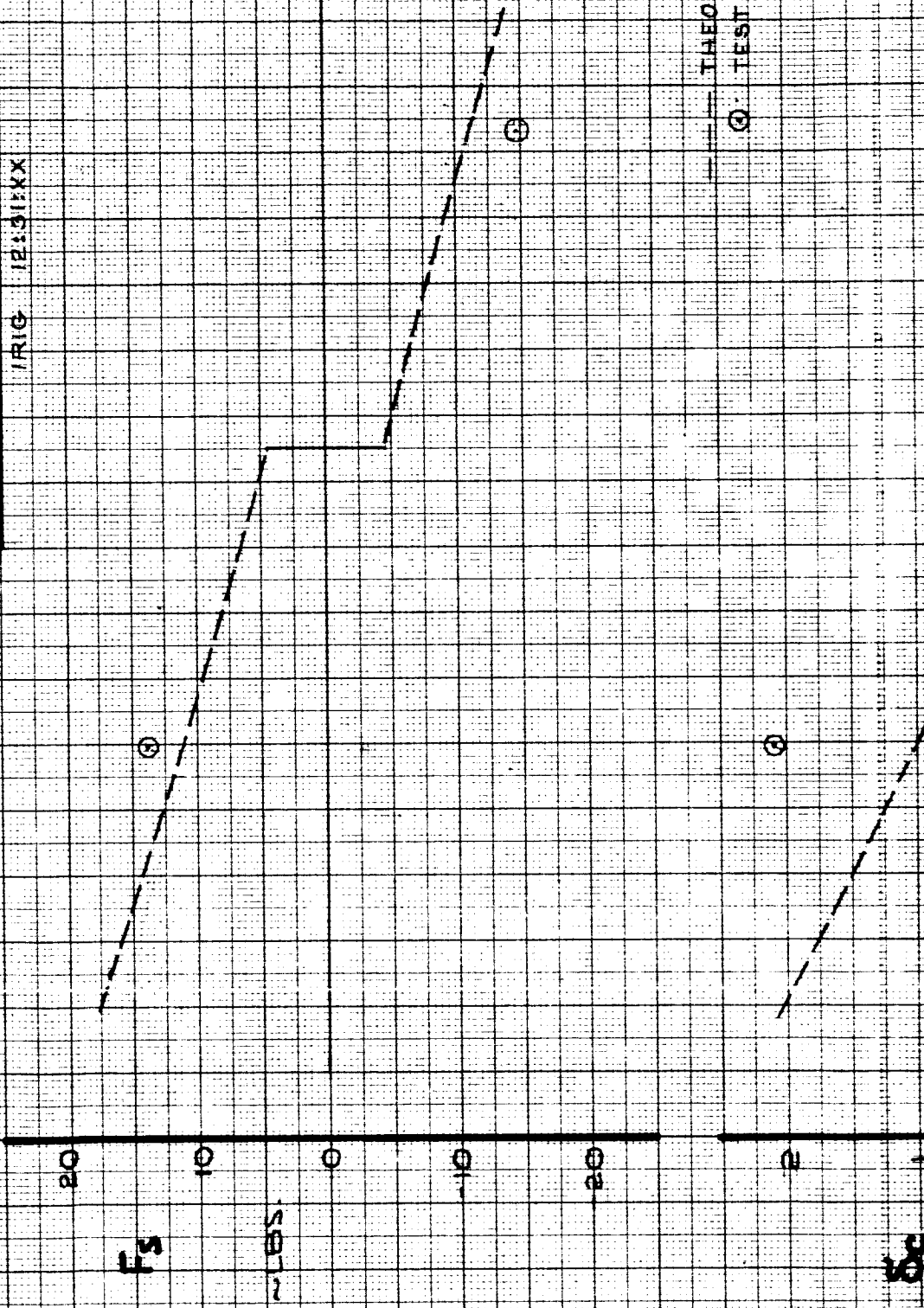


VII-83-2

SPEED STABILITY

AIRPLANE :	367-80	151-B
FL TEST	686-9	686-9
FLAPS	30°	
VL ~ KTS	117	117
ALTITUDE	6100 FT.	SEA LEVEL
G.W. ~ LBS	157000	500000
C.G.	28.5%	25%

IRIG 1231KX

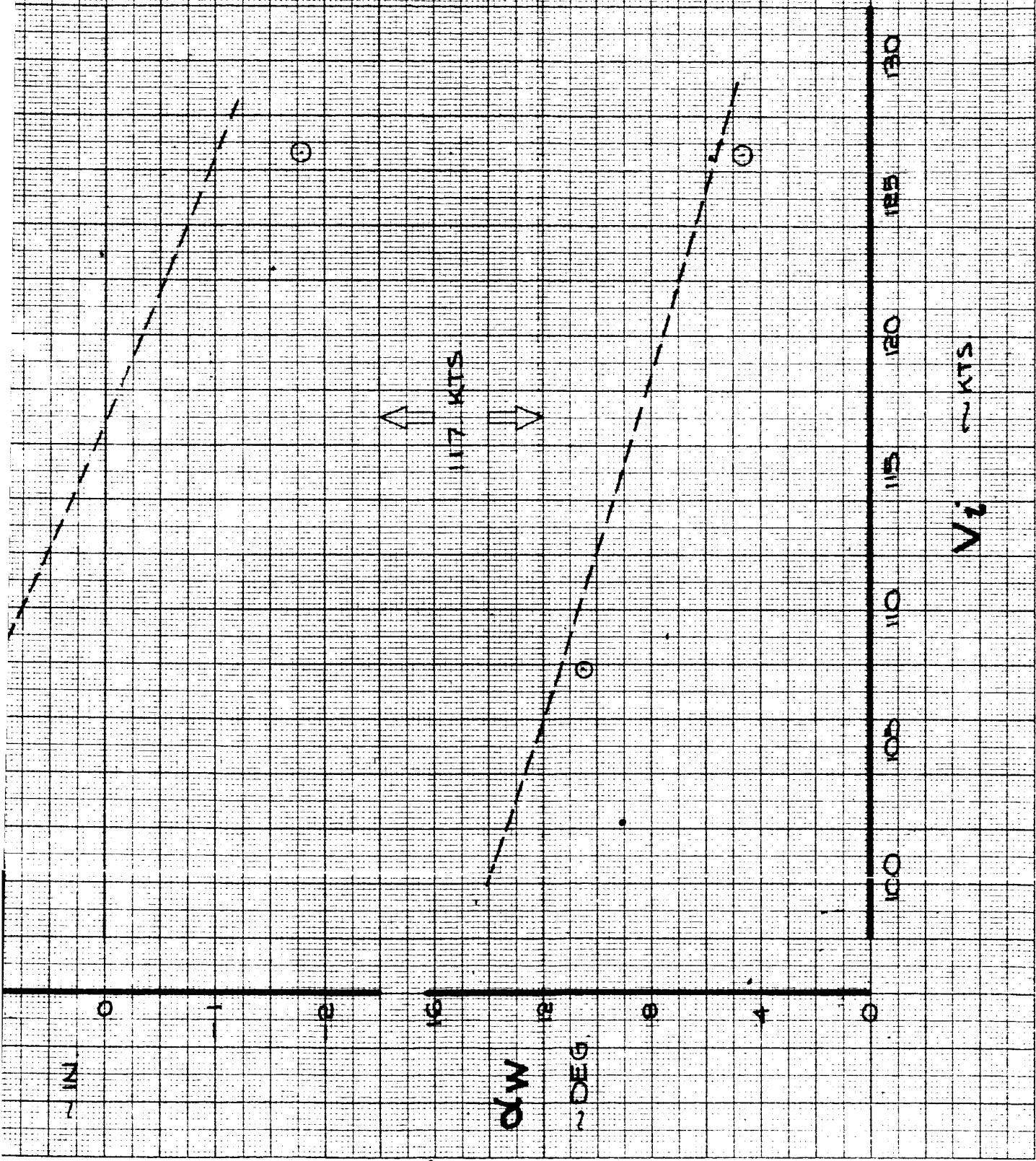


THEORY
 ○ TEST POINT

87

CALC		REVISED	DATE	SPEED STABILITY FL TEST : 686-9 CONFIG. : 151-B	367-80
CHECK					FIG. 59
APPD.				THE BOEING COMPANY	PAGE
APPD.				D6-15000	VII-34

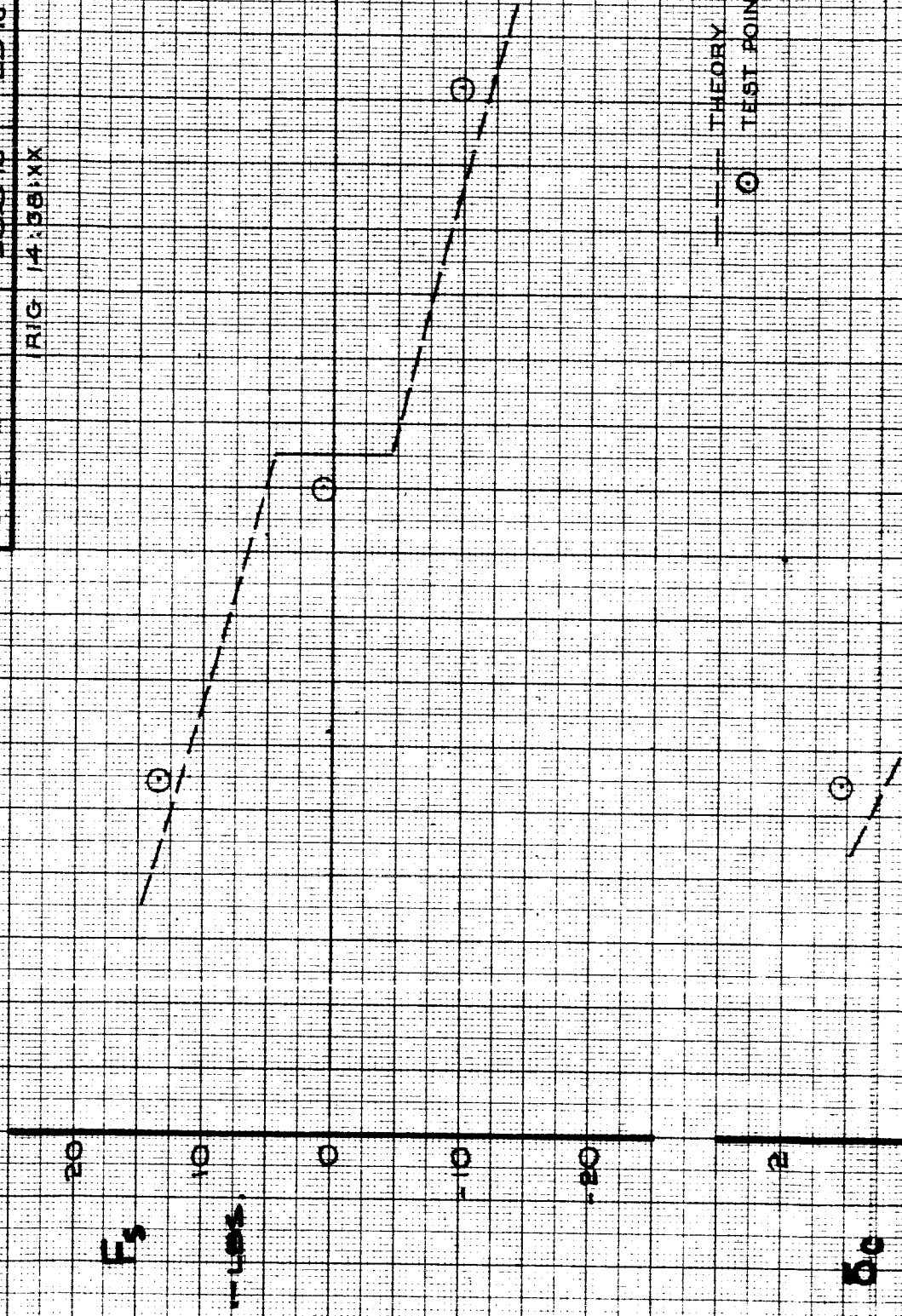
VII-84-2



SPEED STABILITY

AIRPLANE	367-80	151C
FL. TEST	686-8	686-8
FLAPS	30°	
V ₀ (KTS)	117	117
ALTITUDE	3000 FT. SEA LEVEL	
G.W. - LBS.	166000	500000
C.G. -	30.6%	25%

RIG 14381XX

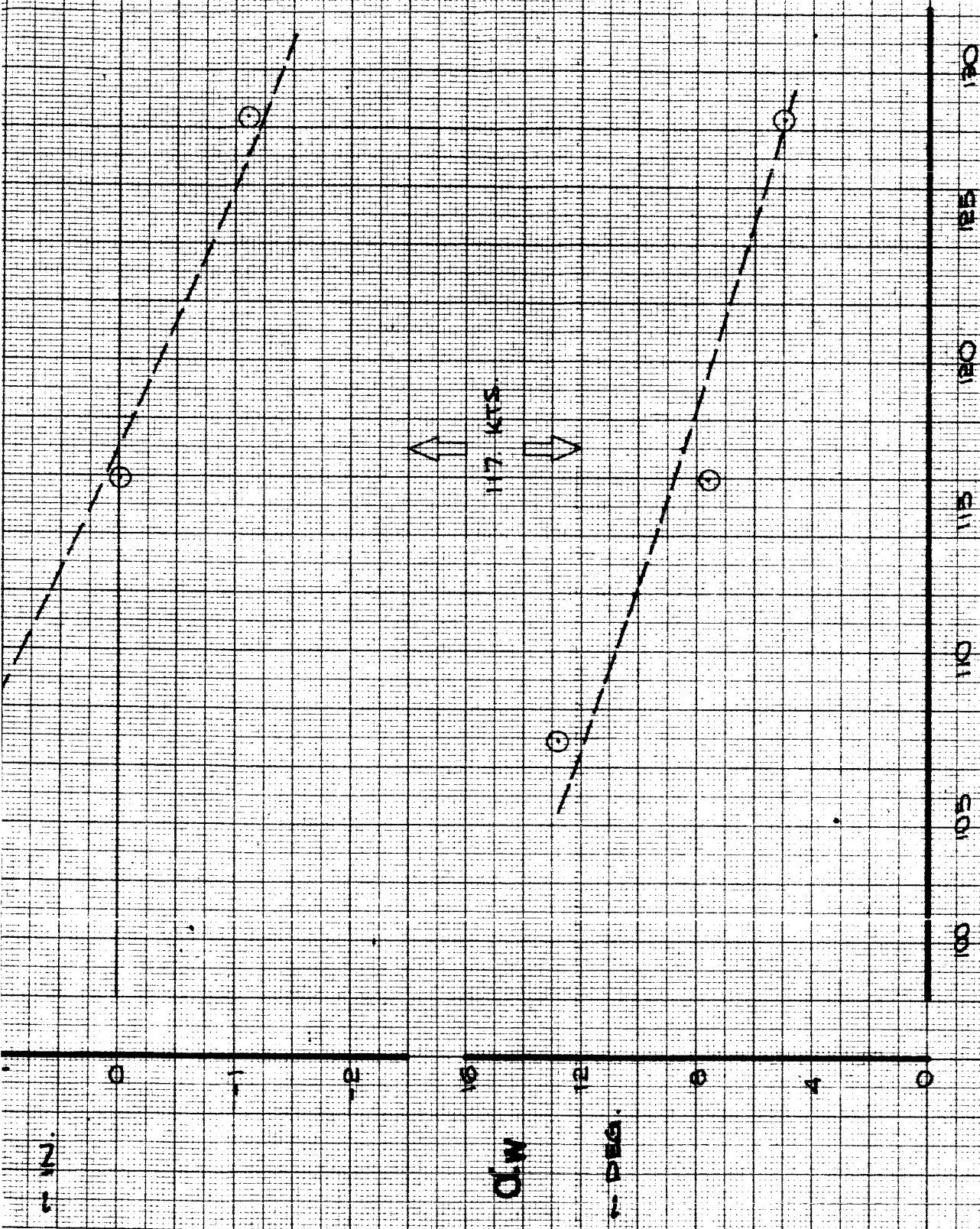


--- THEORY
 ○ TEST POINT

CALC		REVISED	DATE
CHECK			
APPD.			
APPD.			

SPEED STABILITY
 FL. TEST : 686-8
 CONFIG. : 151C

367-80
 FIG. 60

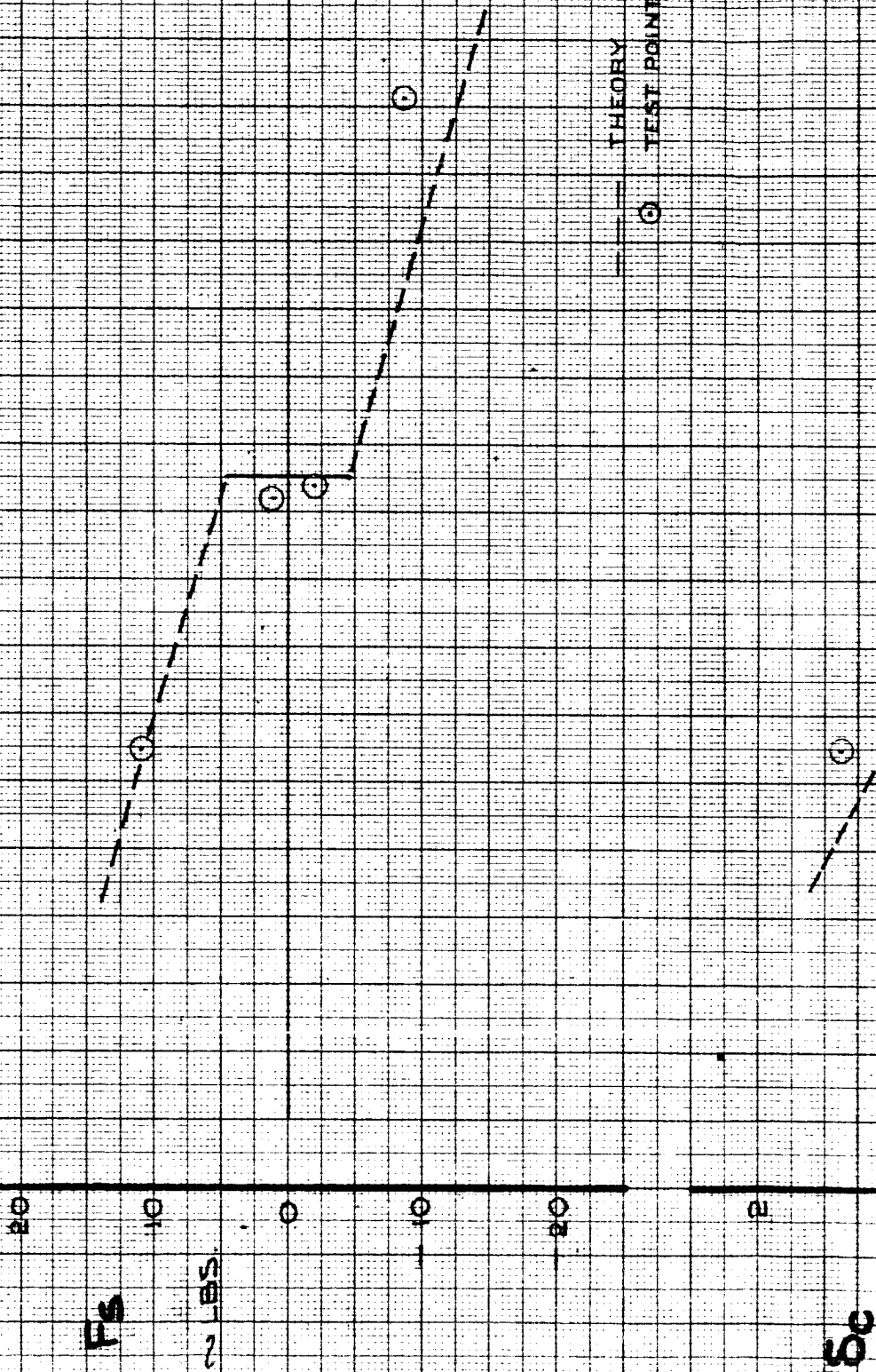


VII-85-2

SPEED STABILITY

AIRPLANE	367-80	158-A
FL. TEST	686-10	686-10
FLAPS	30°	
V ₀ - KTS	117	117
ALTITUDE	5500 FT	SEA LEVEL
G.W. - LBS.	67200	50000
C.G.	30.4%	25%

RIG 131401X



THEORY
TEST POINT

CALC		REVISED	DATE
CHECK			
APPD.			
APPD.			

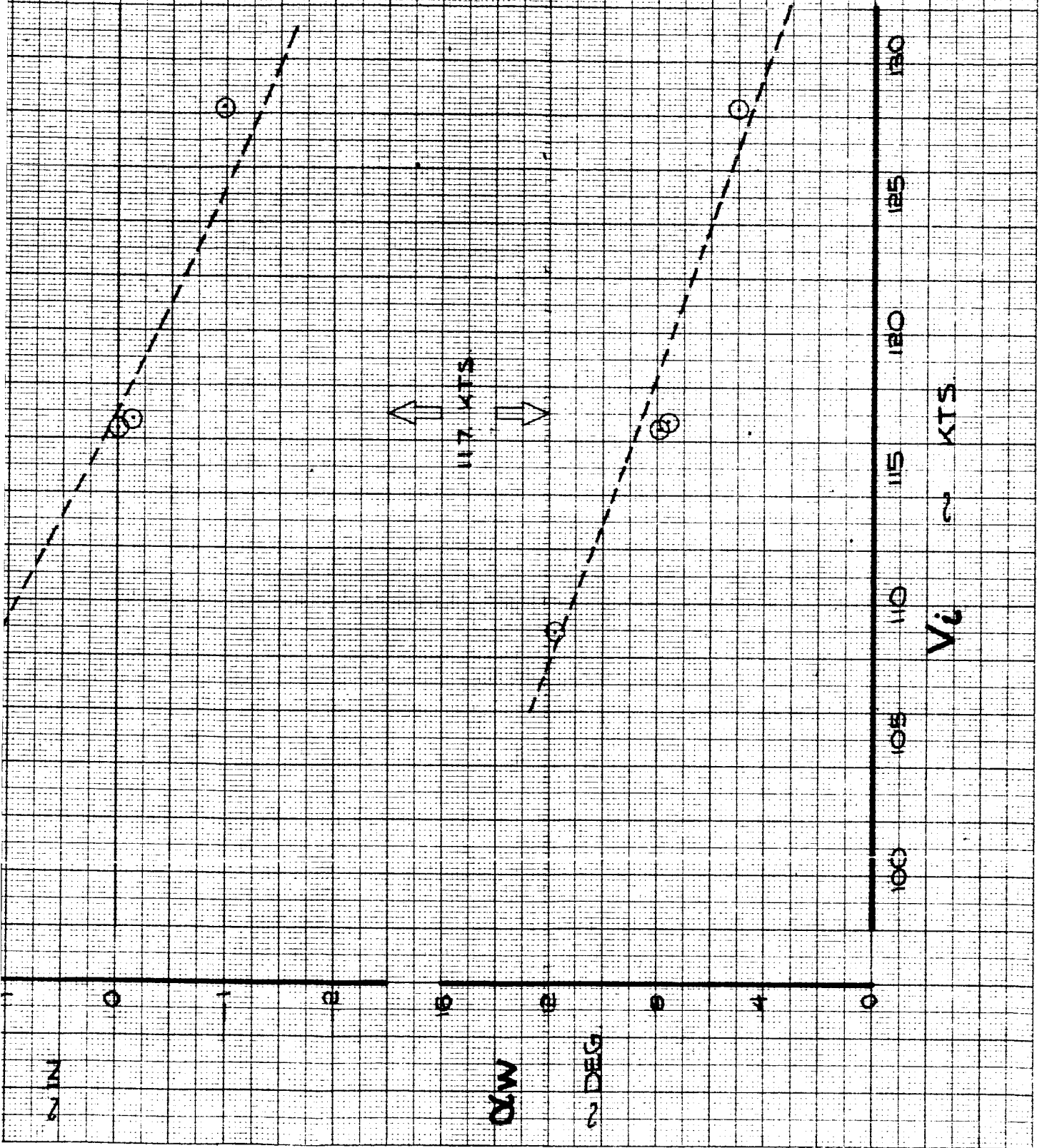
SPEED STABILITY
FL. TEST : 686-10
CONFIG. : 158-A

THE BOEING COMPANY D6-15000

367-80
FIG. 61
PAGE
VII-3c-1

21

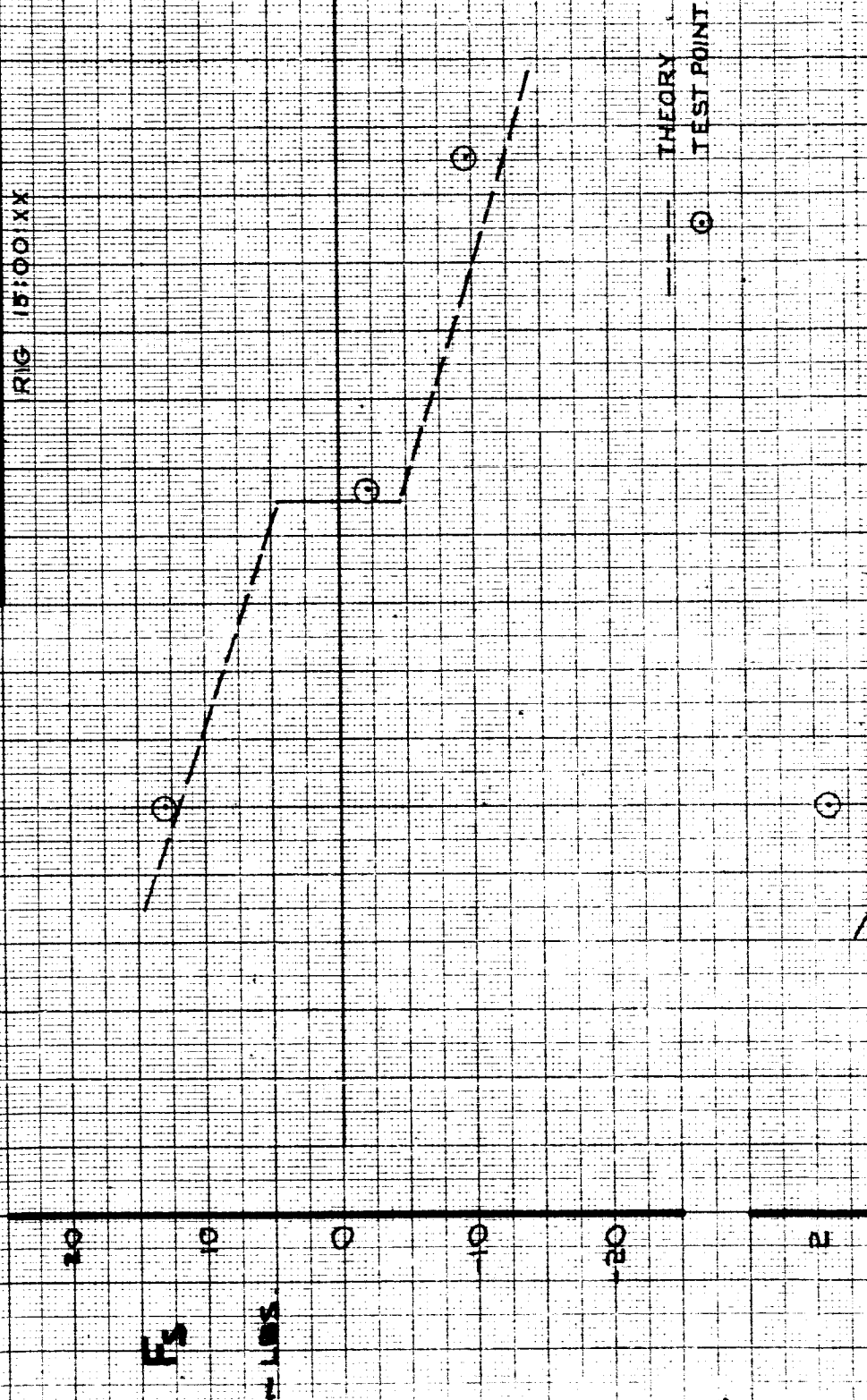
III-86-2



SPEED STABILITY

AIRPLANE : 367-80 159A
 FL. TEST : G86-B
 PLANS : 30
 VC - KTS : 117
 ALTITUDE : 5000 FT SEALEVEL
 GW : 170300 LBS.
 C.G. : 31.0% 259%

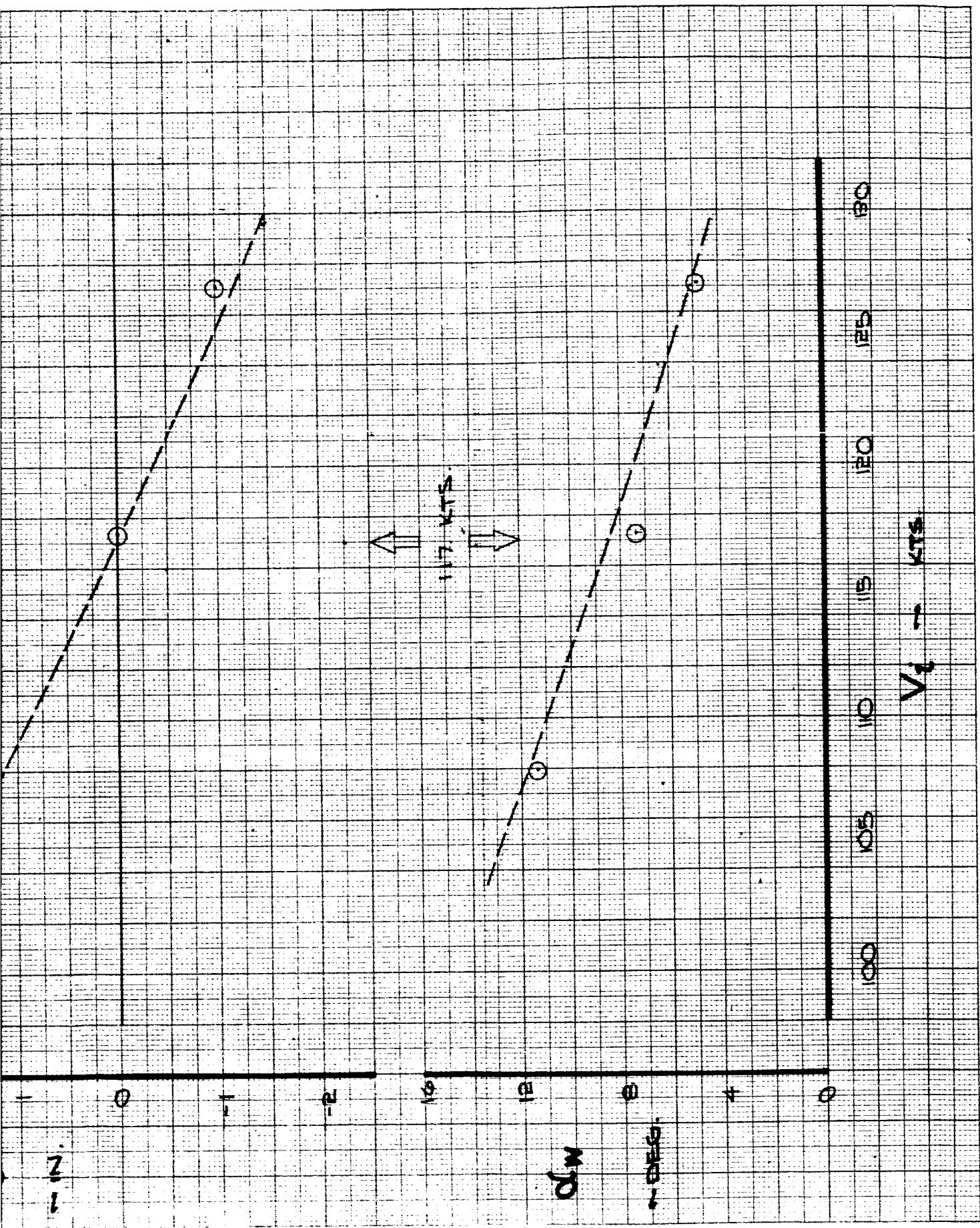
RIG 15:00'XX



CALC			REVISED	DATE
CHECK				
APPD.				
APPD.				

SPEED STABILITY
 FL. TEST : G86-B
 CONFIG. : 159 A

367-80
 FIG. 62



IV-81-2

16

SPEED STABILITY

AIRPLANE	367-80	161B
FL. TEST	686-10	686-10
FLAPS	30°	
V _L - KTS.	117	117
ALTITUDE	8100 FT.	SEA LEVEL
G.W. - LBS.	153000	500000
C.G.	28%	25%

TRIG 14:26:XX



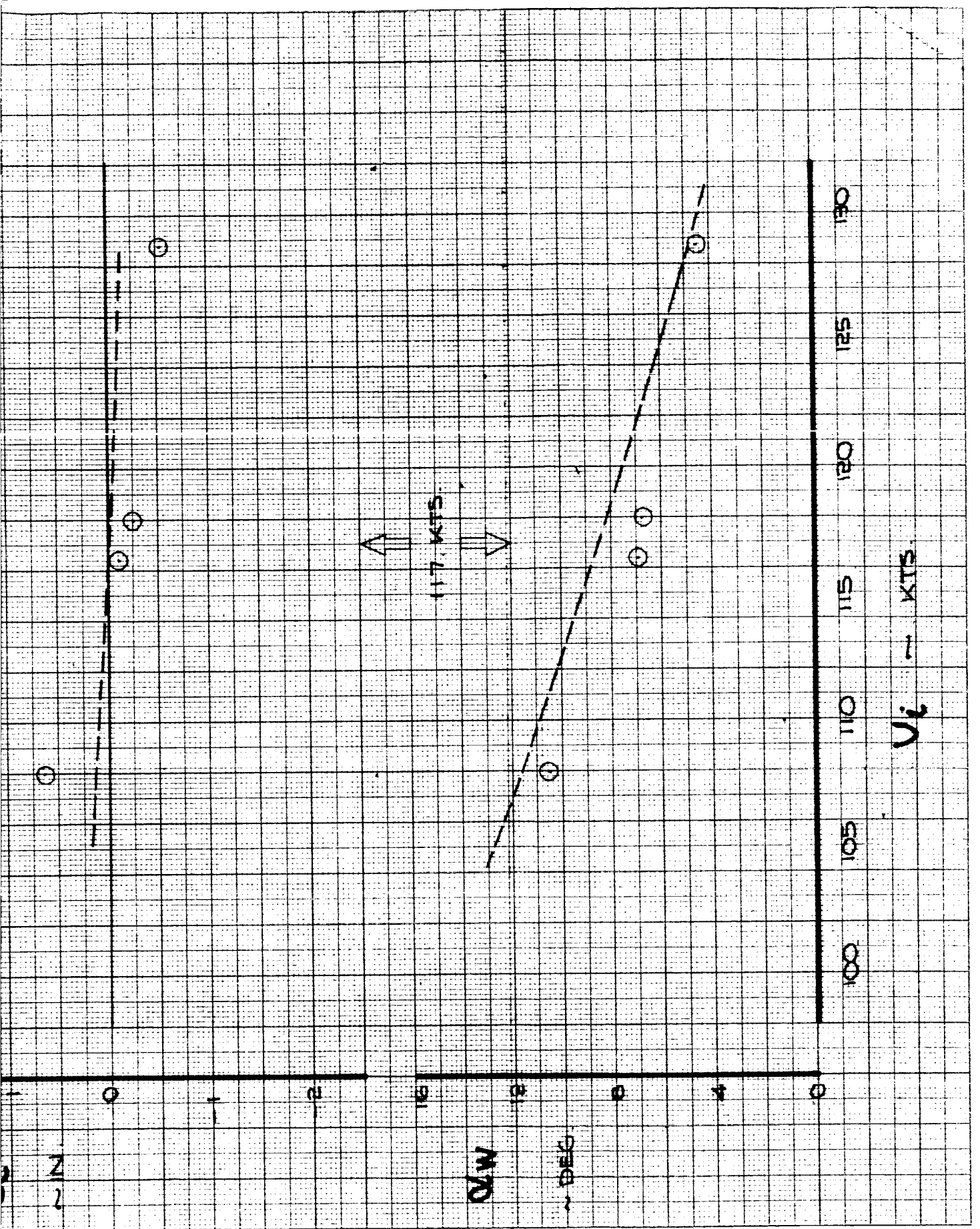
CALC		REVISED	DATE
CHECK			
APPD.			
APPD.			

SPEED STABILITY
 FL. TEST : 686-10
 CONFIG : 161B

THE BOEING COMPANY

D6-15000
 FIG. 63
 PAGE
 VII-53-1

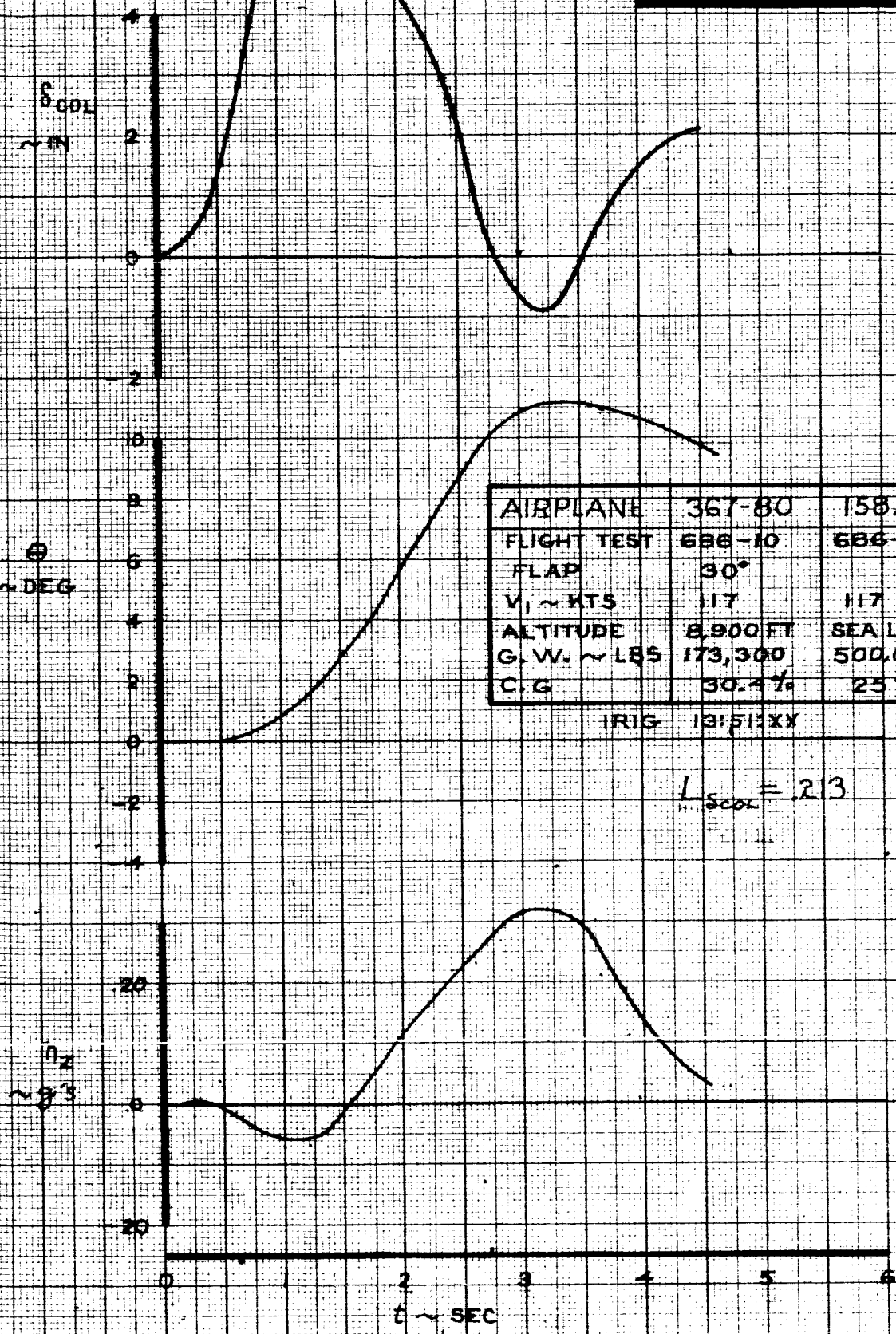
VII-88-2



M70

DEC

PITCH ATTITUDE



AIRPLANE	367-80	158A
FLIGHT TEST	686-10	686-10
FLAP	30°	
$V_1 \sim \text{KTS}$	117	117
ALTITUDE	8,900 FT	SEA LEVEL
G.W. $\sim \text{LBS}$	173,300	500,000
C.G.	30.4%	25%

IRIG 131511XX

$L_{SCOL} = 2.3$

CALC			REVISED	DATE
CHECK				
APR				
APR				

PITCH ATTITUDE
 FLIGHT TEST 686-10
 CONFIGURATION 158A

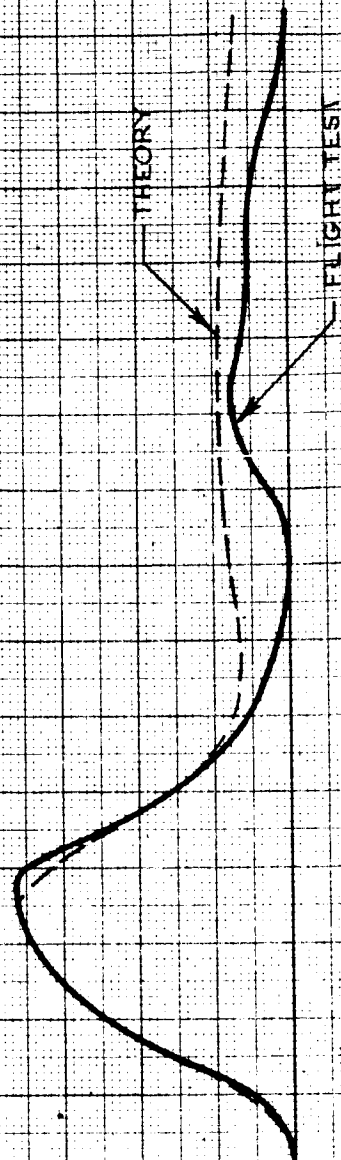
367-80
 FIG. 64
 PAGE VII-89
 THE BOEING COMPANY D6-15000

ELEVATOR PULSE

$$M_x = -1.012$$

$$M_y = 1.174$$

$\Delta \alpha_w$



AIRPLANE	367-80	58 A
FLIGHT TEST	686-10	686-10
FLAPS	30°	
V _i ~ KTS	117	117
ALTITUDE	10,500 FT	SEA LEVEL
G. W. ~ LBS.	173,300	500,000
C.G.	30.2%	25%

CALC		REVISED	DATE
CHECK			
APPD.			
APPD.			

ELEVATOR PULSE
 FLIGHT TEST 686-10
 CONFIGURATION 158 A

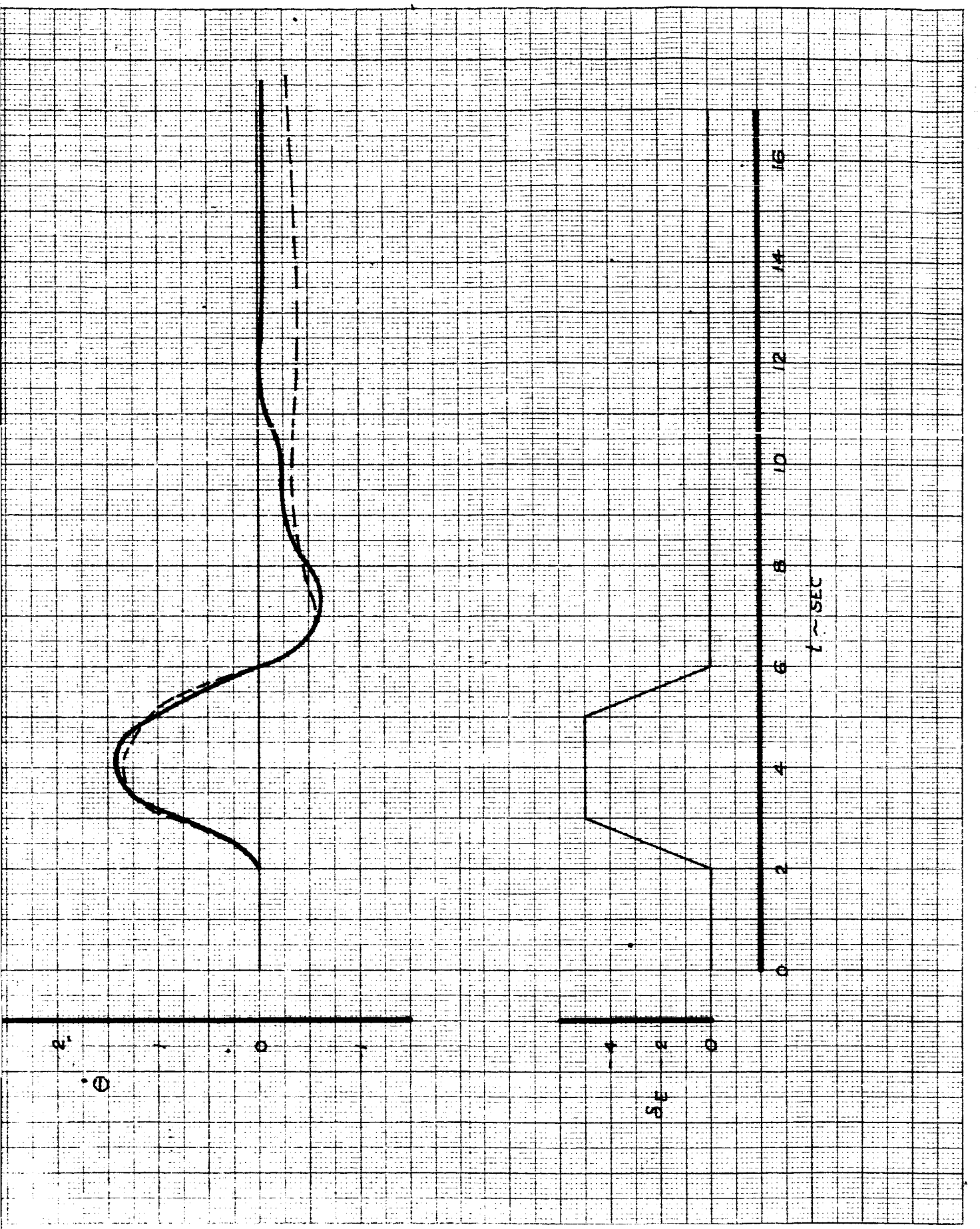
367-80
 FIG. 65

THE BOEING COMPANY D6-15000

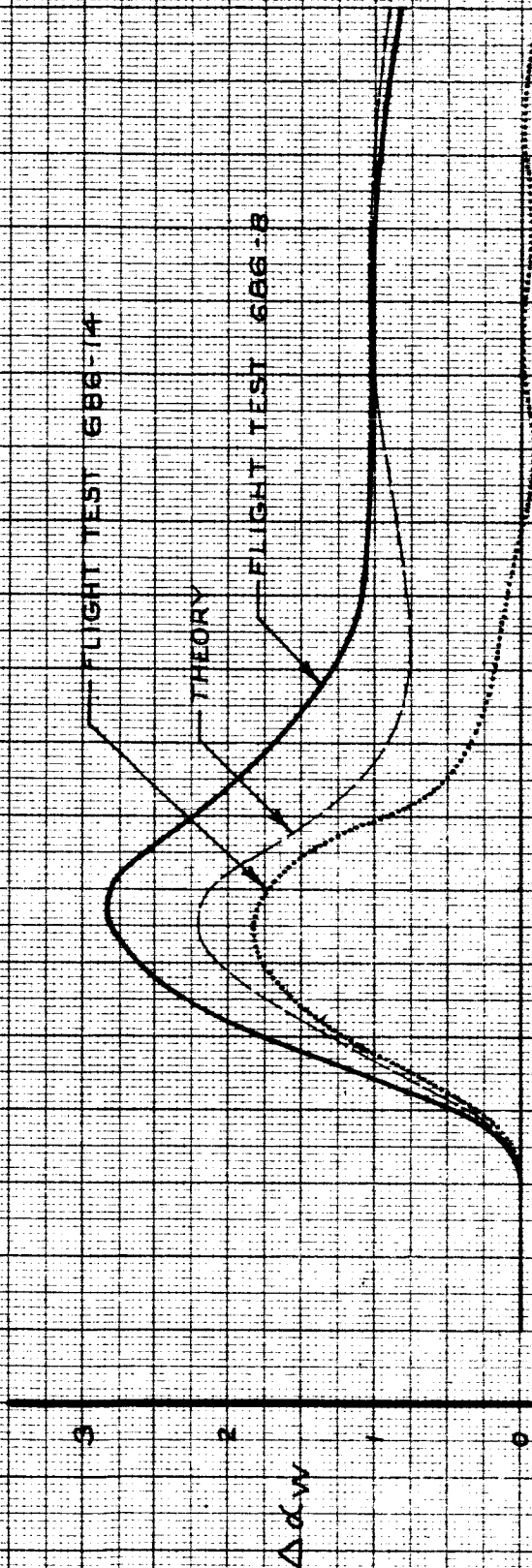
PAGE
 VII-30

93

VII-90-2



ELEVATOR PULSE



AIRPLANE	159 A	367-80	367-80
FLIGHT TEST	686-8 & -14	686-8	686-14
FLAPS	30°		
V ₁ (KTS)	117	117	117
ALTITUDE	SEA LEVEL	6200 FT	6200 FT
G.W. (LBS)	500,000	156,400	148,600
C.G.	25%	30.6%	30.3%
			10:09:XX

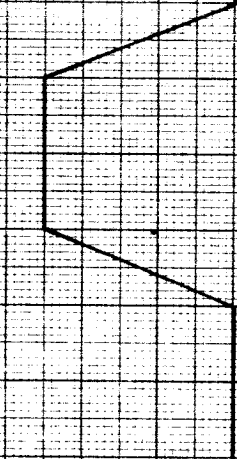
CALC		REVISED	DATE	ELEVATOR PULSE FLIGHT TEST 686-8 & -14 CONFIGURATION 159 A	367-80
CHECK					FIG. 66
APPD.					PAGE
APPD.					VII-11
				THE BOEING COMPANY DG-15000	

h0

1

$$M_A = -506$$

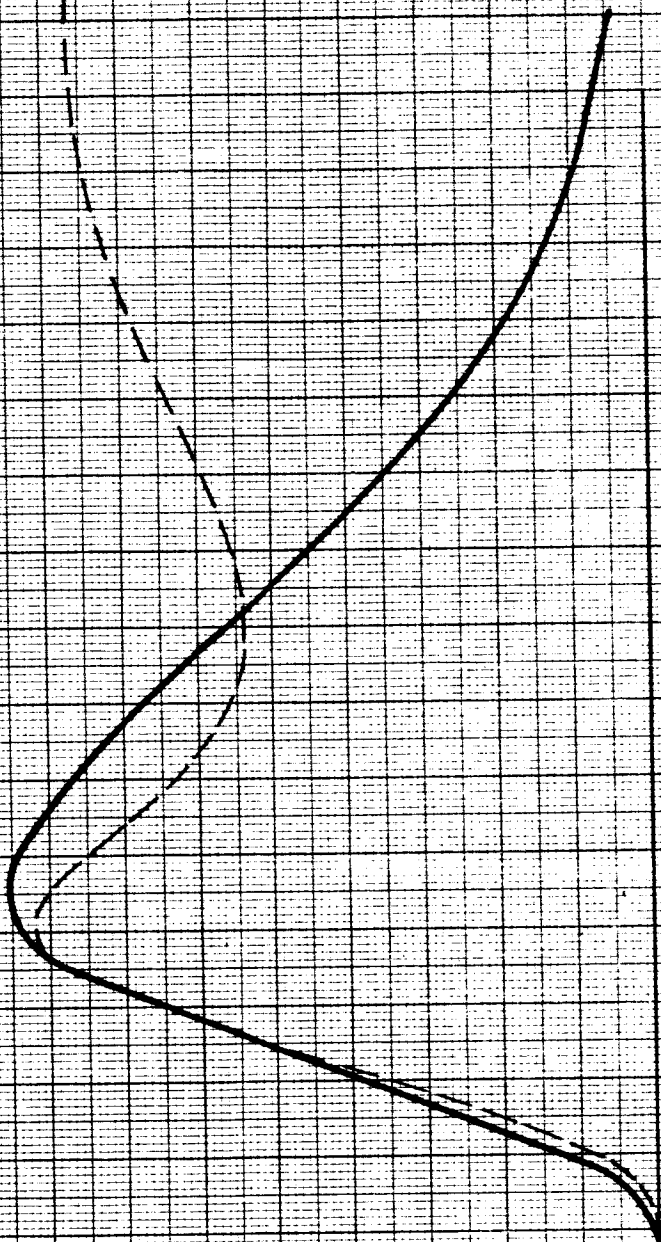
$$M_B = 1174$$



$t \sim \text{SEC}$

VII-91-2

ELEVATOR PULSE



$M_{\alpha} = -1.28$

$M_{\theta} = .587$

AIRPLANE	367-80	161B
FLIGHT TEST	686-10	686-10
FLAPS	30°	
V_i ~ KTS	117	17
ALTITUDE	8,200 FT	SEA LEVEL
G.W. ~ LBS	173,300	500,000
C.G.	30.2%	25%

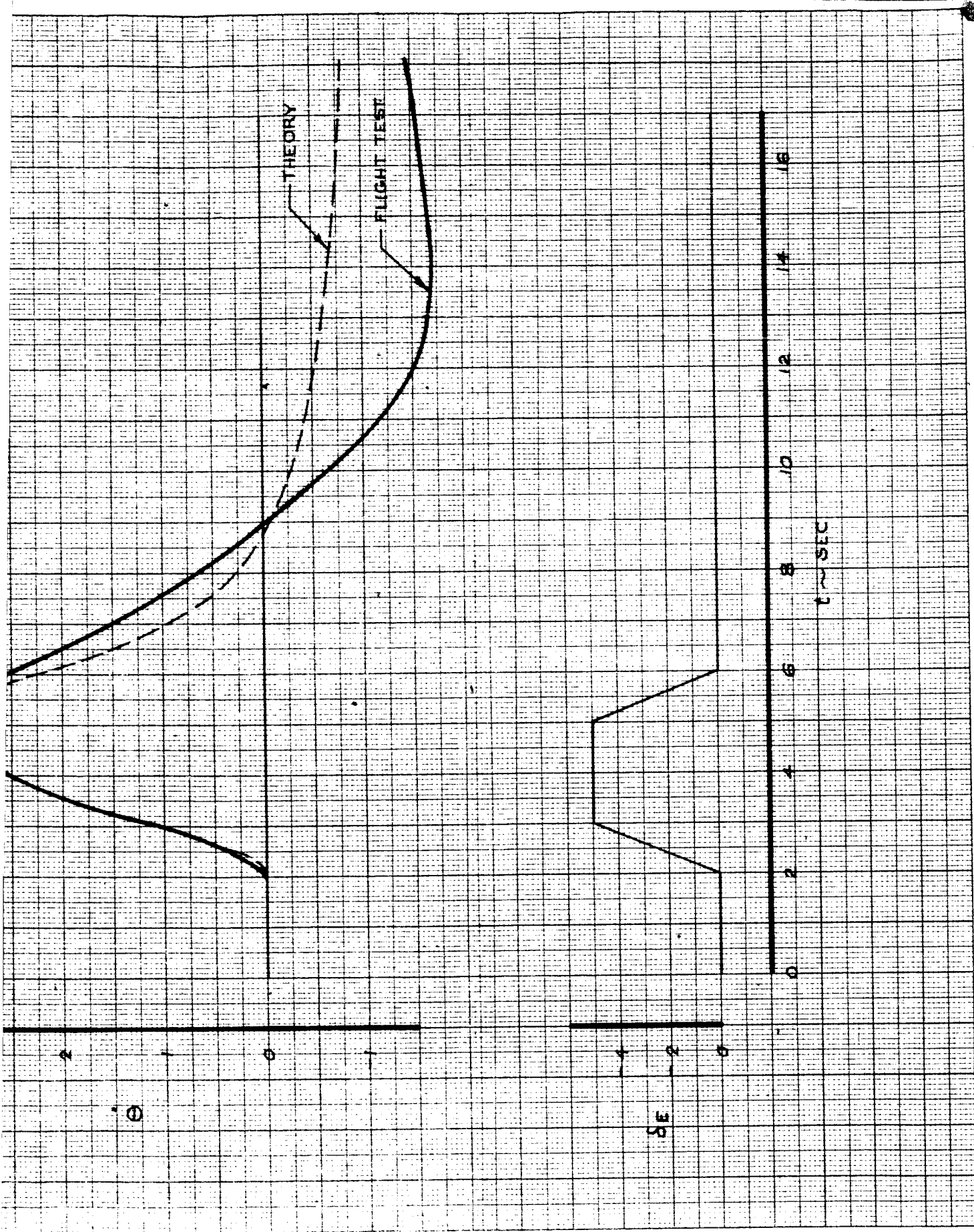
CALC		REVISED	DATE
CHECK			
APPD.			
APPD.			

ELEVATOR PULSE
 FLIGHT TEST 686-10
 CONFIGURATION 161B

367-80
 FIG.67
 PAGE VII-92

THE BOEING COMPANY D6-15005

56



12

B. Ground Based Simulation

The longitudinal characteristics of all the configurations evaluated on the ground based simulator are presented in Table 3. The longitudinal aerodynamic coefficients used to obtain these characteristics are listed in Appendix 1. The effect of elevator lift on pitch response during a step column maneuver is shown for the basic configuration in Fig. 23 (page Vr43). The response of configurations with no elevator lift ($L_{\delta_e} = 0$) and elevator lift opposite the basic configuration ($L_{\delta_e} = -$ basic value) are shown in Figs. 68 and 69 for comparison. The effect of changes in static stability and damping are presented in Figs. 70, 71, and 72 for an elevator pulse. These are comparable to the typical response shown in Fig. 26 (page Vr46).

GROUND BASED CONFIG	L _d 1/SEC·RAD	M _d 1/SEC ²	M RAD/SEC ²	L _{δ_{col}} 1/SEC·IN	M _{δ_{col}} RAD/SEC ² ·IN	M _δ 1/SEC	F _{col} /δ _{col} LB/IN	SHORT PERIOD		PHUGOID		δ _L /δ _{col} DEG./IN
								ω _n RAD/SEC	ζ	ω _n RAD/SEC	ζ	
G-												
100	.571	-.506	.166	.00195	.0219	-.505	4.4	.928	.707	.177	.142	-3.29
100A			.332		.0499		4.4					
100X			.166	.00391	.0219		5.7					
101A			.240	.00195	.0316		4.4					
102			.193		.0176		4.4					
103			.107		.0141							
103A				.00391	.0281							-6.58
105			.166		.0438							
105A			.245		.0646		5.7					
105*			.166	.00588	.0658							-9.87
105 ² X				.01175								
106		-.245		.00195	.0219		4.4	.772	.843	.148	.205	-3.29
107		0.						.575	1.100			
108			.107		.0141							
109			.213		.0282							
109A			.166	.00391	.0438							-6.58
110		+.245		.00195	.0219			.295	2.200			-3.29
111	.302	-.506						.834	.629	.197	.116	
112		-.735						.957	.546	.206	.119	
112A		-.980						1.075	.485	.212	.124	
113		-.343						.732	.716	.184	.124	
113A						-.296		.666	.580	.203	.083	
115		0.				-.585		.420	1.340			
120	.571	-.506				-.242		.817	.605	.201	.081	

CALC	R. Root	2-2-66	REVISED	DATE	GROUND BASED SIMULATION LONGITUDINAL RUN LOG	TABLE
CHECK						3
APR						PAGE
APR						VI-94

THE BOEING COMPANY
RENTON, WASHINGTON D6-15000

AD 1040C-R3

1b

4

8b

TD 1040C-R3

6-7000

GROUND BASED CONFIG	L _d	M _d	M	L _{d_{col}}	M _{d_{col}}	M _θ	F _{col} /δ _{col}	SHORT PERIOD		PHUGOID		δ _e /δ _{col}
								W _n	ζ	W _n	ζ	
G~	1/SEC.RAD	1/SEC ²	RAD/SEC ²	1/SEC.IN	RAD/SEC ² .IN	1/SEC.	LB/IN	RAD/SEC.	-	RAD/SEC.	-	DEG./IN
122A	.571	-.980	.166	-.00195	.0219	-.585	4.4	1.151	.569	.198	.130	-3.29
123	.925	-.506						1.036	.799	.158	.170	
123A				-.00391	.0438							-6.58
123B			.245		.0646		5.7					
124		-.172	.166	-.00195	.0219		4.4	.805	1.000	.099	.416	-3.29
125		.098						.660	1.24			
126		-.245	.107		.0141			.883	.93	.127	.260	
126A			.166	-.00391	.0438							-6.58
127		0	.107	-.00195	.0141			.73	1.115			-3.29
128		-.245				-.245		.725	.92	.160	.091	
129		0						.520	1.195			
130			.166		.0219	-.585		.695	1.115			
131		-.122				-.245		.635	1.040	.128	.169	
132		-.506	.107		.0141			.882	.762	.184	.073	
150	.571		.166		.0219	-.585		.927	.716	C _{Dα} = 1.77 × 8A5/C		
151				+.00195						.177	.140	
151B			.245	+.00165	.0273		5.7					-2.78
151C				0								
151C*			.166		.0219							
151D			.245	+.00391	.0646							-3.29
152		-1.470	.166	-.00195	.0219	-1.173	4.4	1.466	.645	.190	.155	-3.29
153			.332		.0439							
154		-.506	.166		.0219			1.089	.865	.151	.225	
155			.332		.0439							

GROUND BASED SIMULATION
 LONGITUDINAL RUN LOG.
 THE BOEING COMPANY
 RENTON, WASHINGTON D6-15000

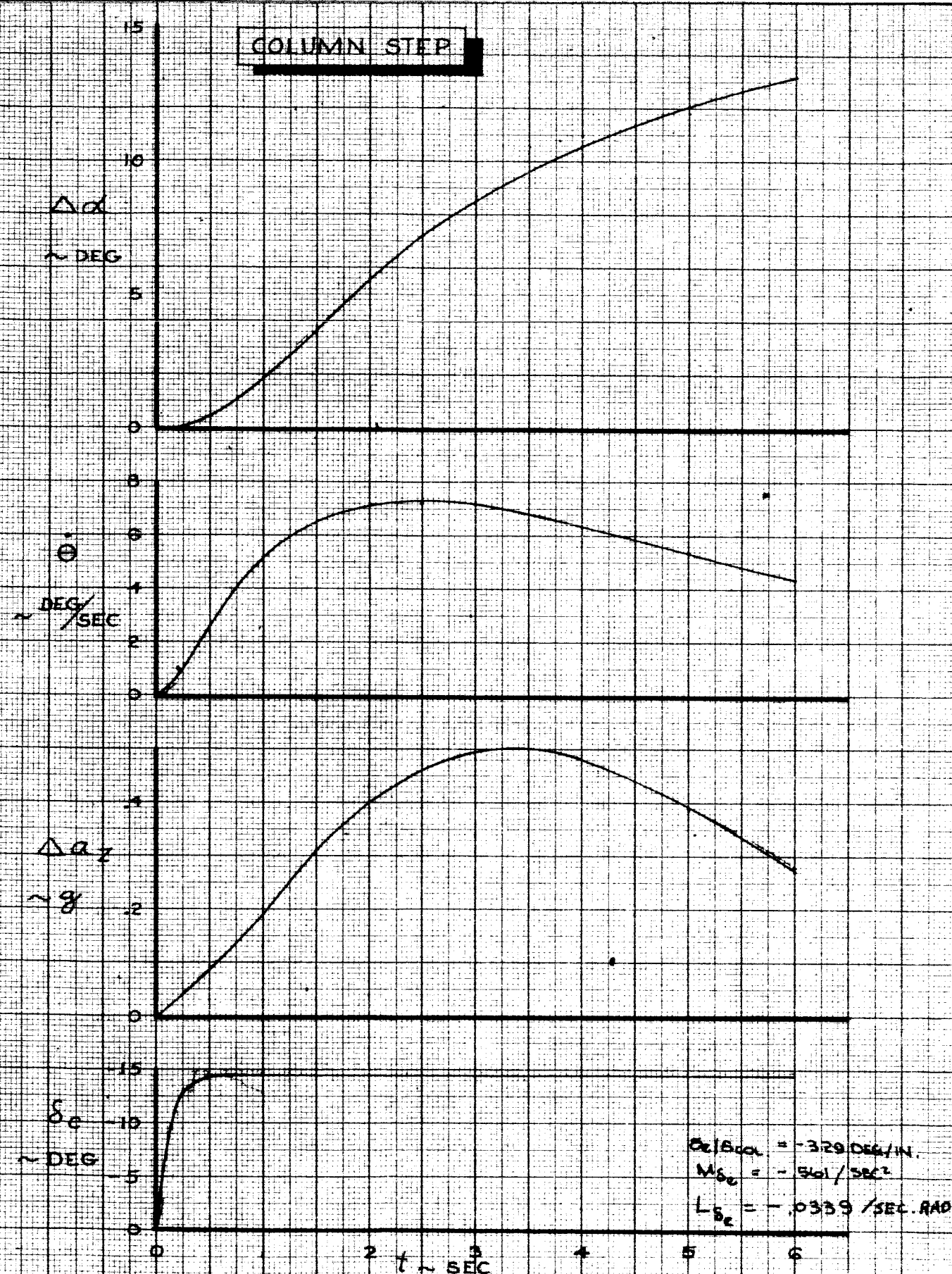
TABLE F1
 3
 PAGE VII-95

GROUND BASED CONFIG.	L α	M α	M	L δ_{COL}	M δ_{COL}	M $\dot{\theta}$	F δ_{COL}	SHORT PERIOD		PHUGOID		δ_f / δ_{col}
								ω_n	ζ	ω_n	ζ	
CALC	1/SEC · RAD	1/SEC ²	RAD/SEC ²	1/SEC · IN	RAD/SEC ² · IN	1/SEC.	LB/IN	RAD/SEC	—	RAD/SEC.	—	DEG/IN
G~	.571	-.980	.332	-.00195	.0439	-.585	4.4	1.151	.569	.198	.130	-3.29
156			.166		.0219	-1.173		1.290	.733	.177	.169	
157						- .585		1.151	.569	.198	.130	
157A								1.290	.733	.177	.169	-6.58
158			.245	-.00391	.0438	-1.173	5.7					
158A			.166			-.585	4.4	1.151	.569	.198	.130	
158A*			.245		.0646		5.7					
158X			.166		.0438	-1.173	4.4	1.290	.733	.177	.169	
159		-.506	.245	-.00165	.0213		5.7					-2.78
159A				-.00391	.0646							-6.58
159B			.166		.0438		4.4	1.466	.645	.190	.155	
160		-1.470										
161		-.122				-.585		.675	.958			
161B			.245		.0646		5.7					
162		-.049	.166		.0438		4.4	.618	1.045			
163	.925	-.980						1.242	.668	1.83	.139	
163A				-.00195	.0219							-3.29

CALC	R. Root	2-2-66	REVISED	DATE
CHECK				
APR				
APR				

66

COLUMN STEP



$G_z/B_{roll} = -329 \text{ DEG/IN.}$
 $M_{\delta_c} = -5601 / \text{SEC}^2$
 $L_{\delta_c} = -0339 / \text{SEC. RAD}$

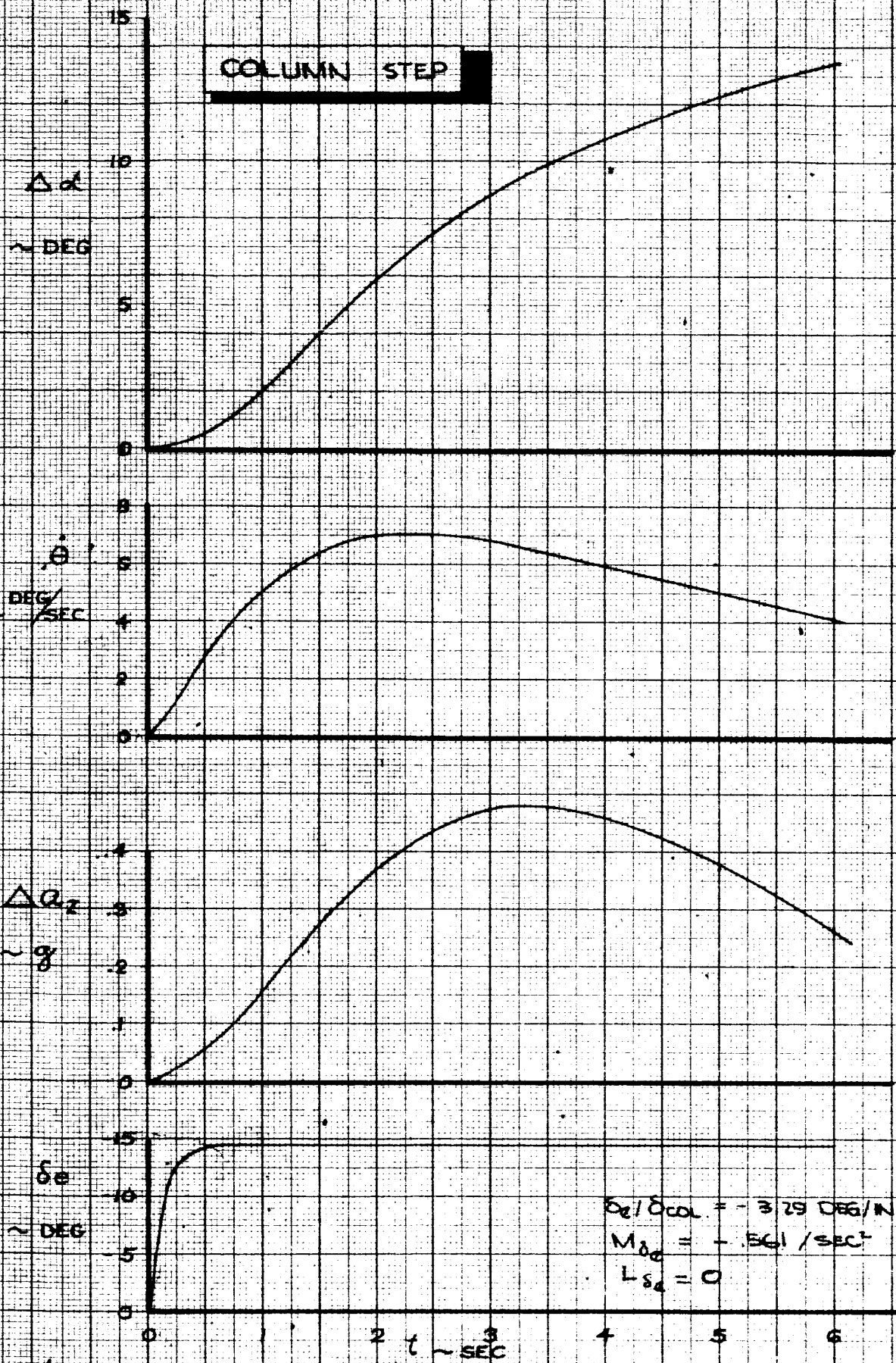
CALC	R. Root	2-2-66	REVISED	DATE
CHECK				
APR				
APR				

COLUMN STEP
GROUND BASED SIMULATOR
CONFIGURATION G151B

THE BOEING COMPANY

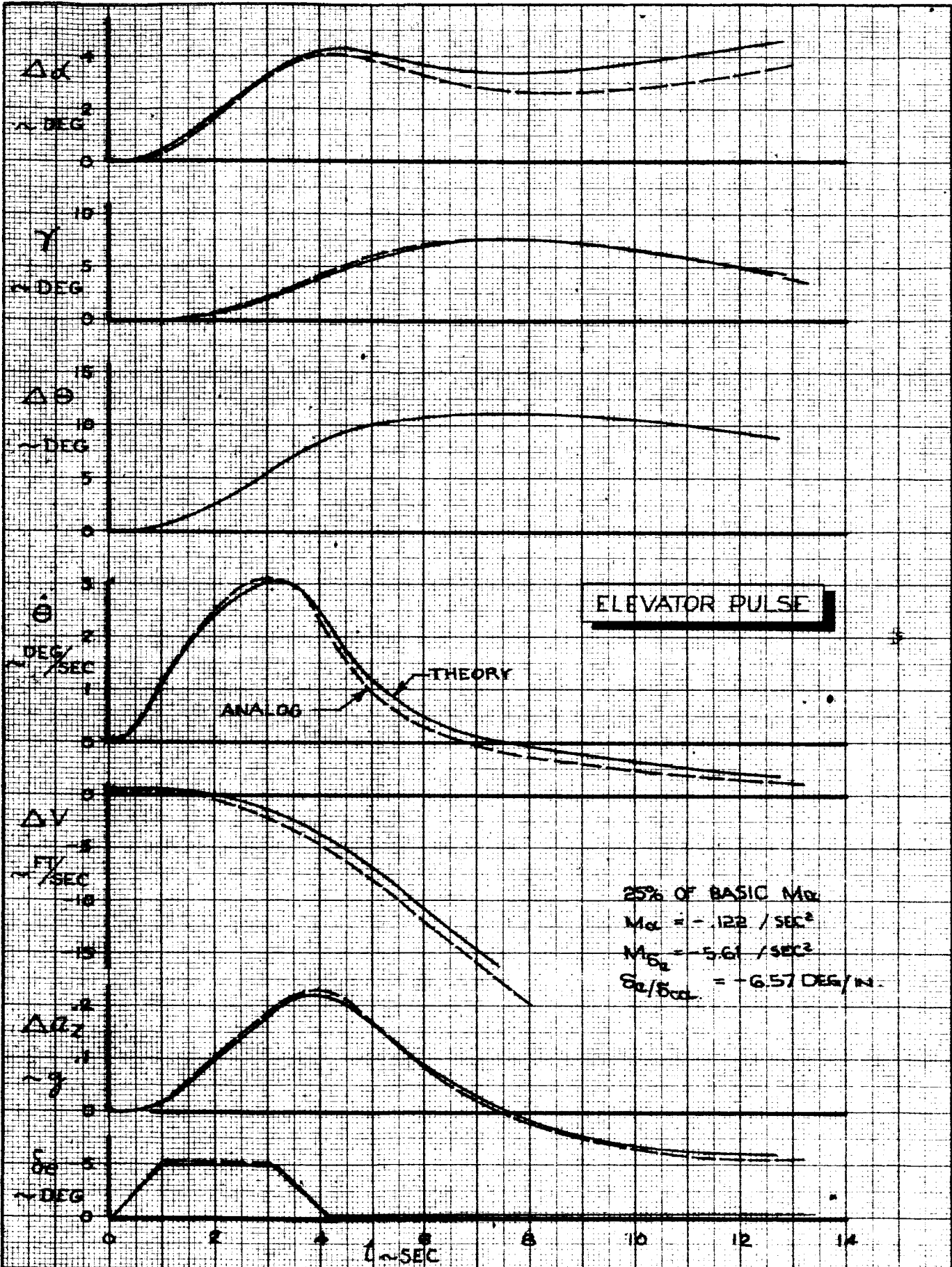
D6-15000
 FIG.68
 PAGE VII-97

COLUMN STEP



$\delta e / \delta \text{col} = -3.29 \text{ DEG/IN.}$
 $M_{\delta e} = -561 / \text{SEC}^2$
 $L_{\delta e} = 0$

CALC	R. Root	2-2-66	REVISED	DATE	COLUMN STEP GROUND BASED SIMULATOR CONFIGURATION G151C THE BOEING COMPANY	D6-15000
CHECK						FIG. 69
APR						PAGE
APR						VII-98



ELEVATOR PULSE

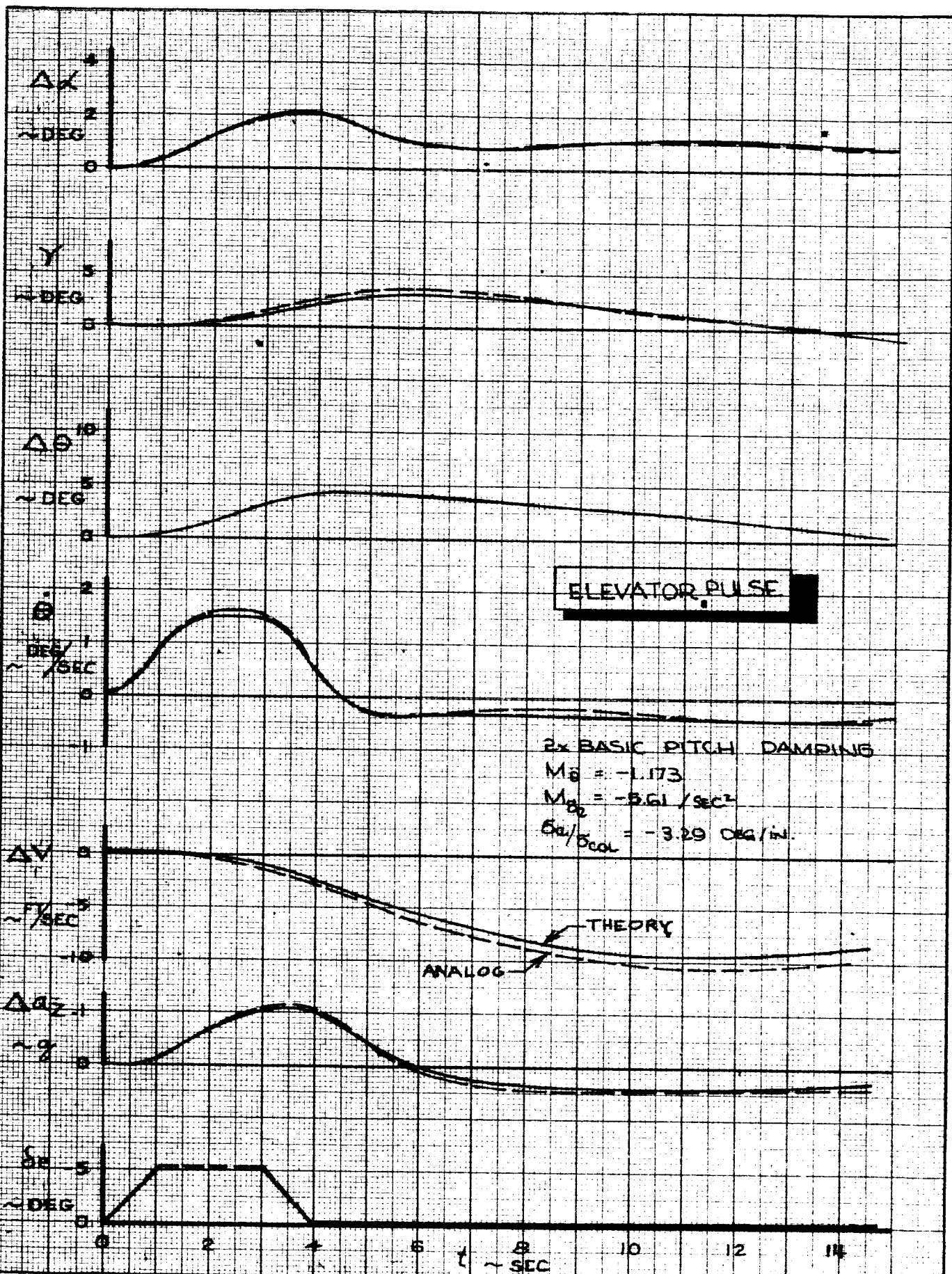
25% OF BASIC MO
 $M_{ax} = -.122 / SEC^2$
 $M_{\dot{\theta}} = -5.61 / SEC^2$
 $G_{\dot{\theta}} = -6.57 DEG/IN$

CALC	R. Root	2-2-66	REVISED	DATE
CHECK				
APR				
APR				

ELEVATOR PULSE
GROUND BASED SIMULATOR
CONFIGURATION G161B
THE BOEING COMPANY

D6-15000
FIG. 70
PAGE
VII-99

102



ELEVATOR PULSE

2x BASIC PITCH DAMPING
 $M_{\theta} = -1.173$
 $M_{\dot{\theta}} = -3.61 / \text{SEC}^2$
 $C_{\dot{\theta}} / \delta_{col} = -3.29 \text{ DEG/IN.}$

THEORY
 ANALOG

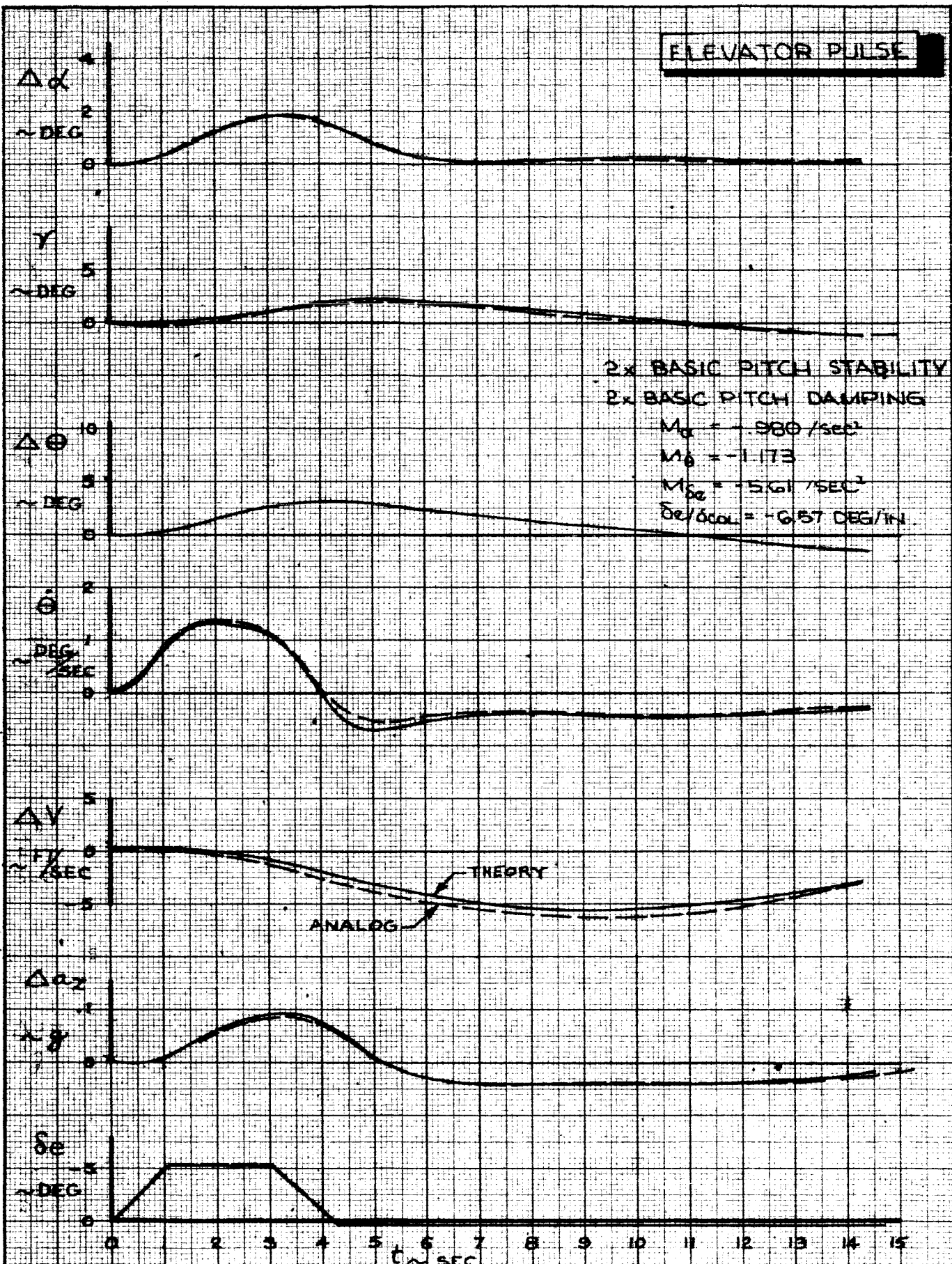
CALC	R. Root	2-266	REVISED	DATE
CHECK				
APR				
APR				

ELEVATOR PULSE
 GROUND BASED SIMULATOR
 CONFIGURATION G159A
 THE BOEING COMPANY

D6-15000
 FIG. 71
 PAGE
 VII-100

103

ELEVATOR PULSE



CALC	R. Root	2-2-66	REVISED	DATE	ELEVATOR PULSE GROUND BASED SIMULATOR CONFIGURATION G158A THE BOEING COMPANY	D6-15000
CHECK						FIG.72
APR						PAGE
APR						VII-101

VIII. LATERAL CONFIGURATION CHARACTERISTICS

A. Airborne Simulation

The characteristics of the four lateral directional configurations evaluated on the airborne simulation which are different from the basic 1209 configuration are documented in this section.

The responses to the documentation maneuvers are summarized or eliminated when there is negligible change from the basic configuration. During all the lateral flight test documentation and evaluation the longitudinal configuration was the basic 101A configuration.

Table 4 contains a summary of the lateral directional configurations evaluated on the Airborne Simulation. The lateral-directional aerodynamic coefficients used to obtain these characteristics are listed in Appendix 1. A summary plot of the steady roll rate maneuver is shown in Fig. 73 for several configurations. The maximum steady state roll rate available agrees fairly well with the theoretical value.

The roll rate reversal data is shown in Figs. 74 thru 77 for four configurations. Comparison of these configurations with the basic, 1209 (Fig. 13), and with each other shows the effect of roll control sensitivity (slope) and total roll control power ($\ddot{\phi}$ max). The roll control power available in flight test is generally lower than theory predicts whereas the sensitivity is accurately predicted.

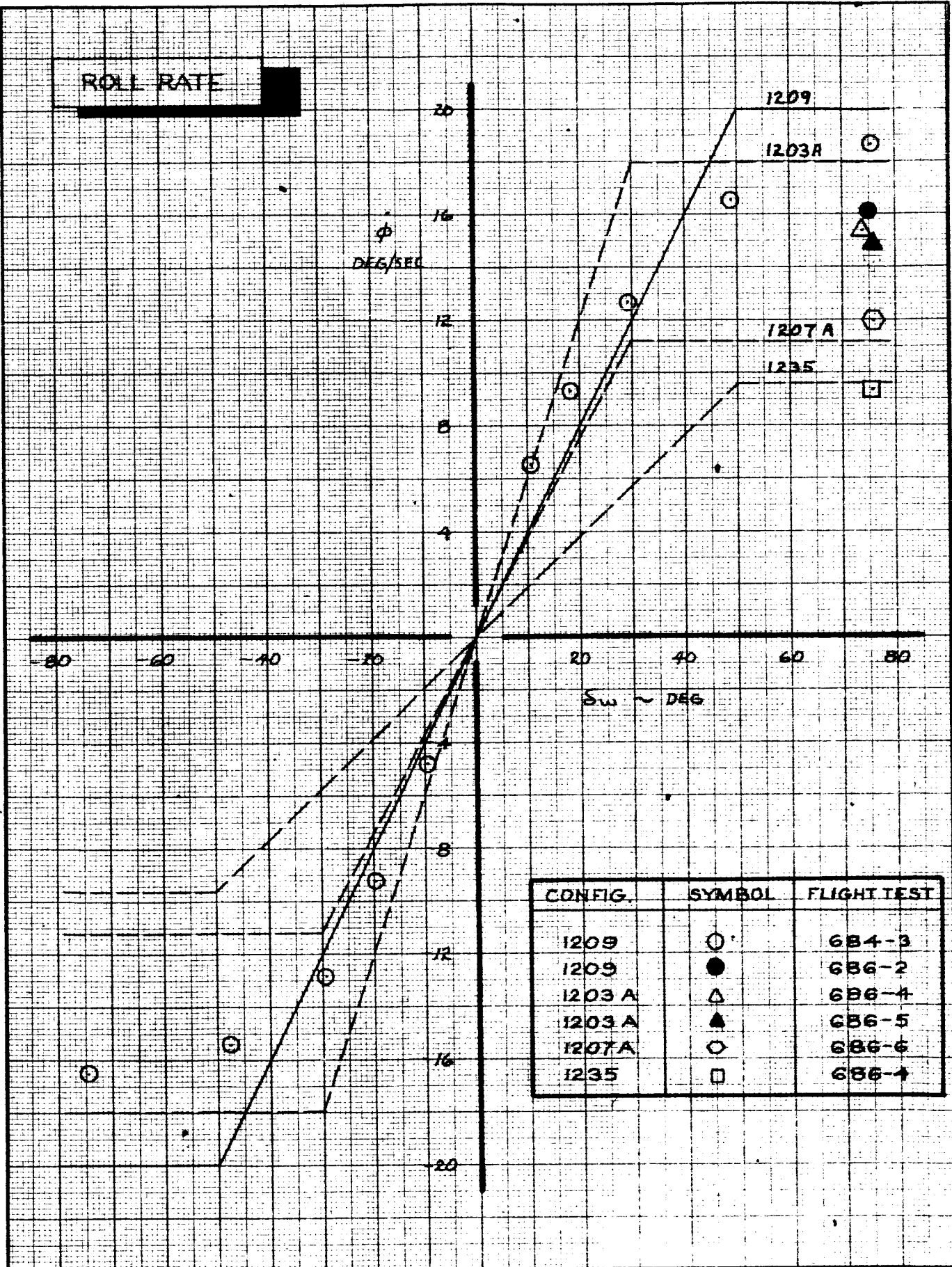
901

CONFIG.	L RAD/SEC ²	$\delta_{W_{EFF}}$ DEG	$L_{\delta W}$ 1/SEC ²	$t_{\delta a_{MAX}}$ SEC	τ_{3D} SEC	P_{SS} RAD/SEC	ϕ_1 DEG	ϕ_2 DEG	DUTCH ROLL		COMMENTS
									ω_n RAD/SEC	ζ	
1209	.267	50	.306	.48	1.14	.348	RT 2.10 LT 2.10	11.3 13.0	.508	.329	BASIC
1203A	.240	30	.458			.358	1.89	10.02			+ ROLL CONTROL SENSITIVITY
1207A	.150	30	.286			.196	1.20	7.25			- ROLL CONTROL POWER
1235	.267	30	.511		.60	.167	1.90	8.95	.533	.380	+ DAMPING IN ROLL + ROLL SENSITIVITY
1237	.250	50	.286	.84	1.14	.326	1.40	9.10	.508	.329	+ TIME TO MAX. AILERON
-80BLC	.323	NON LINEAR	1.200	.48	NON LINEAR	NON LINEAR	4.00	20.72	.513	.564	+ ROLL SENSITIVITY + POWER + DAMPING

MEASURED DURING FLIGHT TEST

ENGR.		REVISED	DATE	AIRBORNE SIMULATION LATERAL RUN LOG	TABLE 4	
CHECK					D6-15000	
APR					THE BOEING COMPANY RENTON, WASHINGTON	VIII-103
APR						

ROLL RATE



CONFIG.	SYMBOL	FLIGHT TEST
1209	○	6B4-3
1209	●	6B6-2
1203 A	△	6B6-4
1203 A	▲	6B6-5
1207A	○	6B6-6
1235	□	6B6-4

CALC		REVISED	DATE
CHECK			
APR			
APR			

SUMMARY OF STEADY ROLL RATES

367-80

FIG. 73

THE BOEING COMPANY DG-15000

PAGE VIII-104

107

A 20° heading change is presented for configuration 1235 in Fig. 78. The high roll damping of this configuration is evident when the time history of the wheel activity is compared to that of the basic 1209 configuration. (Fig. 19).

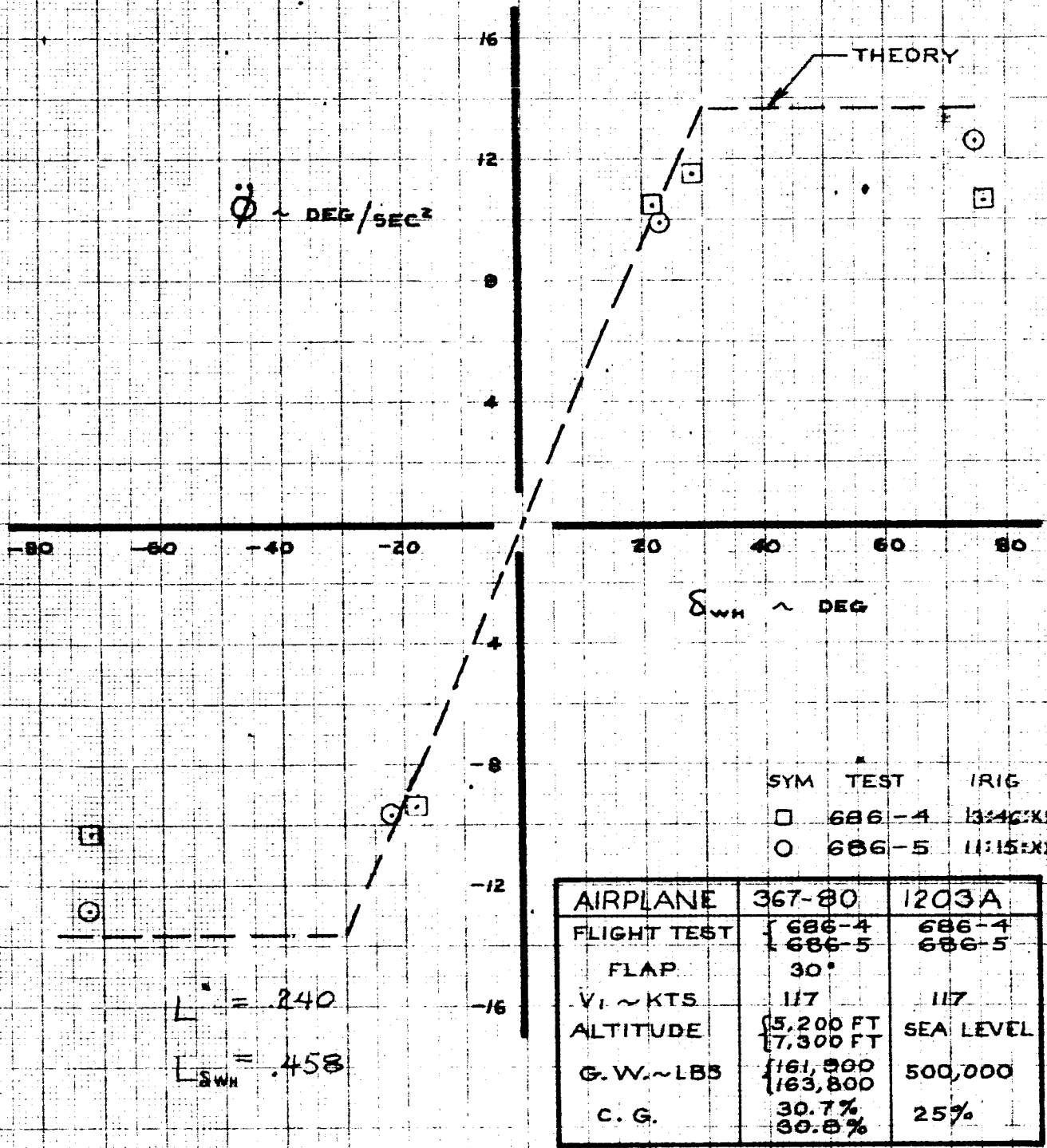
Table 5 shows the results of wheel steps.

TABLE 5

WHEEL STEP

CONFIG.	ϕ_1	ϕ_2	β_1	β_2	δw_1	δw_2
1203A	1.89	10.02	.23	1.76	75.6	75.6
1207A	1.20	7.25	.16	1.00	75.6	75.6
1209 Left	2.10	11.3	.30	1.56	75.6	75.6
1209 Right	2.10	13.0	.41	2.03	75.6	75.6
1235	1.90	8.95	.07	1.12	75.6	75.6
1237	1.40	9.1	.11	1.28	75.6	75.6
-80 BLC	4.00	20.72	.74	2.11	75.6	75.6

ROLL RATE REVERSAL

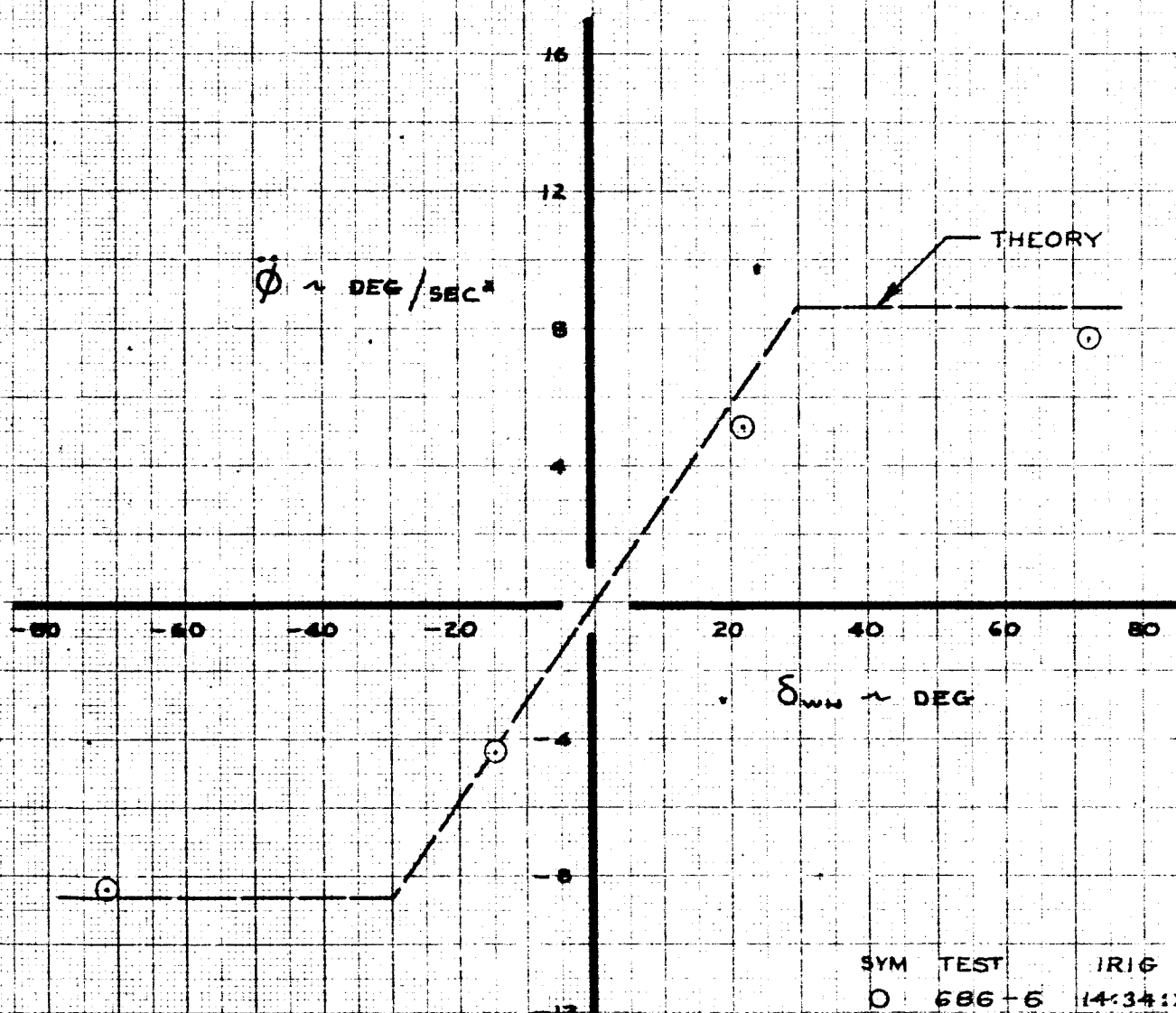


CALC			REVISED	DATE
CHECK				
APR				
APR				

ROLL RATE REVERSAL
 FLIGHT TEST 686-4 & 5
 CONFIGURATION 1203A

367-80
 FIG. 74
 PAGE VIII-106
 THE BOEING COMPANY 06-15000

ROLL RATE REVERSAL



$\dot{\phi} = .150$
 $\dot{\phi} = .286$

SYM TEST IRIG
 O 686-6 14:34:XX

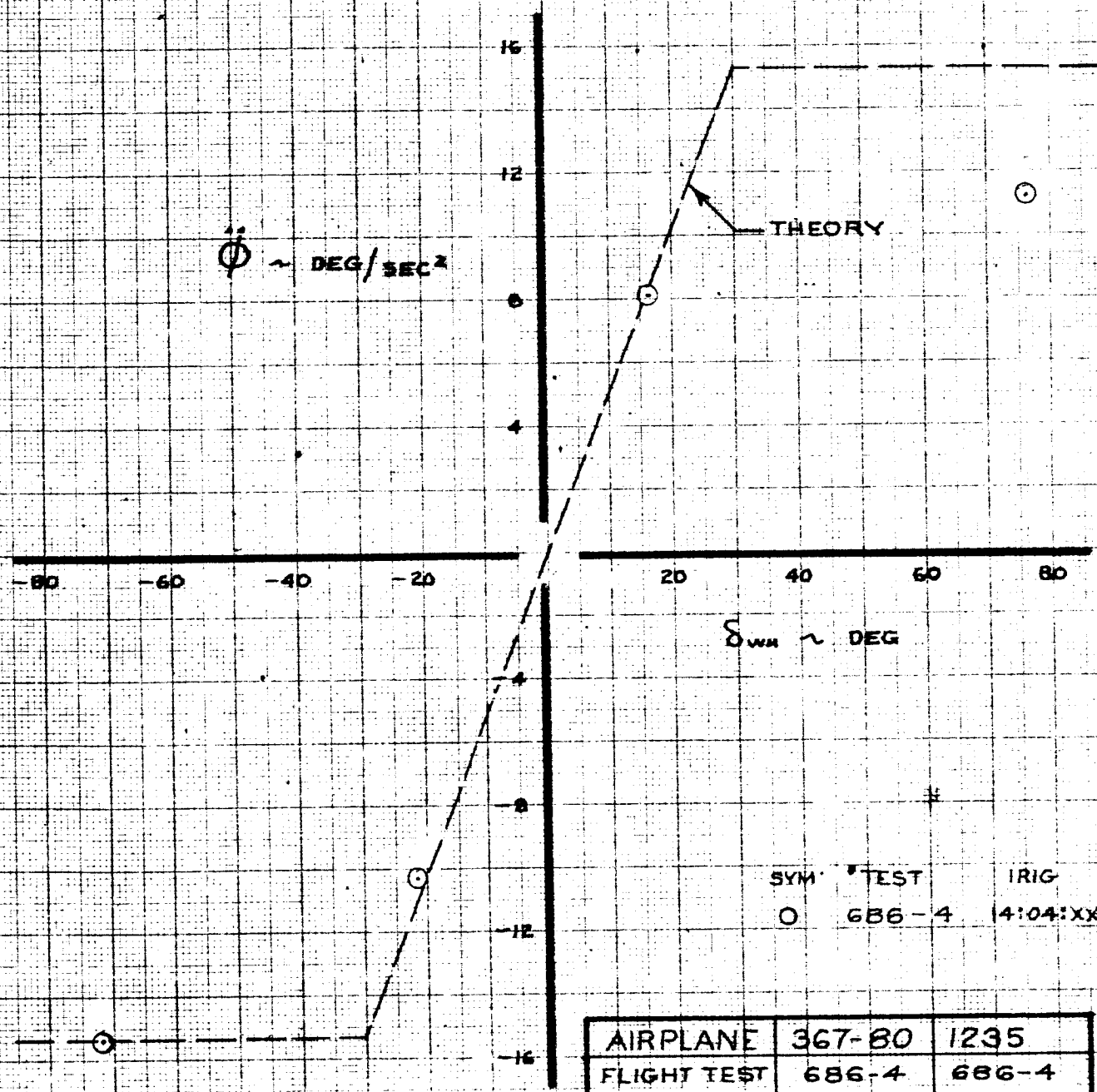
AIRPLANE	367-80	1207A
FLIGHT TEST	686-6	686-6
FLAP	30°	
V ₁ ~ KTS	117	117
ALTITUDE	7,000 FT	SEA LEVEL
G.W. ~ LBS	158,900*	500,000
C.G	30.7%	25%

CALC			REVISED	DATE
CHECK				
APR				
APR				

ROLL RATE REVERSAL
 FLIGHT TEST 686-6
 CONFIGURATION 1207A

367-80
 FIG. 75
 THE BOEING COMPANY DG-15000
 PAGE VIII-107

ROLL RATE REVERSAL



AIRPLANE	367-80	1235
FLIGHT TEST	686-4	686-4
FLAP	30°	
V _I ~ KTS	117	117
ALTITUDE	5,200 FT	SEA LEVEL
G. W. ~ LBS	158,500	500,000
C. G.	29.3%	25.%

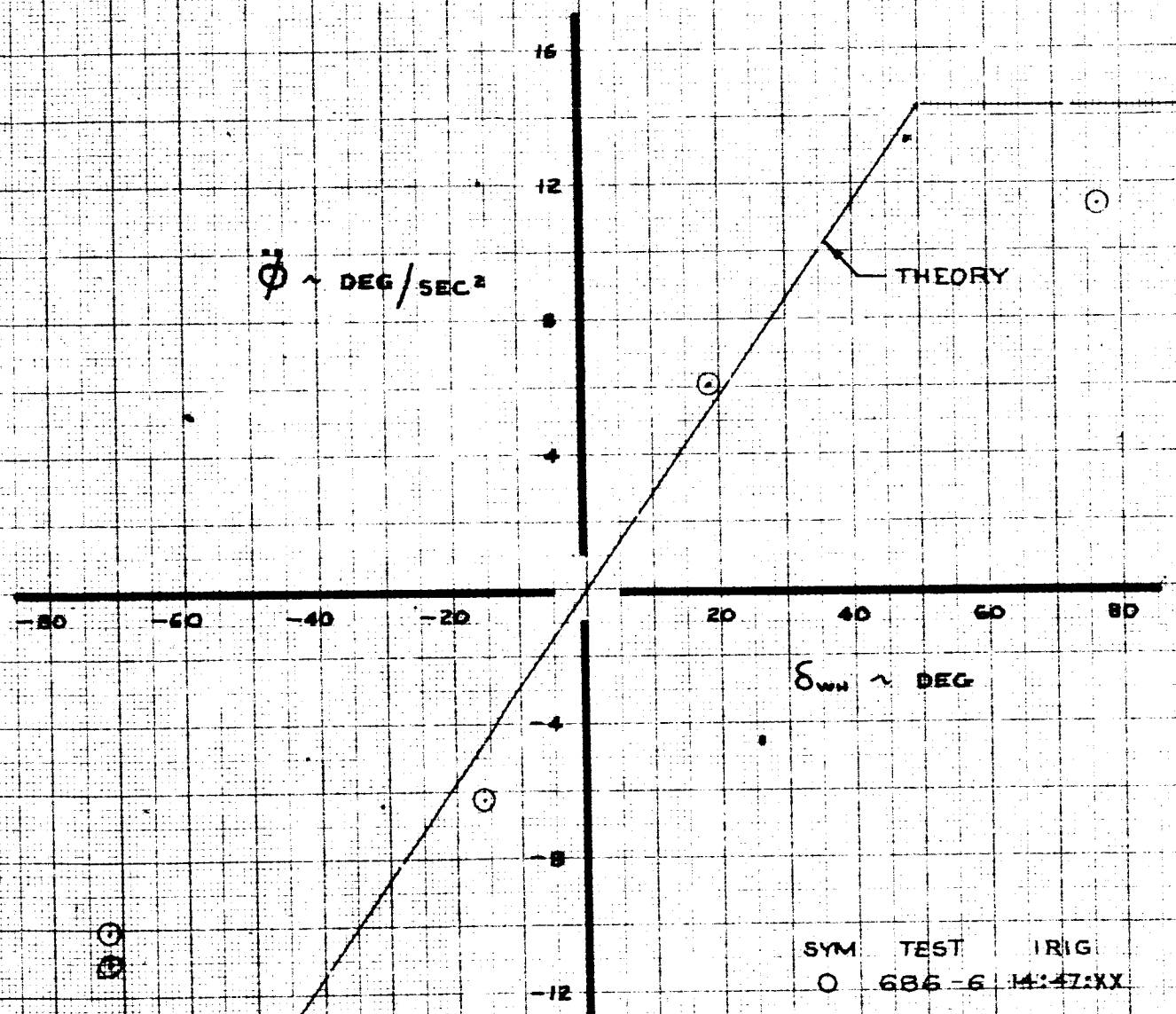
CALC			REVISED	DATE
CHECK				
APR				
APR				

ROLL RATE REVERSAL
FLIGHT TEST 686-4
CONFIGURATION 1235

THE BOEING COMPANY 06-15000

367-80
FIG. 76
PAGE
VIII-108

ROLL RATE REVERSAL



SYM TEST IRIG
 O 686-6 14:47:XX

$L = .250$
 $L_{\delta_{WH}} = .286$

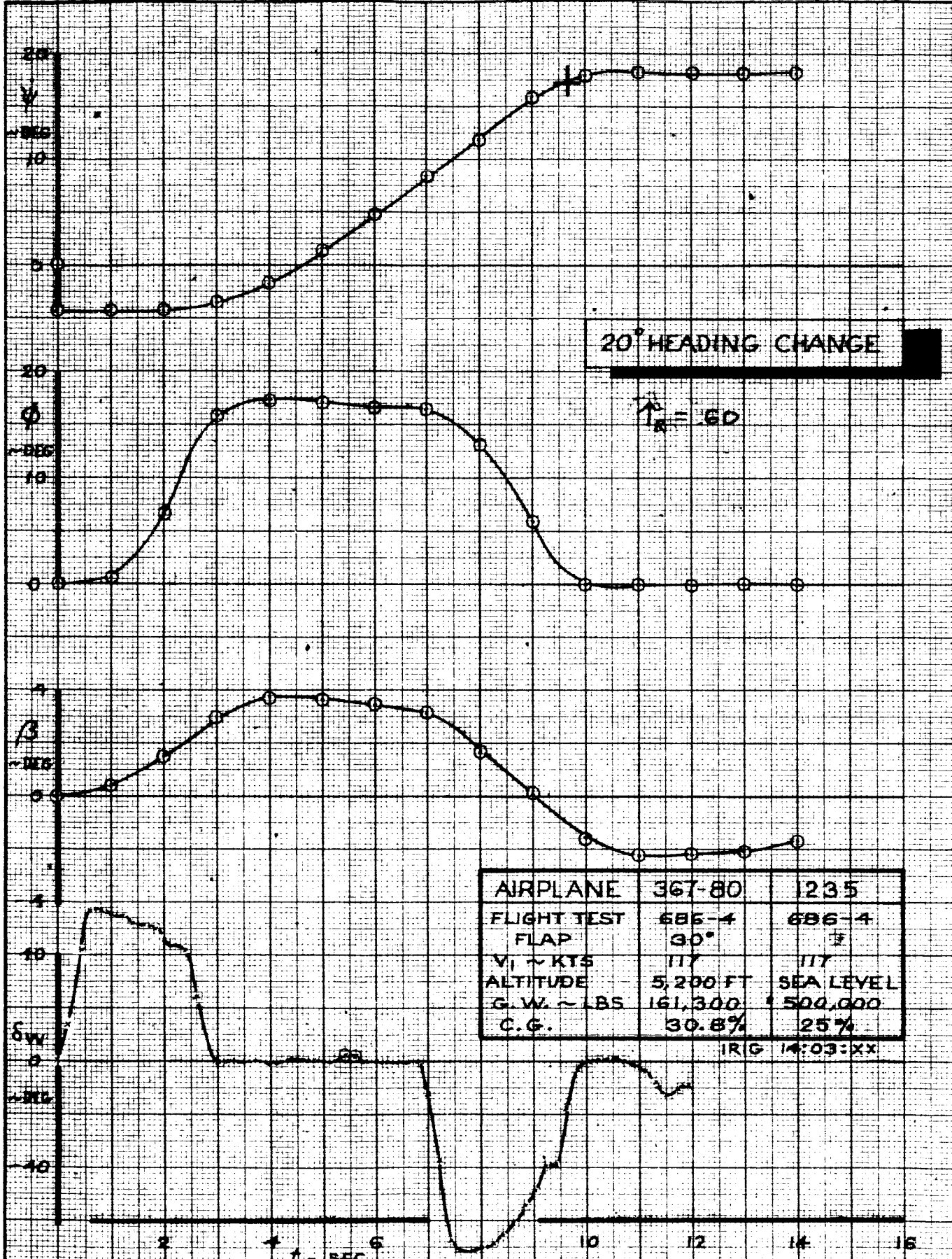
AIRPLANE	367-80	1237
FLIGHT TEST	686-6	686-6
FLAP	30°	
$V_1 \sim \text{KTS}$	117	117
ALTITUDE	6,000 FT	SEA LEVEL
G. W. $\sim \text{LBS}$	162,400	500,000
C. G.	30.7%	25%

CALC			REVISED	DATE
CHECK				
APR				
APR				

ROLL RATE REVERSAL
 FLIGHT TEST 686-6
 COFIGURATION 1237
 THE BOEING COMPANY D6-15000

367-80
 FIG. 77
 PAGE
 VIII-109

112



CALC			REVISED	DATE	20° HEADING CHANGE FLIGHT TEST 686-4 CONFIGURATION 1235	367-80
CHECK						D6-15000
APR						FIG. 78
APR						PAGE
					THE BOEING COMPANY	VIII-110

1/3

B. Ground Based Simulation

The lateral-directional characteristics of all the configurations evaluated on the ground based simulator are presented in Table 6. The aerodynamic coefficients and augmentation system used to obtain these characteristics are listed in Appendix 1. Lateral-Directional aerodynamic characteristics which are equivalent to the basic values with augmentation are also presented. Figures 79, 80, and 81 present roll response ϕ_1 and ϕ_2 as a function of control power for the three augmentation systems used (described in Appendix 1). The effect of roll time constant (T_R) on roll response is presented in Fig. 82 for a step wheel and Fig. 83 for step aileron. Figs. 84 and 85 give roll response for typical configurations with augmentations 2 and 3. A typical roll response with augmentation 1 was presented in Fig. 36 (page VII-57). Figure 86 presents roll response of a configuration with low available aileron rate (60 °/sec).

GROUND BASED CONFIG	L	S _{WH} EFF.	L ₆ WH.	t ₆ a MAX.	τ _{ROLL}	ḡ _{SS}	φ ₁	φ ₂	F _W / S _W	LR SYSTEM	DUTCH ROLL		SPIRAL
											ω _n	ζ	
G ₂	END. PPS	DEG.	1/SEC ²	SEC.	SEC.	DEG/SEC.	DEG.	DEG.	LB/OLB		RAD/SEC.	SEC.	
1	.20	50	.229	.10	1.42	16.3	4.4	14.2	.28	2	.449	.339	2.5
1					1.14	13.1	4.1	15.8		3	.508	.329	18.3
1h					1.42	16.3	4.4	14.2	.14	2	.449	.339	2.5
2	.30		.344			24.4	6.5	21.2	.28				
3	.40		.458			32.6	8.7	28.1					
4	.50		.573			40.7	10.8	35.0					
5	.60		.688			48.9	13.0	42.0					
5A	.80		.917			65.1	17.4	56.2					
5B	1.0		1.146			81.5	21.6	70.					
5C	.15		.172			12.2	3.3	10.9					
5C					1.14	9.8	3.0	12.0		3	.508	.329	18.3
5D	.25		.143			10.2	2.8	9.0		2	.449	.339	2.5
5E	.9		1.031			73.2	19.5	63.					
5F	.10		.115			8.1	2.2	6.8					
5G	.05		.057			1.14	1.0	4.0		3	.508	.329	18.3
5H		90	.032										
5J		30	.096										
6	.15		.286			12.2	3.3	10.9		2	.449	.339	2.5
6					1.14	9.8	3.0	12.0		3	.508	.329	18.3
7A	.10		.191			8.1	2.2	6.8		2	.449	.339	2.5
8	.30	75	.229			14.4	6.5	21.2					
8A	.15		.115			9.8	3.0	12.0		3	.508	.329	18.3
9	.40		.306			14.2	8.7	28.1		2	.449	.339	2.5
10		90	.255										

CALC	R. Root	2-2-66	REVISED	DATE
CHECK				
APR				
APR				

GROUND BASED SIMULATION
LATERAL RUN LOG.
THE BOEING COMPANY
RENTON, WASHINGTON

115

GROUND BASED CONFIG	L	δ_{WH} EFF. DEG.	$L\delta_{WH}$ 1/SEC ²	$t\delta_{QMAX}$ SEC.	τ_{ROLL} SEC.	$\dot{\phi}_{SS}$ DEG/SEC	ϕ_1 DEG	ϕ_2 DEG	$\frac{F_W}{\delta W}$ LB/DEG	26 SYSTEM	DUTCH ROLL		SPIRAL
											ω_n	RAO/SEC	
G2													
11	.30	90	.191	.10	1.42	24.4	6.5	21.2	.28	2	.449	.339	2.5
12	.20		.127			16.3	4.4	14.2					
13	.125		.080			10.2	2.8	9.0					
14	.15		.0955		1.14	9.8	3.0	12.0		3	.508	.329	18.3
16		50	.172	.18	1.42	12.2	3.1	10.2		2	.449	.339	2.5
16					1.14	9.8	2.9	11.5		3	.508	.329	18.3
17	.25		.287		1.42	20.4	5.2	17.0		2	.449	.339	2.5
18	.35		.401			28.5	7.2	24.0					
19	.15		.172	.30		12.2	2.7	9.4		2			
19					1.14	9.8	2.5	10.7		3	.508	.329	18.3
20	.25		.287		1.42	20.4	4.6	15.8		2	.449	.339	2.5
21	.35		.401			28.5	6.2	22.0					
22	.30		.344	.18			6.8	24.8			.403	.223	
23	.20		.229				4.4	16.5					
23A	.15		.172				3.4	12.3					
24	.30		.344		1.03	17.7	5.9	18.6			.474	.377	3.8
25	.15		.172			8.9	3.0	9.2					
25A	.20		.229			11.8	3.9	12.3					
26				.10	1.42	16.3	4.4	14.2			.449	.339	2.5
27													
28													

CALC R. Root
 CHECK
 APR
 APR

REVISED
 DATE

GROUND BASED SIMULATION
 LATERAL RUN LOG.

THE BOEING COMPANY
 RENTON, WASHINGTON

TABLE 6
 DG-15000
 PAGE VIII-112A

116

GROUND BASED CONF.	L	δ _{WH} EFF.	L _g WH.	t _g MAX.	τ _{ROLL}	ḡ _{SS}	φ ₁	φ ₂	F _w / δ _w	LOG SYST.	DUTCH ROLL		SPIRAL	
											ω _n	ζ		
CALC	REVISD	DATE	1/SEC ²	SEC.	SEC.	DEG/SEC	DEG	DEG	LB/IN		RAD/SEC			
CHECK			DEG.									SEC		
APR														
APR														
202A	.25	50	.287	.20	1.14	16.35	5	19.2	.28	3	.508	.329	18.3	1.33
205C	.15		.172			9.8	2.9	11.5						
205F	.10		.115			6.54	1.9	7.6						
207A	.15	30	.286			9.8	2.9	11.5						
216		50	.172	.36			2.5	10.8						
219				.60			1.7	9.5						
219A	.10		.115			6.54	1.1	4.9						
224A	.50		.573	.36	.93	26.6	8.0	31.0	.519		.346	.305	23.5	1.11
231	.16		.184	.20	1.59	14.6	3.4	14.5	.479		.305	.305	11.7	1.70
232A	.26		.298		.72	10.7	4.8	18.2	.529		.367		31.2	.87
233A	.43		.493			17.7	8.0	30.7						
234A	.15		.173			6.19	2.8	10.5						
236	.25		.287	.50	1.14	16.35	4.1	17.9	.508		.329		18.3	1.33
237				.75			3.5	16.3						
1202	.30	50	.344	.20	1.14	19.6	5.7	20.1	.19	1	.508	.329	18.3	1.33
1202A	.25		.287			16.35	4.8	16.7	.19128					
1203	.40		.458			26.1	7.5	26.8	.28					
1203A	.24	30	.459			15.7	4.6	16.0	.19					
1203A ²	.15		.478			16.35	4.8	16.7						
1205C	.15	50	.172			9.80	2.8	10.0	.28					
1205D	.25	75	.191			16.35	4.8	16.7	.19					
1205F	.10	50	.115			6.54	1.9	6.6						

GROUND BASED SIMULATION
LATERAL RUN LOG.
THE BOEING COMPANY
RENTON, WASHINGTON

TABLE 6
D6-15000
PAGE VIII-113

GROUND BASED CONFIG.	L	L _{WH} EFF.	L _{WH}	t _σ MAX.	τ _{BOLL}	P _{SS}	φ ₁	φ ₂	F _W / σ _W	DUTCH ROLL		SPIRAL	
										ω _n	γ	T _{1/2}	φ/β
DEG.	SEC.	DEG.	1/SEC ²	SEC.	SEC.	DEG/SEC	DEG.	DEG.	LB/DEG.	RAD/SEC.		SEC.	
1206	.10	30	.191	.2	1.14	6.54	1.9	6.6	.28	.508	.329	18.3	1.33
1207A	.15		.286			9.8	2.8	10.0	.19				
1209A		75	.115						.19f.28				
1209A	.40		.306			26.2	7.5	26.8	.28				
1222	.30	50	.344	0	1.59	27.4	8.0	27.0		.479	.305	11.7	1.7
1223					1.14	19.6	7.5	22.5		.508	.329	18.3	1.33
1224					.93	16.0	5.6	20.0		.519	.346	23.5	1.11
1230	.15		.172	.2	1.59	13.7	3.1	12.0		.479	.305	11.7	1.7
1231	.16		.184			14.6	3.3	12.9					
1232	.28		.321		.72	11.5	4.6	15.1		.529	.367	31.2	.87
1233	.47		.539			19.4	7.8	24.4	γ				
1233B					.60	16.2	7.4	22.8	.19f.28	.533	.380	38.2	.73
1234B	.15		.172		.72	6.18	2.5	8.0	.28	.529	.367	31.2	.87
1235	.267		.306		.60	9.2	4.2	13.3	.19	.533	.380	38.2	.73
1236	.25		.287	.5	1.14	16.35	3.5	16.0	.28	.508	.329	18.3	1.33
1236B	.43	30	.821	.2	.60	14.8	6.8	21.0	.19	.533	.380	38.2	.73
1237	.25	50	.287	.75	1.14	16.35	3.2	13.0	.28	.508	.329	18.3	1.33
1237A				0			5.3	18.5					

TD 1040C - R3

CALC	R. Root	2-2-66	REVISED	DATE
CHECK				
APR				
APR				

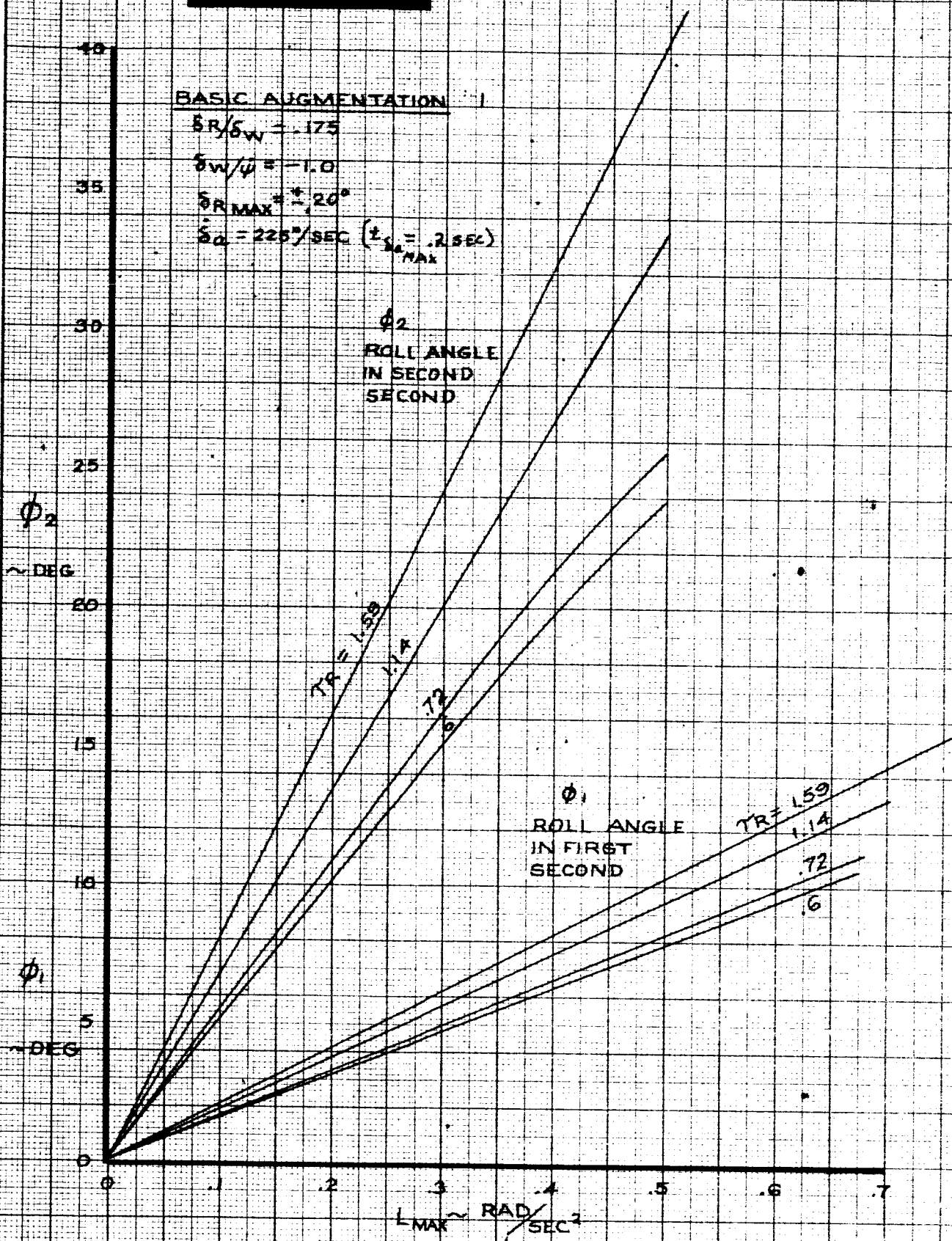
GROUND BASED SIMULATION
LATERAL RUN LOG.
THE BOEING COMPANY
RENTON, WASHINGTON

TABLE
D6-15000
PAGE
VIII-114

811

f

ROLL RESPONSE



CALC	R. Root	2-2-66	REVISED	DATE
CHECK				
APR				
APR				

ROLL RESPONSE - WHEEL STEP
GROUND BASED SIMULATOR
AUGMENTATION 1

THE BOEING COMPANY

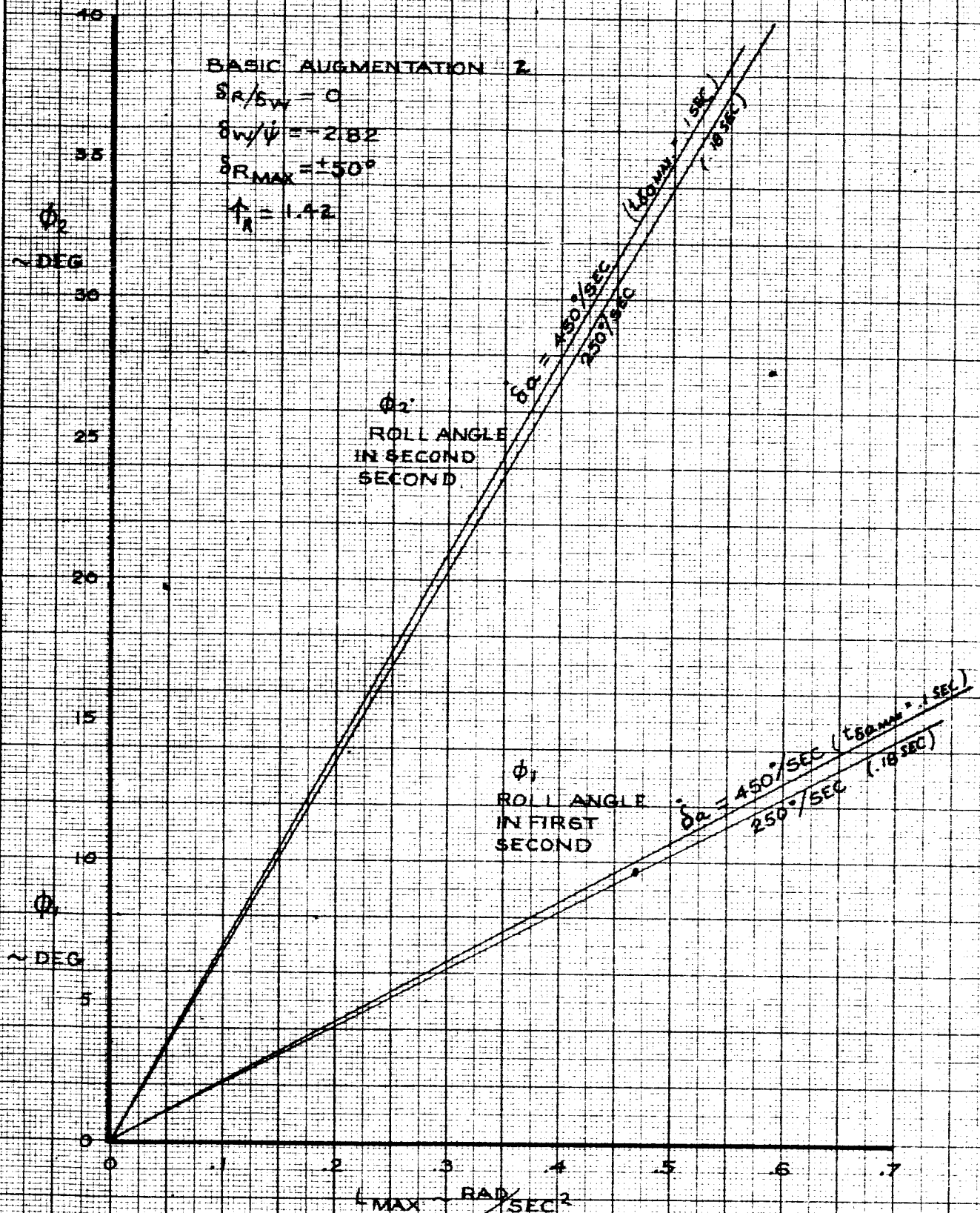
FIG. 79

D6-15000

PAGE VIII-115

119

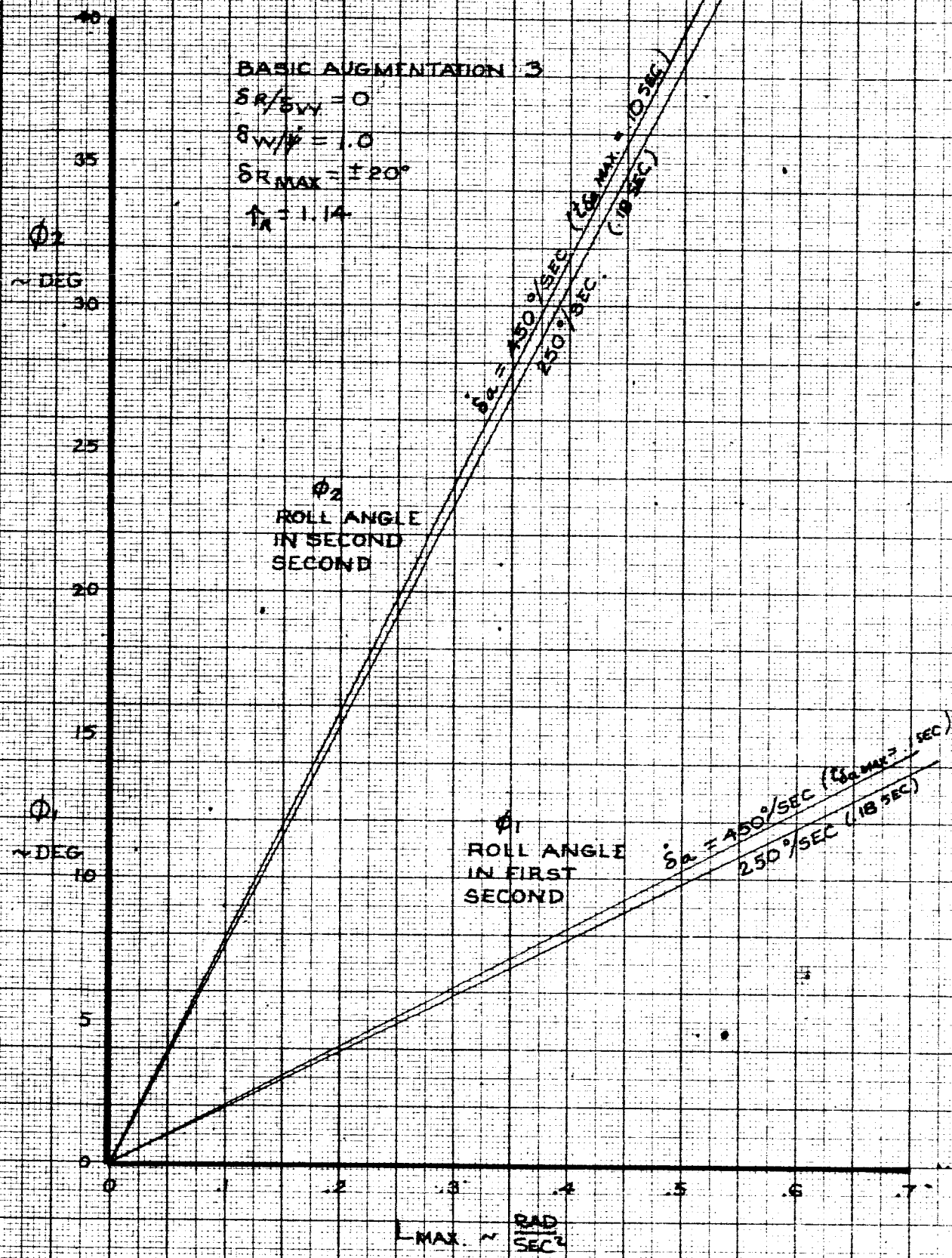
ROLL RESPONSE



CALC	R. Root	2-2-66	REVISED	DATE	ROLL RESPONSE - WHEEL STEP GROUND BASED SIMULATION AUGMENTATION 2 THE BOEING COMPANY	FIG 80
CHECK						D6-15000
APR						PAGE
APR						VIII-116

1.20

ROLL RESPONSE



CALC	R. Root	2-2-66	REVISED	DATE
CHECK				
APR				
APR				

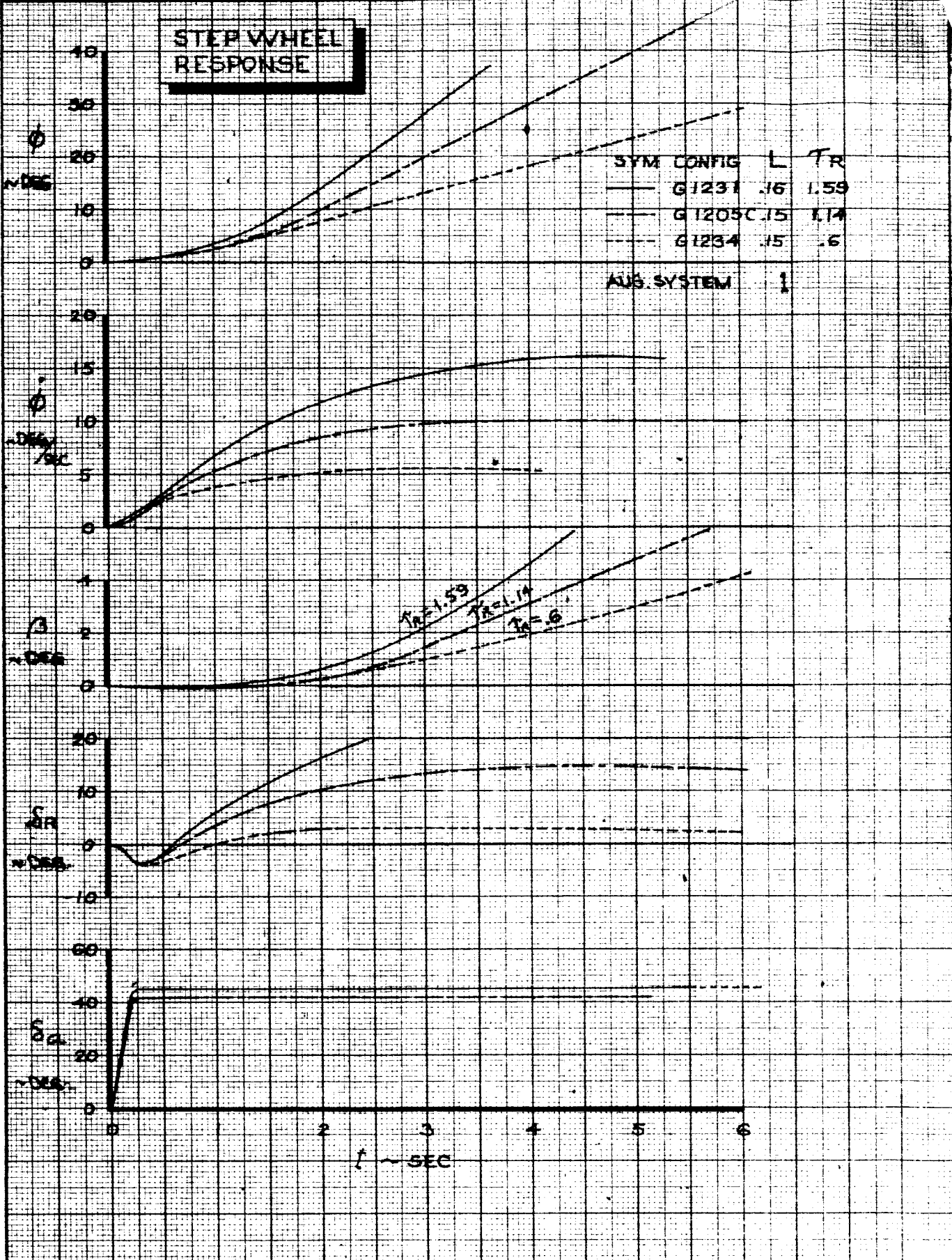
ROLL RESPONSE - WHEEL STEP
 GROUND BASED SIMULATOR
 AUGMENTATION 3

THE BOEING COMPANY

FIG. 81
 D6-15000
 PAGE
 VIII-117

121

STEP WHEEL RESPONSE



CALC	R. Root	2-2-66	REVISED	DATE
CHECK				
APR				
APR				

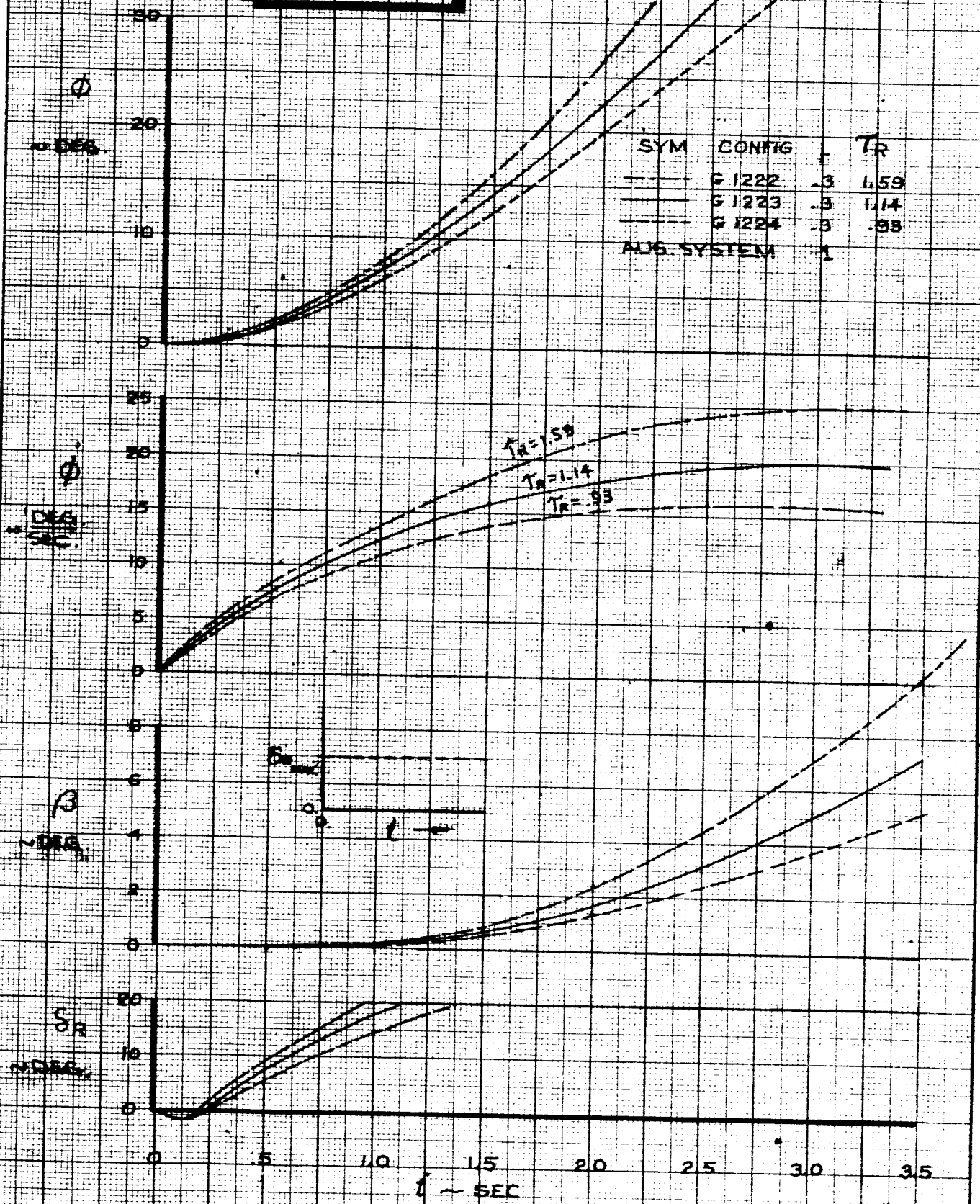
STEP WHEEL RESPONSE
 GROUND BASED SIMULATOR
 EFFECT OF T_R

THE BOEING COMPANY

TD 461 C-84

122

STEP AILERON RESPONSE



SYM	CONFIG	TR
---	G 1222	1.59
---	G 1223	1.14
---	G 1224	.93
---	AUG. SYSTEM	1

CALC	R. Root	2-2-66	REVISED	DATE
CHECK				
APR				
APR				

STEP AILERON RESPONSE
GROUND BASED SIMULATOR
EFFECT OF TR

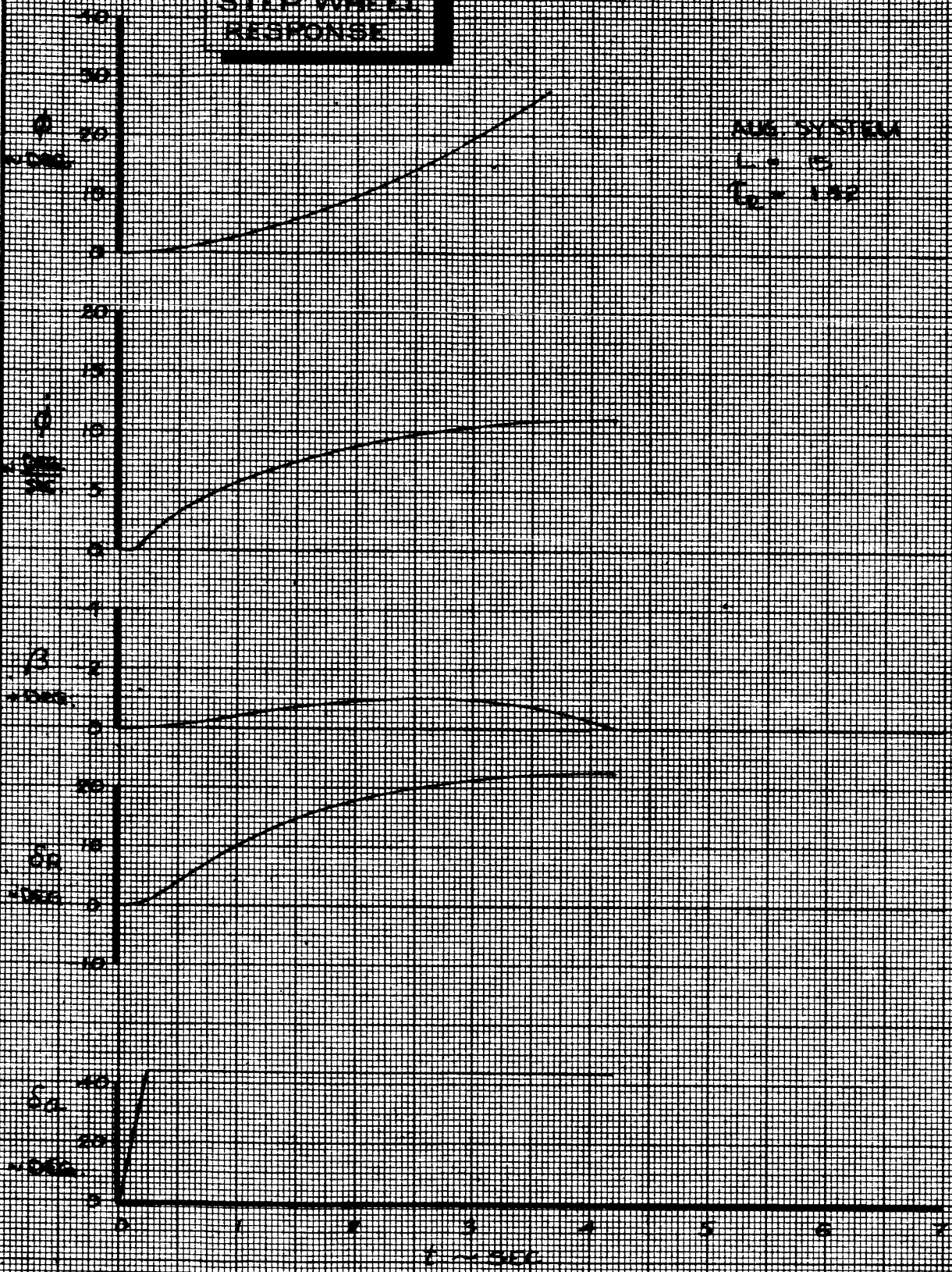
THE BOEING COMPANY

FIG. 83
D6-15000
PAGE
VIII-119

123

STEP WHEEL RESPONSE

AUG SYSTEM 12
 L.P. 15
 G.P. 102

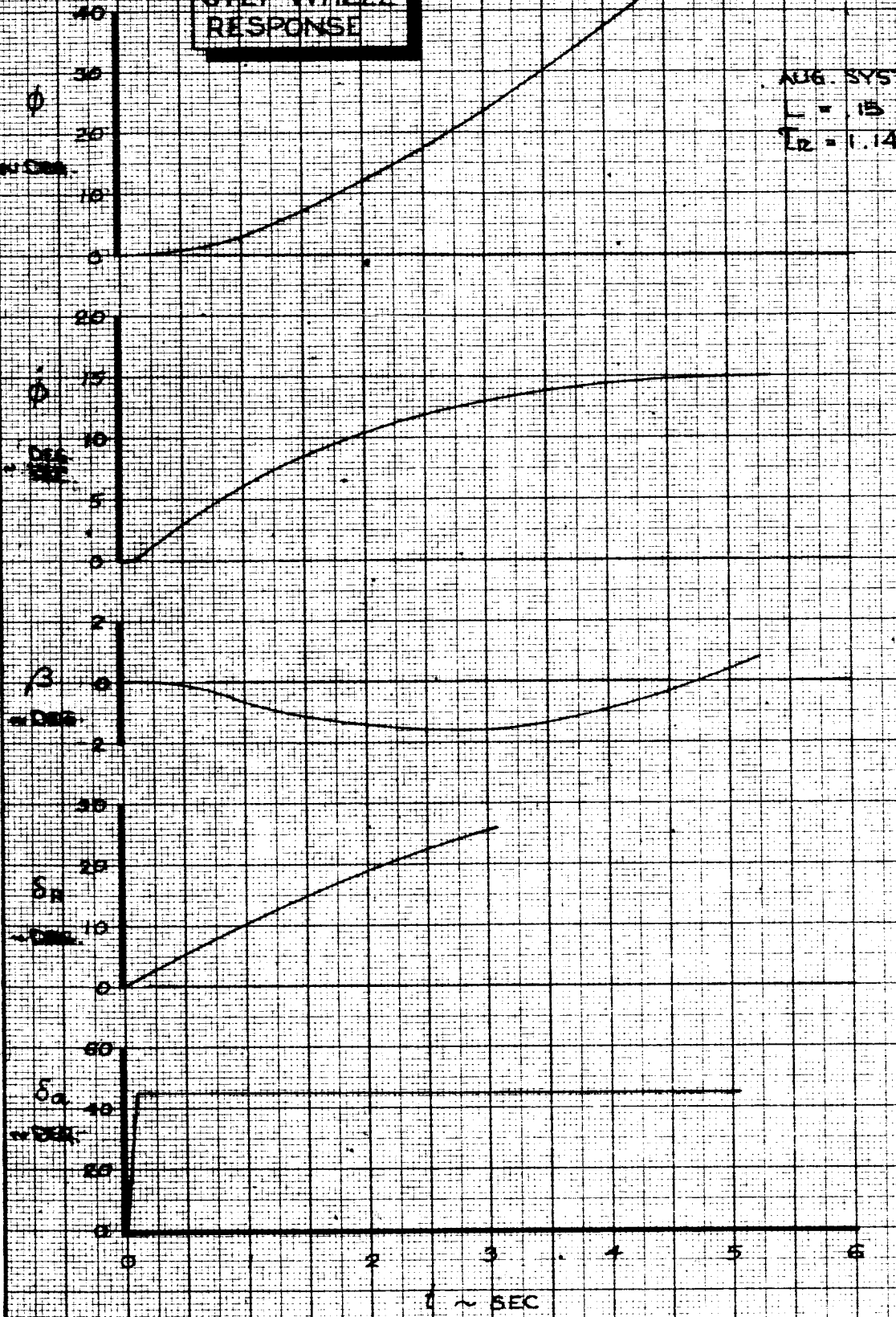


CALC	R. Root	2-2-66	REVISED	DATE	STEP WHEEL RESPONSE GROUND BASED SIMULATOR CONFIGURATION G16	FIG. 84
CHECK						D6-15000
APR						PAGE
APR						VIII-120
					THE BOEING COMPANY	

124

STEP WHEEL RESPONSE

ADG. SYSTEM 3
 $L = 15$
 $L_2 = 1.14$



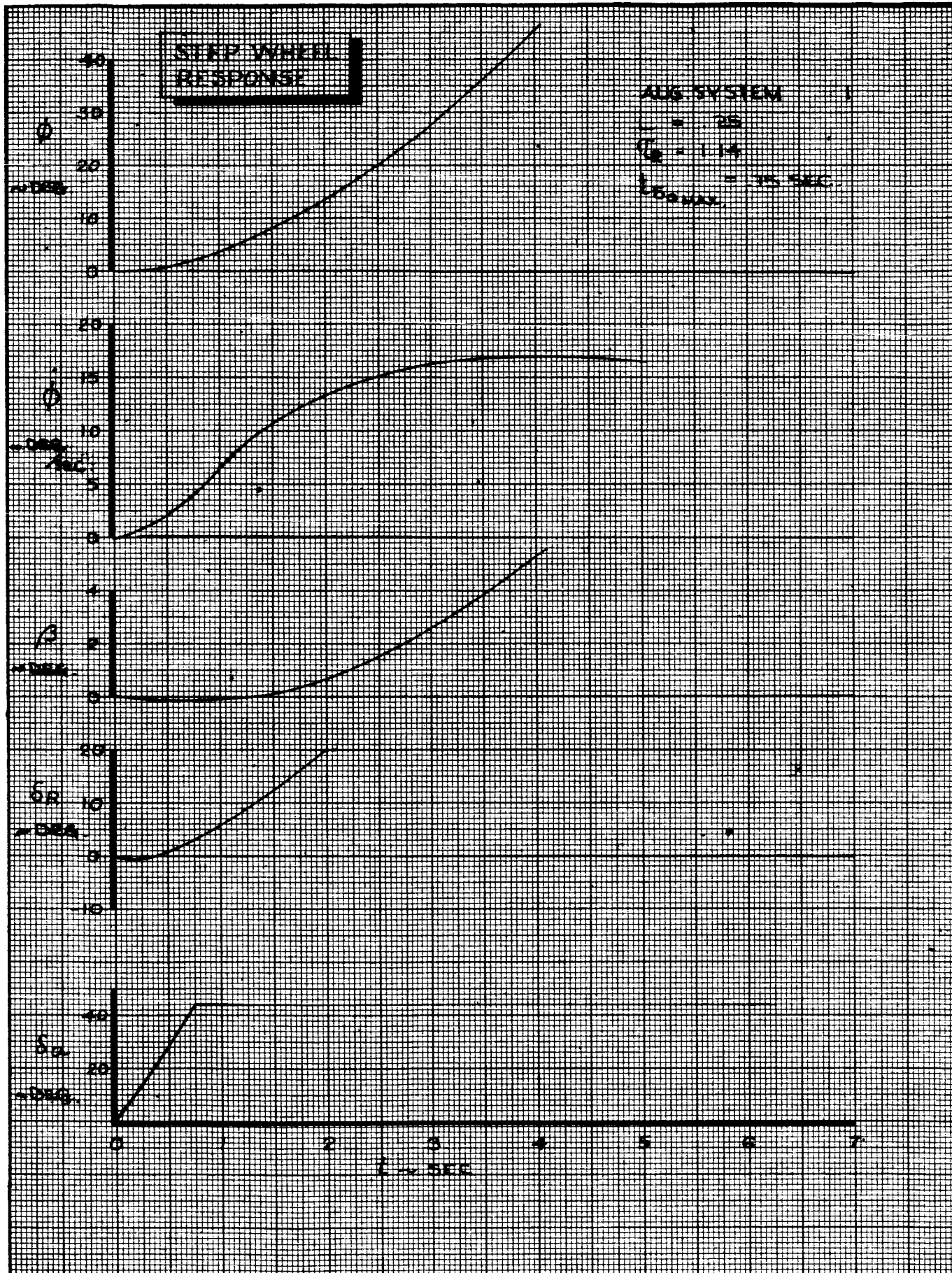
CALC	R. Root	2-2-66	REVISED	DATE
CHECK				
APR				
APR				

STEP WHEEL RESPONSE
 GROUND BASED SIMULATOR
 CONFIGURATION G205 C

THE BOEING COMPANY

FIG. 85
 D6-15000
 PAGE
 VIII-121

10-5



CALC	R. Root	2-2-66	REVISED	DATE	STEP WHEEL RESPONSE GROUND BASED SIMULATOR CONFIGURATION G1237	FIG. 86
CHECK						D6-15000
APR						PAGE
APR						VIII-122
					THE BOEING COMPANY	

1090

IX. DOCUMENTATION OF THE 367-80 WITH BOUNDARY LAYER CONTROL

The longitudinal and lateral characteristics of the 367-80 with Boundary Layer Control (BLC) are documented in Figs. 87 to 96A. The dynamic characteristics are included in Tables 1 and 4 (pages ^{VII}59 and ^{VIII}103). A description in terms of aerodynamic coefficients is given in Appendix 1.

The purpose of going to the BLC configuration was to create the large roll control power required for evaluation. It should be noted, however, that this configuration has many characteristics other than roll control power which are different from the basic 1209 and 101A configuration. The 367-80 (BLC) should not be compared directly to the basic (1209) configuration with the intent of isolating the effects of increased roll control power.

Comments on the flight test and theoretical response to the documentation maneuvers performed are listed below.

Longitudinal

Pitch Rate Reversal

Fig. 87. The pitch control sensitivity is accurately predicted by theory

Wind Up Turn

Figs. 88 & 89. Wind up turn data agrees quite well with the theoretical calculation when the data is shifted to allow for mis-trim.

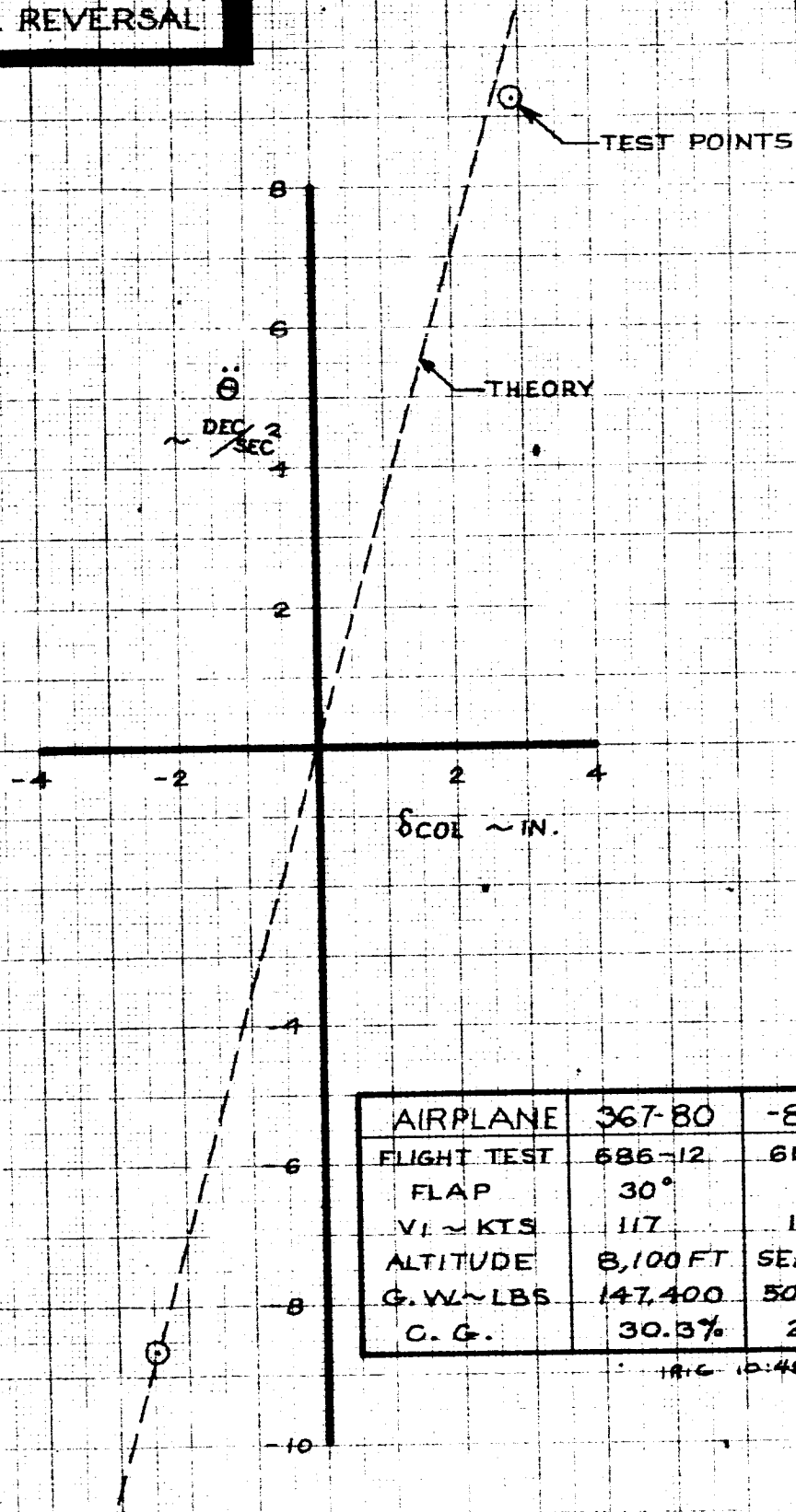
Speed Stability

Fig. 90. A mis-trim in the flight test data is evident when compared to the theory.

Pitch Attitude

Fig. 91. Approximately 3 seconds are required for a pitch attitude change of 9 degrees.

PITCH RATE REVERSAL



AIRPLANE	367-80	-80BLC
FLIGHT TEST	686-12	686-12
FLAP	30°	
V _I ~ KTS	117	117
ALTITUDE	8,100 FT	SEA LEVEL
G. W. ~ LBS	147,400	500,000
C. G.	30.3%	25%

18-C 10:45:XX

CALC			REVISED	DATE
CHECK				
APR				
APR				

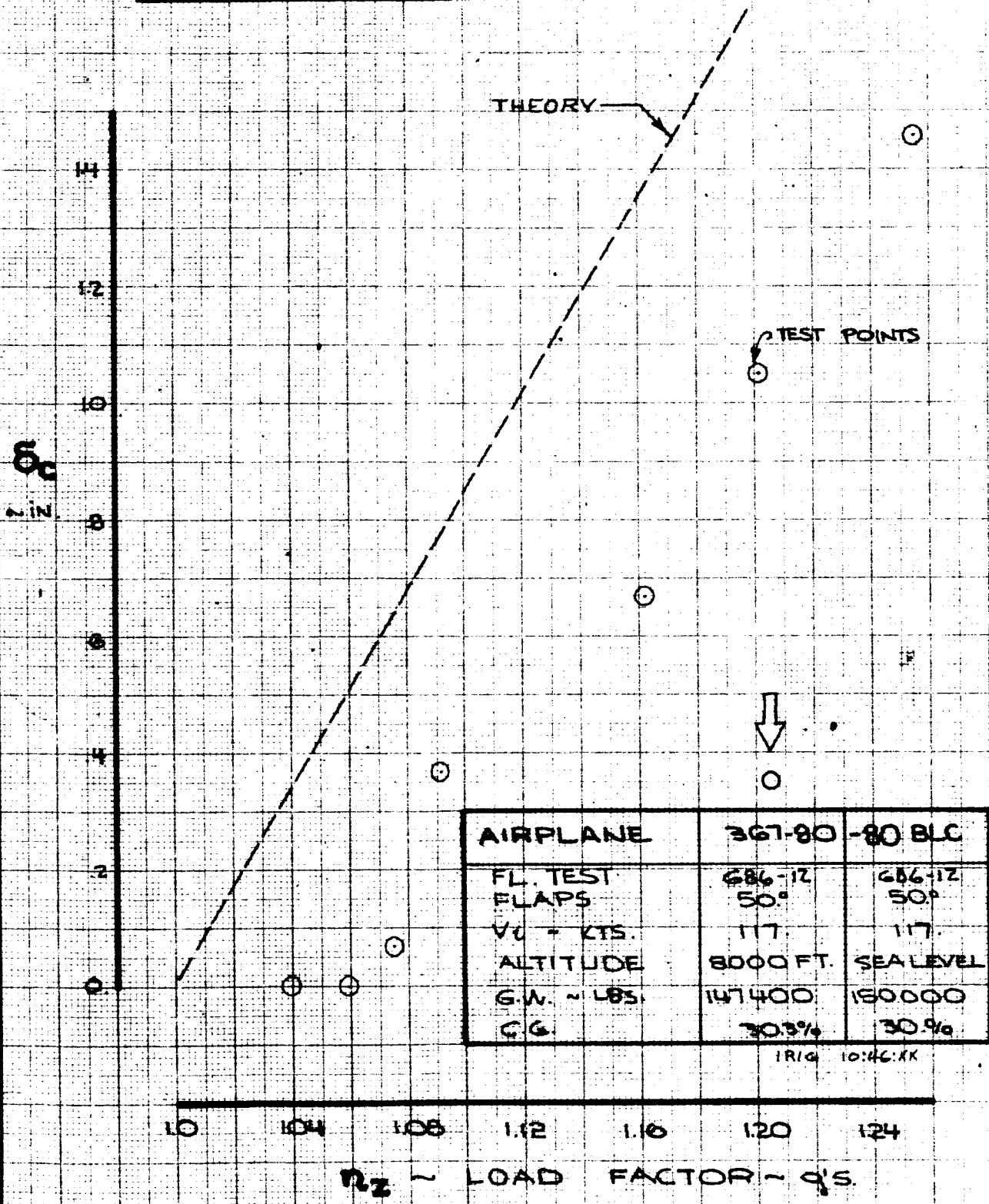
PITCH RATE REVERSAL
 FLIGHT TEST 686-12
 CONFIGURATION -80BLC

THE BOEING COMPANY

367-80
 D6-15000
 FIG. 87
 PAGE
 IX-124

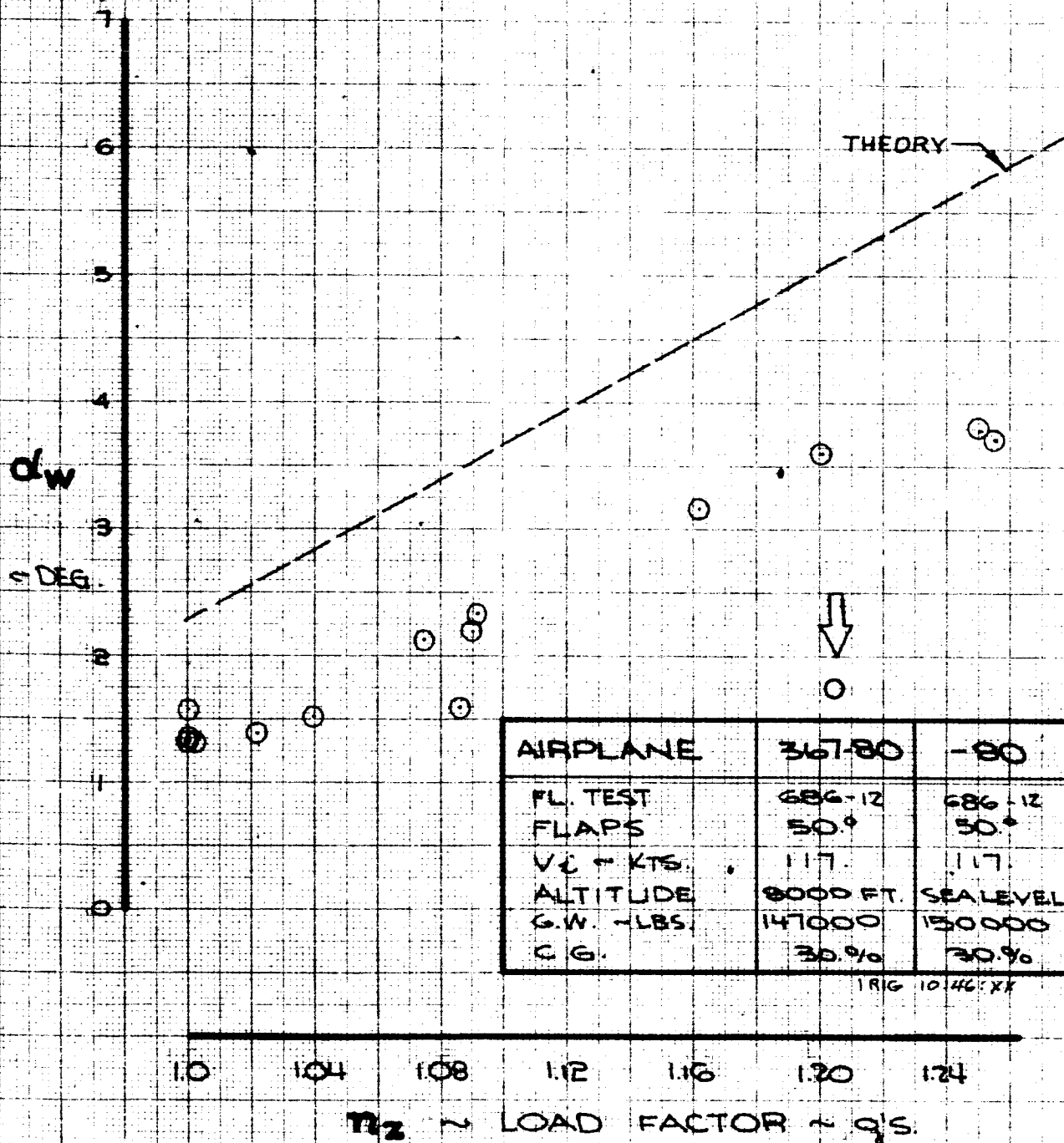
1278

WINDUP TURN



CALC			REVISED	DATE	WINDUP TURN FL. TEST : 686-12 CONFIG. : -80 BLC	367-80
CHECK						D6-15000
APR						FIG. 88
APR						PAGE IX-125
					THE BOEING COMPANY	

WINDUP TURN



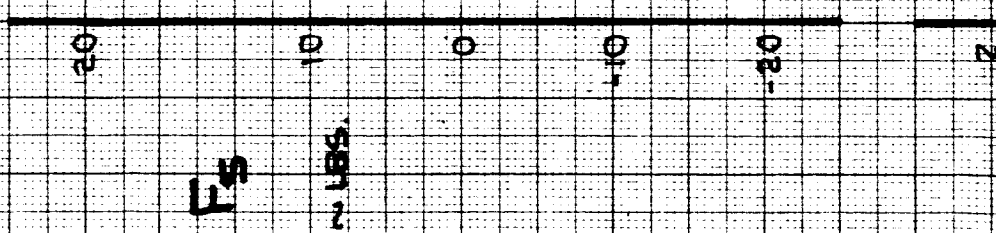
CALC			REVISED	DATE	WINDUP TURN FL. TEST : 686-12 CONFIG. : -80	-80 D6-15000
CHECK						FIG. 89
APR						PAGE
APR						IX-126
					THE BOEING COMPANY	

130

SPEED STABILITY

AIRPLANE	367-80	-80B
FL TEST	686-12	686-12
FLAPS	50%	50%
VL - KTS.	117	117
ALTITUDE	BOOFT SEA LEVEL	
G.W. - LBS.	147000	150000
C.G.	30.3%	30.9%

1815 201714



THEORY
TEST POINT

CALC		REVISED	DATE
CHECK			
APPD.			
APPD.			

SPEED STABILITY
 FL. TEST : 686-12
 CONFIG. : -80B

THE BOEING COMPANY

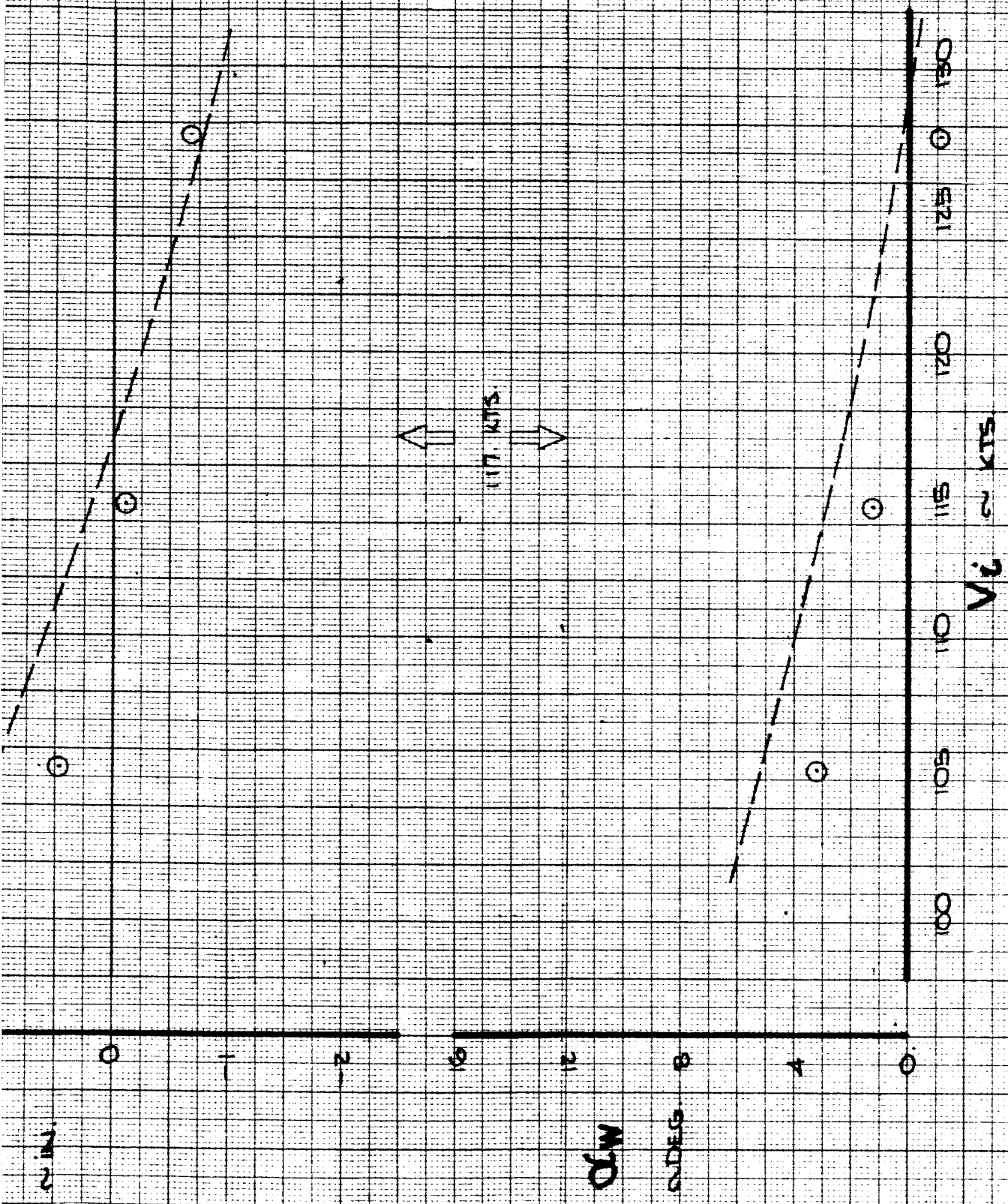
367-80
 D6-15000

FIG. 90

PAGE
 IX-127

131

TR 127-2

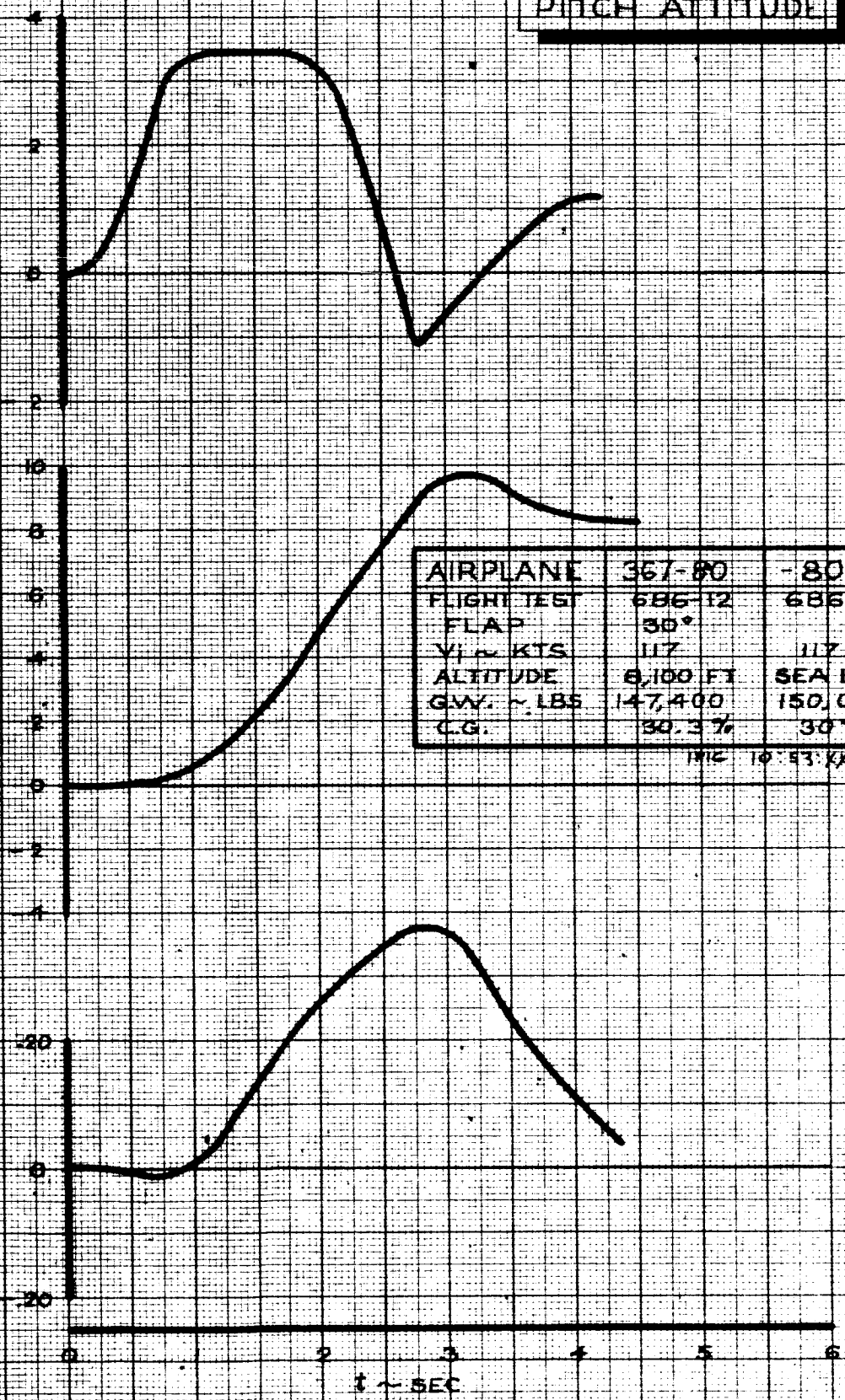


PITCH ATTITUDE

5 DEG
MIN

5 DEG

20
-gS



AIRPLANE	367-80	-80BLC
FLIGHT TEST	686-12	686-12
FLAP	30°	
V ₁ ~ KTS	117	117
ALTITUDE	8,100 FT	SEA LEVEL
GW. ~ LBS	147,400	150,000
C.G.	30.3%	30%

FIG 10-53 XX

CALC		REVISED	DATE
CHECK			
APR			
APR			

PITCH ATTITUDE
FLIGHT TEST 686-12
CONFIGURATION -80BLC

367-80
D6-15000
FIG.91

THE BOEING COMPANY

PAGE
IX-128

1322

Lateral

Steady Roll Rate

Fig. 92. The theoretical and flight test data agree for the steady roll rate.

Roll Rate Reversal

Fig. 93. The theoretical roll acceleration matches the flight test data for small wheel deflections but non-linearity in the airplane characteristic causes inaccuracies for wheel deflections greater than about 15° .

Yaw Rate Reversal

Fig. 94. The yaw rate reversal data agrees fairly well with the theoretically calculated line.

Steady Sideslip

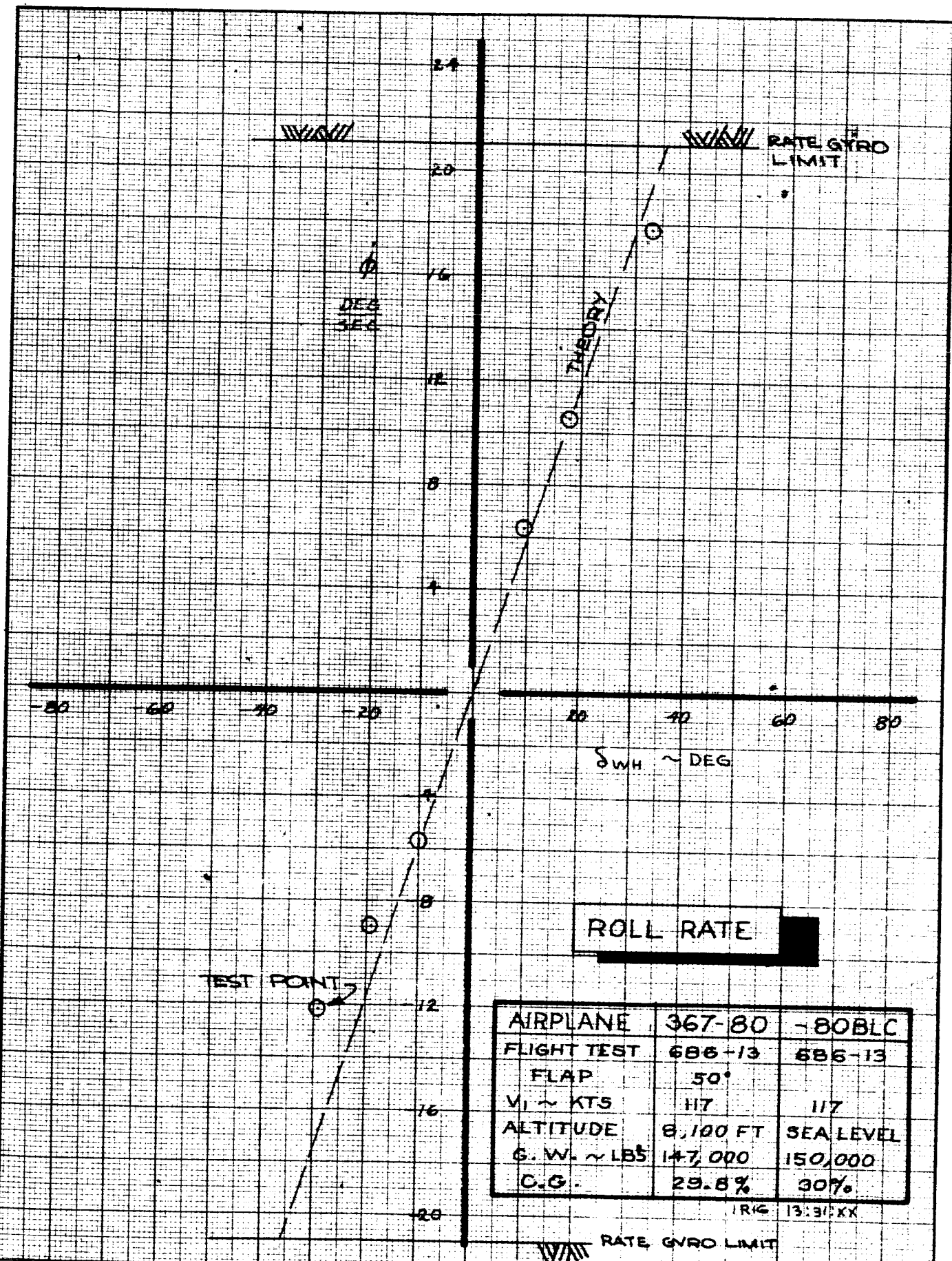
Fig. 95. The steady sideslip characteristics of the 367-80 BLC configuration agree with theory.

Spiral Stability

Fig. 96. The theoretical time to half amplitude in the spiral mode is 124 seconds. The flight test time to half amplitude is 16.3 seconds.

Wheel Step

Fig. 96A. The wheel step took approximately .35 seconds to maximum wheel. The sideslip angle was small in the first second and the roll angle after one second was 3.8° .



ROLL RATE

AIRPLANE	367-80	-80BLC
FLIGHT TEST	686-13	686-13
FLAP	50°	
V ₁ ~ KTS	117	117
ALTITUDE	8,100 FT	SEA LEVEL
G. W. ~ LBS	147,000	150,000
C.G.	29.8%	30%

IRIG 13:31:XX

CALC			REVISED	DATE
CHECK				
APR				
APR				

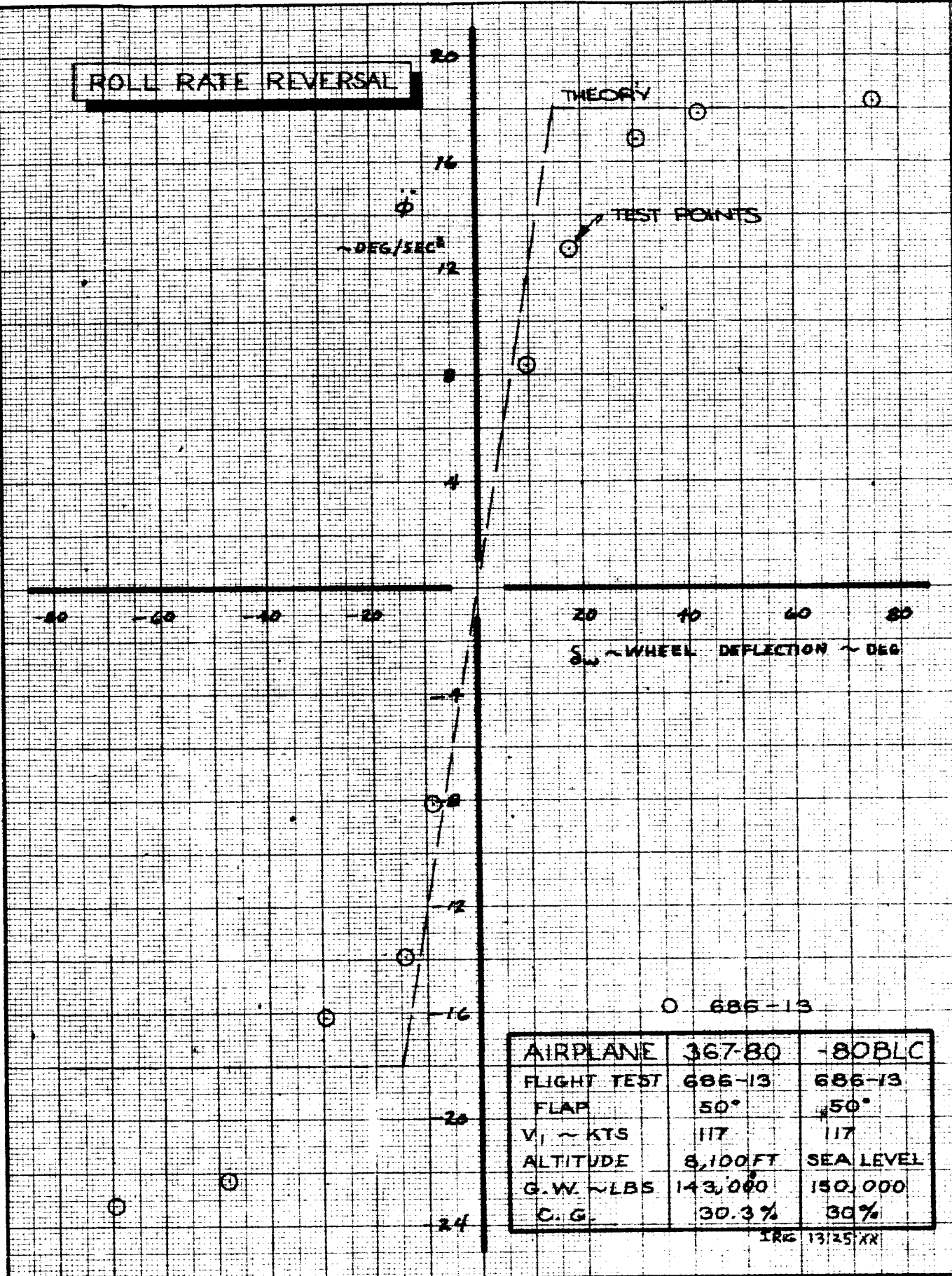
STEADY ROLL RATE
 FLIGHT TEST 686-13
 CONFIGURATION -80BLC

367-80
 DG-15000
 FIG. 92

THE BOEING COMPANY

PAGE
 IX-130

ROLL RATE REVERSAL



AIRPLANE	367-80	-80BLC
FLIGHT TEST	686-13	686-13
FLAP	50°	50°
V ₁ ~ KTS	117	117
ALTITUDE	8,100 FT	SEA LEVEL
G.W. ~ LBS	143,000	150,000
C.G.	30.3%	30%

IRE 13125 XR

CALC			REVISED	DATE
CHECK				
APR				
APR				

ROLL RATE REVERSAL
 FLIGHT TEST 686-13
 CONFIGURATION -80 BLC

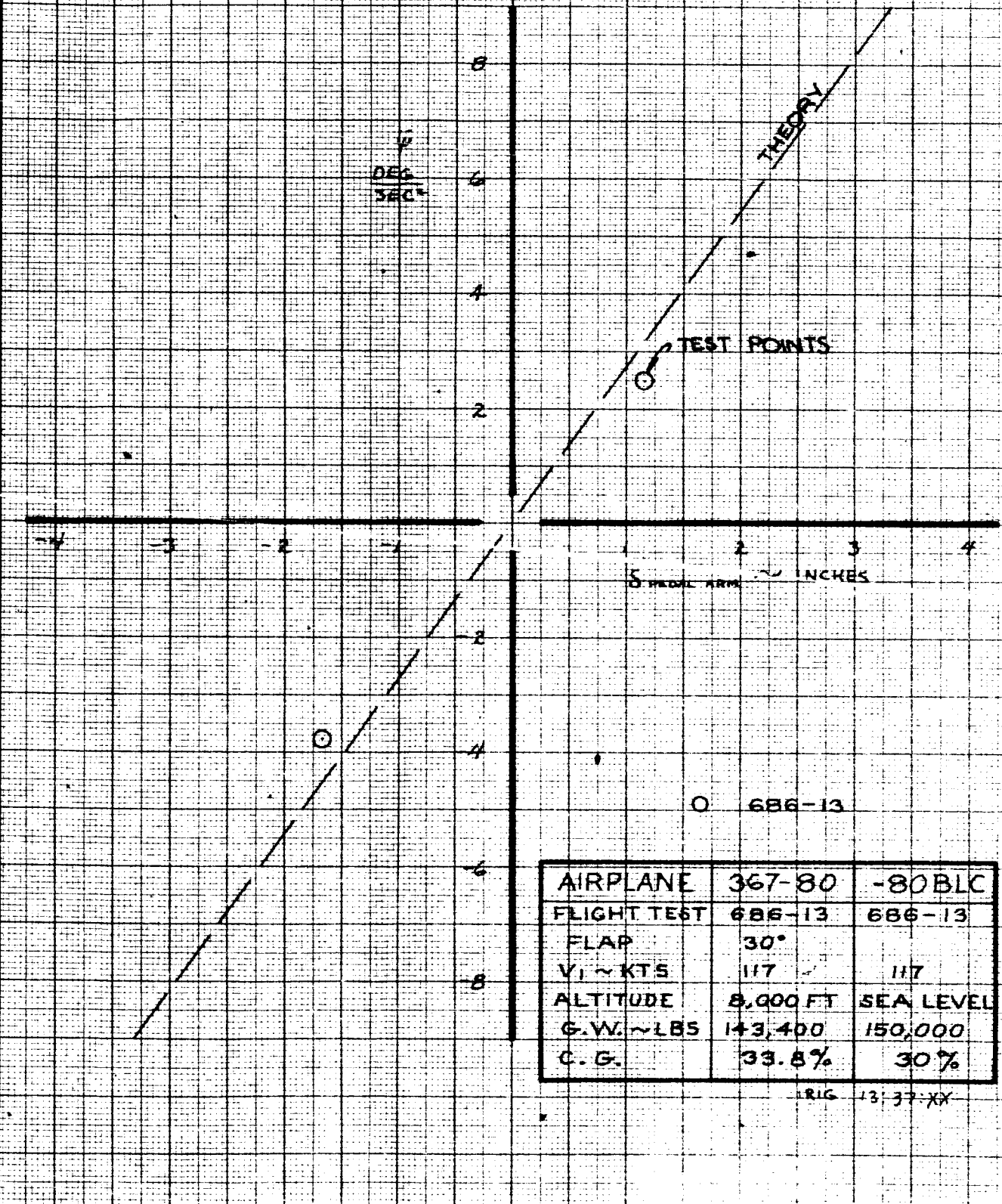
367-80.
 DG-15000
 FIG. 93

THE BOEING COMPANY

PAGE
 IX-131

125

YAW RATE REVERSAL



AIRPLANE	367-80	-80BLC
FLIGHT TEST	686-13	686-13
FLAP	30°	
V ₁ ~ KTS	117	117
ALTITUDE	8,000 FT	SEA LEVEL
G.W. ~ LBS	143,400	150,000
C.G.	33.8%	30%

RIG 13137-XX

CALC			REVISED	DATE
CHECK				
APR				
APR				

YAW RATE REVERSAL
FLIGHT TEST 686-13
CONFIGURATION -80 BLC

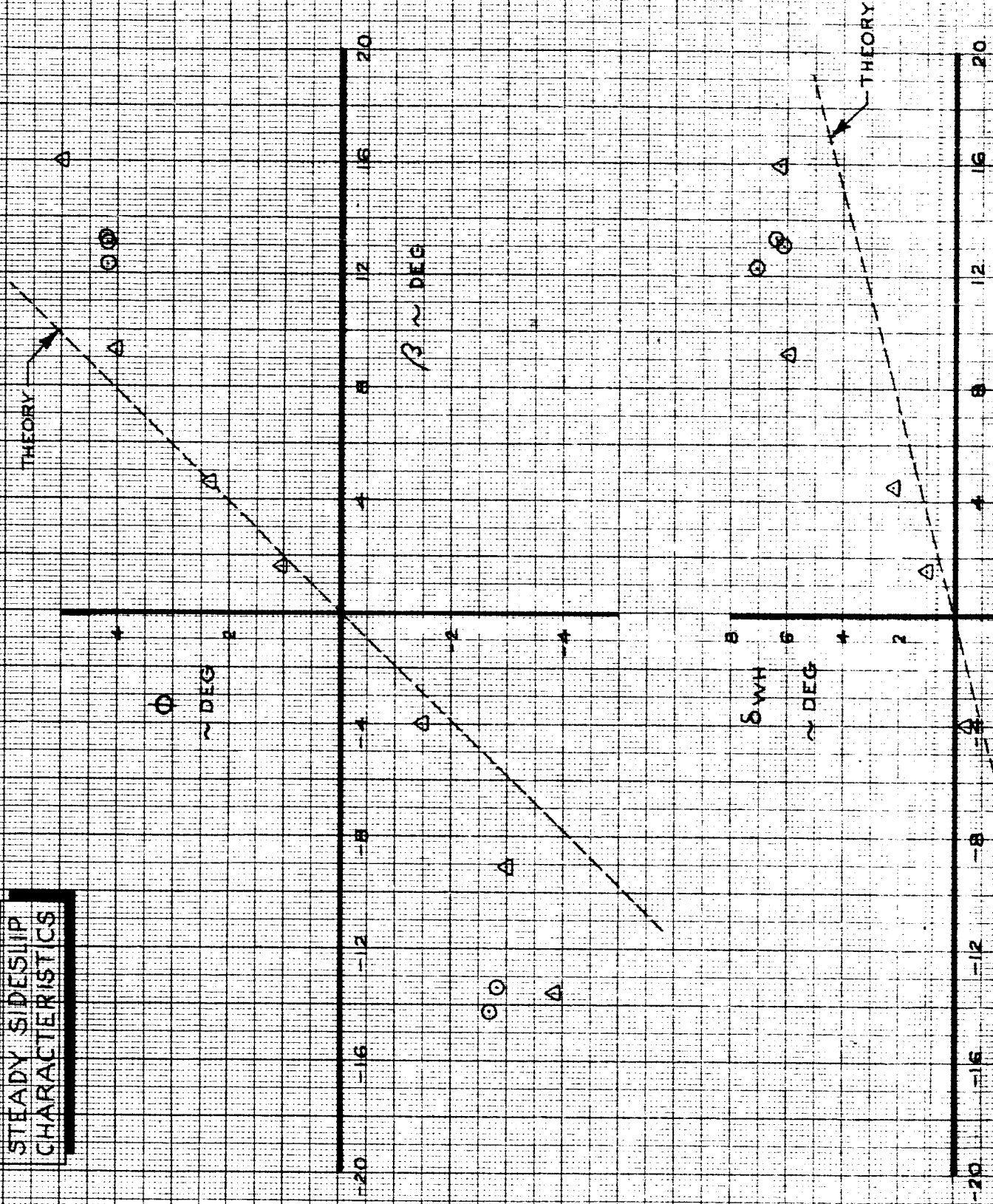
367-80
D6-15000
FIG. 94

THE BOEING COMPANY

PAGE
IX-132

136

STEADY SIDESLIP CHARACTERISTICS

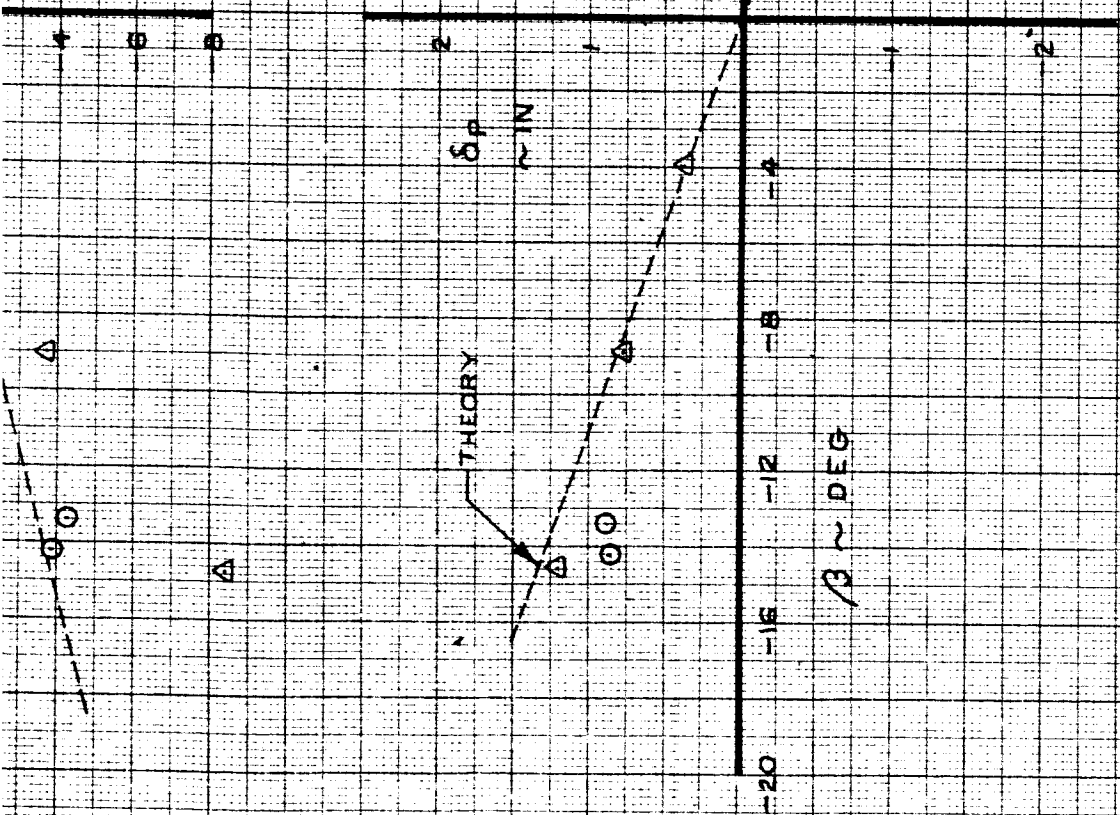


CALC			REVISED	DATE	STEADY SIDESLIP CHARACTERISTICS FLIGHT TEST 686-12 CONFIGURATION -80 BLC	367-80 DG-15000 FIG. 95
CHECK						
APPD.						
APPD.						
					THE BOEING COMPANY	PAGE IX-133

137

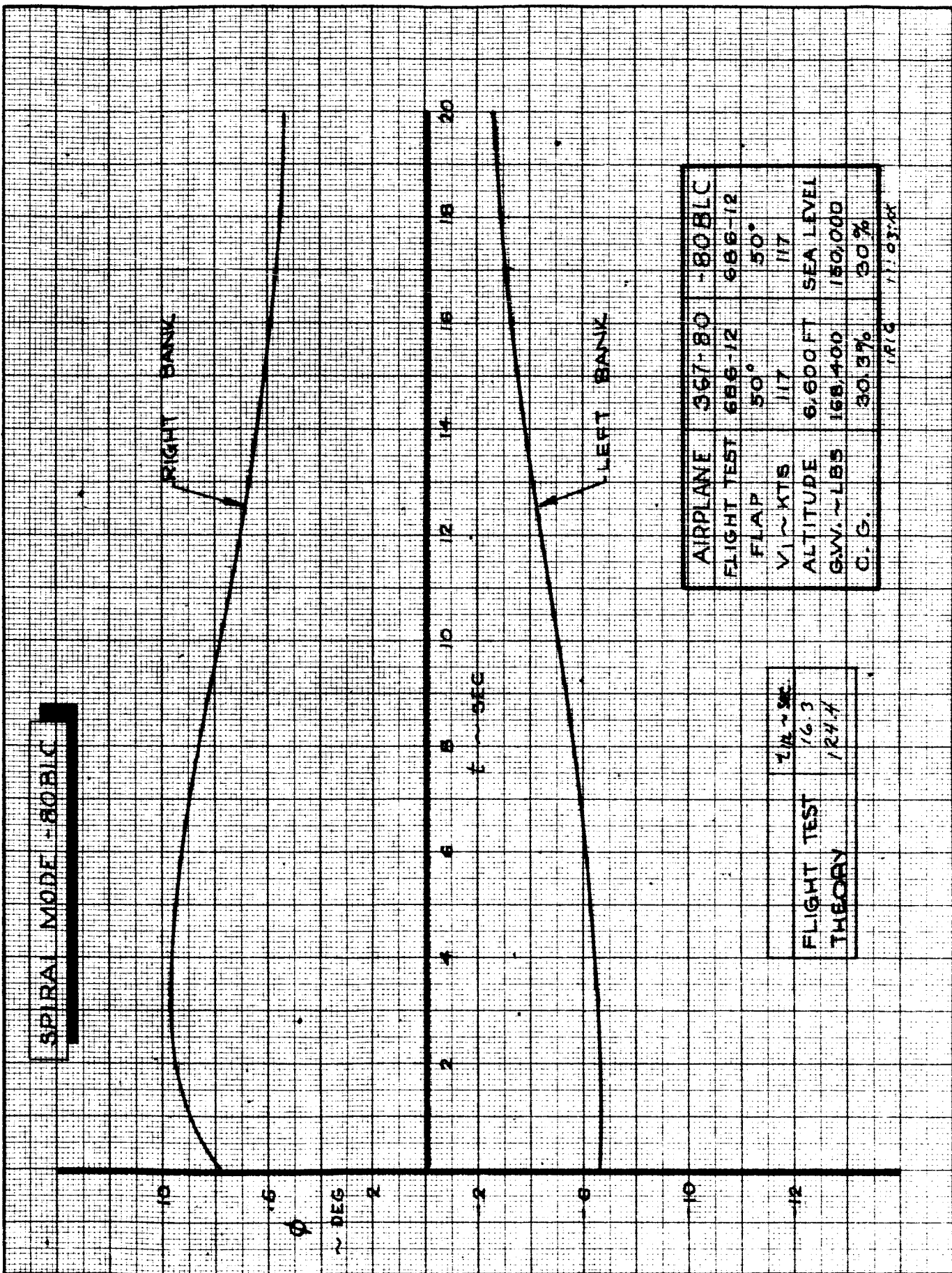
13 ~ DEG

AIRPLANE	BASIC 367-80	367-80	-80 BLC
FLIGHT TEST	659-6	686-12	686-12
FLAP	50°	30°	
ALTITUDE	9,300 FT	9,100 FT	SEA LEVEL
GW. ~ LBS	16,200	143,400	150,000
C.G.	31.5%	30.3%	30
IRIG	17:30:XX	11:06:XX	



TX-133-2

SPIRAL MODE - 80BLC



AIRPLANE	367-80	-80BLC
FLIGHT TEST	686-12	686-12
FLAP	50°	50°
V1 ~ KTS	117	117
ALTITUDE	6,600 FT	SEA LEVEL
G.W. ~ LBS	168,400	150,000
C.G.	30.37%	30%

TIME - SEC	
FLIGHT TEST	16.3
THEORY	12.4

CALC		REVISED	DATE
CHECK			
APR			
APR			

SPIRAL MODE
 FLIGHT TEST 686-12
 CONFIGURATION -80BLC

THE BOEING COMPANY

367-80
 D6-15000
 FIG. 96

PAGE
 IX-134

WHEEL STEP CHARACTERISTICS

ϕ
~ DEG

$\phi = 2072^\circ$

AIRPLANE	367-80	-80BLC
FLIGHT TEST	686-13	686-13
FLAP	50°	50°
V ₁ ~ KTS	117	117
ALTITUDE	7000 FT	SEA LEVEL
G.W. ~ LBS	163,700	150,000
C.G.	30.1%	30%

FIG 13/35 EXX

β
~ DEG

δ_w
~ DEG

t ~ SEC

CALC			REVISED	DATE
CHECK				
APR				
APR				

WHEEL STEP CHARACTERISTICS
 FLIGHT TEST 686-13
 CONFIGURATION -80 BLC
 THE BOEING COMPANY

367-80
 D6-15000
 FIG. 96A
 PAGE
 IX-135

139

X. INFLIGHT - GROUND-BASED SIMULATOR COMPARISON

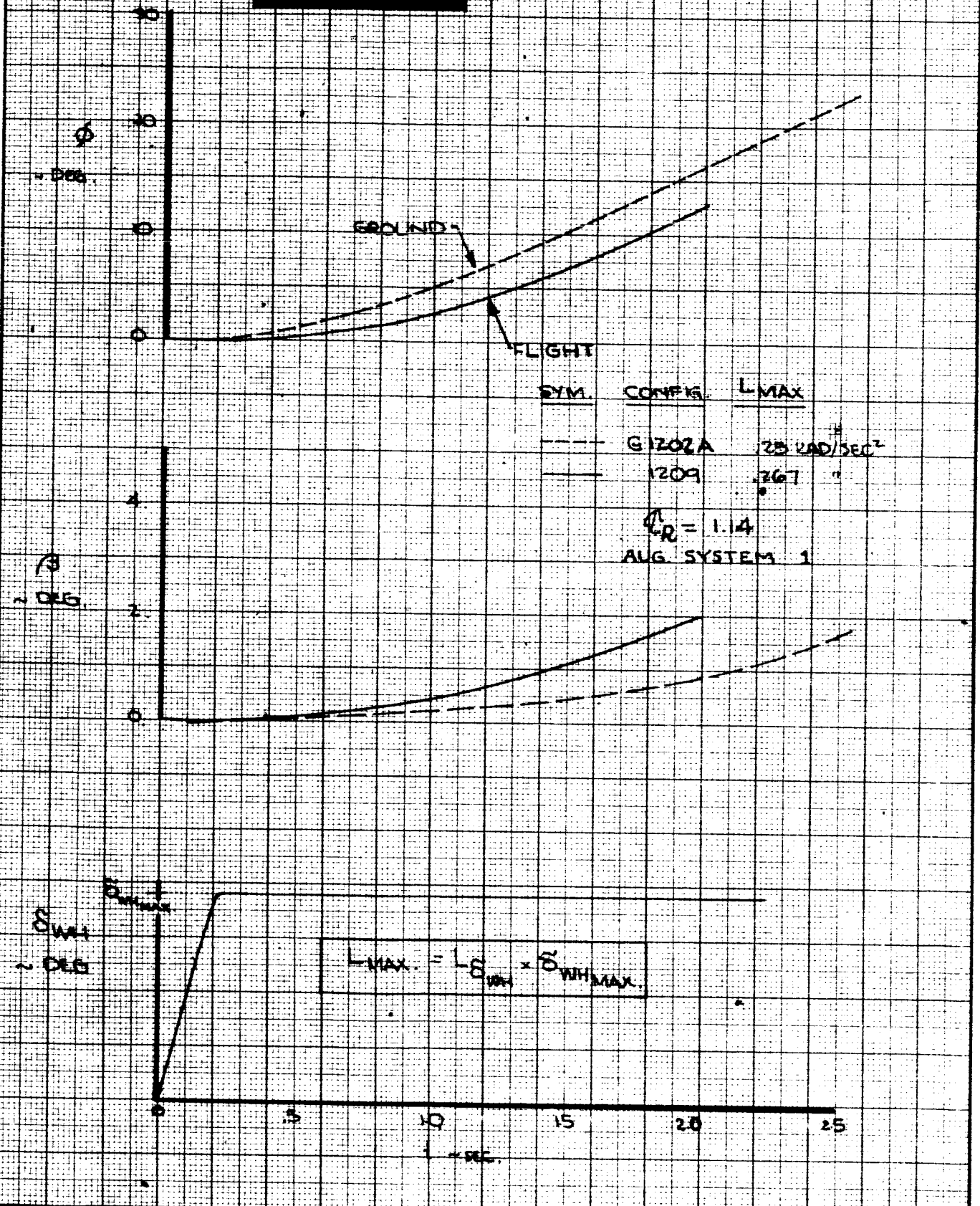
Dynamic characteristics of similar configurations evaluated on the ground based and inflight simulators are presented herein. Figs. 97 and 98 present wheel step and wheel pulse response characteristics comparing configurations G1202A (ground based) and 1209 (inflight). These are similar configurations but the numbers are different because of changes in the in-flight simulator parameters after program initiation. Response differences are due to the different initial response characteristics of the in-flight simulation caused by control surface nonlinearities and aerodynamic lags and a somewhat differently shaped roll control input. The pilot was requested to input a step wheel. The control input shown was the result. Response of these configurations to a rudder pulse is shown in Fig. 99.

Longitudinal response characteristics are presented in Fig. 100 for an elevator pulse and Fig. 101 for a column step comparing similar configurations. Fig. 101 compares the dynamic characteristics of configurations G151C and 151B. These configurations have similar stability, elevator lift and control power and slightly different lift curve slope and lift due to pitch rate ($C_{L\dot{\alpha}}$). They have similar dynamic characteristics. The configuration numbers are different because of changes in the in-flight simulator parameters after program initiation. The responses to a column step of three configurations (101A, 151B, and 151C) evaluated on the inflight simulation are shown in Fig. 102. This figure presents the effect of elevator lift on longitudinal response. Fig. 103 presents the longitudinal response of three configurations (G101A, G151B, G151C), evaluated on the ground based simulator showing the effect of elevator lift.

104

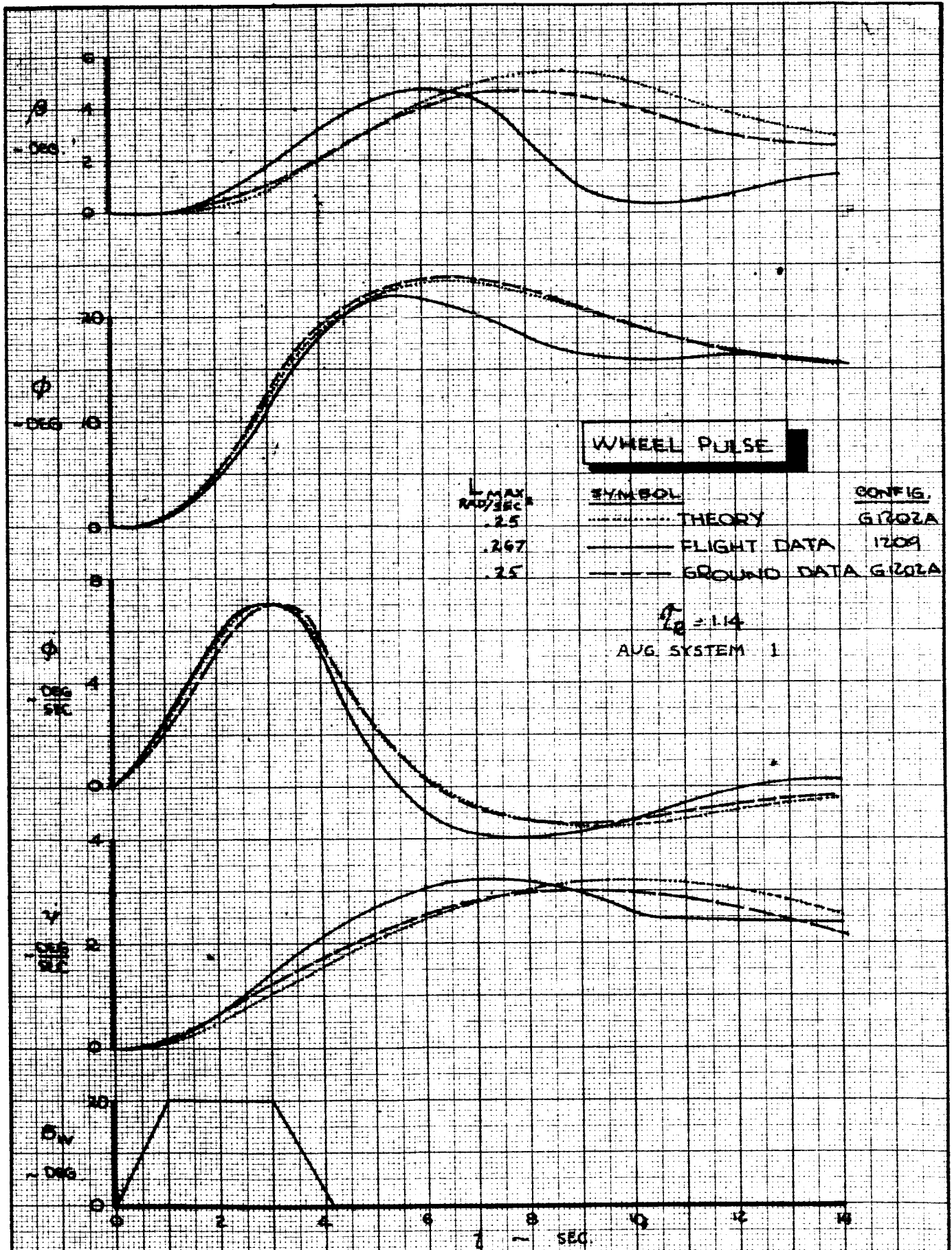
Figs. 104, 105, and 106 compare configurations 101A, 151B, and 151C with G101A, G151B, and G151C as evaluated on the inflight and ground based simulators. Response differences are due to changes in the characteristics as listed in Table 1 and Table 3. Most of the increment in response shown on these curves is due to the difference in elevator lift between the two simulators for a given configuration number.

WHEEL STEP



CALC	R. Root	2-1-66	REVISED	DATE	WHEEL STEP GROUND-FLIGHT COMPARISON CONFIG: G1202A & 1209 THE BOEING COMPANY	D6-15000 FIG. 97 PAGE X-138
CHECK						
APR						
APR						

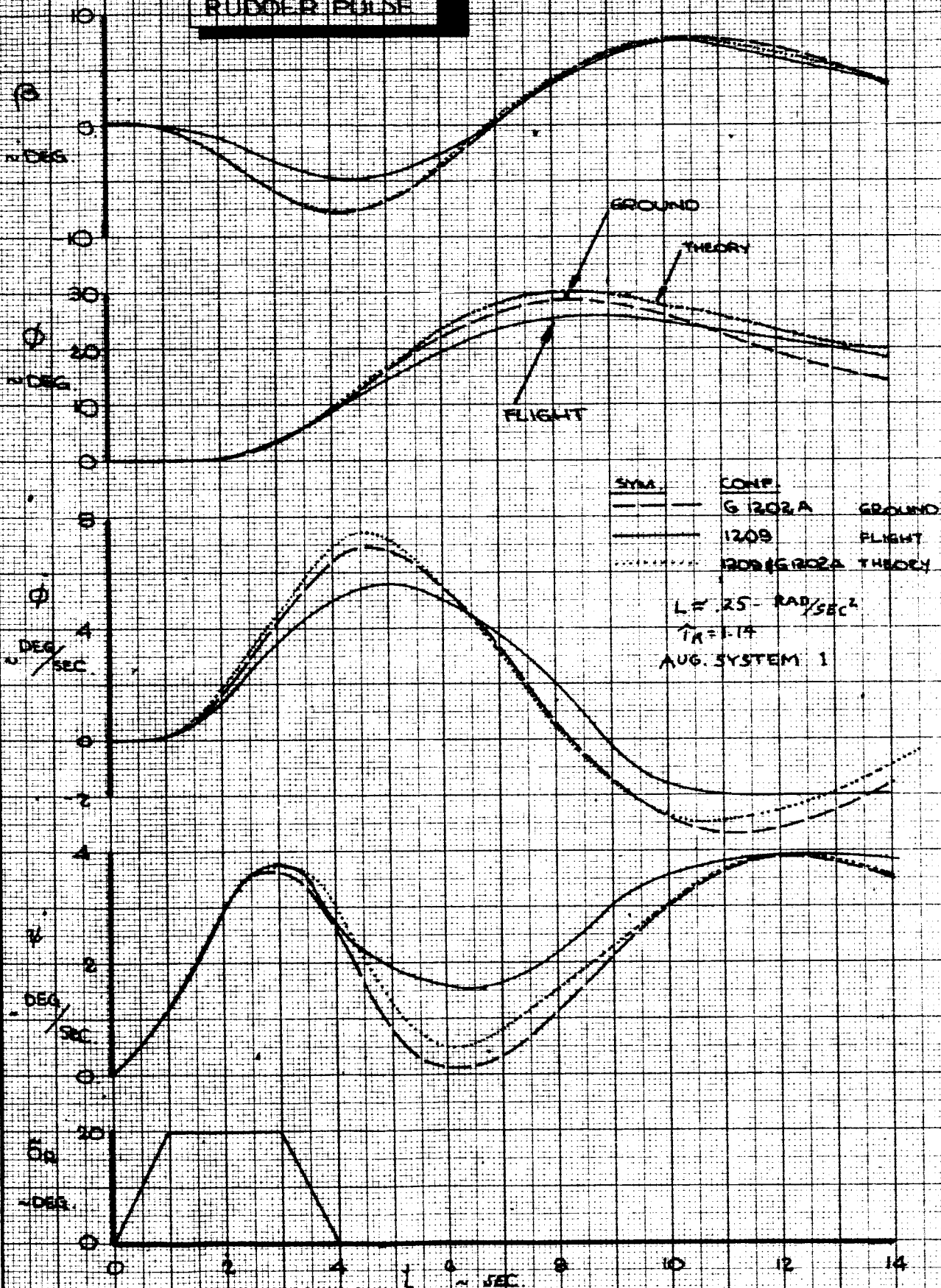
142



CALC	R. Root	2-1-66	REVISED	DATE	CONFIG. G1202A & 1209 WHEEL PULSE DATA COMPARISON	D6-15000 FIG. 98
CHECK						
APR						
APR						
THE BOEING COMPANY					PAGE X-139	

143

RUDDER PULSE



CALC	R. Root	2-1-66	REVISED	DATE	RUDDER PULSE GROUND ~ FLIGHT COMPARISON CONFIG. : G1202A & 1209 THE BOEING COMPANY	D6-15000
CHECK						FIG. 99
APR						
APR						
						PAGE X-140

144

ELEVATOR PULSE

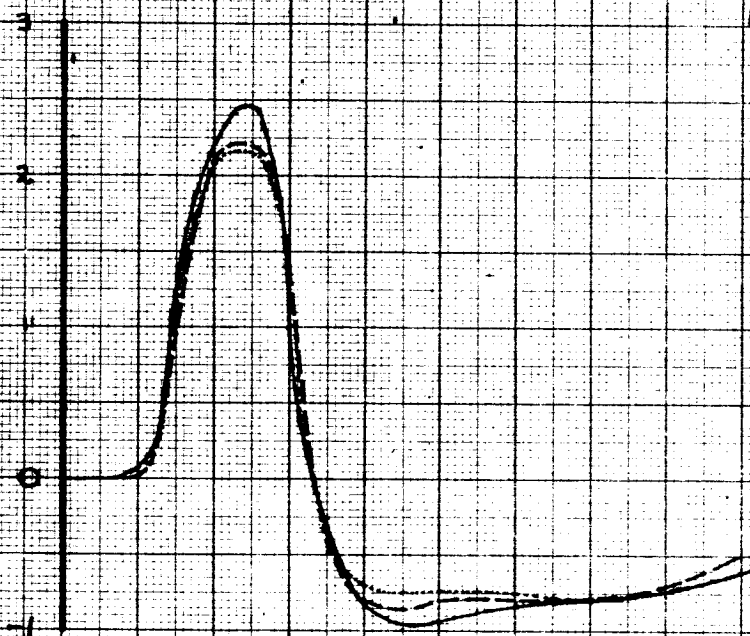
$\Delta Q/W$
DEG



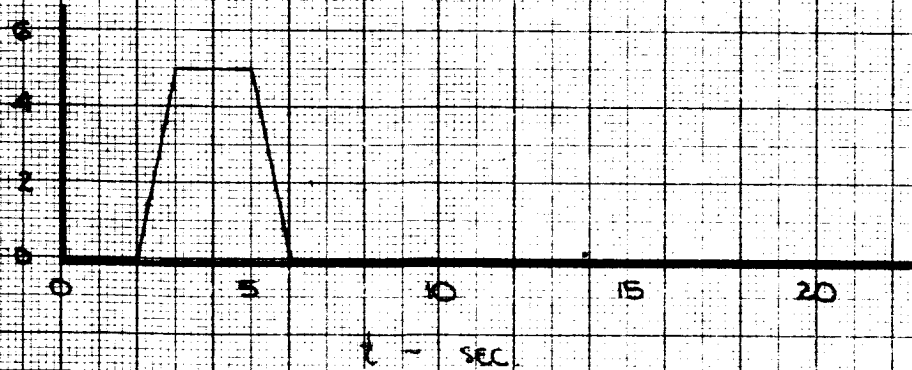
M_{∞} 1/SEC	t_{50} 1/SEC-RAD	SYM.	CONFIGURATION:
-.562	.0701	—	FLIGHT DATA (101A)
-.55	.0333	- - -	GROUND DATA (G101A)
-.562	.0701	· · ·	THEORY (101A)

$M_{\infty} = -.506$

$\Delta Q/W$
DEG

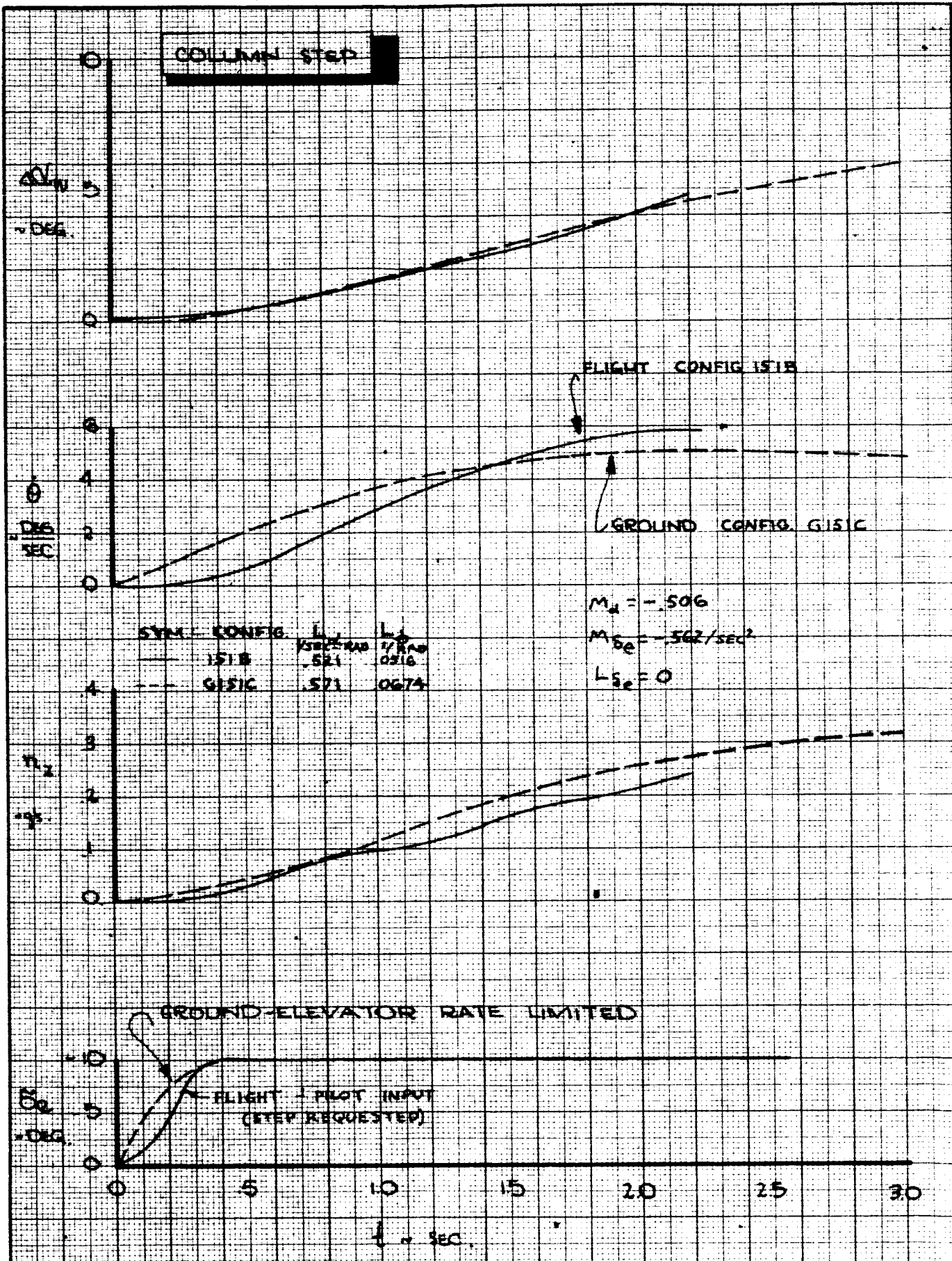


$\Delta Q/W$
DEG

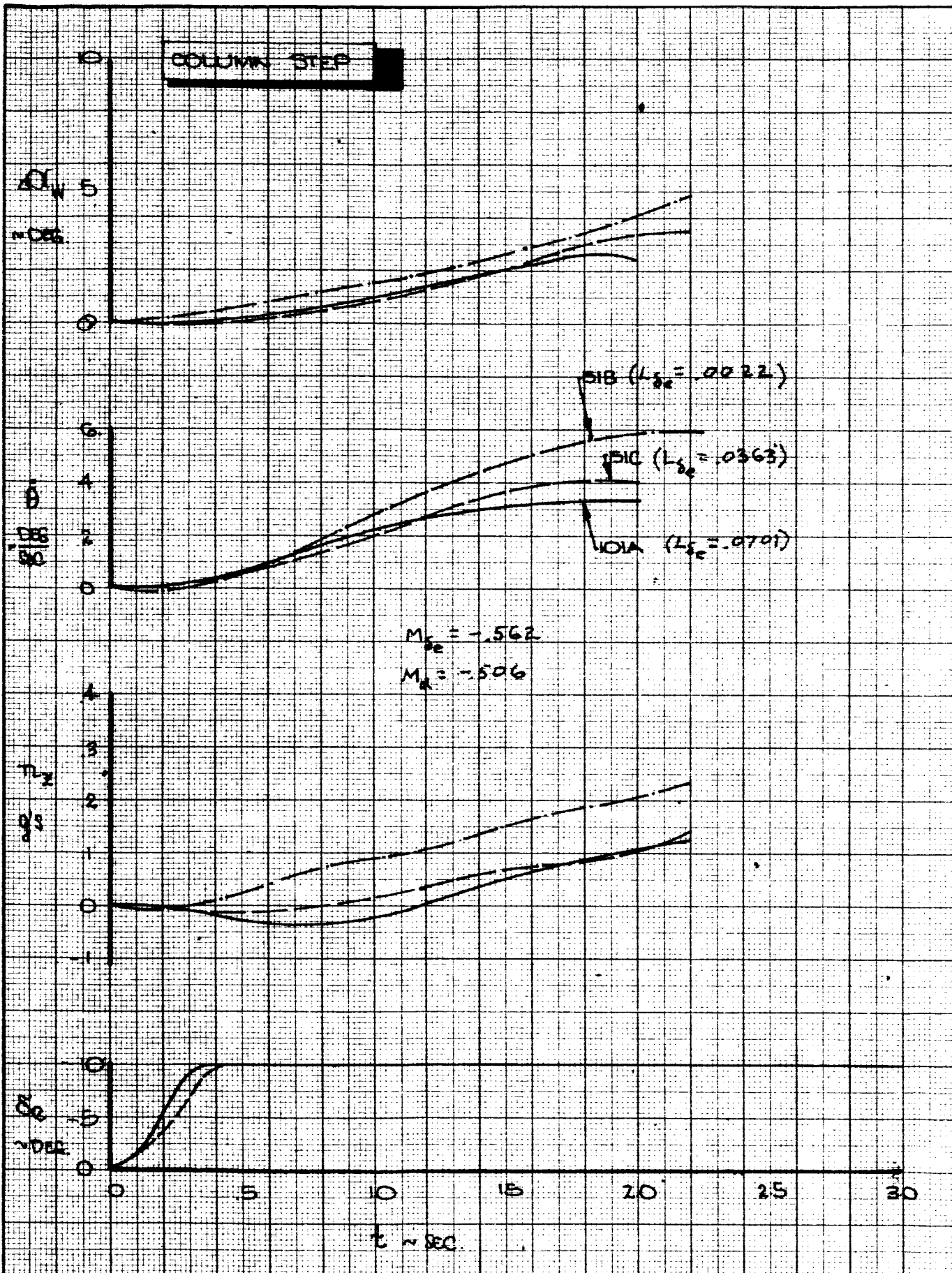


CALC	R. Root	2-2-66	REVISED	DATE	ELEVATOR PULSE GROUND-FLIGHT DATA COMPARISON CONFIG. G101A & 101A THE BOEING COMPANY	D6-15000 FIG.100 PAGE X-141
CHECK						
APR						
APR						

145

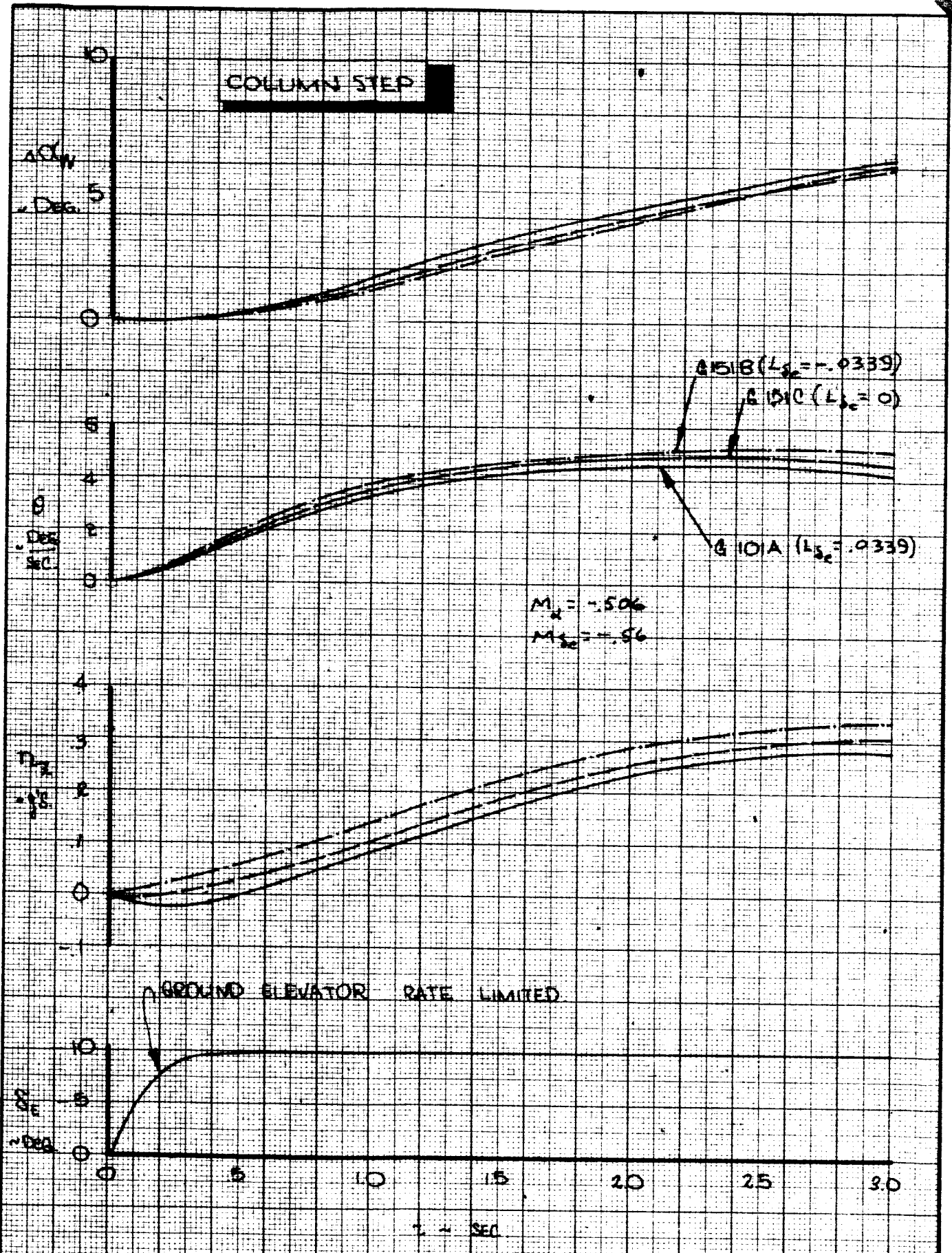


CALC	R. Root	2-2-66	REVISED	DATE	COLUMN STEP GROUND-FLIGHT COMPARISON CONFIG.: G151C & 1518 THE BOEING COMPANY	D6-15000
CHECK						FIG. 101
APR						PAGE
APR						X-142



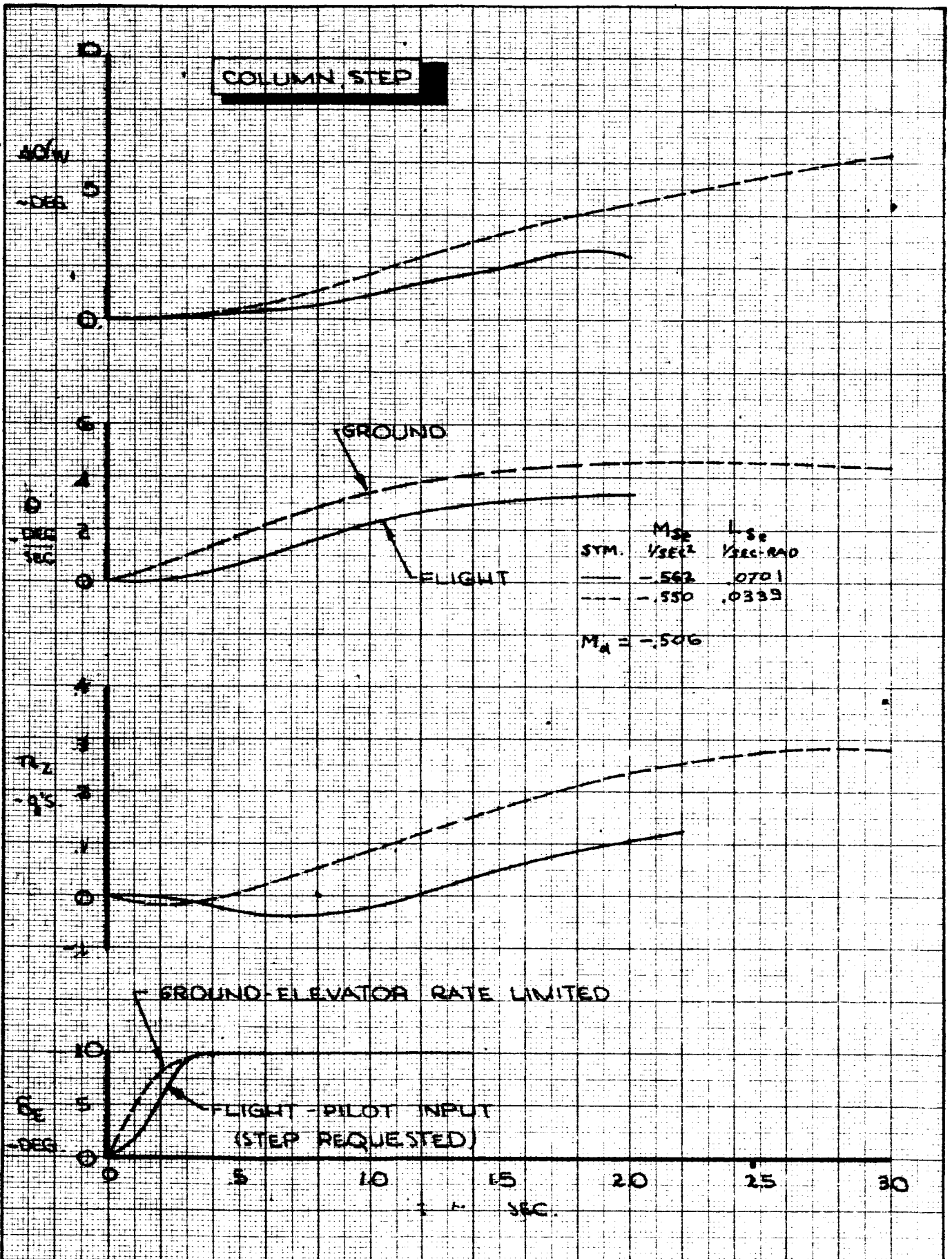
CALC	R. Root	2-9-66	REVISED	DATE	COLUMN STEP FLIGHT DATA COMPARISON CONFIG. 15IC, 15B & 10IA THE BOEING COMPANY	D6-15000
CHECK						FIG. 102
APR						PAGE
APR						X-143

147



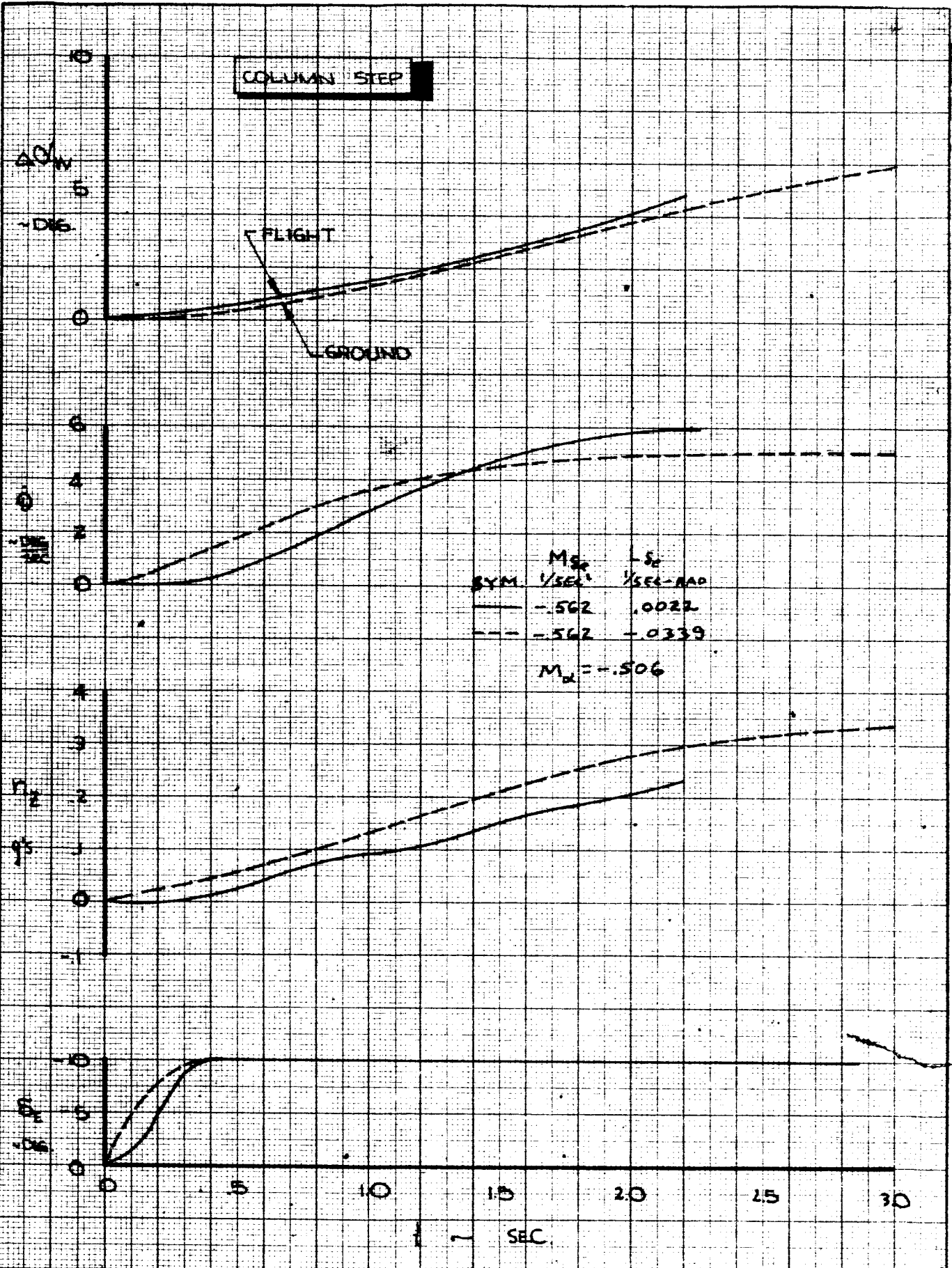
CALC	R. Root	2-4-66	REVISED	DATE	COLUMN STEP GROUND DATA COMPARISON CONFIG. G101A, G151B & G151C THE BOEING COMPANY	D6-15000 FIG. 103 PAGE X-144
CHECK						
APR						
APR						

148



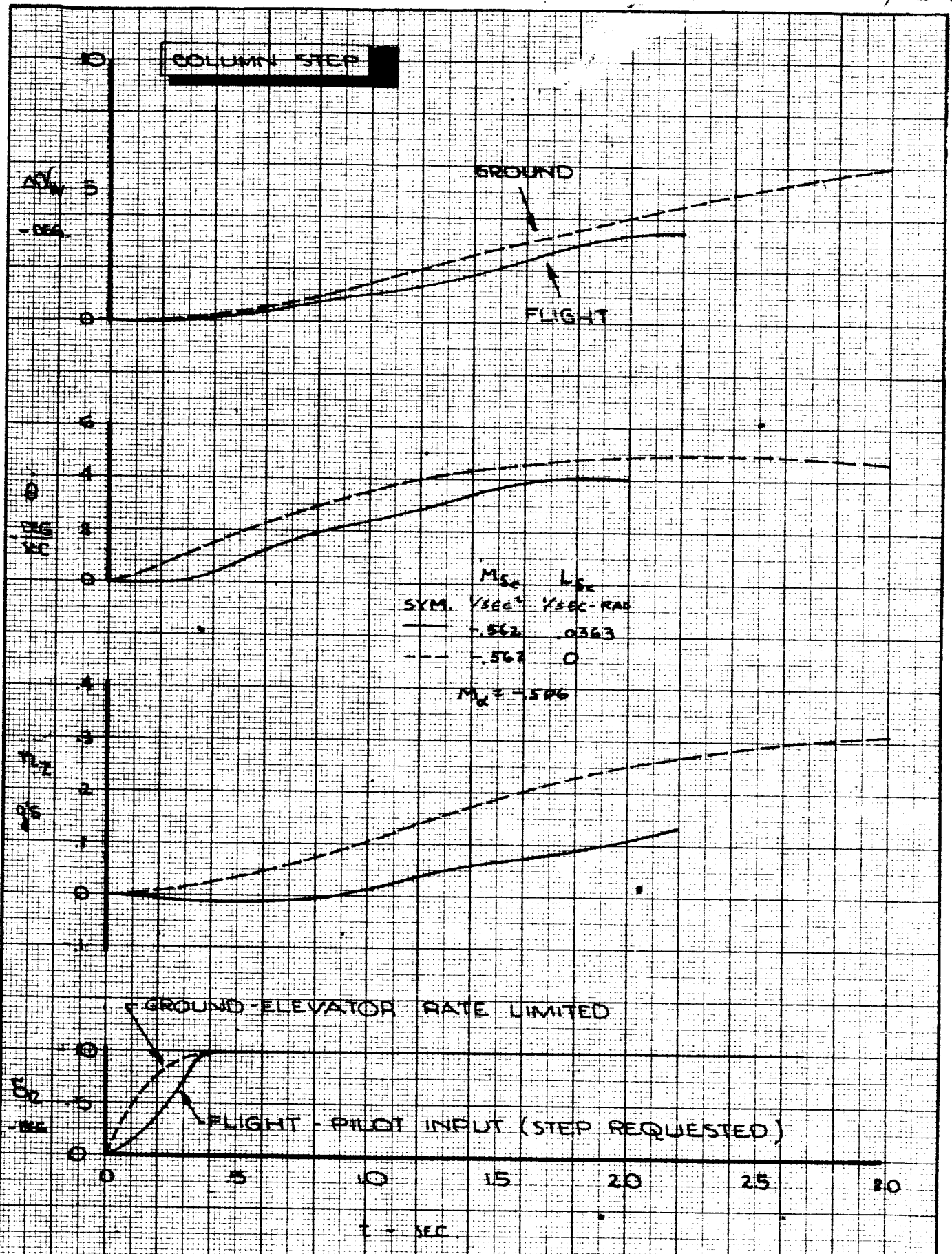
CALC	R. Root	2-2-CC	REVISED	DATE	COLUMN STEP GROUND-FLIGHT COMPARISON CONFIG. GIOIA & IOIA THE BOEING COMPANY	D6-15000
CHECK						FIG.104
APR						PAGE
APR						X-145

bpl.



CALC	R. Root	2-2-66	REVISED	DATE	COLUMN STEP GROUND - FLIGHT COMPARISON CONFIG. G151B & 151B THE BOEING COMPANY	D6-15000
CHECK						FIG. 105
APR						PAGE
APR						X-146

150



CALC	R. Root	2-2-66	REVISED	DATE	COLUMN STEP GROUND-FLIGHT COMPARISON CONFIG. G15IC & 15IC.	D6-15000
CHECK						FIG. 106
APR						PAGE X-147
APR					THE BOEING COMPANY	

151

APPENDIX 1

DESCRIPTION OF THE AMES LARGE TRANSPORT CONFIGURATIONS

A. Airborne Simulator

A description of the basic Ames large transport configuration is given in Table A1-1 and variations from the basic are shown in Table A1-2.

TABLE A1-1

Basic 101A Longitudinal CharacteristicsFlight Condition

V_e	117 Kts
Gross Weight	500,000 lbs.
C. G. Location	25% MAC

Airplane Constants

Wing Area	5500 sq. ft.
Wing Span	215 ft.
MAC	28.75 ft.

Lift Derivatives

$C_{L_{Trim}}$	1.94
$\alpha_{Trim_{wcp}}$	4.7°
$C_{L_{\alpha}}$	6.2 /rad
$C_{L_{\dot{\alpha}}}$	-.537 /rad/sec
$C_{L_{\dot{\theta}}}$.613 /rad/sec
$C_{L_{\dot{\omega}_e}}$.835 /rad

Drag Derivatives

$C_{D_{Trim}}$.45
$C_{D_{\alpha}}$	1.07 /rad

TABLE A1-1 (CONT.)

Pitching Moment Derivatives

$C_{m\dot{\alpha}}$	-2.07 /rad
$C_{m\ddot{\alpha}}$	-.555 /rad/sec
$C_{m\dot{\omega}}$	-2.387/rad/sec
$C_{m\dot{\delta}_E}$	-2.30 /rad
I_y	30.0 x10 ⁶ slug-FT ²

Longitudinal Dynamic Characteristics

Short Period

Damped Natural Frequency	.645 rad/sec
Undamped Natural Frequency	.907 rad/sec
Damping Ratio	.703

Phugoid

Damped Natural Frequency	.170 rad/sec
Undamped Natural Frequency	.172 rad/sec
Damping Ratio	.149

154

TABLE A1-1 (CONT.)

Basic 1209 Lateral - Directional CharacteristicsSide Force Derivatives

$C_{y\beta}$	-.9773	/rad
$C_{y\dot{\phi}}$.06	/rad/sec
$C_{y\dot{\psi}}$.1105	/rad/sec
$C_{y\dot{\beta}}$	-.074	/rad/sec
$C_{y\delta_R}$.2464	/rad
$C_{y\delta_W}$	-.0366	/rad

Rolling Moment Derivatives

$C_{l\beta}$	-.1955	/rad
$C_{l\dot{\phi}}$	-.2442	/rad/sec
$C_{l\dot{\psi}}$.1955	/rad/sec
$C_{l\delta_R}$.00229	/rad
$C_{l\dot{\beta}}$	-.00069	/rad/sec
$C_{l\delta_W}$.0975	/rad
I_{X_B}	17.5×10^6	slug-FT ²

156

TABLE A1-1 (CONT.)

Yawing Moment Derivatives

$C_{n\beta}$.218	/rad
$C_{n\dot{\phi}}$.0905	/rad/sec
$C_{n\dot{\psi}}$	-.2883	/rad/sec
$C_{n\dot{\beta}}$.036	/rad/sec
$C_{n\delta_R}$	-.12	/rad
$C_{n\delta_W}$	-.0001	/rad
I_{Z_B}	45.0×10^6	slug-FT ²
$I_{X_Z_B}$	$.95 \times 10^6$	slug-FT ²

Spiral Divergence

Time Constant	26.5	sec
Time to Half Amplitude	18.3	sec

Roll Coverage

Time Constant	1.14	sec
---------------	------	-----

Dutch Roll

Damped Natural Frequency	.479	rad/sec
Undamped Natural Frequency	.508	rad/sec
Damping Ratio	.329	
$\frac{ \phi }{ \beta }$	1.33	

150

CONFIG.	$C_{m\delta e}$ 1/RAD	$C_{L\delta e}$ 1/RAD	$\delta e/\delta c$	$C_{m\alpha}$ 1/RAD	$C_{L\alpha}$ 1/RAD	$C_{m\dot{\theta}}$ 1/RAD/SEC	$C_{L\dot{\theta}}$ 1/RAD/SEC	$C_{L\delta W}$ 1/RAD	$C_{L\dot{\phi}}$ 1/RAD/SEC	$\delta W_{EFF.}$ DEG
101A	-2.30	.835	-1.5	-2.07	6.2	-2.4	.613			
100	-1.56	.705	-1.5	-2.07	6.2	-2.4	.613			
105A	-2.30	.835	-3.0	-2.07	6.2	-2.4	.613			
105*	-1.56	.705	-4.5	-2.07	6.2	-2.4	.613			
151B	-2.30	.026	-1.5	-2.07	6.2	-2.4	.613			
151C	-2.30	.435	-1.5	-2.07	6.2	-2.4	.613			
151D	-2.30	.026	-3.0	-2.07	6.2	-2.4	.613			
158A	-2.30	.844	-3.0	-4.14	6.57	-4.8	1.17			
159A	-2.30	.844	-1.5	-2.07	6.2	-4.8	1.17			
159B	-2.30	.844	-3.0	-2.07	6.2	-4.8	1.17			
161B	-2.30	.844	-3.0	-.52	5.91	-2.4	.613			
-80BLC	-.917	.297	-2.2	-1.917	5.46	-5.131	0	.180	-3064	
1209								.0975	-2442	50
1203A								.1460	-2442	30
1207A								.0914	-2442	30
1235								.1630	-5100	30
1237								.0914	-2442	50

ENGR.		REVISED	DATE	AIRBORNE SIMULATION AERODYNAMIC CHARACTERISTICS THE BOEING COMPANY RENTON, WASHINGTON	TABLE A1-2
CHECK					D6-15000
APR					A1-6
APR					

A description of Boeing 367-80 with boundary layer control (used as a large transport configuration) is shown in Table A1-3.

TABLE A1-3

367-80 BLC Longitudinal Characteristics

Flight Condition

V_e	117 Kts
Flap Angle	50°
BPR	4:1
Gross Weight	150,000 lbs.
C. G. Location	30% MAC
Speed Brake Trim Angle	6°

Airplane Constants

Wing Area	2821 sq. ft.
Wing Span	130.8 ft.
MAC	20.1 ft.

Lift Derivatives

$C_{L_{Trim}}$	1.14
$\alpha_{Trim_{wcp}}$	2.3°
$C_{L\alpha}$	4.53 /rad
$C_{L\delta_R}$.297
$\frac{\partial C_L}{\partial v}$	-.001875 /ft/sec

Drag Derivatives

$C_{D_{Trim}}$.183
$C_{D\alpha}$.63 /rad

159

TABLE A1-3 (CONT.)

Pitching Moment Derivatives

$C_{m\dot{v}}$	-0.0012	/ft/sec
$C_{m\alpha}$	-1.197	/rad
$C_{m\dot{\alpha}}$	-0.1283	/rad/sec
$C_{m\dot{\epsilon}}$	-0.5131	/rad/sec
$C_{m\dot{\sigma}_g}$	-0.8124	/rad
I_y	2.25×10^6	slug-FT ²

Longitudinal Dynamic CharacteristicsShort Period

Damped Natural Frequency	1.147	rad/sec
Undamped Natural Frequency	1.30	rad/sec
Damping Ratio	.5245	

Phugoid

Damped Natural Frequency	.1342	rad/sec
Undamped Natural Frequency	.1352	rad/sec
Damping Ratio	.1244	

TABLE A1-3 (CONT.)

367-80 BLC Lateral - Directional Characteristics

Side Force Derivatives

$C_{y\beta}$	-0.773	/rad
$C_{y\dot{\phi}}$.3376	/rad/sec
$C_{y\dot{\psi}}$.1035	/rad/sec
$C_{y\beta}$	-.259	/rad/sec
$C_{y\delta_R}$.1992	/rad
$C_{y\delta_W}$	-.032	/rad

Rolling Moment Derivatives

$C_{l\beta}$	-.1507	/rad
$C_{l\dot{\phi}}$	-.1951	/rad/sec
$C_{l\dot{\psi}}$.1407	/rad/sec
$C_{l\beta}$	-.0268	/rad/sec
$C_{l\delta_R}$.0206	/rad
$C_{l\delta_W}$.180	/rad
I_{x_B}	2.57×10^6	slug-FT ²

Yawing Moment Derivatives

$C_{n\beta}$.0555	/rad
$C_{n\dot{\phi}}$	-.0207	/rad/sec
$C_{n\dot{\psi}}$	-.0677	/rad/sec
$C_{n\beta}$.0484	/rad/sec
$C_{n\delta_R}$	-.0777	/rad

151

TABLE A1-3 (CONT.)

Yawing Moment Derivatives (cont'd)

$C_{n\dot{\delta}_W}$.0125	/rad
I_{z_B}	4.73×10^6	slug-FT ²
I_{xz_B}	0	slug-FT ²

367-80 BLC Stability Augmentation System

	<u>Gain</u>	<u>Time Constant</u>
$\frac{\delta_R}{\delta_{WH}}$	0	0
$\frac{\delta_R}{\beta}$	0	0
$\frac{\delta_R}{\beta}$	-1.3	.27 sec
$\frac{\delta_R}{\phi}$	- .5	1.0 sec
$\frac{\delta_A}{\psi}$	- .9	0.1 sec
$\frac{\delta_A}{\beta}$	1.0	0.1 sec
$\frac{\delta_A}{\phi}$	-1.2	0.1 sec

Lateral Dynamic CharacteristicsSpiral Divergence

Time Constant	180.0	sec
Time to Half Amplitude	124.4	sec

Roll Convergence

Time Constant	Non-linear	sec
---------------	------------	-----

102

TABLE A1-3 (CONT.)

Dutch Roll

Damped Natural Frequency	.423	rad/sec
Undamped Natural Frequency	.513	rad/sec
Damping Ratio	.564	
$\frac{ \phi }{ \beta }$.468	

B. Ground Based Simulation

Following is a description of the aerodynamic and physical characteristics of the configurations evaluated on the ground based simulation.

The following information is included:

- a. Basic configuration description (Table A1-4)
- b. Longitudinal changes (Table A1-5)
- c. Lateral Directional changes (Table A1-6)
- d. Lateral Directional Stability Augmentation System (Table A1-7)
- e. Equivalent coefficients (aerodynamic coefficients equivalent to the basic configuration with augmentation) (Table A1-8).

164

CONFIGURATION DESCRIPTION
 AMES LARGE TRANSPORT
 GROUND BASED SIMULATION

BASIC AERODYNAMIC COEFF'S

DRAG : $C_{DTRIM} = .45$
 $C_{D\alpha} = 1.07 \text{ 1/RAD}$

LIFT : $C_{LTRIM} = 1.94$
 $C_{L\dot{\theta}} = .8043 \text{ SEC/RAD}$
 $C_{L\dot{\alpha}} = -.3959 \text{ SEC/RAD}$
 $C_{L\dot{\alpha}} \& C_{L\dot{\delta}_e}$ VARIED

PITCH : $C_{m\dot{\alpha}} = -.555 \text{ SEC/RAD}$
 $C_{m\dot{\omega}} = -.0545 \text{ 1/RAD}$
 $C_{m\dot{\alpha}}, C_{m\dot{\delta}_e} \& C_{m\dot{\omega}}$ VARIED

ROLL : $C_{l\dot{\beta}} = -.395 \text{ 1/RAD.}$
 (UNALG.) $C_{l\dot{\epsilon}} = .3045 \text{ SEC/RAD}$
 $C_{l\dot{\delta}_r} = .00229 \text{ 1/RAD}$
 $C_{l\dot{\epsilon}} \& C_{l\dot{\delta}_w}$ VARIED

YAW
 (UNALG.) $C_{n\dot{\beta}} = .179 \text{ 1/RAD.}$
 $C_{n\dot{\epsilon}} = -.1579 \text{ SEC/RAD}$
 $C_{n\dot{\epsilon}} = -.267 \text{ SEC/RAD}$
 $C_{n\dot{\delta}_a} = .0213 \text{ 1/RAD}$
 $C_{n\dot{\delta}_r} = -.120 \text{ 1/RAD}$

SIDE FORCE
 (UNALG.) $C_{y\dot{\beta}} = -.83 \text{ 1/RAD}$
 $C_{y\dot{\epsilon}} = .572 \text{ SEC/RAD}$
 $C_{y\dot{\epsilon}} = .02995 \text{ SEC/RAD}$
 $C_{y\dot{\delta}_a} = -.0805 \text{ 1/RAD}$
 $C_{y\dot{\delta}_r} = .2464 \text{ 1/RAD}$

PHYSICAL CHARACTERISTICS

WEIGHT = 500000 LBS.
 CENTER OF GRAVITY = .25 \bar{c}
 WING AREA , S = 5,500 FT²
 M.A.C. , \bar{c} = 28.75 FT.
 SPAN , b = 215.0 FT.
 VELOCITY , V = 117.0 KTS.
 = (197.5 FT/SEC)
 α_{TRIM} , α_T = 2.7 DEG.
 (SEA LEVEL) , q = 46.4 LB/FT²

$I_{xx} = 17.5 \times 10^6 \text{ SLUG/FT}^2$
 $I_{yy} = 30.0 \times 10^6 \text{ SLUG/FT}^2$
 $I_{zz} = 45.0 \times 10^6 \text{ SLUG/FT}^2$
 $I_{xz} = .95 \times 10^6 \text{ SLUG/FT}^2$

ENGR.	R. Root	2-1-66	REVISED	DATE	CONFIGURATION DESCRIPTION	TABLE A1-4
CHECK						D6-15000
APR					THE BOEING COMPANY RENTON, WASHINGTON	A1-14
APR						

165

AD 1040C-R3

GROUND BASED CONFIG.	$C_{L\alpha}$ 1/RAD	$C_{m\alpha}$ 1/RAD	$C_{m\dot{\alpha}}$ SEC/RAD	$C_{L\delta e}$ 1/RAD	$C_{m\delta e}$ 1/RAD	$\delta e/\delta col$ DEG/N
G~						
100	6.81	-2.07	-2.39	.409	-1.56	-3.29
100A					-3.12	
100X				.818	-1.56	
101A				.409	-2.25	
102					-1.25	
103					-1.0	
103A						-6.58
105					-1.56	
105A					-2.3	
105*					-1.56	-9.87
105*X				.818		
106		-1.0		.409		-3.29
107		0				
108					-1.0	
109					-2.0	
109A					-1.56	-6.58
110		+1.0				-3.29
111	3.6	-2.07				
112		-3.00				
112A		-4.00				
113		-1.40				
113A		-1.40	-1.21			
115		0	-2.39			
120	6.81	-2.07	-1.00			

CALC	R. Root	2-2-66	REVISED	DATE
CHECK				
APR				
APR				

GROUND BASED SIMULATION
LONGITUDINAL RUN LOG

THE BOEING COMPANY
RENTON, WASHINGTON

TABLE
A1-5
D6-15000
PAGE
A1-15

GROUND BASED CONFIG	$C_{L\alpha}$	$C_{m\alpha}$	$C_{m\dot{\alpha}}$	$C_{L\delta e}$	$C_{m\delta e}$	$\delta e/\delta col$
G~	1/RAD	1/RAD	SEC/RAD	1/RAD	1/RAD	DEG/IN
122A	6.81	-4.00	-2.39	.409	-1.56	-3.29
123	11.0	-2.07				
123A						
123B						
124		-0.50			-1.56	-3.29
125		.40			-1.56	
126		-1.00			-1.00	
126A		-1.00			-1.56	-6.58
127		0			-1.00	-3.29
128		-1.00	-1.00			
129		0	-1.00			
130		0	-2.39		-1.56	
131		-0.50	-1.00		-1.56	
132		-2.07	-1.00		-1.00	
150	6.81		-2.39		-1.56	
151				-.409	-1.56	
151B					-2.30	-2.78
151C				0.	-2.30	
151C*					-1.56	-3.29
151D				-.409	-2.30	-6.58
152		-6.00	-4.80	.409	-1.56	-3.29
153		-6.00			-3.12	
154		-2.07			-1.56	
155		-2.07			-3.12	

$C_{D\alpha} = 1.9$

TD 1040C-R3

CALC	R. Root	2-2-66	REVISED	DATE
CHECK				
APR				
APR				

GROUND BASED SIMULATION
LONGITUDINAL RUN LOG

THE BOEING COMPANY
RENTON, WASHINGTON D6-15000

TABLE
A1-5
PAGE
A1-16

GROUND BASED CONFIG.	CL α	Cm α	Cm $\dot{\alpha}$	CL δe	Cm δe	$\delta e / \delta \text{COL}$
G-	1/RAD	1/RAD	SEC/RAD	1/RAD	1/RAD	DEG/IN
156	6.81	-4.00	-2.39	.409	-3.12	-3.19
157			-4.80		-1.56	
157A			-2.39			
158			-4.80			-6.98
158A			-4.80		-2.3	
158A*			-2.39		-1.56	
158X			-2.39		-2.30	
159		-2.07	-4.80		-1.56	
159A					-2.30	-2.78
159B					-2.30	-6.98
160		-6.00			-1.56	
161		-.50	-2.39		-1.56	
161B		-.50			-2.30	
162		-.20			-1.56	
163	11.00	-4.00				
163A	11.00	-4.00				-3.29

CALC	R. Root	2-2-66	REVISED	DATE
CHECK				
APR				
APR				

GROUND BASED SIMULATION
LONGITUDINAL RUN LOG

THE BOEING COMPANY
RENTON, WASHINGTON D6-15000

GROUND BASED CONFIG	$Cl_{\delta W}$		δW_{EFF}		Cl_P	Aug.
	/RAD	DEG	SEC/RAD			
G~						
1	.073	50	.239	2		
1				3		
1h				2		
2	.110					
3	.146					
4	.183					
5	.219					
5A	.293					
5B	.365					
5C	.054					
5C	.054					
5D	.046					
5E	.330					
5F	.037					
5G	.018					
5H	.010	90				
5J	.030	30				
6	.091					
6	.091					
7A	.061					
8	.073	75				
8A	.037					
9	.098					
10	.082	90				

AD 1040C-R3

CA: C	R. Root	2-2-66	REVISED	DATE
CHECK				
APR				
APR				

GROUND BASED SIMULATION
LATERAL RUN LOG

THE BOEING COMPANY
RENTON, WASHINGTON DG-15000

TABLE
A1-6

PAGE
A1-18

109

AD 1040C-R3

GROUND BASED CONFIG	$C_{L\delta W}$		δW_{EFF}		$C_{L P}$	AUG.
	'/RAD	DEG	SEC/RAD	DEG		
G~						
11	.061	90	-239			2
12	.040					↓
13	.026					↓
14	.030	↓				3
16	.055	50				2
16	.055					3
17	.091					2
18	.128					2
19	.055					2
19	.055					3
20	.091					2
21	.128				↓	
22	.109				-153	
23	.073				↓	
23A	.055				↓	
24	.109				-306	
25	.055				↓	
25A	.073				↓	
26					-239	
27					↓	
28	↓	↓			↓	↓

CALC	R. Root	2-2-66	REVISED	DATE
CHECK				
APR				
APR				

GROUND BASED SIMULATION
LATERAL RUN LOG

THE BOEING COMPANY
RENTON, WASHINGTON DG-15000

TABLE
AI-6
PAGE
AI-19

AD 1040C-R3

GROUND BASED CONFIG	CALC	R. Root	REVISED	DATE	C _{lδw}	δ _{WEFF}	C _{lp}	AUG.
G~					1/RAD	DEG	SEC/RAD	
1206					.061	30	-.239	1
1207A					.091	30		
1209A					.037	75		
1209*					.098	75		
1222					.109	50	-.154	
1223							-.239	
1224							-.306	
1230					.055		-.154	
1231					.059		-.154	
1232					.103		-.410	
1233					.172		-.410	
1233B					.172		-.505	
1234B					.055		-.410	
1235					.098		-.505	
1236					.091		-.239	
1236B					.264	30	-.505	
1237					.091	50	-.239	
1237A					.091	50	-.239	

GROUND BASED SIMULATION
LATERAL RUN LOG

THE BOEING COMPANY
RENTON, WASHINGTON D6-15000

TABLE
A1-6

PAGE
A1-21

26

LATERAL DIRECTIONAL STABILITY AUGMENTATION SYSTEM

BASIC SYSTEM

RUDDER :
$$\delta r = \left[\frac{\delta r}{\beta} \right] \beta + \left[\frac{\delta r}{\dot{\phi}} \right] \dot{\phi} + \left[\frac{\delta r}{\delta w} \right] \delta w$$

WHEEL :
$$\delta w = \left[\frac{\delta w}{\beta} \right] \beta + \left[\frac{\delta w}{\dot{\psi}} \right] \dot{\psi}$$

WHERE :
$$\beta = \left[\frac{\partial}{\psi} \right] \phi - \dot{\psi} = .163 \phi - \dot{\psi}$$

BASIC GAINS

$$\left[\frac{\delta r}{\beta} \right] = - .3$$

$$\left[\frac{\delta r}{\dot{\phi}} \right] = - 2.07$$

$$\left[\frac{\delta w}{\beta} \right] = 1.83$$

AUG. SYSTEM 1

$$\left[\frac{\delta r}{\delta w} \right] = .178$$

$$\left[\frac{\delta w}{\dot{\psi}} \right] = -1.00$$

$$[\delta r_{MAX}] = \pm 20^\circ$$

AUG. SYSTEM 2

$$\left[\frac{\delta r}{\delta w} \right] = 0$$

$$\left[\frac{\delta w}{\dot{\psi}} \right] = -2.82$$

$$[\delta r_{MAX}] = \pm 50^\circ$$

AUG. SYSTEM 3

$$\left[\frac{\delta r}{\delta w} \right] = 0$$

$$\left[\frac{\delta w}{\dot{\psi}} \right] = -1.0$$

$$[\delta r_{MAX}] = \pm 50^\circ$$

ENGR.	R. Root	2-1-66	REVISED	DATE	LATERAL DIRECTIONAL STABILITY AUGMENTATION SYSTEM	TABLE AI-7
CHECK						D6-15000
APR						
APR					THE BOEING COMPANY RENTON WASHINGTON	AI-22

173

EQUIVALENT LATERAL - DIRECTIONAL AERODYNAMIC COEFFICIENTS

YAWING MOMENT

$$\begin{aligned}
 C_{n\dot{\beta}} &= C_{n\dot{\beta}} \text{ BASIC} + C_{n\delta_r} \left(\frac{\delta_r}{\beta} \right) &= .036 \text{ SEC./RAD} \\
 C_{n\dot{\phi}} &= C_{n\dot{\phi}} \text{ BASIC} + C_{n\delta_r} \left(\frac{\delta_r}{\phi} \right) &= .0905 \text{ SEC./RAD} \\
 C_{n\beta} &= C_{n\beta} \text{ BASIC} + C_{n\delta_w} \left(\frac{\delta_w}{\beta} \right) &= .218 \text{ 1/RAD} \\
 C_{n\dot{\psi}} &= C_{n\dot{\psi}} \text{ BASIC} + C_{n\delta_w} \left(\frac{\delta_w}{\dot{\psi}} \right) &= -.267 + .0213 \left(\frac{\delta_w}{\dot{\psi}} \right) \text{ SEC/RAD} \\
 C_{n\delta_w} &= C_{n\delta_w} \text{ BASIC} + C_{n\delta_r} \left(\frac{\delta_r}{\delta_w} \right) &= .0213 - .12 \left(\frac{\delta_r}{\delta_w} \right) \text{ 1/RAD}
 \end{aligned}$$

ROLLING MOMENT

$$\begin{aligned}
 C_{l\dot{\beta}} &= C_{l\dot{\beta}} \text{ BASIC} + C_{l\delta_r} \left(\frac{\delta_r}{\beta} \right) &= -.00069 \text{ SEC/RAD} \\
 C_{l\dot{\phi}} &= C_{l\dot{\phi}} \text{ BASIC} + C_{l\delta_r} \left(\frac{\delta_r}{\phi} \right) &= C_{l\dot{\phi}} + .00229 \left(\frac{\delta_r}{\phi} \right) \text{ SEC/RAD} \\
 C_{l\beta} &= C_{l\beta} \text{ BASIC} + C_{l\delta_w} \text{ BASIC} \left(\frac{\delta_w}{\beta} \right) &= -1955 \\
 C_{l\dot{\psi}} &= C_{l\dot{\psi}} \text{ BASIC} + C_{l\delta_w} \text{ BASIC} \left(\frac{\delta_w}{\dot{\psi}} \right) &= .3045 + .109 \left(\frac{\delta_w}{\dot{\psi}} \right) \text{ SEC/RAD} \\
 C_{l\delta_w} &= C_{l\delta_w} \text{ BASIC} + C_{l\delta_r} \left(\frac{\delta_r}{\delta_w} \right) &= C_{l\delta_w} + .00229 \left(\frac{\delta_r}{\delta_w} \right) \text{ 1/RAD}
 \end{aligned}$$

SIDE FORCE

$$\begin{aligned}
 C_{y\dot{\beta}} &= C_{y\dot{\beta}} \text{ BASIC} + C_{y\delta_r} \left(\frac{\delta_r}{\beta} \right) &= -.074 \text{ SEC/RAD} \\
 C_{y\dot{\phi}} &= C_{y\dot{\phi}} \text{ BASIC} + C_{y\delta_r} \left(\frac{\delta_r}{\phi} \right) &= .060 \text{ SEC/RAD} \\
 C_{y\beta} &= C_{y\beta} \text{ BASIC} + C_{y\delta_w} \left(\frac{\delta_w}{\beta} \right) &= -.9773 \text{ 1/RAD} \\
 C_{y\dot{\psi}} &= C_{y\dot{\psi}} \text{ BASIC} + C_{y\delta_w} \left(\frac{\delta_w}{\dot{\psi}} \right) &= .02995 - .0805 \left(\frac{\delta_w}{\dot{\psi}} \right) \text{ SEC/RAD} \\
 C_{y\delta_w} &= C_{y\delta_w} \text{ BASIC} + C_{y\delta_r} \left(\frac{\delta_r}{\delta_w} \right) &= -.0805 + .2464 \left(\frac{\delta_r}{\delta_w} \right) \text{ 1/RAD}
 \end{aligned}$$

ENGR.	R. Root	2-1-66	REVISED	DATE	EQUIVALENT LATERAL - -DIRECTIONAL AERODYNAMIC COEFFICIENTS.	TABLE A1-B
CHECK						D6-15000
APR						
APR					THE BOEING COMPANY RENTON, WASHINGTON	A1-23

APPENDIX 2

BASIC 367-80 DESCRIPTION

The aerodynamic characteristics of the unaugmented 367-80 inflight simulator are described in Table A2-1 and in Figures A2-1 thru A2-5. Characteristics presented are those used in the control command equations presented in Ref. 1. These equations are used to determine the control gains necessary to augment the aerodynamic characteristics of the 367-80 to the proposed Ames large transport configurations.

Figure A2-1 shows the pitching moment characteristics of the spoilers. The calibration of the inboard to outboard spoilers is presented in Figure A2-2. The lift and drag characteristics of the speed brakes are presented in Figures A2-3 and A2-4. The pitching moment characteristics of the thrust reversers are shown in Figure A2-5.

Several parameters varied during the test flights due to fuel consumption. The center of gravity of the 367-80 airplane varied from 29-31%. The weight varied from approximately 172,000 lbs at take-off to 137,000 at touchdown. The lateral directional moments of inertia vary ± 15 percent from the values shown in Table A2-1. The pitch moment of inertia varies ± 3.3 percent from those presented in Table A2-1.

TABLE A2-1

367-80 Longitudinal CharacteristicsFlight Condition

V_e	117 Kts
Flap Angle	30°
BPR	1
Gross Weight	150,000 lbs.
C. G. Location	30% MAC
Speed Brake Trim Angle	6°

Airplane Constants

Wing Area	2821 sq. ft.
Wing Span	130.8 ft.
MAC	20.1 ft.

Lift Derivatives

$C_{L_{Trim}}$	1.146
$\alpha_{Trim_{wcp}}$	8.5°
$C_{L \alpha}$	5.45 /rad
$C_{L \delta_E}$.52 /rad

Drag Derivatives

$C_{D_{Trim}}$.139
$C_{D \alpha}$.544 /rad

TABLE A2-1 (CONT.)

Pitching Moment Derivatives

$C_{m\alpha}$	-1.11	/rad
$C_{m\dot{\alpha}}$	-.272	/rad/sec
$C_{m\ddot{\alpha}}$	-.710	/rad/sec
$C_{m\delta_E}$	-.975	/rad
I_y	2.25 $\times 10^6$	slug-FT ²

Speed Brakes

$C_{L\delta_{SB}}$	1.11	/rad
$C_{m\delta_{SB}}$	See Fig.	/rad

Longitudinal Dynamic CharacteristicsShort Period

Damped Natural Frequency	1.04	rad/sec
Undamped Natural Frequency	1.42	rad/sec
Damping Ratio	.68	

Phugoid

Damped Natural Frequency	.157	rad/sec
Undamped Natural Frequency	.157	rad/sec
Damping Ratio	.0906	

TABLE A2-1 (CONT.)

367-80 Lateral - Directional CharacteristicsSide Force Derivatives

$C_{y\beta}$	-.838	/rad
$C_{y\dot{\phi}}$.270	/rad/sec
$C_{y\dot{\psi}}$.0727	/rad/sec
$C_{y\dot{\epsilon}}$	0	/rad
C_{yS_R}	.211	/rad
$C_{yS_{WH}}$	-.0252	/rad

Rolling Moment Derivatives

$C_{l\epsilon}$	-.1743	/rad
$C_{l\dot{\phi}}$	-.120	/rad/sec
$C_{l\dot{\psi}}$.104	/rad/sec
$C_{l\dot{\epsilon}}$	0	/rad
C_{lS_R}	.0149	/rad
$C_{lS_{WH}}$.06	/rad
I_{X_B}	2.57×10^6	slug-FT ²

Yawing Moment Derivatives

$C_{n\beta}$.0909	/rad
$C_{n\dot{\phi}}$	-.0179	/rad/sec
$C_{n\dot{\psi}}$	-.1071	/rad/sec

TABLE A2-1 (CONT.)

Yawing Moment Derivatives (cont'd)

$C_{n\dot{\epsilon}}$	-0.0747	/rad
$C_{n\dot{\delta}_R}$	-0.0749	/rad
$C_{n\dot{\delta}_{WH}}$.0030	/rad
I_{z_B}	4.73×10^6	slug-FT ²
I_{xz_B}	$.156 \times 10^6$	slug-FT ²

Lateral Dynamic Characteristics

Spiral Divergence

Time Constant	15.7	sec
Time to Half Amplitude	10.87	sec

Roll Convergence

Time Constant	1.04	sec
---------------	------	-----

Dutch Roll

Damped Natural Frequency	.77	rad/sec
Undamped Natural Frequency	.77	rad/sec
Damping Ratio	.018	
	1.584	

179

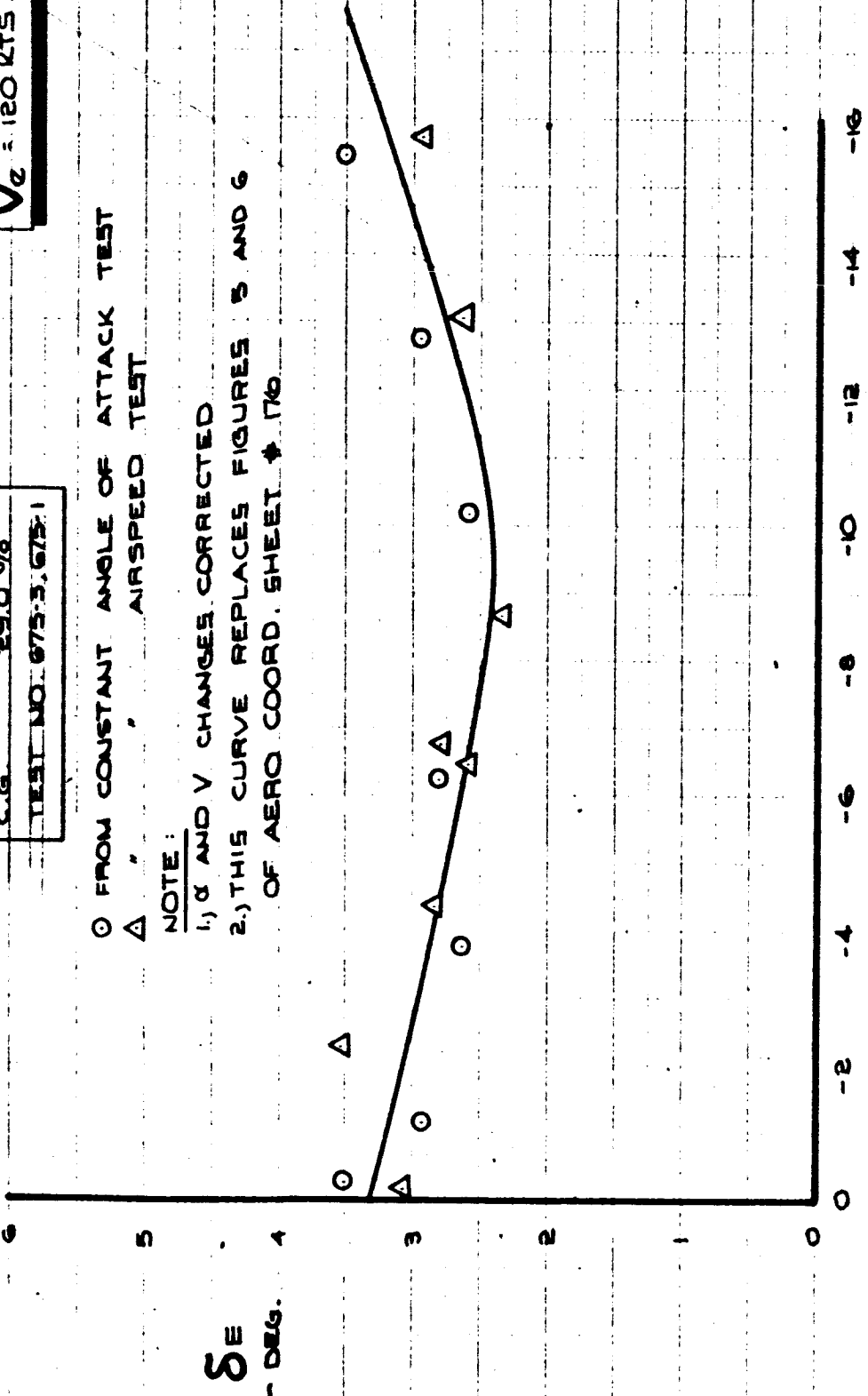
FLAPS 30°
 BRG 10
 G.W. 144,000 LBS
 C.G. 29.0 %
 TEST NO. 675-3, 675-1

$\alpha_{WCP} = 6.3^\circ$
 $V_C = 120 \text{ KTS}$

○ FROM CONSTANT ANGLE OF ATTACK TEST
 △ " " AIRSPEED TEST

NOTE:

- 1.) α AND V CHANGES CORRECTED
- 2.) THIS CURVE REPLACES FIGURES 5 AND 6 OF AERO COORD. SHEET # 170

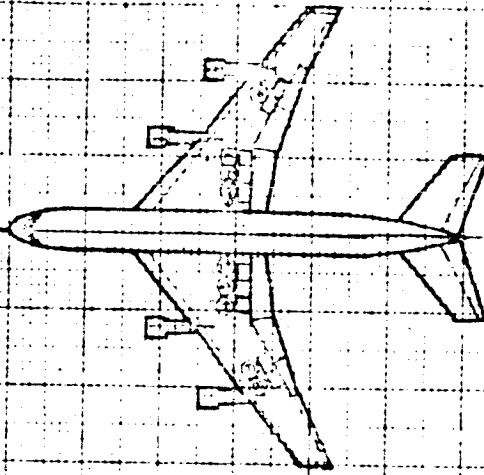


δ SB OUTSIDE - DEG.

CALC	P.S.	11/65	REVISED	DATE
CHECK				
APR				
APR				

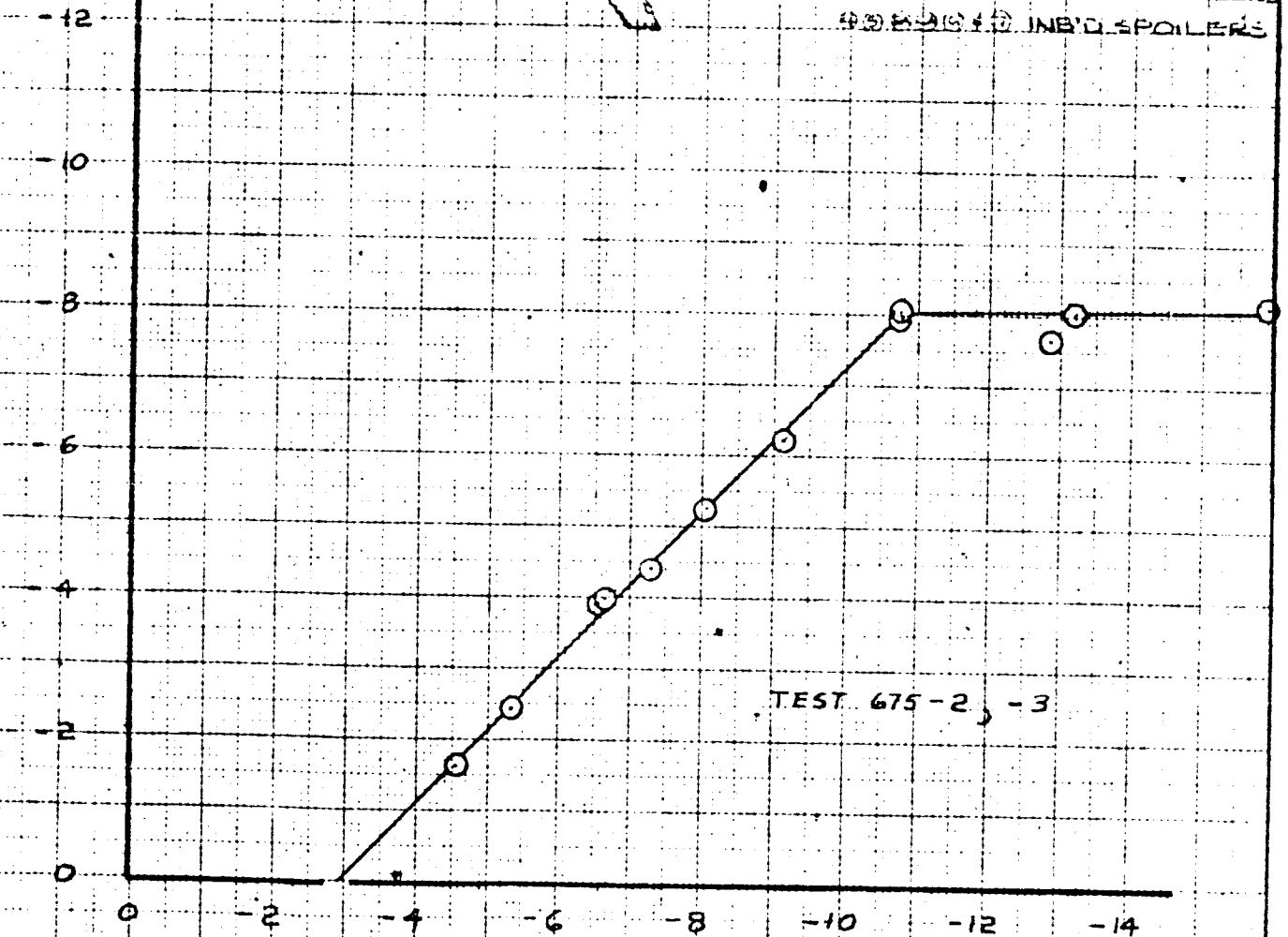
PITCHING MOMENT CHARACTERISTICS OF SPOILERS.
 THE BOEING COMPANY D6-15000

387-80
 FIG. A2-1
 PAGE A2-6



$\delta_{SB_{AVG}}$
INBOARD
~ DEG

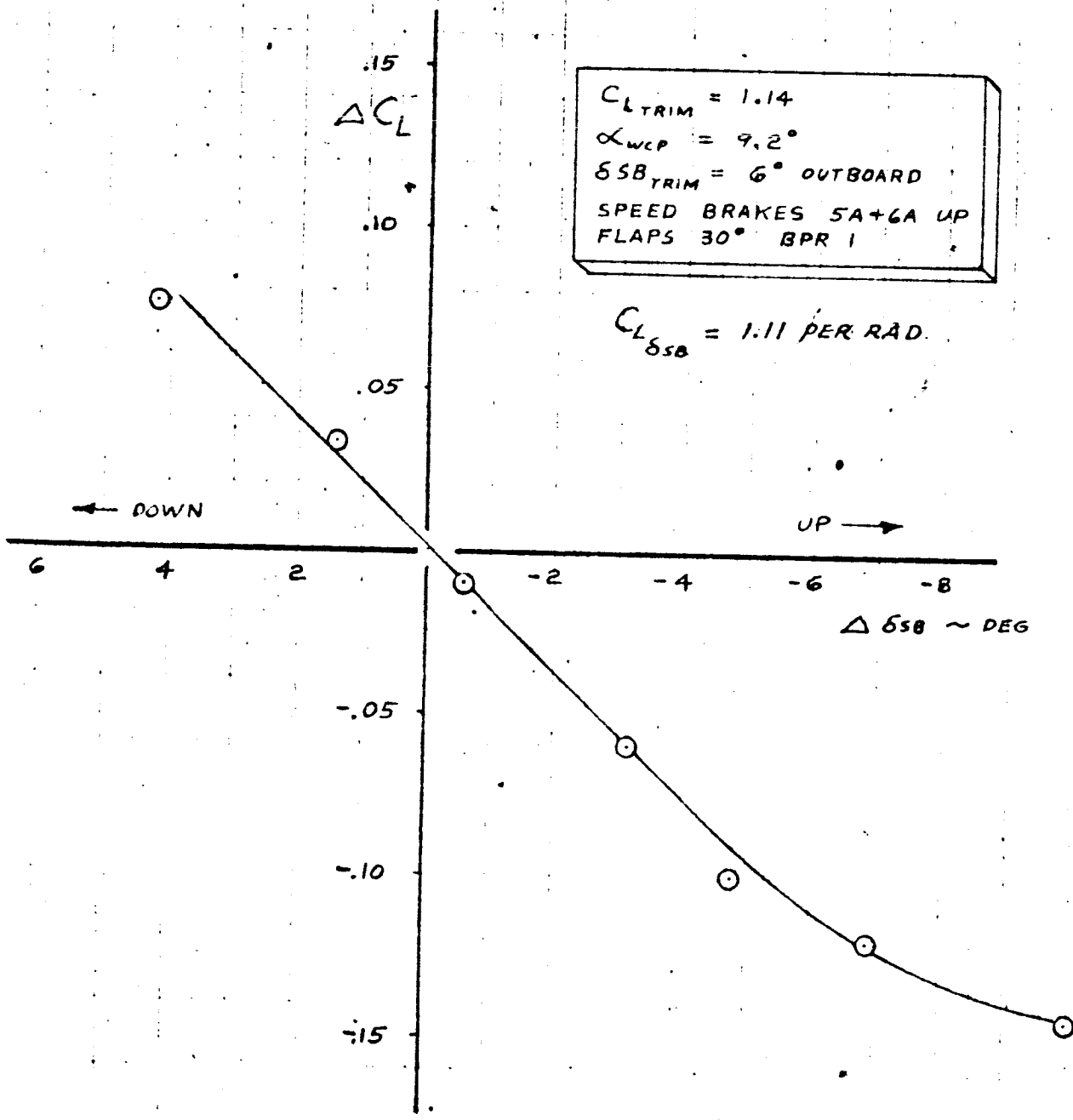
②③④⑤ OUTB'D SPOILERS
⑥⑦⑧⑨⑩ INB'D SPOILERS



TEST 675-2, -3

$\delta_{SB_{AVG}}$ OUTBOARD ~ DEG

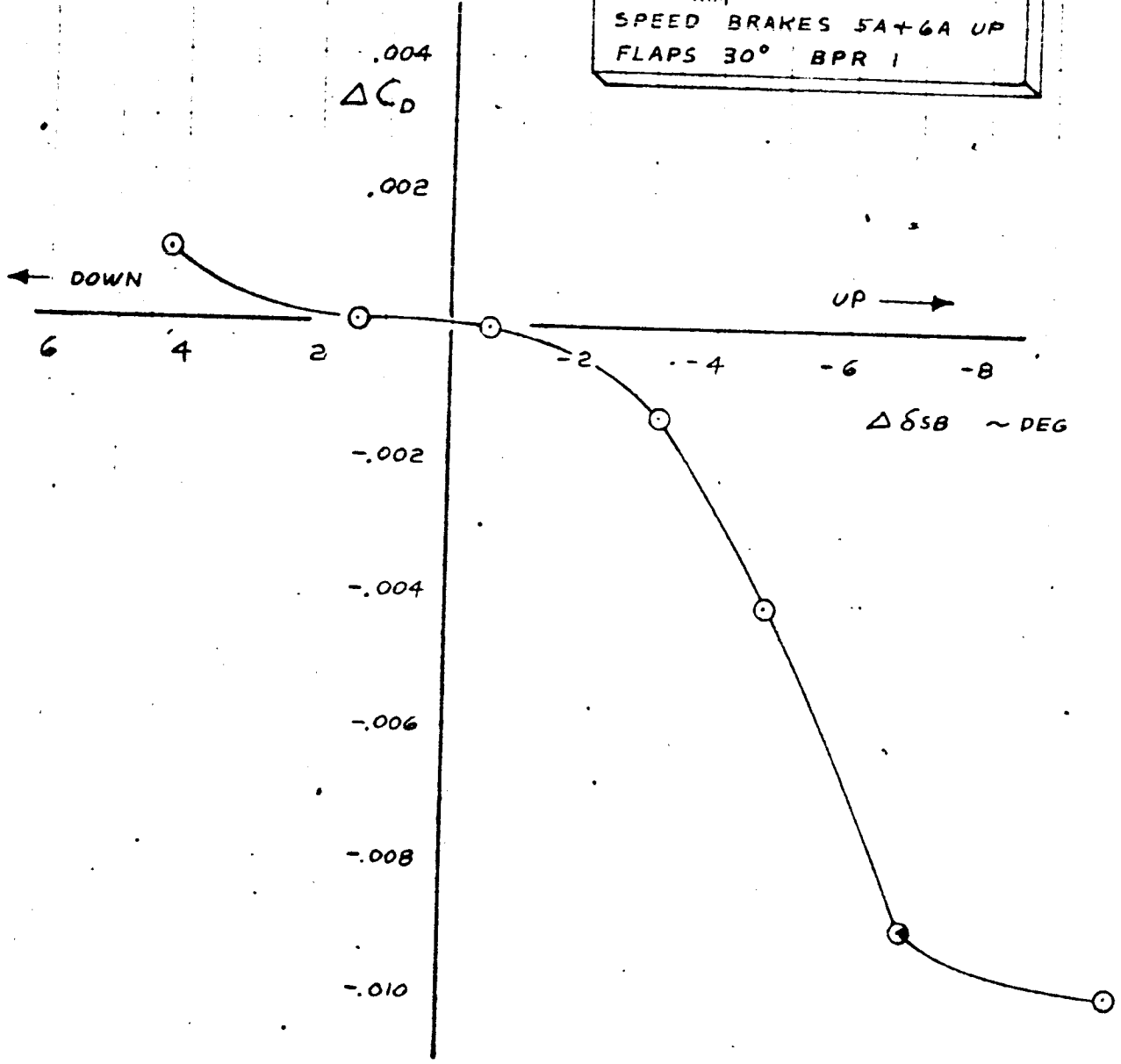
CALC	W.M.E.	11-1-65	REVISED	DATE	SPEED BRAKE OPERATION CALIBRATION TESTS	367-80
CHECK						FIG. A2-2
APR					THE BOEING COMPANY DG-15000	PAGE
APR						A2-7



TEST 675-2,-3

CALC	W.M.E.	10-29-58	REVISED	DATE	SPEED BRAKE CHARACTERISTICS LIFT	367-80
CHECK						FIG. A2-3
APR						THE BOEING COMPANY D6-15000
APR						

$C_{L\text{TRIM}} = 1.14$
 $\alpha_{WCP} = 9.2^\circ$
 $\delta_{SB\text{TRIM}} = 6^\circ$ OUTBOARD
 SPEED BRAKES 5A+6A UP
 FLAPS 30° BPR 1

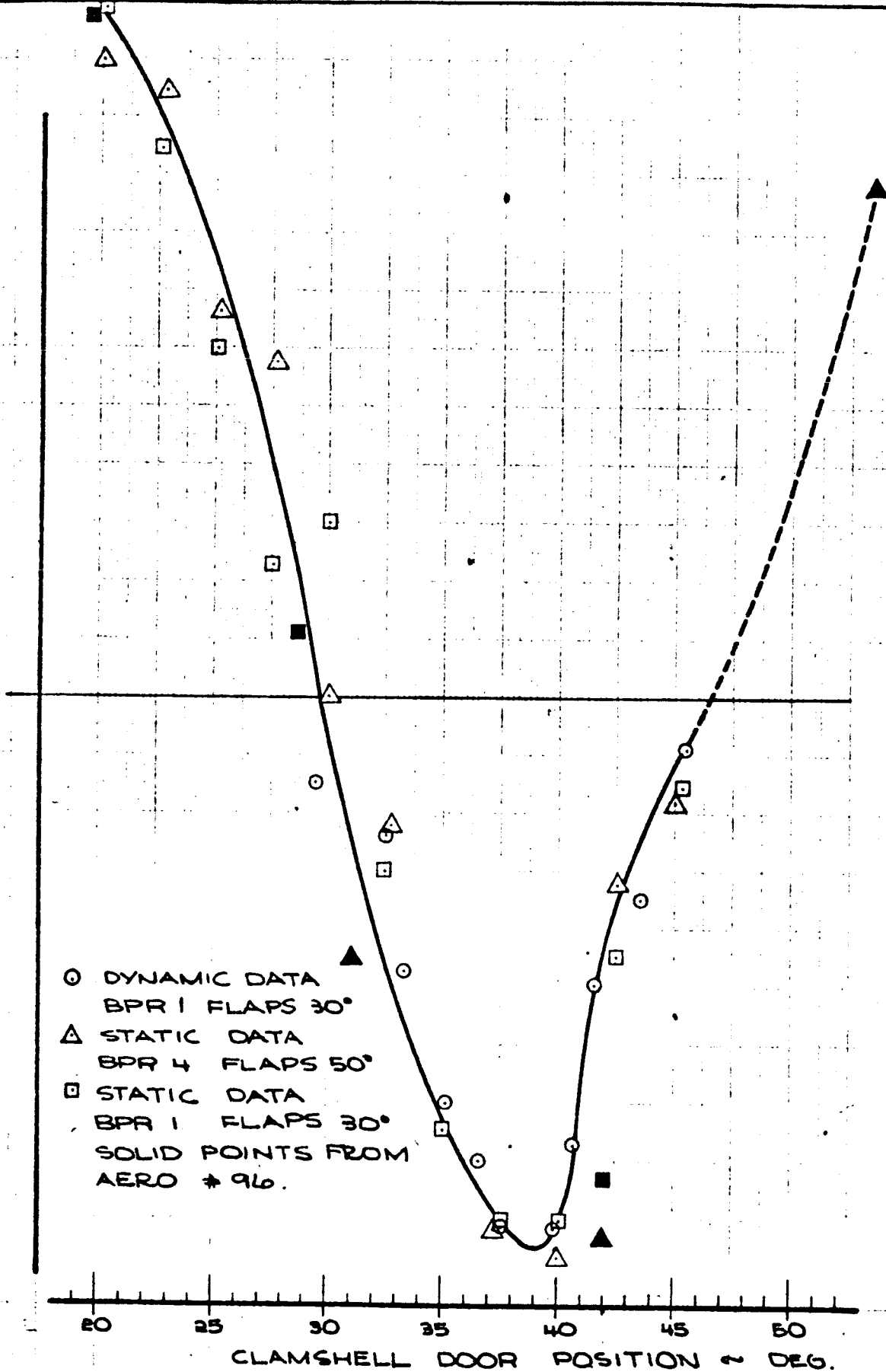


TEST 675-2, -3

CALC	W. M. E.	10-29-65	REVISED	DATE	SPEED BRAKE CHARACTERISTICS DRAG	367-80
CHECK						FIG AR-4
APR						
APR						
					THE BOEING COMPANY	06-15000
						PAGE A2-9

ELEVATOR TO TRIM δ DEG.

10
8
6
4
2
0
-2
-4
-6
-8
-10



CALC			REVISED	DATE
CHECK				
APR				
APR				

FLIGHT TEST DATA
THRUST REVERSER PITCH. M.

767-80

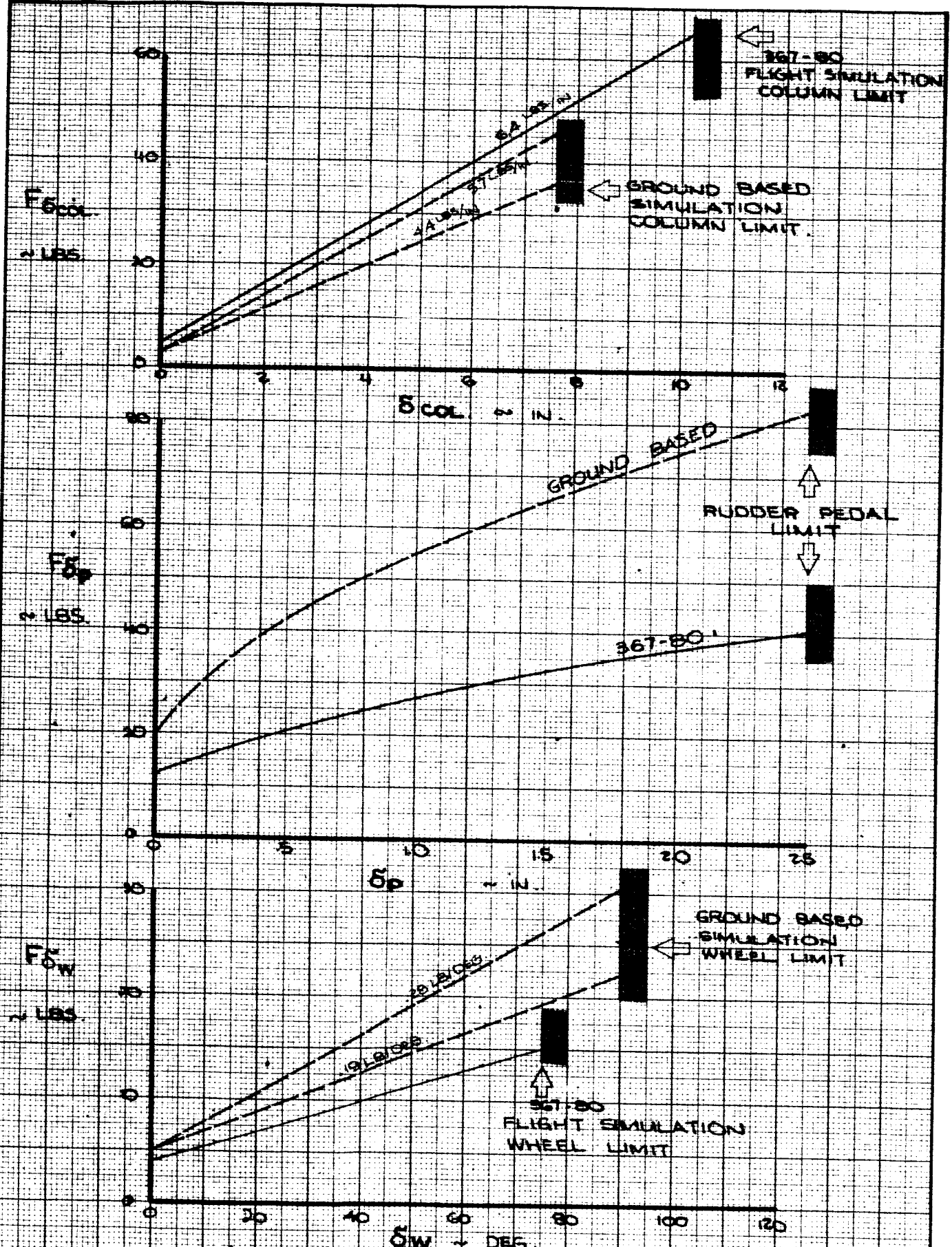
FIG. A2-5

THE BOEING COMPANY D6-15000

PAGE
A2-10

APPENDIX 3

Typical control system force characteristics for the ground based and airborne simulations are presented in Fig. A3-1, for column, wheel, and rudder pedals. Wheel and Column forces were varied on the ground based simulation during the evaluations. These variations are listed in Tables 3 and 6 of section VII and VIII. Forces were kept constant on the airborne simulation. The pilots had the capability of varying column force characteristics in flight, but little variation was noted.



CALC	R. Root	2-2-66	REVISED	DATE
CHECK				
APR				
APR				

CONTROL SYSTEM FORCE CHARACTERISTICS

THE BOEING COMPANY

APPENDIX 4**Derivation of Theory**

The theoretical characteristics presented for the control pulses and steps were obtained from 6-degree-of-freedom digital computer programs. The theoretical equations involved can be found in Reference 2.

The theoretical characteristics of the documentation maneuvers performed other than the pulses and steps are derived on the following pages.

APPENDIX 4

THEORETICAL CALCULATIONS

Speed Stability

$$C_L = C_{L_0} + C_{L_\alpha} \Delta\alpha + C_{L_\dot{\alpha}} \dot{\alpha} + C_{L_{\dot{0}}} \dot{0} + C_{L_V} \Delta V + C_L \delta_E \delta E \quad (1)$$

and

$$C_M = C_{M_0} + C_{M_\alpha} \Delta\alpha + C_{M_{\dot{0}}} \dot{0} + C_{M_\dot{\alpha}} \dot{\alpha} + C_{M_V} \Delta V + C_M \delta_E \delta E \quad (2)$$

For the steady state case $\dot{0} = \dot{\alpha} = 0$ and equations (1) and (2) become

$$C_L = C_{L_0} + C_{L_\alpha} \Delta\alpha + C_{L_V} \Delta V + C_L \delta_E \delta E \quad (3)$$

and

$$C_M = C_{M_0} + C_{M_\alpha} \Delta\alpha + C_{M_V} \Delta V + C_M \delta_E \delta E. \quad (4)$$

Differentiating equation (3)

$$\frac{d C_L}{dV} = C_{L_\alpha} \frac{d \Delta\alpha}{dV} + C_{L_V} + C_L \delta_E \frac{d \delta E}{dV} \quad (5)$$

Rearranging terms in equation (5) gives

$$\frac{d \Delta\alpha}{dV} = \frac{1}{C_{L_\alpha}} \left[\frac{d C_L}{dV} - C_{L_V} - C_L \delta_E \frac{d \delta E}{dV} \right] \quad (6)$$

Differentiating equation (4)

$$0 = C_{M_\alpha} \frac{d \Delta\alpha}{dV} + C_{M_V} + C_M \delta_E \frac{d \delta E}{dV} \quad (7)$$

Substituting equation (6) into equation (7) gives

$$0 = \frac{C_{M_\alpha}}{C_{L_\alpha}} \left[\frac{d C_L}{dV} - C_{L_V} - C_L \delta_E \frac{d \delta E}{dV} \right] + C_{M_V} + C_M \delta_E \frac{d \delta E}{dV} \quad (8)$$

Solving for $\frac{d \delta E}{dV}$ in equation (8)

$$\frac{d \delta E}{dV} = \frac{C_{M_\alpha} C_{L_V} - C_{M_\alpha} \frac{d C_L}{dV} - C_{M_V} C_{L_\alpha}}{C_{L_\alpha} C_M \delta_E - C_{M_\alpha} C_L \delta_E} \quad (9)$$

187

Speed Stability

The lift equation is

$$L_0 = \frac{1}{2} \rho V^2 S C_{L_0} \tag{10}$$

Differentiating equation (10)

$$0 = \frac{1}{2} \rho S (C_{L_0} 2V dV + V^2 dC_L)$$

Solving this for dC_L gives

$$\frac{dC_L}{dV} = -\frac{2C_{L_0}}{V} \tag{11}$$

Substituting equation (11) into equation (9)

$$\frac{d\delta_E}{dV} = \frac{C_{M\alpha} C_{L_V} + C_{M\alpha} \frac{2C_{L_0}}{V} - C_{M_V} C_{L\alpha}}{C_{L\alpha} C_{M\delta_E} - C_{M\alpha} C_{L\delta_E}} \tag{12}$$

Substituting equation (11) into equation (6) gives

$$\frac{d\alpha}{dV} = \frac{1}{C_{L\alpha}} \left[\frac{-2C_{L_0}}{V} - C_{L_V} - C_{L\delta_E} \frac{d\delta_E}{dV} \right] \tag{13}$$

Integrating equation (12) yields

$$\delta_E = \int_{V_0}^V \frac{d\delta_E}{dV} dV = \frac{C_{M\alpha} C_{L_V} - C_{M_V} C_{L\alpha}}{C_{L\alpha} C_{M\delta_E} - C_{M\alpha} C_{L\delta_E}} \int_{V_0}^V \frac{dV}{V} + \frac{C_{M\alpha} \frac{2C_{L_0}}{V} - C_{M_V} C_{L\alpha}}{C_{M\delta_E} C_{L\alpha} - C_{M\alpha} C_{L\delta_E}} \int_{V_0}^V \frac{dV}{V}$$

$$\delta_E = + \frac{2C_{L_0} C_{M\alpha}}{C_{M\delta_E} C_{L\alpha} - C_{M\alpha} C_{L\delta_E}} \ln \frac{V}{V_0} - \frac{C_{M_V} C_{L\alpha} - C_{L_V} C_{M\alpha}}{C_{M\delta_E} C_{L\alpha} - C_{M\alpha} C_{L\delta_E}} (V - V_0) \tag{14}$$

$$\delta_{COL} = \left(\frac{1}{\delta_E / \delta_{COL}} \right) \delta_E$$

$$F_S = \left(\frac{F_S}{COL} \right) \delta_{COL}$$

Speed Stability

Integrating equation (13) yields

$$\alpha = \left(\frac{d\alpha}{dV} \right) dV = - \frac{1}{C_{L\alpha}} \left[\int_{V_0}^V \frac{2 C_{L_0}}{V} dV + \int_{V_0}^V C_{LV} dV + \int_{V_0}^V C_{LE} \frac{d\delta_E}{dV} dV \right]$$

$$= - \frac{2 C_{L_0}}{C_{L\alpha}} \ln V/V_0 - \frac{C_{LV}}{C_{L\alpha}} (V - V_0) - C_{LE} \delta_E$$

THEORETICAL CALCULATIONS

Wind Up Turn

$$C_L = C_{L_0} + C_{L_\alpha} \alpha + C_{L_{\dot{\theta}}} \dot{\theta} + C_{L_{\dot{\alpha}}} \dot{\alpha} + C_{L_V} V + C_{L_{\delta_E}} \delta_E \quad (1)$$

and

$$C_m = C_{m_0} + C_{m_\alpha} \alpha + C_{m_{\dot{\theta}}} \dot{\theta} + C_{m_{\dot{\alpha}}} \dot{\alpha} + C_{m_V} V + C_{m_{\delta_E}} \delta_E \quad (2)$$

The increments from trim are

$$\Delta C_L = C_L - C_{L_0} = (n-1)C_{L_0} \quad (3)$$

and

$$\Delta C_m = C_m - C_{m_0} = 0.$$

For the steady state case $V = \text{constant}$ and $\dot{\alpha} = 0$. Solving for the steady state $\Delta \delta_E$ in equation (2) gives

$$\Delta \delta_E = - \frac{C_{m_\alpha} \Delta \alpha + C_{m_{\dot{\theta}}} \dot{\theta}}{C_{m_{\delta_E}}} \quad (4)$$

and solving for $\Delta \alpha$ in equation (1) gives

$$\Delta \alpha = \frac{C_L - C_{L_0} - C_{L_{\dot{\theta}}} \dot{\theta} - C_{L_{\delta_E}} \Delta \delta_E}{C_{L_\alpha}} \quad (5)$$

Substituting equation (3) into equation (5)

$$\Delta \alpha = \frac{(n-1)C_{L_0} - C_{L_{\dot{\theta}}} \dot{\theta} - C_{L_{\delta_E}} \Delta \delta_E}{C_{L_\alpha}} \quad (6)$$

Equations (4) and (6) can be combined with $\dot{\theta} = \frac{(n^2 - 1)}{n} g/v$ (chapter 9, page 301, Reference 2) for a wind up turn to give

$$\frac{\Delta \delta_E}{(n-1)} = \frac{-C_{m_\alpha} C_{L_0} + \frac{(1+n)}{n} (C_{L_{\dot{\theta}}} C_{m_\alpha} - C_{L_\alpha} C_{m_{\dot{\theta}}}) g/v}{C_{m_{\delta_E}} C_{L_\alpha} - C_{L_{\delta_E}} C_{m_\alpha}} \quad (7)$$

$$\frac{\Delta \delta_c}{(n-1)} = \frac{\Delta \delta_E}{(n-1)} \cdot \frac{(\delta_c)}{(\delta_E)} \quad (8)$$

Wind Up Turn

From Equation 6

$$\frac{\Delta\alpha}{(n-1)} = \frac{C_{L_0} - C_{L_0} \frac{(n+1)g}{n v} - C_{L_0} C_R \frac{\delta E}{(n-1)}}{C_{L_\alpha}}$$

or

$$\frac{(n-1)}{\Delta\alpha} = \frac{C_L}{C_{L_0} - C_{L_0} \frac{(n+1)g}{n v} - C_{L_0} C_R \frac{(\delta E)}{(n-1)}}$$

193

THEORETICAL CALCULATIONS

Steady Sideslip

The yawing moment equation is

$$C_n = C_{n_0} + C_{n_\beta} \beta + C_{n_{\dot{\beta}}} \dot{\beta} + C_{n_{\dot{\psi}}} \dot{\psi} + C_{n_{\dot{\phi}}} \dot{\phi} + C_{n_{\delta_R}} \delta_R + C_{n_{\delta_{WH}}} \delta_{WH} \quad (1)$$

The side force equation is

$$C_y = C_{y_0} + C_{y_\beta} \beta + C_{y_{\dot{\beta}}} \dot{\beta} + C_{y_{\dot{\phi}}} \dot{\phi} + C_{y_\phi} \phi + C_{y_{\delta_{WH}}} \delta_{WH} + C_{y_{\delta_R}} \delta_R + C_{y_{\dot{\psi}}} \dot{\psi} \quad (2)$$

The rolling moment equation is

$$C_l = C_{l_0} + C_{l_\beta} \beta + C_{l_{\dot{\beta}}} \dot{\beta} + C_{l_{\dot{\phi}}} \dot{\phi} + C_{l_{\dot{\psi}}} \dot{\psi} + C_{l_{\delta_{WH}}} \delta_{WH} + C_{l_{\delta_R}} \delta_R \quad (3)$$

For the steady state case equation (1), (2) and (3) become

$$0 = C_{n_\beta} \beta + C_{n_{\delta_R}} \delta_R + C_{n_{\delta_{WH}}} \delta_{WH}, \quad (4)$$

and

$$0 = C_{y_\beta} \beta + C_{y_{\delta_R}} \delta_R + C_{y_\phi} \phi + \cancel{C_{y_{\delta_{WH}}} \delta_{WH}} \text{ negligible} \quad (5)$$

$$0 = C_{l_\beta} \beta + C_{l_{\delta_{WH}}} \delta_{WH} + C_{l_{\delta_R}} \delta_R \quad (6)$$

Combining equations (4) and (6) yields

$$\frac{\delta_R}{\beta} = \frac{-C_{n_\beta} C_{l_{\delta_{WH}}} + C_{l_\beta} C_{n_{\delta_{WH}}}}{C_{n_{\delta_R}} C_{l_{\delta_{WH}}} - C_{n_{\delta_{WH}}} C_{l_{\delta_R}}}$$

and

$$\frac{\delta_{WH}}{\beta} = \frac{-C_{n_{\delta_R}} C_{l_\beta} + C_{n_\beta} C_{l_{\delta_R}}}{C_{n_{\delta_R}} C_{l_{\delta_{WH}}} - C_{n_{\delta_{WH}}} C_{l_{\delta_R}}}$$

also

$$\frac{\delta_P}{\beta} = \frac{\delta_R}{\beta} \frac{\delta_P}{\delta_R}$$

Steady Sideslip

From equation (2)

$$\frac{\phi}{\beta} = -\frac{1}{C_{Y\phi}} \left[C_{Y\beta} + C_{Y\delta_R} \frac{\delta_R}{\beta} \right] \quad (6)$$

Substituting $C_L = C_{Y\phi}$ in equation (6)

$$\frac{\phi}{\beta} = -\frac{1}{C_L} \left[C_{Y\beta} + C_{Y\delta_R} \frac{\delta_R}{\beta} \right]$$

194

THEORETICAL CALCULATION

Steady Roll Rate

The rolling moment equation is

$$C_l = \frac{I_{xx}}{qsb} \ddot{\phi} = C_{l\beta} \beta + C_{l\dot{\beta}} \dot{\beta} + C_{l\dot{\phi}} \dot{\phi} + C_{l\dot{\psi}} \dot{\psi} + C_{l\delta_{WH}} \delta_{WH}^{WH} + C_{l\delta_R} \delta_R^{R} \quad (1)$$

For a steady state roll rate $\ddot{\phi} = 0$, so equation (1) becomes

$$0 = C_{l\beta} \beta + C_{l\dot{\beta}} \dot{\beta} + C_{l\dot{\phi}} \dot{\phi} + C_{l\dot{\psi}} \dot{\psi} + C_{l\delta_{WH}} \delta_{WH}^{WH} + C_{l\delta_R} \delta_R^{R} \quad (2)$$

If the flight test maneuver to determine steady roll rate is performed correctly then $\delta_R = \beta = \dot{\psi} = \dot{\beta} = 0$. The flight test data was adjusted to fit these conditions so

$$0 = C_{l\dot{\phi}} \dot{\phi}_{SS} + C_{l\delta_{WH}} \delta_{WH}^{WH}$$

$$\frac{\dot{\phi}_{SS}}{\delta_{WH}} = \frac{C_{l\delta_{WH}}}{C_{l\dot{\phi}}}$$

THEORETICAL CALCULATION

Roll Acceleration

The rolling moment equation is

$$C_L = \frac{I_{XX}}{qsb} \ddot{\phi} = C_{L\beta} \beta + C_{L\dot{\beta}} \dot{\beta} + C_{L\dot{\phi}} \dot{\phi} + C_{L\psi} \psi + C_{L\delta_{WH}} \delta_{WH} + C_{L\delta_R} \delta_R \quad (1)$$

The roll rate reversal data was measured at a point where $\dot{\phi} = \psi = \beta = \delta_R = \dot{\beta} = 0$
so equation (1) becomes

$$\frac{I_{XX}}{qsb} \ddot{\phi} = C_{L\delta_{WH}} \delta_{WH}$$

solving for $\ddot{\phi} / \delta_{WH}$

$$\frac{\ddot{\phi}}{\delta_{WH}} = C_{L\delta_{WH}} \frac{qsb}{I_{XX}}$$

THEORETICAL CALCULATIONS

Yaw Acceleration

The yawing moment equation is

$$C_n = \frac{I_{zz}}{qsb} \ddot{\psi} = C_{n\beta} \beta + C_{n\dot{\beta}} \dot{\beta} + C_{n\dot{\psi}} \dot{\psi} + C_{n\dot{\phi}} \dot{\phi} + C_{n\delta_R} \delta_R + C_{n\delta_{WH}} \delta_{WH} \quad (1)$$

The roll rate reversal data was measured at a point where $\beta = \dot{\beta} = \dot{\psi} = \dot{\phi} = \delta_{WH} = 0$

so equation (1) becomes

$$\frac{I_{zz}}{qsb} \ddot{\psi} = C_{n\delta_R} \delta_R$$

solving for $\ddot{\psi} / \delta_R$

$$\ddot{\psi} / \delta_R = C_{n\delta_R} \frac{qsb}{I_{zz}}$$

Multiplying equation (2) by the pedal to rudder gearing gives

$$\ddot{\psi} / \delta_P = C_{n\delta_R} \frac{qsb}{I_{zz}} \left(\frac{\delta_R}{\delta_P} \right)$$

197

THEORETICAL CALCULATIONS

Pitch Acceleration

The pitching moment equation is

$$C_M = \frac{I_{yy}}{qsc} \ddot{\theta} = C_{M\alpha} \Delta\alpha + C_{M\dot{\theta}} \dot{\theta} + C_{M\ddot{\alpha}} \ddot{\alpha} + C_{M\dot{U}} \dot{U} + C_{M\delta E} \delta E \quad (1)$$

The pitch acceleration was measured at a point where $\Delta\alpha = \dot{\theta} = \ddot{\alpha} = \dot{U} = 0$

so equation (1) becomes

$$\frac{\ddot{\theta}}{\delta E} = C_{M\delta E} \frac{qsc}{I_{yy}} \quad (2)$$

Multiplying equation (2) by the column to elevator gearing gives

$$\frac{\ddot{\theta}}{\delta_{COL}} = C_{M\delta E} \frac{qsc}{I_{yy}} \left(\frac{\delta e}{\delta_{COL}} \right)$$

APPENDIX 5

A. Ground Based Analog Simulation Description

The ground-based flight simulator used for these studies was the Ames Research Center, moving-base transport simulator with a color TV visual scene. The visual scene, projected to simulate daylight flying, was produced by the Ames Research Center landing-approach color image generator. The simulation solved the six degree of freedom equations of motion of the airplane and presented the solutions in cab motions, instrument readings, and visual display changes. Linearized aerodynamic coefficients were used in the equations of motion. The equations of motion are given in Table A5-1.

The moving-base transport simulator utilized a transport-type (C-130) cab with conventional seating, instrumentation, and controls for two pilots. The left hand seat was used for these tests. A hydraulic feel system allowed for variation of the control system parameters. The instrument panel included the following instruments:

1. Air-speed
2. Altitude
3. Rate of climb
4. Angle of attack
5. Angle of sideslip
6. Turn and slip
7. Heading
8. Attitude
9. Localizer and glide slope error.

TABLE A5-1

Ground Based Simulation Equations of Motion:

DRAG

$$C_D = C_{D_{\alpha=0}} + C_{D_{\alpha}} \alpha$$

$$\dot{V} = \frac{1}{m} (T_N - g S C_D - W \sin \gamma)$$

$$V = V_T = \int \dot{V} dt + V_0 \quad (V_0 = \text{initial velocity})$$

$$x = x_0 + \int (V \cos \gamma \cdot \cos \psi) dt \quad (x_0 = \text{initial distance from runway threshold})$$

$$V_e = \sqrt{g} V + V_{eUST}$$

$$g = \frac{V_e^2}{295}$$

$$T_N = T_{N_0} + \frac{\partial T_N}{\partial V} u \quad (T_{N_0} = \text{initial net thrust for trim})$$

$$u = V - V_0$$

PITCH

$$C_m = C_{m_g} g + C_{m_{\dot{\alpha}}} \dot{\alpha} + C_{m_{\alpha=0}} + C_{m_{\alpha}} \alpha + C_{m_{\delta_e}} \delta_e + C_{m_{i_H}} i_H$$

$$I_{YY} \frac{\dot{g}}{573} = g S \bar{c} C_m$$

$$g = \int \dot{g} dt$$

TABLE A5-1 (CONT.)

$$C_{n_w} = C_{n_{\delta_s}} \delta_s + C_{n_{\delta_a}} \delta_a + C_{n_{\delta_r}} \delta_r + C_{n_{\beta_w}} \beta_w + C_{n_p} (P) + C_{n_r} (r)$$

$$I_{xx} \frac{\dot{r}}{57.3} = I_{xz} \left(\frac{\dot{r}}{57.3} \right) + g S b C_{\ell}$$

$$I_{zz} \frac{\dot{r}}{57.3} = g S C_n b$$

$$P = \int \dot{P} dt$$

$$r = \int \dot{r} dt$$

$$\dot{\phi} = P + r \frac{g}{57.3}$$

$$\dot{\psi} = r \cos \phi + g \sin \phi$$

$$\phi = \int \dot{\phi} dt + \phi_0 \quad (\phi_0 = \text{initial roll angle})$$

$$\psi = \int \dot{\psi} dt + \psi_0 \quad (\psi_0 = \text{initial yaw angle})$$

SIDE FORCE

$$C_Y = C_{Y_{\delta_s}} \delta_s + C_{Y_{\delta_r}} \delta_r + C_{Y_{\beta_w}} \beta_w + C_{Y_p} (P) + C_{Y_r} (r) + C_{Y_{\delta_w}} \delta_w$$

$$a_Y = \frac{1}{m} (g S C_Y + W \sin \phi + T \frac{\beta_r}{57.3})$$

$$\dot{\beta}_p = P \frac{g}{57.3} - r + \frac{57.3}{V} a_y$$

$$\beta_p = \int \dot{\beta}_p dt + \beta_0 \quad (\beta_0 = \text{initial sideslip angle})$$

$$\beta = \beta_p + \beta_{GUST}$$

$$S_Y = S_{Y_0} + \int V \sin \psi_p dt \quad (S_{Y_0} = \text{initial lateral distance from runway})$$

$$\dot{\psi}_p = \int \left(\frac{a_y}{V} \cos \phi - g \sin \phi \right) dt$$

1001

TABLE A5-1 (CONT.)

$$\dot{\alpha}_p = \alpha_0 + \int (g + 57.3 \frac{a_z}{V}) dt \quad (\alpha_0 = \text{initial } \alpha \text{ for trim})$$

$$\alpha = \alpha_p + \alpha_{GUST}$$

$$\theta = \gamma + \alpha_p$$

LIFT

$$C_L = C_{L\alpha=0} + C_{L\alpha} \alpha + C_{L\delta_e} \delta_e + C_{L i_H} i_H + C_{L\dot{\alpha}} \dot{\alpha} + C_{Lg} g$$

$$(C_{L\alpha=0} + C_{L\alpha} \alpha \text{ limited to } C_{L_{MAX.}})$$

$$-a_z = \frac{1}{M} (g S C_L - W \cos \phi \cos \gamma)$$

$$\dot{\gamma} = - \frac{57.3}{V} (a_z \cos \phi + a_y \sin \phi)$$

$$\gamma = \int \dot{\gamma} dt - \gamma_0 \quad (\gamma_0 = \text{initial flight path angle})$$

$$\dot{h} = V \sin \gamma$$

$$h = \int \dot{h} dt + h_0 \quad (h_0 = \text{initial altitude})$$

ROLL AND YAW

$$C_l = C_{lW} - C_{nW} \frac{\alpha}{57.3} \quad (C_{lW} \text{ and } C_{nW} \text{ defined below})$$

$$C_n = C_{nW} + C_{lW} \frac{\alpha}{57.3}$$

$$C_{lW} = C_{l\delta_s} \delta_s + C_{l\delta_a} \delta_a + C_{l\delta_r} \delta_r + C_{l\beta_w} \beta_w + C_{lp} (P) + C_{lr} (r)$$

The pilots outside view was limited to the visual TV scene by blocking out all windows not directly in front of him.

Motion of the cab was controlled by three linear hydraulic servo actuators. These were operated differentially or synchronously for three degrees of motion; roll, pitch, and heave (vertical). The actuators were controlled in a closed loop fashion by the simulation. The roll axis of motion was scaled down by a factor of two so that a simulated roll angle of ten degrees produced five degrees of cab roll motion. This resulted in less side acceleration error apparent to the pilot in a steady turn due to gravity. The pilot received the proper roll cues from the instruments and visual scene. A tabulation of the moving-base transport simulator physical characteristics is shown in Table A5-2.

The visual scene was produced by a closed circuit color television system which utilized a scale contour map including roads, buildings and fields, as well as the runway to which the approaches were conducted. A color television camera was positioned by electric servos and driven closed loop by the simulation. The scope of the simulated airplane movements was limited only by the boundaries of the contour map. Descent through a cloud layer was simulated by obliterating the picture to a pre-selected altitude. The tabulated physical characteristics of the visual display system are shown in Table A5-2.

TABLE A5-2
SYSTEM CAPABILITIES

Ames Moving-Base Transport Simulator

Motions Generated:	<u>Acceleration</u>	<u>Displacement</u>
Roll	1 Rad/Sec ²	± 9°
Pitch	0.5 Rad/Sec ²	+ 14° - 6°
Heave (vertical)	± 0.8g (from ambient)	24 inches

Ames Landing-Approach Color Television Display

Motions Generated	<u>Velocity</u>	<u>Displacement</u>
Roll	0.35 Rad/Sec	--
Pitch	0.52 Rad/Sec	--
Yaw	0.17 Rad/Sec	360°
Lateral	240 Knots	2 1/2 miles
Vertical	6000 ft/min.	1500 ft. to 20 ft.
Longitudinal (runway length)	240 knots --	9 miles 10,000 ft. (model scale 1:1200)

APPENDIX 6

The following is a description of the documentation maneuvers performed by the evaluation pilots:

Longitudinal Maneuvers

- Pitch Rate Reversal** The airplane was trimmed by the safety pilot before engaging simulation. After stabilizing in steady flight pitch rate reversals were performed. The maneuver was initiated by applying a sharp column input, then quickly applying a step column input in the opposite direction. The column was stabilized, the airspeed held within 2 knots of trim, and the angle of attack held within 1° of trim when the pitch rate reversed.
- Column Step** From a stabilized flight condition, an aft column step was applied with amplitude sufficient to give a 1.2g maneuver. Recover was initiated after peak load factor was reached.
- Wind Up Turn** Wind up turns to 45° bank angle were performed, stabilizing in 5° bank increments.
- Speed Stability** The safety pilot trimmed the airplane in level flight. From initial trim the speed was increased and decreased in 5 kts increments using elevator only.
- Phugoid** The airspeed was decreased 10 kts from trim using elevator only. The controls were released and the phugoid was allowed to continue for two cycles. If the phugoid was divergent the maneuver was repeated with an initial 5 knot decrease in airspeed.

2-205

Pitch Attitude

A precision pitch attitude change of 5° to 10° was performed in minimum time, using the flight director for attitude reference.

Elevator Pulse

The airplane was trimmed in the initial configuration by the safety pilot before engaging simulation. The column pulse was then applied from the computer.

Lateral Maneuvers**Steady Roll Rate**

The airplane was stabilized in a steady turn and step wheel inputs were applied.

Roll Rate Reversal

The roll rate reversals were initiated by pulsing the wheel sharply, then applying the specified step wheel input in the opposite direction. When done properly the wheel was stabilized and the sideslip angle was less than 2° when the roll rate reversed.

Yaw Rate Reversal

After the safety pilot trimmed the airplane, the yaw rate reversal was initiated by the evaluation pilot with an 8° sharp rudder input followed by an opposite rudder step input as required. When done properly the sideslip was less than 2° and the rudder pedals were stabilized when the yaw rate reversed.

Steady Sideslip

With the airplane in the trimmed condition the evaluation pilot stabilized in a 10° sideslip, released the controls, and re-stabilized in level flight.

Spiral Stability

The configuration was stabilized in a 10° right turn and the controls were released. Recovery was initiated when the bank angle reached either 5° or 20° .

206

20° Heading Change The evaluation pilot performed a 20° heading change in minimum time.

Wheel Step With the airplane in level flight a full wheel step was applied rapidly with recovery initiated when the bank angle reached 15°.

Wheel Pulse The airplane was trimmed in the initial configuration by the safety pilot before engaging simulation. The wheel pulse was applied from the computer.

Rudder Pulse The airplane was trimmed in the initial configuration by the safety pilot before engaging simulation. The rudder pulse was applied from the computer.